PAGES 1537–1656

ISSN 0003–2654

The Analyst

A monthly international journal dealing with all branches of the theory and practice of analytical chemistry, including instrumentation and sensors, and physical, biochemical, clinical, pharmaceutical, biological, environmental, automatic and computer-based methods

Vol.117 No.10 October 1992

The Analyst

The Analytical Journal of The Royal Society of Chemistry

Editorial Manager, Analytical Journals: Judith Egan

Editor, *The Analyst*
Harpal S. Minhas
The Royal Society of Chemistry,
Thomas Graham House, Science Park,
Milton Road, Cambridge CB4 4WF, UK
Telephone 0223 420066.
Fax 0223 423623. Telex No. 818293 ROYAL.

US Associate Editor, *The Analyst*
Dr J. F. Tyson
Department of Chemistry,
University of Massachusetts,
Amherst MA 01003, USA
Telephone 413 545 0195
Fax 413 545 4490

Senior Assistant Editor
Paul Delaney

Assistant Editors
Brenda Holliday, Sheryl Youens

Editorial Secretary: Navlette Dennis

Advertisements: Advertisement Department, The Royal Society of Chemistry, Burlington House, Piccadilly, London, W1V 0BN. Telephone 071-437 8656. Telex No. 268001. Fax 071-437 8883.

The Analyst (ISSN 0003–2654) is published monthly by The Royal Society of Chemistry, Thomas Graham House, Science Park, Milton Road, Cambridge CB4 4WF, UK. All orders, accompanied with payment by cheque in sterling, payable on a UK clearing bank or in US dollars payable on a US clearing bank, should be sent directly to The Royal Society of Chemistry, Turpin Distribution Services Ltd., Blackhorse Road, Letchworth, Herts SG6 1HN, United Kingdom. Turpin Distribution Services Ltd., is wholly owned by the Royal Society of Chemistry. 1992 Annual subscription rate EC £276.00, USA $589, Rest of World £310.00. Purchased with *Analytical Abstracts* EC £604.00, USA $1299.00, Rest of World £669.00. Purchased with *Analytical Abstracts* plus *Analytical Proceedings* EC £712.00, USA $1527.00, Rest of World £791.00. Purchased with *Analytical Proceedings* EC £351.00, USA $749.00, Rest of World £395.00. Air freight and mailing in the USA by Publications Expediting Inc., 200 Meacham Avenue, Elmont, NY 11003.

USA Postmaster: Send address changes to: *The Analyst*, Publications Expediting Inc., 200 Meacham Avenue, Elmont, NY 11003. Second class postage paid at Jamaica, NY 11431. All other despatches outside the UK by Bulk Airmail within Europe, Accelerated Surface Post outside Europe. PRINTED IN THE UK.

Information for Authors

Full details of how to submit material for publication in *The Analyst* are given in the Instructions to Authors in the January issue. Separate copies are available on request.

The Analyst publishes papers on all aspects of the theory and practice of analytical chemistry, fundamental and applied, inorganic and organic, including chemical, physical, biochemical, clinical, pharmaceutical, biological, environmental, automatic and computer-based methods. Papers on new approaches to existing methods, new techniques and instrumentation, detectors and sensors, and new areas of application with due attention to overcoming limitations and to underlying principles are all equally welcome. There is no page charge.

The following types of papers will be considered:

Full research papers.

Communications, which must be on an urgent matter and be of obvious scientific importance. Rapidity of publication is enhanced if diagrams are omitted, but tables and formulae can be included. Communications receive priority and are usually published within 5–8 weeks of receipt. They are intended for brief descriptions of work that has progressed to a stage at which it is likely to be valuable to workers faced with similar problems. A fuller paper may be offered subsequently, if justified by later work. Although publication is at the discretion of the Editor, communications will be examined by at least one referee.

Reviews, which must be a critical evaluation of the existing state of knowledge on a particular facet of analytical chemistry.

Every paper (except Communications) will be submitted to at least two referees, by whose advice the Editorial Board of *The Analyst* will be guided as to its acceptance or rejection. Papers that are accepted must not be published elsewhere except by permission. Submission of a manuscript will be regarded as an undertaking that the same material is not being considered for publication by another journal.

Regional Advisory Editors. For the benefit of potential contributors outside the United Kingdom and North America, a Group of Regional Advisory Editors exists. Requests for help or advice on any matter related to the preparation of papers and their submission for publication in *The Analyst* can be sent to the nearest member of the Group. Currently serving Regional Advisory Editors are listed in each issue of *The Analyst.*

Manuscripts (four copies typed in double spacing) should be addressed to:

Harpal S. Minhas, Editor, *The Analyst,*
Royal Society of Chemistry,
Thomas Graham House,
Science Park, Milton Road,
CAMBRIDGE CB4 4WF, UK *or*:

Dr. J. F. Tyson
US Associate Editor, *The Analyst*
Department of Chemistry
University of Massachusetts
Amherst MA 01003, USA

Particular attention should be paid to the use of standard methods of literature citation, including the journal abbreviations defined in Chemical Abstracts Service Source Index. Wherever possible, the nomenclature employed should follow IUPAC recommendations, and units and symbols should be those associated with SI.

All queries relating to the presentation and submission of papers, and any correspondence regarding accepted papers and proofs, should be directed either to the Editor, or Associate Editor, *The Analyst* (addresses as above). Members of the Analytical Editorial Board (who may be contacted directly or via the Editorial Office) would welcome comments, suggestions and advice on general policy matters concerning *The Analyst.*

Fifty reprints are supplied free of charge.

ROYAL SOCIETY OF CHEMISTRY

ESSENTIAL FOR MASS SPECTROMETRISTS

Mass Spectrometry Bulletin Hard Copy

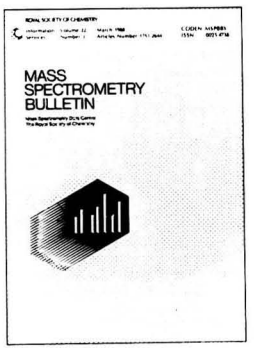

Mass Spectrometry Bulletin (MSB) is published monthly and contains bibliographic details of recently published literature on mass spectrometry, ion processes, ionization techniques and particle-impact phenomena. **MSB** provides the most comprehensive coverage of ALL areas of mass spectrometry.

Items included in **MSB** are selected from over 900 primary journals, books and conference proceedings. Approximately 880 items are included in each issue and are assigned to one of 34 subject sections. In addition, selected terms are provided with each **MSB** entry, highlighting the mass spectrometric content of the original document.

Each monthly issue includes a subject index, author index, compounds classification index, elements index and general index for the easy location of items of interest.

Mass Spectrometry Bulletin PC Version

Now with NEW software

The Mass Spectrometry Bulletin PC Version (MSB pc) provides easy access to the world's recently published literature. **MSB pc** saves much invaluable time and effort, fulfilling current awareness needs efficiently and allowing complex searches to be completed in seconds, in the convenience of the office or lab.

MSB pc runs on IBM pc compatible machines.

A free demonstration disk is available on request

MSB pc Features:

- Comprehensive coverage of ALL areas of mass spectrometry.
- **Simple creation of personal database subsets**
- **Monthly updates easily added to the database**
- Fast, flexible and extremely easy to use
- Includes an established software package – **ideaList**
- Full database management facilities

SUBSCRIPTION PRICES FOR 1992

Mass Spectrometry Bulletin Hard Copy
EC £355.00 USA $730.00 Rest of World £392.00

Mass Spectrometry Bulletin PC Version
EC £495.00 (plus VAT in the UK) USA £950.00 Rest of World £520.00

Special Package Price (for both PC and Printed versions)
EC £700.00 (plus VAT in the UK) USA $1,410 Rest of World £770.00

Those who already subscribe to the printed version may order the pc version for only
EC £345.00 (plus VAT in the UK) USA £680.00 Rest of World £378.00

To subscribe or for further details, please contact:
Mike Corkill, Royal Society of Chemistry
Thomas Graham House, Science Park, Milton Road
Cambridge CB4 4WF, United Kingdom
Tel: +44 (0)223 420066
Fax: +44 (0)223 423623
Telex: 818293 ROYAL

ROYAL SOCIETY OF CHEMISTRY
Information Services

Mössbauer Spectroscopic Investigation of the Sorption of Iron by Polyether-type Polyurethane-foam Sorbents

Štefan Palágyi* and Tibor Braun
Institute of Inorganic and Analytical Chemistry, Eötvös University, P.O. Box 123, H-1443 Budapest, Hungary
Zoltau Homonnay and Attila Vértes
Department of Nuclear Chemistry, Eötvös University, P.O. Box 32, H-1518 Budapest, Hungary

The results of a study on the nature of the iron species sorbed by polyether-type open-cell polyurethane (PU) foam membranes are presented. The study has included freshly prepared anionic $^{57}Fe^{III}$–halo complexes and $^{57}Fe(SCN)_3$, in addition to the cationic $^{57}Fe^{II}$–phenanthroline complex. Conclusions concerning the most probable nature of the sorbed species have been drawn from the comparison of Mössbauer spectra for frozen Fe–PU foam complexes with the spectra for corresponding iron-containing frozen aqueous solutions and extracts in suitable organic solvents. For Fe^{III} compounds, diethyl ether, and for the Fe^{II} complex, acetone, pentyl alcohol and nitrobenzene were used as organic solvents. The spectra were recorded at 80 K and evaluated to obtain isomer shifts, quadrupole splittings and internal magnetic fields for different iron species.

Keywords: *Mössbauer spectroscopy; iron; polyurethane foam sorbent; polyurethane foam membrane; sorption mechanism*

The use of resilient open-cell polyether-type polyurethane (PU) foam membranes as sorbents is a relatively novel advance in the field of separation science.[1–3] Polyurethane-foam sorbents can be used, in principle, unloaded or loaded with various reagents. The mechanism of the sorption by reagent-loaded PU is characterized, first of all, by the nature of the physically or chemically immobilized (loaded) reagents in the foam structure. It seems that in these instances the main function of the PU-foam backbone itself is to serve as a solid quasi-spherical membrane-like support for the loading reagents. On the other hand, unloaded PU-foam membranes are not chemically inert and, owing to their polymeric nature and/or their different functional groups or heteroatoms, may well take part in the sorption processes. The studies of the possible mechanism of the sorption of metals indicate that, owing to the complex chemical nature of the polyether-type PU-foam membrane material, several mechanisms could be involved simultaneously.[2] Some of the mechanisms taken into account separately are: ether-like solvent extraction, ligand addition or exchange, anion exchange and cation chelation, *etc.*, including adsorption and absorption.[3–13]

Investigation of these mechanisms has been carried out by the use of various physical and nuclear measurements. Mössbauer spectroscopy has been used previously in the study of the nature of the species sorbed by PU foam from $Fe(SCN)_3$ solution.[9] It was found that a neutral $Fe(SCN)_3$ species is most probably sorbed by both the polyether and polyester foams investigated. A comparison of the spectra obtained with those of frozen aqueous and diethyl ether solutions of $Fe(SCN)_3$ indicated the similarity of the diethyl ether extracted and PU-foam sorbed species. As the complexes of Fe^{III} are mostly six-coordinated, a species such as $Fe(SCN)_3 \cdot D_3$ could be assigned to the sorbed species, where D represents some donor group of the polymer.

In this paper, results of a study of the nature of the iron species sorbed by the PU-foam membranes are presented. The study has been extended to some other anionic Fe^{III}–halo complexes, and to the cationic Fe^{II}–phenanthroline complex. Because of the enhanced sorption of these complexes with a polyether-type foam in comparison with a polyester-type foam, only the former was investigated thoroughly.

* On leave from the Institute of Radioecology and Applied Nuclear Techniques, Kosice, Czechoslovakia.

As reported recently,[14] polyether-type PU foam does not sorb chloro complexes of Fe^{II}. From a comparison of the behaviour of the anionic Fe^{II} and Fe^{III} chloro complexes ($FeCl_4^{2-}$ and $FeCl_4^-$, respectively) on the polyether-type PU foams with that in diethyl ether,[15–17] the similarity of these sorbents to etheric extractants was evident. This similarity, and the similarities in the sorption of typical pseudo-halides, *i.e.*, thiocyanates, including $Fe(SCN)_3$, on polyether-type foam, and in the extraction of these with liquid ethers, led to the concept of the solid etheric solvent-extraction mechanism of metal-ion sorption by polyether-type polyurethanes.[6,7,18–21]

It was reported recently[22] that Fe^{II} can also be sorbed on the polyether-type PU foam as an Fe^{II}–1,10-phenanthroline chelate with bulky monovalent anions, *e.g.*, ClO_4^-. Iron(II) forms a cationic complex with phenanthroline, $Fe(phen)_3^{2+}$,[15,17] The ion pair formed with perchlorate, $Fe(phen)_3(ClO_4)_2$, is not soluble in diethyl ether[23] despite the fact that 1,10-phenanthroline alone is soluble. This indicates that the mechanism of Fe^{II} sorption on PU foam is different from the above-mentioned ether-like solvent extraction and it can be expected that it will be analogous to the extraction of ion pairs with oxygenated organic solvents.[15]

In this paper, conclusions concerning the most probable nature of the sorbed species have been drawn from a comparison of the Mössbauer spectra for frozen Fe–PU foam complexes with the spectra for corresponding Fe-containing frozen aqueous solutions and extracts in suitable organic solvents.

Experimental

Preparation of Aqueous Solutions of Fe^{III} Complexes

All the chemicals used were of analytical-reagent grade. Iron enriched in ^{57}Fe (95%) was used in the sample preparations. The metallic iron (10 mg) was dissolved in concentrated (12 mol dm^{-3}) hydrochloric acid solution. The $FeCl_2$ solution was then oxidized to $FeCl_3$ with several drops of concentrated (14 mol dm^{-3}) nitric acid and concentrated hydrogen peroxide, while boiling. The valence state Fe^{III} was confirmed by the thiocyanate reaction. Finally, the solution was diluted with de-ionized water to obtain 0.005 mol dm^{-3} $^{57}FeCl_3$ solution in approximately 5 mol dm^{-3} HCl.

A solution of $^{57}FeBr_3$ of the same Fe^{III} concentration in 5 mol dm^{-3} HBr was prepared from the $FeCl_3$, and re-extracted from diethyl ether (see below) with de-ionized water. The iron

was recovered from its aqueous solution as $FeBr_3$ after several evaporations to dryness with concentrated hydrobromic acid (12 mol dm^{-3}) on a hot-plate. Finally, the solution of $^{57}FeBr_3$ was diluted with de-ionized water to the desired concentration.

A solution of $^{57}Fe(SCN)_3$ was prepared from $FeBr_3$ by elution with acetone from PU foam (see below). The solution was evaporated to dryness, and Fe^{III} was recovered as $Fe(NO_3)_3$ after several evaporations to dryness with concentrated nitric acid (14 mol dm^{-3}). Finally, the solution of 5 mmol dm^{-3} $^{57}Fe(SCN)_3$ was prepared from 0.5 mol dm^{-3} KSCN in 1 mol dm^{-3} HNO_3.[9]

Solutions of Fe^{III} bromide or thiocyanate can be equally well prepared also, either by the aqueous elution of $FeCl_3$ from PU foam or by the aqueous re-extraction of $FeBr_3$ from diethyl ether, as described above. The desired compounds can be easily prepared also from the diethyl ether solutions by evaporation to dryness.

Preparation of Etheric Solutions of Fe^{III} Complexes

The solutions of $^{57}FeCl_3$, $^{57}FeBr_3$ and $^{57}Fe(SCN)_3$ in diethyl ether were prepared by several successive extractions from 20 cm^3 of the aqueous solutions in a ratio of 1 + 1 v/v. The final concentration of Fe in these solutions was adjusted simply by evaporation of a portion of the diethyl ether.

Preparation of Aqueous Solutions of Fe^{II} Complexes

The enriched metallic ^{57}Fe (10 mg) was dissolved in concentrated (12 mol dm^{-3}) hydrochloric acid as before. The $FeCl_2$ solution was then used in further experiments. The solution was neutralized with several drops of aqueous 25% NH_3, and the pH was adjusted to about 4. The saturated tris(phenanthroline)iron(II) chloride (orange colour) was prepared by the addition of solid 1,10-phenanthroline. The $^{57}Fe(phen)_3(ClO_4)_2$ was finally prepared by addition of a sufficient volume of 5 mol dm^3 $HClO_4$. Before the sorption of Fe^{II} complexes on PU foam, the solutions were diluted to 20 cm^3 with 5 mol dm^3 $HClO_4$.

Preparation of Organic Solutions of Fe^{II} Complexes

The solution of $Fe(phen)_3(ClO_4)_2$ in pentyl alcohol was prepared by extraction of this complex from its aqueous solution (1–2 cm^3) in a volume ratio of 1 + 1. Using another portion of aqueous solution, the solution of $Fe(phen)_3(ClO_4)_2$ in nitrobenzene was prepared in the same way. The acetone solution of this complex was prepared either by the elution of $Fe(phen)_3(ClO_4)_2$ from PU foam (see below) or by repeated evaporation of a pentyl alcohol or nitrobenzene solution of this complex with acetone.

Preparation of Fe^{II} and Fe^{III} Complexes Loaded on PU Foam

A polyether-type open-cell PU foam was used (Chemical Works, Sajobabony, Hungary) with a density of 30 kg m^{-3}. The foam was cut into 10 cm high cylindrical plugs, 2 cm in diameter.[24,25] The foam cylinders were placed into 20 cm^3 plastic syringes and were washed, compressing and releasing successively with 50 cm^3 of 1 mol dm^{-3} HCl, de-ionized water and acetone. Finally, the cylinders were air dried. The mass of the 10 cm cylindrical plugs was 0.88 ± 0.01 g. Finally, 5 cm high cylinders were used in the experiments.

The sorption experiments were carried out using the pulsated-column technique,[24,25] with use of 20 cm^3 plastic syringes each filled with a 5 cm high washed PU-foam cylinder. The volume of the aqueous phase was 20 cm^3 in each instance. The foam plugs were equilibrated with aqueous solutions of Fe^{II} or Fe^{III} complexes for 30 min, pulsating the foam cylinder in the solution at about three strokes per minute. After the last compression, the foam cylinders were dried, first, between two sheets of filter-paper and then in air.

Preparation of Frozen Samples for Analysis

The measurements were carried out at 80 K. Before the measurements, the samples were frozen in liquid nitrogen. The volume of each aqueous solution was reduced to about 1 cm^3 by evaporation on a hot-plate. Etheric solutions were concentrated to the same volume by evaporation in air. The other organic solutions were used in their concentrated form without further treatment.

A 0.35 or 0.6 cm thick copper ring (1.5 cm i.d. and 0.35 cm wall thickness) was used as a sample container (according to the volume of the samples required for obtaining sufficient counts of the spectra), mounted between two transparent thin plastic foils, fixed between two copper sample-holder rings. The filling of the sample container, immersed in liquid nitrogen, was carried out by means of a syringe dispenser.[26] The frozen liquid was in the form of small beads (of about 0.2 cm in diameter). Polyurethane-foam cylinders with sorbed compounds were compressed and frozen directly in the plastic syringes used for sorption. The compressed plugs, of 0.2–0.3 cm thickness, mounted in the sample holder without the sample container. For the measurements, freshly prepared solutions and Fe–foam complexes were used. Finally, the sample holder was inserted into a hollow cold finger that was firmly connected to a specially manufactured liquid-nitrogen container.[26] The container was then positioned between the irradiation and detection facilities.

Mössbauer Spectroscopy Measurements

The Mössbauer spectrometer was equipped with a Ranger Electronic transducer (Ranger Scientific, Burleson, TX, USA) and control unit. An ICA-70 multichannel analyser (KFKI, Budapest, Hungary) was coupled with a conventional NaI(Tl) scintillation detector. A $^{57}Co(Pd)$ source of about 7.4 × 10^8 Bq activity was used. Isomer shifts relative to metallic iron at room temperature, are reported in Table 1. The transducer was operated at a velocity of 12 mm s^{-1}.

The collection of spectra usually took several hours. Sextets, doublets and singlets of Lorentzian lines were used for the fitting of the spectra.

Results and Discussion

Sorption of ^{57}Fe Samples

The sorption capacity of the PU foam was determined by a spectrophotometric method based on the reaction between Fe^{III} and thiocyanate and by gravimetry [supposing $H(FeCl_4)$ to be the sorbed species]. The two analytical results were in good agreement. A capacity of 52 mg g^{-1} of Fe in PU foam was found. In our Mössbauer measurements 4 mg cm^{-1} of

Table 1 Mössbauer parameters obtaind at 80 K for $Fe(phen)_3(ClO_4)_2$ in different frozen solutions and absorbed in PU foam. Typical errors are ±0.001 and 0.005 mm s^{-1} for isomer shifts and quadrupole splittings, respectively

Medium	Isomer shift relative to α-Fe at room temperature/ mm s^{-1}	Quadrupole splitting/ mm s^{-1}
PU foam	0.381	0.280
Water	0.409	0.258
Pentyl alcohol	0.397	0.213
Acetone	0.396	0.232
Nitrobenzene	0.390	0.248

^{57}Fe in PU foam has never been exceeded, which is less than half of the saturation value.

In the preparation of the $FeCl_3$ sorbate on PU foam, hydrochloric acid concentration of 5 mol dm^{-3} was chosen. It was found that, at this concentration, a higher sorption efficiency can be obtained without damage to the PU-foam structure.[1,4,14] At higher hydrochloric acid concentrations, polyether foams become unstable and decompose by dissolution in the concentrated acid.[1] As is known, the optimum extraction of $FeCl_3$ with diethyl ether takes place in 5–6 mol dm^{-3} HCl.[15,16] Therefore, this HCl concentration can well serve as a reference for mutual comparison of the sorption and extraction efficiency.

In accordance with earlier observations,[14,18,19,27] Fe is sorbed efficiently on PU foams from acidic chloride solutions as an anionic $FeCl_4^-$ chloro complex, similarly as in the extraction with diethyl ether.[15–17] Our experiments confirmed these results, and under our conditions, in 5 mol dm^{-3} HCl, $FeCl_3$ was sorbed quantitatively and, as the material balance showed (increase in the mass of the PU-foam cylinder), it was actually in the form of $H(FeCl_4)$. However, our observations showed that the sorption of $FeBr_3$ in 5 mol dm^{-3} HBr on the PU foam is different in nature, because the material balance revealed a marked increase in the mass of the PU cylinder. Therefore, it can be supposed that, in this instance, $FeBr_3$ is sorbed in the form of an $H(FeBr_m)$ polybromic complex (where $m > 4$), probably as a result of the partial oxidation of Br^- to Br_2 by nitric acid.

The sorption of $^{57}Fe(SCN)_3$ on the PU foam requires an appreciable excess of thiocyanate, while the acidity of the aqueous solution is of lesser importance.[20] However, the increased acidity could initiate decomposition and polymerization of thiocyanate or isothiocyanic acid.[15] From the increase in the mass of the PU foam plug it can be supposed that, under the described conditions, the ratio of Fe to thiocyanate was about 1 : 30 in the foam.

The sorption of an Fe^{II}–phenanthroline complex on PU foams in the presence of Cl^- failed. It was also found that $Fe(phen)_3(ClO_4)_2$ cannot be extracted into diethyl ether or chloroform. To keep the iron in the Fe^{II} valence state it is advisable to add some (several tens of milligrams) of $NH_2OH{\cdot}HCl$ to the aqueous solution to prevent its oxidation to Fe^{III} before the addition of phenanthroline. From the measurement of the mass of the PU-foam plug, before and after sorption, it can be concluded that the foam sorbs exactly as much 1,10-phenanthroline and ClO_4^- accompanying anion as follows from the stoichiometry of the $Fe(phen)_3(ClO_4)_2$ complex. This is a confirmation of the previous results that the $Fe(phen)_3^{2+}$ chelate can be successfully used for the determination of some anions, including ClO_4^- by spectrophotometry.[23,28]

It should be noted that the efficiency of the sorption of the Fe^{II} and Fe^{III} complexes investigated by PU foams was 95–100% and the recovery from the foam with acetone amounted to 100%.

Analysis of ^{57}Fe Samples

Investigation of Fe^{III} complexes

Successful Mössbauer experiments could be performed in the systems containing Cl^- or SCN^-. In addition to the PU-foam absorbed complexes, aqueous and etheric frozen solutions were analysed. The attempt to study the Br^--containing system failed because of the absorption of a very large amount of polybromic acid (as discussed above) on the PU foam. The heavy bromine atom absorbs the 14.4 keV of gamma-radiation very effectively, thus preventing the recording of a Mössbauer spectrum.

The two series of Mössbauer spectra can be seen in Figs. 1 and 2. Each spectrum contains a magnetically split component (sextet) and a singlet or a doublet. Useful conclusions can be drawn from the parameters of the sextet. The observed magnetic splitting in this instance is due to the $S = 5/2$ spin state of the paramagnetic Fe^{3+}. Normally, we do not see any hyperfine field for a paramagnetic Fe^{III} bulk compound, because the interaction between the neighbouring Fe^{3+}, and between the Fe^{3+} and the crystal lattice, results in a very rapid back-and-forth change in spin orientation (paramagnetic spin relaxation) and even in the very short Mössbauer time window (the mean lifetime of an $^{57}Fe^m$ nucleus is about 10^{-7} s) the observed mean hyperfine field is zero. However, the rate of paramagnetic spin relaxation can be reduced under appropriately set experimental conditions. As, in our example, the spectra were recorded at 80 K where the spin–lattice relaxation is slow (*i.e.*, sufficiently slow to observe a quasi-constant magnetic field at the ^{57}Fe nucleus), we have to take account of the spin–spin relaxation time only. The obvious choice is dilution. If the Fe^{3+} ions are well separated from each other the likelihood of their direct interaction is highly reduced and the rate of spin–spin relaxation decreases. This explains why very dilute solutions were used in the Fe^{III} experiments and never saturated the PU foam with the Fe^{III} complexes.

The magnetic field at the $^{57}Fe^{3+}$ nucleus having an unperturbed d^5 configuration with $S = 5/2$ spin cannot be

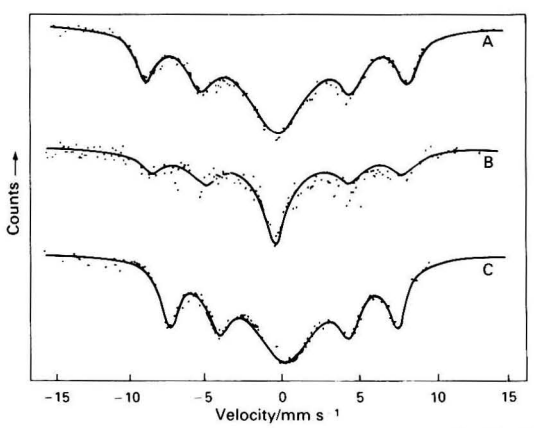

Fig. 1 Mössbauer spectra recorded at 80 K in the Fe^{3+}–Cl^-–X system. Lettering indicates: X = water (A); X = diethyl ether (B); and X = PU foam (C)

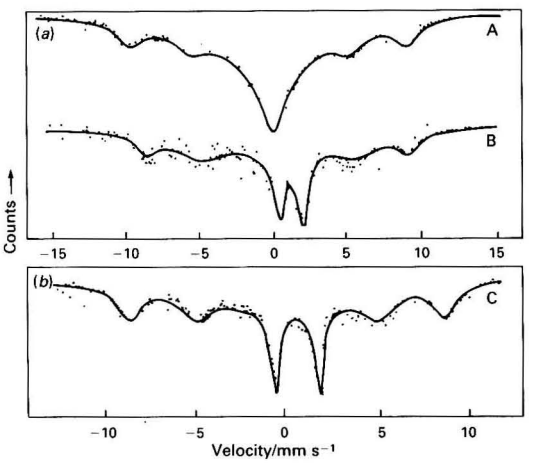

Fig. 2 Mössbauer spectra recorded at 80 K in the Fe^{3+}–SCN^-–X system. Lettering indicates: X = water (A); X = diethyl ether (B); and X = PU foam (C)

Table 2 Internal magnetic fields at the ^{57}Fe nucleus in different systems at 80 K as derived from Mössbauer spectra

System	Internal magnetic field/ MA m^{-1}
Fe^{3+}/Cl^-/water	43.9 ± 0.1
Fe^{3+}/Cl^-/diethyl ether	41.5 ± 0.4
Fe^{3+}/Cl^-/PU foam	37.6 ± 0.1
Fe^{3+}/SCN^-/water	44.6 ± 0.1
Fe^{3+}/SCN^-/diethyl ether	44.1 ± 0.4
Fe^{3+}/SCN^-/PU foam	42.9 ± 0.2

measured experimentally because the ever present coordination entities (the solvent molecules, if nothing else) donate electrons to the free *d* orbitals with necessarily opposite spins and hence reduce the mean magnetic field. As a consequence, the observed mean magnetic field is characteristic of the coordination sphere of the Fe^{3+}, and its change could indicate the exchange of coordinating species or some new interaction.

The Mössbauer data obtained for the chloride- and thiocyanate-containing system are summarized in Table 2. The spectra were evaluated with respect to a sextet with varying linewidth for the 1–6, 2–5 and 3–5 line pairs and a central doublet or singlet. Singlets can be observed because parts of the Fe^{III} species happen to be too close to each other in the random frozen solution, causing a fast spin–spin relaxation that occurs too quickly. The doublets appearing in the Fe–thiocyanate–diethyl ether and Fe–thiocyanate–PU systems denote the presence of Fe^{II} species. This is as a result of the partial decomposition of the thiocyanate complex under our experimental conditions, which involve a redox reaction between Fe^{3+} and SCN^- (ref. 15) (precipitation of sulfur could be observed). Neither the presence of a paramagnetic singlet nor the doublet of the Fe^{II} species affected the evaluation of the effective magnetic field from the parameters of the sextet.

From a comparison of the hyperfine field data it is clear that the behaviour of the two systems differs. The variation of the hyperfine field values is greater when the coordination entity is chloride. This observation does not support the assumption that free tetrahedral $FeCl_4^-$ ions exist in all of these systems. The most plausible explanation is that in the aqueous system we assume that tetrahedral $FeCl_4^-$ ions are present, where the high H^+ concentration suppresses the coordination ability of the water molecules by protonating them. This is also supported by the high magnetic field.[29] The value of the magnetic field can decrease, in the etheric solution, if a six-coordinated species forms with two diethyl ether ligands. However, for the PU-absorbed species the value of the magnetic field is unexpectedly low and oxygen donor groups cannot be responsible for such a large decrease. A strong ligand, probably the isocyanate groups of the PU foam, must be coordinated to the Fe^{3+}. In the thiocyanate-containing system, the tendency of the variation of the hyperfine fields is the same, although the difference between the frozen etheric and aqueous solutions is almost within the experimental error. For the PU-foam absorbed species, the hyperfine field, again, is smaller, indicating some more intense charge transfer to the free *d* orbitals of the Fe^{3+} from the groups of the PU foam. On the basis of the magnetic fields, probably a six-coordinated species forms in all instances, in agreement with an earlier conclusion.[9]

Investigation of Fe^{II} complexes

The Mössbauer spectra recorded for $Fe(phen)_3(ClO_4)_2$ at 80 K, in different solvents and also absorbed in PU foam, are shown in Fig. 3. Each spectrum was evaluated to one quadrupole doublet except when the solvent was water. In this instance a two-doublet fit was necessary. According to its

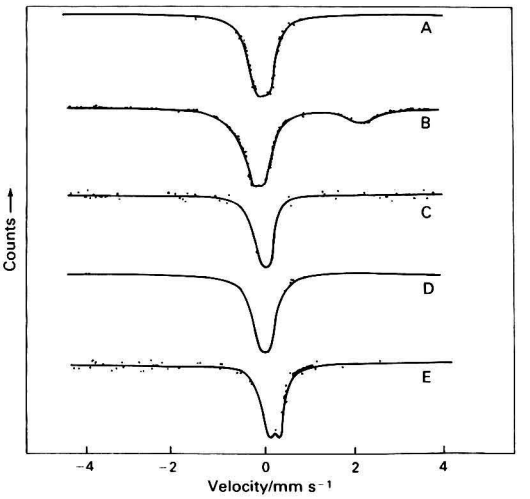

Fig. 3 Mössbauer spectra of $[Fe(phen)_3](ClO_4)_2$, recorded at 80 K, as absorbed in PU foam (A) and in different frozen solutions [water (B); pentyl alcohol (C); acetone (D); and nitrobenzene (E)]

Mössbauer parameters, the second doublet was probably due to the residual high-spin species,[30] which is irrelevant to the present study. The parameters obtained for the different systems are listed in Table 1.

All the listed parameters are typical for low-spin Fe^{II} complexes, as expected. It can be seen that there is virtually no difference in the parameters as the medium is changed even if those for the PU foam-absorbed complex are extreme (lowest isomer shift and highest quadrupole splitting). It is clearly shown that the strong chelate molecule cannot be perturbed appreciably either by the molecules of the applied solvents or by the PU foam. This suggests that any change in the vicinity of the Fe^{II} complex must affect only the outer ligand sphere, and this determines the mechanism of absorption.

Conclusions

As can be seen from the Mössbauer spectroscopic investigations of the anionic Fe^{III} complexes, the differences in the nature of chloride- and thiocyanate-containing systems are apparent.

The observations do not support the assumption that free $FeCl_4^-$ is present in all of the chloride-containing systems, except water. In the etheric solution, most probably a six-coordinated complex, $H(FeCl_4)\cdot 2(C_2H_5)O$, is formed with two diethyl ether ligands. With the PU foam-sorbed complexes, a strong ligand, probably two isocyanate donor groups of the PU foam coordinate with the Fe^{3+} ion in the resulting $H(FeCl_4)\cdot 2D$ complex.

In the thiocyanate-containing system, the difference between aqueous and etheric solutions is almost negligible, and $Fe(SCN)_3$ species are present in both solvents. With the PU foam-sorbed species, probably a six-coordinated complex, $Fe(SCN)_3\cdot 3D$, is formed with some of the donor groups of the PU foam, in agreement with an earlier observation.[9]

The Mössbauer spectra of $Fe(phen)_3(ClO_4)_2$ in various solvents that are sorbed on the PU foam exhibit no significant differences. This suggests that the nature of this cationic Fe^{II} complex in the PU foam is essentially the same as in the aqueous and organic solvents used.

This work was supported by the Hungarian Fund for Basic Research (OTKA), which is gratefully acknowledged.

References

1 Braun, T., Navratil, J. D., and Farag, A. B., in *Polyurethane Foam Sorbents in Separation Science*, CRC Press, Boca Raton, FL, 1985.
2 Braun, T. *Fresenius' Z. Anal. Chem.*, 1989, **333**, 785.
3 Palagyi, S., and Braun, T., in *Preconcentration Techniques for Trace Elements*, eds. Alfassi, Z. B., and Wai, C. M., CRC Press, Boca Raton, FL, 1992, pp. 363–700.
4 Bowen, H. J. M., *J. Chem. Soc. A*, 1970, 1082.
5 Korkisch, J., Steffan, I., and Navratil, J. D., *Radioact. Waste Manage.*, 1972, **6**, 349.
6 Gesser, H. D., Bock, E., Baldwin, W. G., Chow, A., McBride, D. W., and Lipinsky, W., *Sep. Sci.*, 1976, **11**, 317.
7 Braun, T., and Farag, A. B., *Anal. Chim. Acta*, 1978, **98**, 133.
8 Hamon, R. F., Khan, A. S., and Chow, A., *Talanta*, 1982, **29**, 313.
9 Abbas, M. N., Vertes, A., and Braun, T., *Radiochem. Radioanal. Lett.*, 1982, **54**, 17.
10 Al-Bazi, S. J., and Chow, A., *Talanta*, 1984, **31**, 431.
11 Hamon, R. F., and Chow, A., *Talanta*, 1984, **31**, 963.
12 Khan, A. S., Baldwin, V. G., and Chow, A., *Can. J. Chem.*, 1987, **65**, 1103.
13 Brackenbury, K. F. G., Jones, L., and Koch, K. R., *Analyst*, 1987, **112**, 459.
14 Drtil, M., Tölgyessy, J., and Braun, T., *Fresenius' J. Anal. Chem.*, 1990, **338**, 50.
15 Sandell, E. B., and Onishi, H., *Photometric Determination of Metals*, Wiley, New York, 4th edn., 1978, pt. 1.
16 Koch, O. G., and Koch-Dedic, G. A., *Handbuch der Sprenanalyse*, Springer, Berlin, 1973.
17 De, A. K., Khopkar, S. M., and Chalmers, R., *Solvent Extraction of Metals*, Van Nostrand Reinhold, London, 1970.
18 Gesser, H. D., Horsfall, G. A., Gough, K. M., and Kravchuk, B., *Nature (London)*, 1982, **268**, 1082.
19 Oren, I. J., Gough, K. M., and Gesser, H. D., *Can. J. Chem.*, 1979, **57**, 2032.
20 Braun, T., and Abbas, M. N., *Anal. Chim. Acta*, 1982, **134**, 321.
21 Maloney, M. P., Moody, G. J., and Thomas, J. D. R., *Analyst*, 1980, **105**, 1087.
22 Bhattacharya, S., Roy, S. K., and Chakraborty, A. K., *Talanta*, 1990, **37**, 1109.
23 Knizek, M., *Chem. Listy*, 1968, **62**, 299.
24 Braun, T., and Palagyi, S., *Anal. Chem.*, 1979, **51**, 1697.
25 Palagyi, S., and Braun, T., *J. Radioanal. Chem.*, 1979, **51**, 269.
26 Vertes, A., and Nagy, D. L., *Mössbauer Spectroscopy of Frozen Solutions*, Akadémiai Kiadó, Budapest, 1991.
27 Drtil, M., and Tölgyessy, J., *Chem. Listy*, 1990, **84**, 550.
28 Yamamoto, Y., Kotsuji, K., Kinuwaki, S., and Sawamura, H., *J. Chem. Soc. Jpn.*, 1964, **85**, 869.
29 Vértes, A., Korecz, L., and Burger, K., *Mössbauer Spectroscopy*, Akadémiai Kiadó, Budapest, 1979, p. 323.
30 Ganguli, P., Gütlich, P., Müller, E. W., and Irler, W., *J. Chem. Soc., Dalton Trans.*, 1981, 441.

Paper 2/01224C
Received March 6, 1992
Accepted May 27, 1992

Near Near Infrared Spectroscopy for Quantitative and Qualitative Quality Control

Tamzin A. Lafford,* Yvette Cornélis and Peter Forster
Ciba-Geigy AG, CH-4002 Basel, Switzerland

Absorbance spectra from near near infrared (NNIR; 800–1050 nm) spectroscopy of organic liquids are measured using a silicon diode array spectrometer. No sample dilution is necessary as the absorbance values are low. Multi-component analysis applied to complete NNIR spectra provides both quantitative and qualitative information, essential in industrial quality control. Acceptable accuracy (error <1%) is achieved in the quantitative analysis of mixtures of non-interacting substances, and it is also possible to analyse alcohols in non-polar solvents, where intermolecular H-bonding occurs. Principal component regression was also performed on the NNIR data to give qualitative information.

Keywords: *Near near infrared spectroscopy; multi-component analysis; quality control; principal component regression; diode array spectrometer*

Spectrophotometry is widely used in industrial quality control. Quantitative analysis is carried out in the ultraviolet/visible (UV/VIS) region (190–820 nm) on the basis that the Beer–Lambert law is obeyed, assuming intermolecular interactions are negligible. Concentrations are calculated from absorbance data at only one or two wavelengths. As absorbance values are high in this region, it is necessary to dilute samples accurately prior to measurement and analysis.

Lately, infrared (IR; 2500–15 000 nm) and near infrared (NIR; 1000–2500 nm) spectroscopy have more frequently been used to obtain qualitative information. In the past, this has been achieved by visual comparison of the sample spectrum with a reference. A great improvement on this method was the use of factor analysis of NIR spectra.[1] A 'learning set' of several reference spectra is required, against which the sample spectrum is compared. The results of the analysis are plotted in factor space, the spectra of each different substance forming a separate cluster of points. The sample can be identified by its relative position in the factor space.

Multicomponent analysis (MCA) is a simple least-squares regression algorithm.[2,3] It uses the data at all the wavelengths considered, if so desired. However, for accuracy, it is necessary that the Beer–Lambert law is obeyed at every wavelength taken. The method is currently being used in the UV/VIS region in this laboratory with increasing success. A standards list consisting of one spectrum of each of the relevant pure components is compiled by the user. The MCA then compares the test spectrum with the standards and constructs the least-squares fit from a linear combination. The proportions required of each spectrum are converted into component concentrations. A chi-squared 'error of fit', normalized with respect to the system noise and sensitivity, is also returned. This is a measure of how closely the reconstructed spectrum fits the test data. It is a sensitive qualitative measure; a poor fit can indicate that the standards chosen are not appropriate to the sample composition, or that some intermolecular interaction occurs that influences the sample spectrum. The standards list can then be revised, or the wavelength range considered adjusted to improve the fit.

Sample preparation is not necessary for NIR measurements but quantitative analysis is complicated, as the spectra contain overlapping bands and are strongly influenced by intermolecular interactions. Multicomponent analysis using reference spectra is not viable, and more complex algorithms such as principal component regression (PCR) and partial least-squares using factors rather than reference spectra[4] are required. These involve tedious calibration procedures.

Spectra from near near infrared (NNIR; 800–1050 nm) spectroscopy of many organic liquids exhibit sharper bands with less overlap than the NIR spectra. The NNIR spectra are conveniently measured with silicon diode arrays, no sample dilution and almost no sample preparation is required as the absorbances are low. The aims of this investigation were: (*i*) to establish whether the simple MCA algorithm is applicable despite the necessarily high sample concentrations; and (*ii*) to determine whether NNIR spectra are sufficiently individual to allow one substance to be distinguished from another.

Experimental

The NNIR absorbance spectra were measured using an HP 8452a extended visible diode array spectrometer (Hewlett-Packard). It was equipped with a multi-cell transporter holding two quartz cells of 10.0 mm optical pathlength.

To counteract instrumental drift, it proved necessary to simulate a double beam apparatus. One cell (the 'blank') was filled with solvent (CCl_4). The other was a flow-through cell connected to an AMICA 5000 dynamic diluter[5] from which the sample, accurately diluted as required, was delivered. The diluter was driven by the system software. The spectrum of the blank was always measured directly after the sample spectrum, and then subtracted from it mathematically.

Measurements are also sensitive to the effects of turbulence following the injection of the liquid into the cell. Turbulence causes fluctuations in the refractive index of the sample, which then appears as noise in the absorbance spectrum. This was overcome by a stabilization time of 180 s prior to the measurement.

The spectra of pure organic liquids and of concentrations down to 40% v/v in CCl_4 were recorded. Propan-1-ol was measured down to 0.05% concentration. Some two-component mixtures were also investigated over the range from 95 to 5% v/v.

Multicomponent analysis was performed within the instrument software, which was written in this laboratory. The standards list in each case consisted of spectra of the relevant pure substances and included a flat 'dummy' spectrum to account for any flat drift in the baseline of the instrument between measurements.

For treatment by PCR the data were transferred to the ICAP software package (Bran and Luebbe). The spectra were usually differentiated before analysis to eliminate the effects of any baseline offset between them (the substitute for the flat dummy in the MCA software package).

* Present address: School of Physics, University of Bath, Claverton Down, Bath, UK, BA2 7AY.

Results and Discussion

NNIR Spectra of Liquids

Spectral features in the NNIR are sharper than in the NIR. Pure organic liquids show low absorbances (0.02–0.07 using a 10.0 mm light path) with a characteristic peak around 900 nm for aliphatic compounds. This is shifted to shorter wavelengths for aromatic compounds. Some typical spectra are shown in Fig. 1. The spectrum of water, by contrast, has a peak at 980 nm with an absorbance of 0.2.

Quantitative Analysis

Dilutions in CCl_4

The observance of the Beer–Lambert law in the NNIR by many organic liquids was confirmed. This was carried out by checking the correlation of the absorbance at a given wavelength with the concentration. The wavelength chosen was at a maximum in the spectrum, in order to minimize the influence of noise. (For alcohols, it was necessary to ignore the peak at about 970 nm, see below.) The standard error of estimate of the linear regression in terms of absorbance was $S_{y,x}$ <0.0001 in most cases. Therefore, the Beer–Lambert law is closely followed.

Multicomponent analysis was carried out over the whole NNIR range on the spectra recorded. For toluene, benzene and heptane of concentrations from 100 to 40% in CCl_4 a calculation error (residual concentration) of better than 0.5% relative was achieved. Poorer accuracy was obtained with some other substances, *e.g.*, cyclohexane and 1,4-dioxane, which have two possible molecular configurations. The proportions present of each configuration depend on the temperature, which was not necessarily constant during the measurements. Problems with electronic interference have so far frustrated attempts at temperature stabilization of the samples. Improved results are expected upon implementation of thermostatic control. It will then be interesting to see how well MCA in the NNIR can differentiate between molecular configurations.

In studying alcohols diluted in CCl_4 an absorbance peak that did not obey the Beer-Lambert law was found. It occurs between 960 and 980 nm, depending on the alcohol (see Fig. 2). It is assigned to an overtone of the OH-stretching vibration, and its amplitude *versus* concentration characteristic is influenced by the degree of intermolecular hydrogen bonding.[6,7]

This self-association of alcohols in non-polar solvents precludes the application of MCA over the entire NNIR wavelength range. The reliability of the analysis can be improved in two ways: (*i*) by restricting the wavelength range so that the region of the OH peak is excluded; or (*ii*) by including in the MCA standards list the spectrum of a very dilute sample (*e.g.*, 1%). Such a spectrum is dominated by the OH peak. The apparent concentration of this standard together with the calculated concentration of the pure standard gives a revised estimate of the alcohol concentration.

The relative accuracies of the above methods are illustrated in Fig. 3 for dilutions of propan-1-ol in CCl_4. As the alcohol concentration decreases, the OH peak becomes more significant and corrections are more important. (In the following figures the true concentration is that prepared with the dynamic dilutor.)

Two-component mixtures

Some mixtures of two absorbing pure liquids were also investigated. The concentration of one component relative to the other ranged from 5 to 95% v/v. The MCA could be performed with an error of better than 1% if the components did not interact (*e.g.*, by H-bonding). The results of MCA on toluene–heptane mixtures are given in Fig. 4.

Qualitative Analysis

Multicomponent analysis algorithm

The software used for the MCA has the advantage that quantitative and qualitative information are delivered simultaneously. The concentration is calculated, and the normalized error of fit can be used as a qualitative indicator as it measures how closely the test spectrum can be matched by a linear combination of the standard spectra (see above).

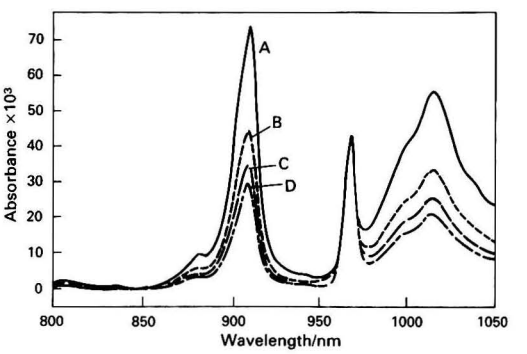

Fig. 2 NNIR spectrum of *tert*-butanol in CCl_4. A, 100; B, 63; C, 50; and D, 42% v/v. (Pathlength = 10.0 mm)

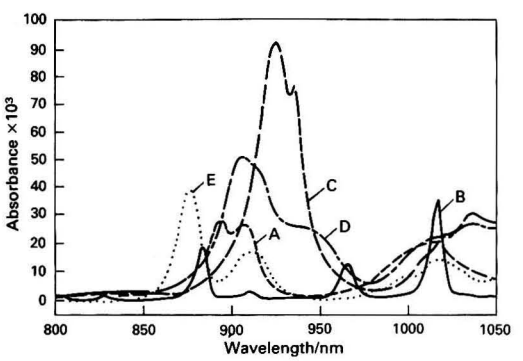

Fig. 1 NNIR absorbance spectra of pure organic liquids. A, Acetone; B, chloroform; C, cyclohexane; D, tetrahydrofuran; and E, toluene

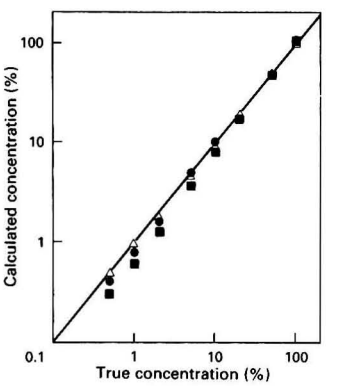

Fig. 3 Accuracy of MCA on propan-1-ol. ■, 800–1050 nm; △, 800–1050 nm (1% propan-1-ol standard included); and ●, 800–946 nm. The solid line represents the ideal regression line ($y = x$)

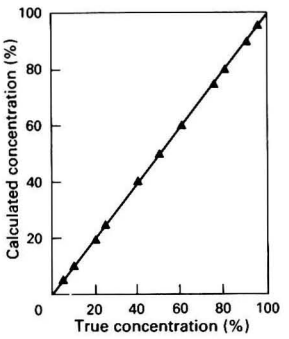

Fig. 4 Accuracy of MCA on toluene–heptane mixtures. The calculated toluene concentrations are plotted. The solid line represents the ideal regression line ($y = x$)

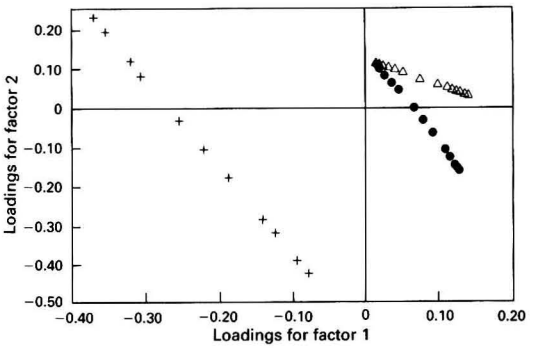

Fig. 5 Projection in factor 1/factor 2 plane, of the PCR results. +, Toluene–cyclohexane; △, propan-1-ol–ethanol; and ●, propan-1-ol–1,4-dioxane. The first differential was taken before the analysis. Four factors were used

Steps can be taken to improve a bad fit (*e.g.*, by restricting the wavelength range considered, as with the alcohols, see under Dilutions in CCl_4), but it is necessary to decide the extent to which this is reasonable. A persistently poor fit indicates that the sample is incompatible with the standards selected.

Principal component regression

The NNIR spectra are also suitable for analysis by PCR. The spectra of two-component mixtures are separated into well defined clusters in factor space, as shown in Fig. 5. Here, the clusters have degenerated into lines as the data cover wide concentration ranges. The end of a line corresponds to 95% concentration of one of the components. Note the near-coincidence of two of the lines at one end: this occurs where the mixtures both contain 95% propan-1-ol.

It is also possible to construct a quantitative model within the PCR software. This requires more work than with the MCA in order to build a set of calibration spectra. The spectra of 0.05–100% propan-1-ol in CCl_4 were examined in this way. The process yielded two factors: factor one with an eigenvalue of 0.2829 and factor two 0.0024. The former correlates well with the concentration ($r = 0.999$, relative standard deviation = 0.7%). Factor 2 improves the concentration prediction for very weak solutions (relative standard deviation = 0.6%) where the OH peak is dominant in the spectrum (see under Dilutions in CCl_4). It describes the evolution of intermolecular interactions with the alcohol concentration.

Conclusions

Spectrometry in the NNIR region (800–1050 nm) is suitable for routine industrial quality control. The NNIR spectra are readily measured using silicon diode arrays, and time-consuming sample preparation is eliminated as the absorbance values are low.

Unlike NIR spectra, NNIR spectra of organic liquids contain distinct bands. The simple, rapid MCA algorithm is applicable and delivers quantitative and qualitative information simultaneously. For liquids with no intermolecular interactions, this method can be applied directly to the entire NNIR spectrum. It is also possible to study substances such as alcohols in non-polar solvents if the interactions are taken into account.

The NNIR spectra are also suitable for qualitative analysis by PCR. Distinct clusters are formed in factor space by the spectra of the different substances investigated. Construction of a quantitative model with this algorithm is also possible, but requires a calibration set of many spectra. Similarly, more complex algorithms are also available.

It is hoped to improve the present system further by stabilizing the sample temperature. The use of cells with longer optical pathlengths should improve the signal-to-noise ratio, although it might be necessary to extend the stabilization time to allow for the greater turbulence.

References

1 Gemperline, P. J., and Weber, L. D., *Anal. Chem.*, 1989, **61**, 138.
2 Brown, C. W., Lynch, P. F., Obremski, R. J., and Lavery, D. S., *Anal. Chem.*, 1982, **54**, 1472.
3 Perkampus, H. H., *UV-VIS-Spektroskopie und ihre Anwendungen*, Springer-Verlag, Berlin, 1986.
4 Fuller, M. P., Ritter, G. L., and Draper, C. S., *Appl. Spectrosc.*, 1988, **42**, 217.
5 Valser, P. E., and Bartels, H., *Am. Lab.*, 1982, **12**(2), 32.
6 Shinomiya, K., and Shinomiya, T., *Bull. Chem. Soc. Jpn.*, 1990, **63**, 1093.
7 Kunst, M., van Duijn, D., and Bordewijk, P., *Ber. Bunsenges. Phys. Chem.*, 1979, **83**, 840.

Paper 1/06422C
Received December 23, 1991
Accepted June 9, 1992

Spectrophotometric Enzyme-amplified Immunoassay for Thyroid Stimulating Hormone

Robert Wilson
Research Centre for Advanced Science and Technology, University of Tokyo, Tokyo, Japan

Thyroid stimulating hormone (TSH) regulates the function of the thyroid gland. Its determination at low concentrations in serum is useful in the diagnosis of hyperthyroidism. In this paper, it is detected using a spectrophotometric enzyme-amplified immunoassay. The reporter enzyme is alkaline phosphatase and its substrate is flavin adenine dinucleotide phosphate (FADP). Reaction with alkaline phosphatase converts FADP into flavin adenine dinucleotide (FAD), which, unlike FADP, re-activates apo-D-amino acid oxidase (apo-AOD). Re-activation of apo-AOD allows the product of the reporter enzyme to be amplified. The lower limit of detection for TSH by this method is 0.06 μU cm^{-3}. This compares with 0.54 μU cm^{-3} for an identical assay in which *p*-nitrophenyl phosphate was the substrate for alkaline phosphatase. Contaminating alkaline phosphatase was removed from the reagents by affinity chromatography.

Keywords: *Enzyme-amplified immunoassay; thyroid stimulating hormone; flavin adenine dinucleotide phosphate; apo-D-amino acid oxidase; affinity chromatography*

Enzyme amplification has been used to enhance the speed and sensitivity of various analytical techniques.[1–6] In these systems the substrate is either the analyte or a compound present at a concentration proportional to that of the analyte. It is cycled enzymically to increase the amount of a detectable product. In the enzyme-amplified immuno-assisted assay described by Self,[1] for example, the analyte is placental alkaline phosphatase (PLAP). This is used to dephosphorylate NADP and produce a stoichiometric amount of NAD. The NAD is cycled between alcohol dehydrogenase and diaphorase to produce a coloured dye. The amount of dye produced can be related to the concentration of PLAP by reference to a calibration graph.

In this paper, an enzyme-amplification system based on phosphorylated flavin adenine dinucleotide (FADP) is described. Flavin adenine dinucleotide (FAD) is the coenzyme of D-amino acid oxidase (AOD). The coenzyme can be removed to yield apo-AOD.[7] Removal of FAD is reversible and re-activation of the apo-enzyme has been used in sensitive assays to detect the coenzyme.[7,8] If FAD is phosphorylated it is unable to re-activate apo-AOD. Treatment with alkaline phosphatase, however, converts it into FAD. Therefore, FADP and apo-AOD can be used to detect alkaline phosphatase according to the scheme shown in Fig. 1. In the work described here, FADP was prepared by phosphorylating FAD with orthophosphoric acid. It was then used in an enzyme-amplified immunoassay for thyroid stimulating hormone (TSH) in which alkaline phosphatase was the enzyme label.

Experimental

Materials

D-Amino acid oxidase (AOD; E.C. 1.4.3.3) Type I from porcine kidney, alkaline phosphatase (E.C. 3.1.3.1) {4000 DEA units per milligram of enzyme protein [1 DEA (diethanolamine) unit is the amount of alkaline phosphatase that will hydrolyse 1 μmol of *p*-nitrophenyl phosphate per minute at 37 °C, in DEA buffer (1 mol dm^{-3}) that also contains *p*-nitrophenyl phosphate (15 mmol dm^{-3}) and magnesium chloride (0.5 mmol dm^{-3})]} from bovine intestinal mucosa, peroxidase (POD; E.C. 1.11.1.7) Type II from horseradish, FAD, L-histidyldiazobenzylphosphonic acid attached to agarose, eight-channel multiple pipettes and the enzyme-immunoassay kit for TSH (Catalogue No. SIA 120-A) were all obtained from Sigma (St. Louis, MO, USA). The immunoassay kit contained the following components: microtitre plates with immobilized antibodies to TSH, conjugate solution (antibodies to TSH labelled with alkaline phosphatase), TSH solution (12 μU cm^{-3} cross-standardized to a World Health Organization primary standard), diluent for the TSH solution (the diluent was pH 7.5 buffered protein solution that contained a surfactant and 0.1% sodium azide as a preservative), and a buffered surfactant wash solution. These components were used in all the immunoassays. All other reagents were of the highest grade commercially available. The plate reader was from Tosoh (Tokyo, Japan). The plate shaker was from Scientific Industries (Bohemia, NY, USA).

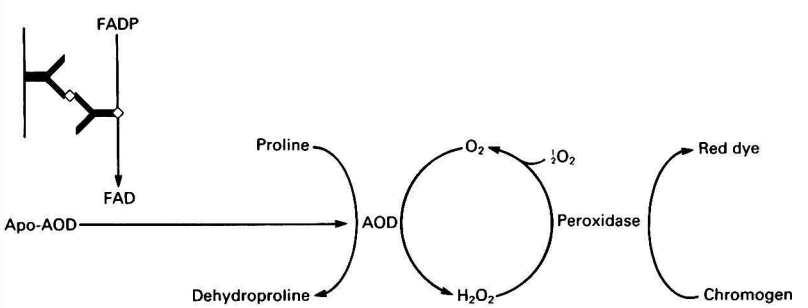

Fig. 1 Schematic representation of enzyme amplified immunoassay for TSH

General Methods

Alkaline phosphatase-free peroxidase was prepared by the method of Landt *et al.*[9] for phosphatase removal rather than purification; it was used in all assays involving FADP. Alkaline phosphatase solutions were prepared by diluting the commercial solution with 0.1 mol dm^{-3} tris(hydroxymethyl)methylamine (Tris) buffer (pH 9.5) that contained bovine serum albumin (BSA) (10 g dm^{-3}), Triton X-100 (0.5 g dm^{-3}), D-proline (50 mmol dm^{-3}), dihydroxybenzenesulfonic acid (DHBS) (5 mmol dm^{-3}) magnesium nitrate (1 mmol dm^{-3}) and zinc nitrate (0.1 mmol dm^{-3}). Bovine serum albumin and Triton X-100 helped to prevent adsorption of alkaline phosphatase on the walls of the container. The molarity of alkaline phosphatase in these solutions was based on a relative molecular mass of 140 kDa[10] and the assumption that all protein (biuret) in the commercial material was alkaline phosphatase. All buffer solutions were adjusted to the correct pH at 25 °C and all work was carried out at this temperature. The limit of detection, where calculated, was taken as the analyte concentration equivalent to twice the standard deviation of eight zero calibrators.

Preparation of Apo-AOD

Two methods were used to prepare apo-amino acid oxidase (apo-AOD). The first method has been described by Decker and Hinkkanen.[7] In the second method, AOD (10 mg) dissolved in 5 cm^3 of 10 mmol dm^{-3} buffer (pH 8.5) was dialysed against 3 × 250 cm^3 of 0.1 mol dm^{-3} Tris buffer (pH 8.5) that contained potassium bromide (1 mol dm^{-3}) and ethylenediaminetetraacetic acid (EDTA) (5 mmol dm^{-3}) for a total of 36 h at 4 °C in darkness, and then against 3 × 250 cm^3 of 0.1 mol dm^{-3} Tris buffer (pH 8.5) for 36 h at 4 °C in darkness.

Standardization of Apo-AOD

Apo-amino acid oxidase was diluted 1 + 9 with 0.1 mol dm^{-3} Tris buffer (pH 8.5) that contained 4-aminoantipyrine (4AP) (0.5 mmol dm^{-3}). Solutions of FAD (0–10 μmol dm^{-3}) were prepared in 0.1 mol dm^{-3} Tris buffer (pH 9.5). This buffer contained D-proline (50 mmol dm^{-3}), DHBS (5 mmol dm^{-3}), POD (0.1 mg cm^{-3}), magnesium nitrate (1 mmol dm^{-3}) and zinc nitrate (0.1 mmol dm^{-3}). The apo-AOD solution (100 mm^3) and FAD solution (100 mm^3) were added to the wells of a microtitre plate. After 10 min the absorbance was measured at 492 nm.

Stability of Apo-AOD *versus* pH

The apo-AOD solution was dialysed against 1 dm^3 of de-ionized water for 24 h. It was then diluted 1 + 9 with buffer solutions (10 mmol dm^{-3}) that contained 4AP (0.5 mmol dm^{-3}). In the pH range 3–5 the buffer solution was sodium citrate, in the range 6–8 sodium phosphate and in the range 9–10 sodium carbonate. The apo-AOD solutions were maintained at a temperature of 25 °C for 24 h in darkness. During this time they were assayed for activity after 0, 4, 8 and 24 h, by mixing them with 0.1 mol dm^{-3} Tris buffer (pH 8.5), that contained POD (0.1 mg cm^{-3}), D-proline (50 mmol dm^{-3}), DHBS (5 mmol dm^{-3}) and FAD (10 μmol dm^{-3}).

Re-activation of Apo-AOD *versus* pH

The apo-AOD was diluted 1 + 9 with de-ionized water that contained 4AP (0.5 mmol dm^{-3}). The rate of re-activation was determined by mixing apo-AOD solution (100 mm^3) and buffer solution (100 mm^3) in the wells of a microtitre plate. Buffer solutions in the pH range 7.0–9.5 contained Tris (0.2 mol dm^{-3}), FAD (100 nmol dm^{-3}), POD (0.1 mg cm^{-3}), D-proline (50 mmol dm^{-3}) and DHBS (5 mmol dm^{-3}). The amount of colour development was measured after 60 min.

Preparation of FADP

This was prepared according to the method described by Wilson.[11] A 50 mg amount of FAD was added to 2 cm^3 of anhydrous dimethyl sulfoxide, the mixture was sonicated to dissolve the FAD, and the solvent was evaporated under vacuum at 30–40 °C. Orthophosphoric acid (1 mol dm^{-3}) in dimethyl sulfoxide (100 mm^3) and *N*,*N*-diisopropylethylamine (200 mm^3) were then added, with sonication. Next, 100 mm^3 of trichloroacetonitrile were added to the solution, followed by further sonication. After 20 min the reaction was terminated by addition of glacial acetic acid to a final concentration of 50% v/v. The product was loaded onto a column packed with diethylaminoethyl (DEAE)-cellulose equilibrated with 50% v/v aqueous acetic acid. Monophosphate derivatives of FAD were eluted with a gradient of 100–400 mmol dm^{-3} ammonia in 50% v/v aqueous acetic acid. The eluate was dried by rotary evaporation at 30 °C and stored at −20 °C.

Determination of the FAD Liberated From FADP

Alkaline phosphatase converts FADP into FAD by acting as a phosphatase, but this enzyme also has a low level of phosphodiesterase activity.[12] This results in cleavage of FAD and renders the coenzyme unable to re-activate apo-AOD. When determining the amount of FAD that can be liberated from a given amount of FADP, therefore, it is important to keep the phosphodiesterase activity to a minimum. This entails using a small amount of alkaline phosphatase. It is also important to use a low concentration of substrate to ensure that orthophosphate released during the reaction does not inhibit alkaline phosphatase.

Assuming that FADP had the same molar absorption coefficient as FAD ($\varepsilon = 11.3\ dm^3\ mmol^{-1}\ cm^{-1}$)[7] a 1 μmol dm^{-3} solution was prepared in 0.1 mol dm^{-3} Tris buffer (pH 9.5). This buffer also contained POD (0.1 mg cm^{-3}), D-proline (50 mmol dm^{-3}), DHBS (5 mmol dm^{-3}), magnesium nitrate (1 mmol dm^{-3}) and zinc nitrate (0.1 mmol dm^{-3}). The FADP solution was mixed 1 + 1 with an alkaline phosphatase solution (0.1 DEA units cm^{-3}) made up in the same buffer. At zero time, and at 10 min intervals thereafter, aliquots were assayed for FAD by mixing them 1 + 1 with apo-AOD prepared in 0.1 mol dm^{-3} pyrophosphate buffer (pH 8.5) that contained 4AP (0.5 mmol dm^{-3}). The amount of FAD present was determined, with use of the plate reader, at 492 nm, with reference to a calibration graph. The experiment was continued for 90 min, *i.e.*, until the amount of FAD remained constant for five successive measurements.

Stability of FADP

The stability of FADP in solution was investigated at 4 and 25 °C. The FADP was dissolved in 0.1 mol dm^{-3} Tris buffer (pH 8.5) to a concentration of 50 μmol dm^{-3} ($\varepsilon_{450} = 18.0\ dm^3\ mmol^{-1}\ cm^{-1}$). This buffer also contained 4AP (0.5 mmol dm^{-3}). At appropriate intervals, this solution was assayed for FAD as described previously.

Removal of Phosphatase from Apo-AOD

Contaminating phosphatase was removed from apo-AOD by the method of Landt *et al.*[9] for phosphatase removal rather than purification. The apo-AOD (1 cm^3) was loaded dropwise onto a column packed with L-histidyldiazobenzylphosphonic acid agarose (1 cm^3 of gel in an 8 mm i.d. column). Phosphatase-free AOD was eluted with 0.1 mol dm^{-3} Tris buffer (pH 8.5) and collected in a volume of 5 cm^3. To this was added 4AP to a final concentration of 1 mmol dm^{-3}.

Effect of FADP on the Re-activation of apo-AOD by FAD

The apo-AOD solution was used for the assay for FAD in the range 0–250 nmol dm^{-3} in the presence of FADP at a final concentration of 25 μmol dm^{-3}, according to the method for standardization of apo-AOD that has already been described. The results were compared with the amount of colour development observed in the absence of FADP.

Optimization of FADP Concentration

In an assay for alkaline phosphatase the final FADP concentration was varied between 0 and 50 μmol dm^{-3}. The apo-AOD–AP solutions were diluted 1 + 1 with FADP solutions made up in 0.1 mol dm^{-3} Tris buffer (pH 8.5) immediately prior to the assay. The product (apo-AOD–FADP solution) was then mixed 1 + 1 with a 2 pmol dm^{-3} alkaline phosphatase solution (100 mm^3) and the amount of colour development after 1 h was measured.

Re-activation of Apo-AOD by Alkaline Phosphatase *versus* pH

The apo-AOD–FADP solution was prepared as described previously except that FADP was dissolved in, and the apo-enzyme was eluted from the affinity column with, de-ionized water. The rate of re-activation was determined by mixing apo-AOD–FADP solution (100 mm^3) and 2 pmol dm^{-3} phosphatase (100 mm^{-3}) in the pH range 7.0–9.5. The extent of colour development after 1 h was measured.

Assay for Alkaline Phosphatase

Alkaline phosphatase was assayed in the range 0–1 pmol dm^{-3}. To each well of a microtitre plate was added 100 mm^3 of alkaline phosphatase solution and 100 mm^3 of apo-AOD–FADP solution prepared as described previously. The plate was then covered with aluminium foil. After 1 h the absorbance of the solutions in the wells was measured at 492 nm with reference to a reagent blank that contained no D-proline. For comparison, identical amounts of alkaline phosphatase were assayed in 0.1 mol dm^{-3} diethanolamine buffer (pH 9.8) with *p*-nitrophenyl phosphate (10 mmol dm^{-3}) as the substrate. This buffer also contained magnesium nitrate (1 mmol dm^{-3}) and zinc nitrate (0.1 mmol dm^{-3}). The absorbance was measured at 405 nm.

Immunoassay for TSH

Solutions of TSH (100 mm^3) in the range 0–5 μU cm^{-3} were added to the wells of a microtitre plate coated with antibodies to TSH. The plate was then covered with plastic cling film and gently shaken at room temperature for 1 h. At the end of this time the wells were washed out five times with a buffered surfactant solution. After each wash, the plate was inverted and vigorously blotted against a clean paper towel to remove as much of the wash solution as possible. After washing, an alkaline phosphatase-labelled antibody solution (100 mm^{-3}) was added to the wells of the plate. It was then incubated for 1 h and washed as described previously. After washing, the extent of colour development associated with known amounts of TSH was measured as described for the alkaline phosphatase assay except that the concentration of apo-AOD was increased by a factor of ten, the FADP was made up in the POD–proline–DHBS solution, and the extent of colour development was measured after 30 min. During this time the plate was gently shaken. For comparison, an immunoassay in which nitrophenyl phosphate was the substrate was carried out as in the alkaline phosphatase assay except that the plate was gently shaken and colour development was measured after 30 min.

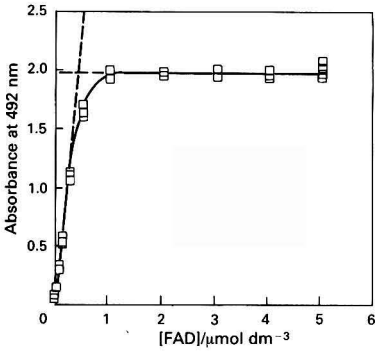

Fig. 2 Standardization of apo-AOD. The graph was extrapolated as shown and the binding molarity taken as the FAD concentration at the point where the lines crossed (230 nm). This was multiplied by the dilution factor (1 + 19) to find the binding molarity of the original solution (4.6 μmol dm^{-3})

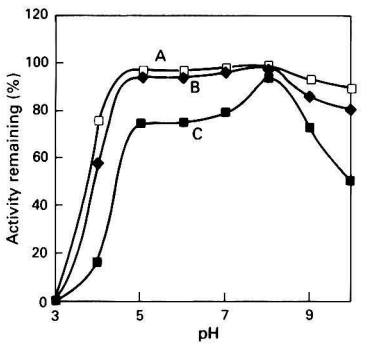

Fig. 3 Variation of the stability of apo-AOD with pH at 25 °C. A, 4; B, 8; and C, 24 h

Results and Discussion

Apo-AOD

The method used to prepare apo-AOD is based on that of Decker and Hinkkanen.[7] In the original method, sodium pyrophosphate buffer was used instead of Tris. The latter buffer was used in this work because the apo-AOD is used to detect alkaline phosphatase in an immunoassay. In this assay, sodium pyrophosphate, itself a substrate for alkaline phosphatase, would act as a competitive inhibitor, but Tris promotes the reaction by acting as a transphosphorylating agent.[13]

The apo-AOD was standardized by plotting absorbance at 492 nm against FAD concentration, as shown in Fig. 2. The lower limit of detection for FAD was 4.3 nmol dm^{-3}. The binding molarity was found by extrapolation, as shown in the diagram. Typically, apo-AOD prepared in Tris buffer had a binding molarity of 4.6 μmol dm^{-3} prior to dilution. The amount of residual FAD was 46 nmol dm^{-3} (about 1% of the binding molarity). The apo-AOD prepared in sodium pyrophosphate buffer solution had a lower binding molarity of about 3.7 μmol dm^{-3}. The amount of residual FAD in this material was also about 1% of the binding molarity.

A plot of percentage activity remaining *versus* pH is shown in Fig. 3 from which it can be seen that the apo-enzyme has maximum stability at about pH 8.0. In this work a slightly higher pH (8.5) was used to facilitate comparison with previous work in this area. Investigation of the stability in 0.1 mol dm^{-3} Tris buffer at this pH showed that there was no detectable loss of activity after 8 h at 25 °C or 1 week at 4 °C.

FADP

The average yield of FADP was about 18% m/m. A solution with an absorbance of 1.0 at 450 nm in 0.1 mol dm^{-3} Tris buffer (pH 8.5) contained enough FADP to yield a 56 μmol dm^{-3} solution of FAD after treatment with alkaline phosphatase. Therefore, a molar absorption coefficient of 18 dm^3 $mmol^{-1}$ cm^{-1} was assigned to it. The extent of colour development observed when FAD was assayed in the presence of FADP (50 μmol dm^{-3}) was only 50% of that observed in the absence of FADP. This indicates that FAD must compete with FADP for the binding site of apo-AOD. Taking into account the molar absorption coefficient and the 50% decline in colour development, the amount of FAD present in the material, as a percentage of FADP, was calculated to be 0.02%. When an aqueous solution of FADP (50 μmol dm^{-3}) was stored at 25 °C for 8 h no hydrolysis to FAD could be detected. After 1 week at 4 °C, however, some hydrolysis (about 1%) did occur.

Assays for Alkaline Phosphatase and TSH

The optimum concentration of FADP in assays for alkaline phosphatase was about 20 μmol dm^{-3}, as shown in Fig. 4. At concentrations in excess of 25 μmol dm^{-3} the extent of colour development decreases, presumably because FADP interferes with the re-activation of apo-AOD by FAD. A plot of colour development *versus* pH for the re-activation of apo-AOD by alkaline phosphatase acting on FADP is shown in Fig. 5. This indicates that the optimum pH is about 9.0, slightly higher than the optimum pH for the re-activation of apo-AOD by FAD, which is about pH 8.5. In the alkaline phosphatase assay this pH was attained by mixing equal volumes of pH 8.5 and pH 9.5 Tris buffer solutions. A plot of colour development *versus* alkaline phosphatase concentration is shown in Fig. 6. The lower limit of detection for alkaline phosphatase was 12 fmol dm^{-3} (2.5 amol of phosphatase per well). The lower limit of detection with nitrophenyl phosphate as the substrate was 160 fmol dm^{-3}.

When alkaline phosphatase was not removed from the apo-enzyme the background absorbance was about 1.0 after 10 min. If the background absorbance increases at a rate per hour of more than 0.2 relative to a reagent blank the apo-AOD should be passed through the affinity column again. When the plate was not covered in aluminium foil there was a slow increase in the background absorbance owing to photoreduction of FADP followed by the formation of hydrogen peroxide (this also occurs with other flavins such as FAD and is not peculiar to FADP). As a result, the background absorbance after 1 h in a well-lit laboratory is more than double that observed when light is excluded. This leads to an increase in the noise-to-signal ratio and a slight decline in the lower limit of detection.

The concentration of apo-AOD used in the TSH immunoassay was ten times greater than that used in the alkaline phosphatase assay in order to extend the range over which TSH could be detected. A plot of colour development *versus* TSH concentration is shown in Fig. 7. The lower limit of detection for TSH in the amplified immunoassay was 0.06 μU cm^{-3}. The precision of the assay was good [relative standard deviation (RSD) <10%] for all concentrations of TSH that were assayed. The limit of detection with nitrophenyl phosphate as the chromogen was 0.54 μU cm^{-3} (RSD <10% for all concentrations of TSH assayed). For comparison, Obzansky *et al.*,[14] who used an amplifier based on FADP

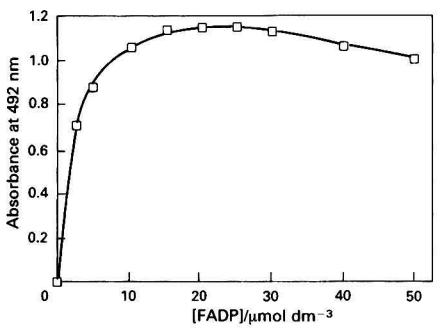

Fig. 4 Effect of FADP concentration on the amount of colour development in the presence of picomolar concentrations of alkaline phosphatase

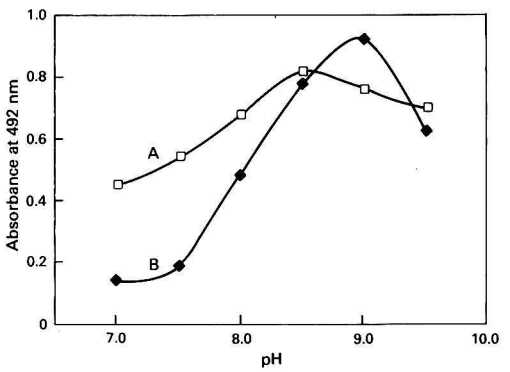

Fig. 5 Variation of the rate of re-activation with pH. A, Re-activation by FAD; and B, re-activation by alkaline phosphatase acting on FADP

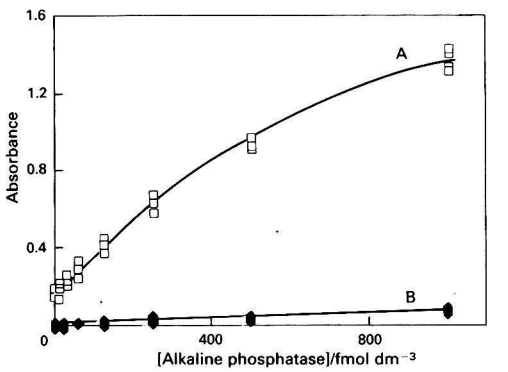

Fig. 6 Alkaline phosphatase assay. A, FADP assay; and B, nitrophenyl phosphate assay

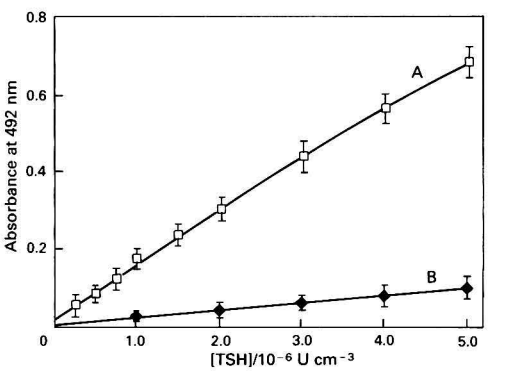

Fig. 7 TSH immunoassay. Error bars are equivalent to ±1 SD of the mean (n = 6). A, FADP assay; and B, nitrophenyl phosphate assay

in conjunction with a releasable-linker immunoassay for TSH, reported a limit of detection that could have been in the range 0.05–0.1 μU cm^{-3}.

Conclusion

The enzyme amplification system described here can be used to enhance the sensitivity or decrease the time required to carry out immunoassays. The main obstacle encountered in bringing this work to a successful conclusion was the removal of contaminating alkaline phosphatase from the reagents. If this is not done the noise-to-signal ratio is unacceptably high. As yet, the full potential of the amplification system described here has not been realized. In the present study it has been used with a chromophore, which, compared with certain other POD substrates, has a low molar absorption coefficient. It was chosen because, unlike them, it has an absorbance spectrum that does not overlap with that of FADP and because it is stable at the appropriate pH. As an alternative, however, it is possible to detect the hydrogen peroxide produced by AOD luminometrically.[7] This results in a significant improvement in sensitivity and will be the subject of a subsequent paper.

This work was supported by the Japan Society for the Promotion of Science. This support is gratefully acknowledged.

References

1 Self, C. H., *J. Immunol. Methods*, 1985, **76**, 389.
2 Habron, S., Eggelte, H. J., and Rabin, B. R., *Anal. Biochem.*, 1991, **198**, 47.
3 Bates, D. L., *Trends Biotechnol.*, 1987, **5**, 204.
4 Cardosi, M. F., Birch, S. W. B., Smith, B. M., and Johannsson, A., *Electroanalysis*, 1989, **1**, 297.
5 Scheller, F., Siegbahn, N., Danielsson, B., and Mosbach, K., *Anal. Chem.*, 1985, **57**, 1740.
6 Kirstein, D., Danielsson, B., Scheller, F., and Mosbach, K., *Biosensors*, 1989, **4**, 231.
7 Decker, K., and Hinkkanen, A., in *Methods of Enzymatic Analysis*, ed. Bergmeyer, H. U., VCH, Weinheim, 3rd edn., 1985, vol. 7.
8 DeLuca, C., Weber, M. M., and Kaplan, N. O., *J. Biol. Chem.*, 1956, **223**, 559.
9 Landt, M., Boltz, S. C., and Butler, L. G., *Biochemistry*, 1978, **17**, 915.
10 Keesey, J., *Biochemica Information*, Boehringer Mannheim Biochemicals, IN, USA, 1987, p. 8.
11 Wilson, R., Ph.D. Thesis, Cranfield Institute of Technology, UK, 1990.
12 Daniel, H., Binninger, E., and Rehner, G., *Int. J. Vitam. Nutr. Res.*, 1983, **53**, 109.
13 Chappelet-Tordo, D., Fosset, M., Iwatsubo, M., Gache, C., and Lazdunski, M., *Biochemistry*, 1974, **13**, 1789.
14 Obzansky, D. M., Rabin, B. R., Simons, D. M., Tseng, S. Y., Severing, D. M., Eggelte, H., Fischer, M., Habron, S., Stout, R. W., and Di Paolo, M. J., *Clin. Chem. (Winston-Salem, N.C.)* 1991, **37**, 1513.

Paper 2/01842J
Received April 7, 1992
Accepted June 1, 1992

Column Dead-time Determination Methods Based on the Isothermal Retention-time Behaviour of a Homologous Series in Chromatography

Paddy Fleming
Regional Technical College, Ballinode, Sligo, Ireland

In this paper, the theory of chromatographic retention behaviour of the members of a homologous series is tested, which is based on the hypothesis that the ratio of the adjusted retention times of any two consecutive members of any homologous series in an isothermal column is constant. The paper shows how the dead time of a column can be calculated from the slope and intercept of a linear graph of the gross retention times of the $n + 1$th homologue members *versus* the gross retention times of the nth homologue members, and a method is outlined whereby equal weighting can be given to all the experimental retention times of the homologue members used in the said plot.

Keywords: *Chromatography; retention time; dead time; homologue*

The gross retention time, t_R, of a solute in chromatography, although it is directly observable, is of little interest in itself because it is the sum of two time intervals that are not directly observable. The two time intervals in question are the time a solute spends in the mobile phase (t_m) and the time a solute spends in the stationary phase (t'_R). The latter time interval, which is referred to as the adjusted or net retention time, is of greater interest to chromatographers. However, it cannot be determined unless t_m, which is referred to as the dead time of the column, is known. The isothermal gross chromatographic retention times ($t_{R,n}$), of at least three consecutive members of a homologous series have been exploited to calculate, using various mathematical methods, the dead time of a column, and hence, the adjusted retention time, $t'_{R,n}$, of each homologue member was determined. The subscript 'R' which denotes retention, will henceforth be omitted from the text. The sole directly observable fact, as noted by Sevcik and Lowentap[1] is that the ratio of the differences between the gross retention times of any three consecutive homologous members, t_n, t_{n-1} and t_{n-2}, is a constant, *i.e.*,

$$(t_n - t_{n-1})/(t_{n-1} - t_{n-2}) = \text{constant} > 1 \qquad (1)$$

where n refers to the carbon number of a homologue member. It follows from the above experimentally observed fact that the ratio of the differences between the net retention times of any three consecutive members of a homologous series, t'_n, t'_{n-1} and t'_{n-2}, is also equal to the same constant in eqn. (1), as $t_n = t'_n + t_m$. Consider a hypothetical homologue member of zero carbon number having a gross retention time, t_0, greater than t_m. The time t_0 is equivalent to the 'real' column dead time, introduced by Smith *et al.*[2] Fig. 1 shows a simulated chromatographic separation of the first three members of such a homologous series. The net retention time, t'_0, of the hypothetical zero carbon number homologue is equal to the 'd' term introduced into eqn. (18) in the paper by Smith *et al.*[2]

If, as Parcher and Johnson[3] showed, the inert gases are retained in gas–liquid chromatography (GLC), albeit in small amounts, then the mathematical dead-time calculation, based on the gross retention times of at least three consecutive members of a homologous series, is the only estimate available of the time solute components spend in the mobile phase. However, the caveat must be acknowledged, according to Sharples and Vernon,[4] that a slight error in the gross retention of the mid-component of a set of three closely spaced homologue members will cause a large consequential error in the mathematical dead time.

The dead-time calculations of Touabet *et al.*[5] on alkane retention times in GLC are based on an iterative method by Wentworth.[6] Touabet *et al.*[5] established that the experimental gross retention time of methane was significantly higher than the mathematical dead time of the column. Smith *et al.*[7] investigated higher (than linear) degree polynomial fits between the logarithm of the adjusted retention time and carbon number in order to obtain improved accuracy, only to find the results more difficult to interpret. Tarjan *et al.*[8] concluded that, if accurate retention times had been available then, the simple mathematical method, involving three consecutive alkanes, would have been as good as the more complicated computerized statistical and iterative methods.

Wainwright *et al.*[9] investigated the retention behaviour of the homologous series of alkylbenzenes in reversed-phase high-performance liquid chromatography (RP-HPLC) and in GLC, and found the mathematical dead times thereby calculated to be satisfactory for the RP-HPLC columns and unsatisfactory for the varying-polarity GLC columns. Ashes *et al.*[10] found no statistical difference between the average dead times calculated from four homologous series on each of four GLC stationary phases. Haken *et al.*[11] observed that mathematical dead-time calculations were more affected by small changes in the retention times of alkanes than by the method of calculation. Wainwright *et al.*[12] concluded that the mathematical dead-time estimate, based on the retention times of alkane homologues, was more accurate than the retention time of methane. Wainwright *et al.*[12] also found that the retention time of methane was always greater than the mathematical dead time and that there was excellent agreement between the observed retention time for methane and

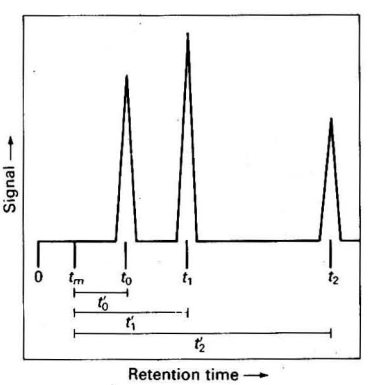

Fig. 1 Gross retention times of the first three members of a homologous series, $n = 0, 1, 2$, are shown. The dead time is not shown as a peak because it arises from a calculation on the gross retention times

the retention time for methane calculated from the observed retention times of the C_5–C_9 alkanes on the assumption that a linear relationship existed between the logarithm of the net retention time and the number of carbon atoms for the alkane homologous series.

Vernon and Suratman[13] warned that sample size and composition could influence retention times in computerized GLC techniques. Overaa[14] discussed a Fibonacci-based search process to find a value for t_m (based on retention times, t_n, of selected members of a homologous series) that minimized the number of individual regression analyses necessary to provide the best straight-line fit between $\ln(t_n - t_m)$ and n, thereby maximizing the relative standard deviation (r^2).

The definition of dead time in liquid chromatography (LC) and hence its determination is less straightforward. Alhedai *et al.*[15] defined two dead times in HPLC, *i.e.*, the 'kinetic' dead time being the solute time in the mobile phase, which is assumed to occupy all the interstitial volume in the column, and the 'thermodynamic' dead time, which assumes that part of the interstitial volume contains static mobile phase, which does not contribute to retention. Levin and Grushka[16] calculated the dead time of an RP-HPLC column by using directly determined capacity ratios and the retention times of various systems' peaks and found the calculated dead times to be equal to or greater than the retention time of 'non-retained' peaks. Daignault *et al.*[17] proposed a method to approach a limiting value for dead time in HPLC, which involved injecting about 10^{-9} mol of a simple inorganic anion onto a reversed-phase column with a simple methanol–water mobile phase and using the resulting retention time to calculate the void volume of the column; hence, its dead time could be known for any given carrier flow rate. Montes *et al.*[18] determined the void volume for a given column–mobile phase system from the experimental retention volumes of a homologous series of compounds, for which there was a free energy correlation between the distribution coefficients and the carbon numbers for each member of the homologous series. van Tulder *et al.*[19] evaluated and generalized the method of Grobler and Balizs[20] for the calculation of the dead time in HPLC. The Grobler and Balizs method was proposed for the isothermal retention data from consecutive homologues, whereas van Tulder *et al.* generalized the same method for homologues that are separated by equidistant carbon numbers. The Grobler and Balizs method requires two consecutive linear regressions to be excecuted before the dead time can be calculated. van Tulder *et al.* suggested guidelines for the optimum selection of both the homologues and the number of homologues, which afforded the most precise value for the dead time. Margarit-Roig *et al.*[21] suggested a dead-time method based on observing the retention time of 2,4-dinitrophenylhydrazine, chromatographed on a chemically bonded-phase RP-HPLC column, as a function of the percentage of water in the mobile phase. Krstulovic *et al.*[22] found that the dead time in RP-HPLC depended on mobile-phase composition and on the molecular size of the solute used, and that all the homologous series studied yielded linear log t'_n *versus* n plots of constant slope. Smith *et al.*,[23] having reviewed the various dead-time methods in LC, suggested that the conventional mathematical treatment of the retention data for a homologous series could become as commonly adopted a dead-time determination method as in gas chromatography.

In this paper, a general theory of the isothermal retention behaviour of the members of a homologous series in GLC is presented. The theory is based on the testable hypothesis that the ratio of the adjusted isothermal retention times of any two consecutive members of a homologous series is constant. In the paper the hypothetical zero carbon-number member of the homologous series, which was originally introduced by Smith *et al.*,[2] is used, but it associates with it a gross retention time that is greater than t_m. The dead time of a column is calculated from the characteristics of a linear graph of the gross retention time of the $n + 1$th homologue member *versus* the gross retention time of the nth homologue member, and a method is outlined whereby equal weighting is given to all the experimental retention times of the homologue members used in the said plot.

Derivation of Experimental Quantities

The dependence of the net retention time of a homologue member on its carbon number is assumed to be such that the constant value for the ratio in eqn. (1) ensues. It is observed in the isothermal chromatographic separation of a homologous mixture that the spacing between consecutively eluted members increases with increasing carbon number. If it is assumed that the ratio of the net retention times of any two consecutive members of the homologous series is constant, R, and is greater than unity and that the net retention time of the hypothetical $n = 0$ homologue member is finite, *i.e.*, $t'_0 > 0$, then

$$t'_n/t'_{n-1} = t'_{n-1}/t'_{n-2} = \ldots\ldots = t'_2/t'_1 = t'_1/t'_0 = R > 1 \quad (2)$$

It can be seen from eqn. (2) that

$$t'_n = t'_0 R^n \quad (3)$$

Eqn. (3), where t'_n increases geometrically with n, is equivalent to the standard linear relationship between the logarithm of the net retention time and the carbon number of a homologue member, as

$$\log_{10} t'_n = \log_{10} t'_0 + n \times \log_{10} R = A + n \times B \quad (4)$$

where A ($= \log_{10} t'_0$) and B ($= \log_{10} R$) are constants.

The ratio R, as defined by eqn. (2), is not observed directly because the net retention times are not directly observable. However, eqn. (2) can be re-written as follows:

$$(t'_n/t'_{n-1}) - 1 = (t'_{n-1}/t'_{n-2}) - 1 \quad (5)$$

Eqn. (5) can be simplified to read

$$(t'_n - t'_{n-1})/t'_{n-1} = (t'_{n-1} - t'_{n-2})/t'_{n-2} \quad (6)$$

Eqn. (6) can be further re-arranged to read

$$(t'_n - t'_{n-1})/(t'_{n-1} - t'_{n-2}) = t'_{n-1}/t'_{n-2} = R \quad (7)$$

It can be seen, by comparing eqn. (7) with eqn. (1), that the observable constant defined in eqn. (1) is equal to the constant defined in eqn. (2). An experimental value of R, based on the gross retention times of any three consecutive members of a homologous series, is now available for use in eqn. (3). The net retention time of the $n = 0$ homologue member can be derived as follows. As

$t'_n = t_n - t_m = t'_0 R^n$ and $t'_{n-1} = t_{n-1} - t_m\, t'_0 R^{n-1}$, therefore,

$$t'_0 = (t_n - t_{n-1})/(R^n - R^{n-1}) \quad (8)$$

Similarly, the net retention time of the xth homologue member is given by

$$t'_x = t'_0 R^x = (t_n - t_{n-1}) R^{x-n+1}/(R - 1) \quad (9)$$

The dead time, t_m, is given by the expression:

$$t_m = t_n - t'_n = t_n - t'_0 R^n = (R t_{n-1} - t_n)/(R - 1) \quad (10)$$

The first Grobler and Balizs regression equation is contained in eqn. (8), *i.e.*, $\ln(t_n - t_{n-1})$ *versus* n. The slope of this graph is $\ln R$ and its intercept is $\ln[t'_0(1 - R^{-1})]$. The gross retention time of every member of the homologous series employed in this first regression is used twice, *i.e.*, these gross retention times are given double weighting, except for the first and the last members, which are used once only. The second Grobler and Balizs regression equation may now be executed as per eqn. (10), *i.e.*, t_n *versus* R^n. The slope of this graph is t'_0 and its intercept is the dead time t_m.

Eqn. (10) is equivalent to that derived by Hansen and

Andresen.[24] The gross retention time of the xth homologue member is given by $t_x = t'_x + t_m$ and is as follows:

$$t_x = [(R^{x-n+1} - 1)t_n - (R^{x-n+1} - R)t_{n-1}]/(R - 1) \quad (11)$$

The net retention times calculated *via* eqns. (8) and (9), and the ratio R calculated *via* eqn. (1) are unaffected by any systematic error that could occur in the measurement of the gross retention times, t_n, $t_n - 1$ and t_{n-2}, involved in the respective calculations, because the systematic error 'cancels out' in the calculations. However, the gross retention times, t_m and t_x, defined in eqns. (10) and (11), respectively are affected by a systematic error in the measurement of the gross retention times. If the observed gross retention times are τ_n, τ_{n-1} and τ_{n-2}, and $t_n = \tau_n + \varepsilon$, *etc.*, where ε is the systematic error, then the calculated dead time, τ_m, is related to the true dead time *via* eqn. (10) as follows:

$$\tau_m = (R\tau_{n-1} - \tau_n)/(R - 1) = [R(t_{n-1} - \varepsilon) - t_n + \varepsilon]/(R - 1) = (Rt_{n-1} - t_n)/(R - 1) - \varepsilon = t_m - \varepsilon \quad (12)$$

Similarly, it can be shown, *via* eqn. (11), that $\tau_x = t_x - \varepsilon$.

Therefore, if all the measured gross retention times of the homologous series are subjected to the same systematic error, then the calculated gross retention times will also be similarly affected, while the calculated net retention times will be unaffected.

Eqn. (10) can also be expressed in another equivalent form as follows:

$$t_n = Rt_{n-1} + (1 - R)t_m \quad (13)$$

Eqn. (13) appears as eqn. (3) in a paper by Berendsen *et al.*[25] and it yields a linear relationship when t_n is plotted against t_{n-1} with a slope of R and an intercept of $(1 - R)t_m$. Note that the gross retention time of every member of the homologous series used in the experiment is plotted twice (first as an abscissa and then as an ordinate) when eqn. (13) is applied, except the first member (used only as an abscissa) and the last member (used only as an ordinate). The dead time is conveniently calculated from the characteristics of the linear plot *via* t_m = intercept/(1 − slope). The characteristic constant of the homologous series, R, is given by the slope of the same linear plot. The single regression required contrasts with the two regressions required for the same data by the Grobler and Balizs method.

The t_0 used in eqn. (3) of the paper by Berendsen *et al.*[25] is not to be confused with the t_0 defined in the introduction.

Experimental

Materials

The experimental data analysed herein were published by Smith *et al.*[26] and appear in the first of three sections in Table 1 of that paper. The data consist of 18 individual isothermal separations of the C_5–C_{10} alkane series on a single column operated with a thermal-conductivity detector. The same data were analysed in Table 3 of a paper by Wainwright and Haken.[27] The gross retention times for a mixture of methane ($n = 1$) and air from 16 injections on the same column under identical conditions, and as given in Table V of ref. 26, are also analysed in this paper. Reference is also made in this paper to the results of Berendsen *et al.*[25]

Analysis

The experimental data of Smith *et al.*[26] yielded a set of 90 coordinate points when plotted according to eqn. (13), and the regression characteristics of the linear plot were slope = 1.832 ± 0.003 and intercept = −45.05 ± 0.36. This indicates a mathematical dead time of t_m(s) = 54.2 ± 0.6. Smith *et al.*[26] calculated t_m, *etc.*, by using the same set of data obtained by each of three methods.[20,28,29] The method of Guardino *et al.*[28] is used to calculate t_m by an iterative method and then to evaluate $\log_{10} R$ and t'_0 *via* a least-squares linear regression. The modified simplex method for non-linear parameter estimation is used to calculate iteratively t_m, $\log_{10}R$ and t'_n *via* an optimization process described by Nelder and Mead.[29] The optimum number of homologues required to obtain the most precise dead time for a given value for slope R is, according to van Tulder *et al.*,[19] given by 1 + 3/ln R. Therefore, the optimum number of homologues in this instance is six. Each of the 18 isothermal separations of the C_5–C_{10} alkane series mentioned above was applied to eqn. (13) by using linear regression and the slope, R; the dead times, t_m = intercept/(1 − slope), are presented in Table 1.

The average dead time and its standard error were calculated from Table 1 to yield 54.2 ± 0.2. The average slope and its standard error were likewise calculated to yield 1.831 ± 0.003.

The Student's two-tail t-test was applied to the paired differences between the dead times listed in Table 1 and the corresponding dead times listed in each column of Table II of ref. 26 or Table 3 of ref. 27. The null hypothesis (H_0) asserts that the method proposed in this paper for calculating the dead time agrees with each of the dead time calculation methods used by Smith *et al.*,[26] *i.e.*, that the population mean difference (μ_d) is zero; H_0: $\mu_d = 0$. The number of determinations was $n = 18$ and, therefore, the number of degrees of freedom is $\nu = n - 1 = 17$. A largest calculated t-value of 0.9617 was achieved when the results calculated *via* the proposed method were compared with the modified simplex results tabulated in column six of both of the aforementioned Table II and Table 3. The t-test at the 5% level of significance yields $t_{0.025,\ 17} = 2.571$. All the calculated t-values were much less than the critical value. Therefore, at the 5% level of significance, the null hypothesis is accepted, *i.e.*, the set of dead time calculations listed in Table 1 is equal to the other six sets of dead time calculations listed in both of the above-mentioned Table II of ref. 26 and Table 3 of ref. 27.

The methane retention times for 16 separations of methane and air are reported in Table V of ref. 26 for the same column and detector to which the measurements in Table 1 refer. Dixon's Q-test was used to reject, at the 90% confidence level, three outliers of the 16 methane retention times listed in the

Table 1 Values obtained for the slope and corresponding column dead-time (t_m) when the straight line eqn. (13) was applied to the isothermal retention times listed in the first 18 rows of Table 1 in ref. 26 or in Table 3 of ref. 27

GLC separation number	First 'run' on eqn. (13)		Second 'run' on eqn. (13)	
	Slope $1/R_1$	Dead time $1/t_{m_1}$	Slope $2/R_2$	Dead time $2/t_{m_2}$
1	1.8472	54.467	1.8571	54.957
2	1.8371	55.287	1.8413	55.501
3	1.8338	54.433	1.8317	54.334
4	1.8323	54.973	1.8235	54.536
5	1.8452	54.768	1.8468	54.830
6	1.8122	53.989	1.8076	53.743
7	1.8455	55.287	1.8324	55.142
8	1.8305	53.907	1.8310	53.927
9	1.8271	53.839	1.8207	53.515
10	1.8350	54.289	1.8359	54.332
11	1.8247	53.702	1.8191	53.421
12	1.8336	53.913	1.8386	54.162
13	1.8286	53.689	1.8257	53.530
14	1.8370	53.981	1.8487	54.547
15	1.8268	53.667	1.8222	53.430
16	1.8177	53.341	1.8140	53.143
17	1.8276	53.786	1.8264	53.729
18	1.8286	53.887	1.8286	53.887

Table 2 Average retention times (s) from 18 isothermal separations of C_5–C_{10} alkanes as calculated from Table I of ref. 26. The retention times listed in parentheses were calculated from the otherwise listed retention times as per eqn. (15) and refer to the so-called 'peripheral' members, C_4 and C_{11}, of the alkane series*

(C_4)	C_5	C_6	C_7	C_8	C_9	C_{10}	(C_{11})
(60.52)	65.80	75.39	93.16	125.58	184.86	293.58	(492.65)

* The characteristics of eqn. (13), *i.e.*, slope and intercept, based on the C_5–C_{10} data are 1.832 and −45.06, respectively. The respective characteristics of eqn. (13) based on the C_4–C_{11} data are 1.831 and −44.99.

said Table V. The remaining 13 methane retention times yielded an average retention time and standard error of t_1 = 55.3 ± 0.1. This compares favourably with a corresponding value of t_1 = 55.2 ± 0.2, calculated from the average gross isothermal retention times of the C_5–C_{10} alkane series listed in Table 2 *via* eqn. (2), by using $R = 1.831 \pm 0.003$ and $t_m = 54.2 \pm 0.2$:

$$t_1 = (t_n - t_m)R^{1-n} + t_m \qquad (14)$$

Conclusions

The material presented in this paper concerning the chromatographic retention behaviour of a homologous series of compounds has appeared in one form or another over the last 30 years. Previously, the apparent linear relationship between the logarithm of the adjusted retention time and the carbon number of a homologue member was the working hypothesis in the determination of the dead time of a column. However, it is not possible to prove this hypothesis through direct experimental observations because the adjusted retention time cannot be known before the dead time of the column is known. This paper is based solely on the working hypothesis that the ratio of the adjusted retention times of any two consecutive members of a homologous series is a constant. This latter hypothesis is not only subject to direct experimental proof by eqn. (13), but it also embraces the aforementioned hypothesis and other experimental dead time methods such as that of Grobler and Balizs.[20] According to Said *et al.*,[30] eqn. (2) is experimentally valid for a large span of carbon values in an alkane series.

The analysis presented by Sevcik[31] and by Sevcik and Lowentap[1] on this subject presented difficulties that were addressed by Smith *et al.*[2] by arbitrarily assigning a net retention time to a theoretical alkane of carbon number zero. The same concept is used in this paper, but it is postulated *ab initio* rather than as an afterthought, and the conventional retention relationships are derived therefrom.

Equation (13) allows the mathematical dead time of a column and the ratio of the net retention times of two consecutive members of a homologous series to be measured graphically from the gross retention times in the same column of at least three consecutive members of a homologous series. Equation (13) is easier to understand and apply for these purposes than any of the other equivalent methods[20,28,29] it was compared with above and it yields comparable results. The average gross retention time for methane calculated *via* eqn. (14) from the gross retention times of alkanes published by Smith *et al.*[26] and experimental values for R and t_m was equal to the average gross retention time for methane determined directly by Smith *et al.*[26] The paper also shows that gross retention times, calculated from experimental gross retention times, which all suffer from a systematic error, contain the same systematic error, whereas adjusted retention times, although likewise calculated, are unaffected by systematic error.

Although a minimum of three consecutive homologue members is required when applying eqn. (13), it is recommended that the criterion of van Tulder *et al.*[19] on this matter should be followed. The gross retention times of the peripheral members of any such set of homologue members receive half the weighting of the central members when applied to eqn. (13) as set out above. This bias can be counteracted using the slope and intercept from the first 'run' on eqn. (13) to generate artifically an extra pair of peripheral gross retention times from the original set of gross retention times using eqn. (13) in the following form on the experimental data points:

$$t_{n \pm x} = (t_n - t_m)R^{\pm x} + t_m \qquad (15)$$

This new set of data, *i.e.*, the original set of experimental gross retention times plus the two artificially generated peripheral gross retention times, can now be used for a second 'run' on eqn. (13) to generate new values for its slope and intercept. The two artificially generated peripheral retention times act as a balanced coordinate pair, *i.e.*, while one of the artificially generated peripheral retention times acts as an abscissa for the lowest experimental carbon number homologue member used, then the other artificially generated peripheral retention time acts as an ordinate for the highest experimental carbon number homologue member used. The above manoeuvre ensures that all the experimental gross retention times act both as abscissae and as ordinates when applied *via* linear regression to eqn. (13). It is also recommended that replicate separations should be performed so as to minimize the effect of random errors.

The general chemical expression for the nth member of a straight chain homologous series is $(CH_2)_n$ X, where X is the hypothetical zero carbon number member of the series, *e.g.*, if X is H_2, then the homogous series is the alkane series, *etc.* Berendsen *et al.*[25] shows, in Fig. 2 of that reference, the logarithm of the capacity factor (k) *versus* carbon number for seven straight chain homologous series in a given HPLC column under constant chromatographic conditions. All seven plots have the same slope, but diverse intercepts. This suggests that the adjusted retention time of the hypothetical zero carbon-number member, t'_0, varies from homologous series to homologous series, but that the adjusted retention times of the higher order homologue members increases by the same multiplying factor, $R > 1$, for each homologous series. The analysis put forward in this paper offers theoretical support to those observations, *i.e.*, the addition of a CH_2 monomer to straight chain homologous series has the same multiplicative effect on the adjusted retention times of all the members of all homologous series under fixed chromatographic conditions. The average mathematical dead time in the paper by Berendsen *et al.*[25] with 136 ± 1 s. The least retained, a homologous series of alcohols, had t'_0 = 4.5s, while the most retained, a homologous series of alkylphenyls, had t'_0 = 54.5 s.

There is no such species in chromatography as an 'unretained compound' as even the hypothetical zero carbon number homologue member has a finite adjusted retention time.

The author is grateful for the critical and constructive comments of the referees.

References

1 Sevcik, J., and Lowentap, M. S. H., *J. Chromatogr.*, 1978, **147**, 75.
2 Smith, R. J. Haken, J. K., and Wainwright, M. S., *J. Chromatogr.*, 1985, **331**, 389.
3 Parcher, J. F., and Johnson, D. M., *J. Chromatogr. Sci.*, 1980, **18**, 267.
4 Sharples, W. E., and Vernon, F., *J. Chromatogr.*, 1978, **161**, 83.
5 Touabet, A., Badjah Hadj Ahmed, A. Y., Maeck, M., and Meklati, B. Y., *HRCC J. High Resolut. Chromatogr. Chromatogr. Commun.*, 1986, **9**, 456.

6 Wentworth, W. E., *J. Chem. Educ.*, 1965, **42**, 96.
7 Smith, R. J., Haken, J. K., Wainwright, M. S., and Madden, B. G., *J. Chromatogr.*, 1985, **328**, 11.
8 Tarjan, G., Nyiredy, S., Gyor, M., Lombosi, E. R., Lombosi, T. S., Budahegyi, M. V., Meszaros, S. Y., and Takacs, J. M., *J. Chromatogr.*, 1989, **472**, 1.
9 Wainwright, M. S., Nicass, C. S., Haken, J. K., and Chaplin, R. P., *J. Chromatogr.*, 1985, **321**, 287.
10 Ashes, J. R., Mills, S. C., and Haken, J. K., *J. Chromatogr.*, 1978, **166**, 391.
11 Haken, J. K. Wainwright, M. S., and Smith, R. J., *J. Chromatogr.*, 1977, **133**, 1.
12 Wainwright, M. S., Haken, J. K., and Srisukh, D., *J. Chromatogr.*, 1979, **179**, 160.
13 Vernon, F., and Suratman, J. B., *Chromatographia*, 1983, **17**, 597.
14 Overaa, P., *Lab. Pract.*, 1986, **39**, 25.
15 Alhedai, A., Martire, D. E., and Scott, R. P. W., *Analyst*, 1989, **114**, 869.
16 Levin, S., and Grushka, E., *Anal. Chem.*, 1989, **61**, 2428.
17 Daignault, L. G., Jackman, D. C., and Rillema, D. P., *Chromatographia*, 1989, **27**, 156.
18 Montes, M., Usero, J. L., Del Arco, A., Izquierdo, C., and Casado, J., *J. Chromatogr.*, 1989, **481**, 97.
19 van Tulder, P. J. M., Franke, J. P., and de Zeeuw, R. A., *HRCC J. High Resolut. Chromatogr. Chromatogr. Commun.*, 1987, **10**, 191.
20 Grobler, A., and Balizs, G., *J. Chromatogr. Sci.*, 1974, **12**, 57.
21 Margarit-Roig, L., Diaz-Marot, A., and Gassiot-Matas, M., *Afinidad*, 1986, **406**, 525.
22 Krstulovic, A. M., Colin H., and Guiochon, G., *Anal. Chem.*, 1982, **54**, 2438.
23 Smith, R. J., Nicass, C. S., and Wainwright, M. S., *J. Liq. Chromatogr.*, 1986, **9**, 1387.
24 Hansen, H. L., and Andresen, K., *J. Chromatogr.*, 1968, **34**, 246.
25 Berendsen, G. E., Schoenmakers, P. J., de Galan, L., Vigh, G., Varga-Puchony, Z., and Inczedy, J., *J. Liq. Chromatogr.*, 1980, **3**, 1669.
26 Smith, R. J., Haken, J. K., and Wainwright, M. S., *J. Chromatogr.*, 1978, **147**, 65.
27 Wainwright, M. S., and Haken, J. K., *J. Chromatogr.*, 1980, **184**, 1.
28 Guardino, K., Albaiges, J., Firpo, G., Rodriguez-Vinals, R., and Gassiot, M., *J. Chromatogr.*, 1976, **118**, 13.
29 Nelder, J. A., and Mead, R., *Comput. J.*, 1965, **7**, 308.
30 Said, A. S., Tabarak, M. H., and Dadkhah, A. A., *HRCC J. High Resolut. Chromatogr. Chromatogr. Commun.*, 1989, **12**, 342.
31 Sevcik, J., *J. Chromatogr.*, 1977, **135**, 183.

Paper 1/03722F
Received July 22, 1991
Accepted June 25, 1992

Characterization of Amines by Fast Black K Salt in Thin-layer Chromatography

Ilkka Ojanperä
Department of Forensic Medicine, University of Helsinki, Kytösuontie 11, SF-00300 Helsinki, Finland
Kristiina Wähälä and Tapio A. Hase
Department of Chemistry, University of Helsinki, Vuorikatu 20, SF-00100 Helsinki, Finland

Amines were characterized on a silica gel thin-layer chromatographic (TLC) plate with the diazonium reagent Fast Black K salt (FBK) and with subsequent novel procedures: acid treatment or treatment with *N*-(1-naphthyl)ethylenediamine in acid solution. The differentiation of primary, secondary and tertiary aliphatic and aromatic amines was demonstrated, with special attention to drug substances. By using the *N*-(1-naphthyl)ethylenediamine treatment a 5-fold improvement in the detection limits for aliphatic secondary amines was achieved compared with FBK alone, allowing detection of 0.01 μg of methamphetamine and 0.04 μg of methyl phenidate. The structures of the coloured reaction products were elucidated by spectroscopic and TLC methods. An unexpected reaction was observed with dialkylanilines, which reacted by *N*-coupling with various diazonium salts with cleavage of an alkyl group.

Keywords: *Fast Black K salt; thin-layer chromatography; amines; diazo coupling; forensic analysis*

Thin-layer chromatography (TLC) possesses a unique advantage among chromatographic techniques in allowing post-chromatographic derivatization of immobilized analytes. This makes possible the sequential use of a wide variety of derivatization reagents. A sample can also be run on several parallel tracks of the TLC plate and each track can then be treated with different reagents. The combined information obtained from a retardation factor (R_F) and from colour reactions provides a powerful means for analyte characterization that can be superior to more expensive instrumental techniques.

In a recent paper,[1] we showed the ability of a diazonium reagent, Fast Black K salt (FBK), to differentiate between sub-microgram amounts of aliphatic amines by colour and elucidated the structures of the coloured products. Primary amines form a violet and secondary amines an orange–red or red product, whereas tertiary amines do not react. However, differentiation of the respective types of arylamines and also aliphatic amines from arylamines was found to be more difficult.

This paper describes improved differentiation methods for aliphatic amines and also shows that aromatic amines and phenols are readily discerned by the novel FBK techniques. Drug substances are included to demonstrate the value of these methods in drug analysis, particularly in toxicological drug screening.

Experimental

Materials

Diazonium salts FBK [2,5-dimethoxy-4-(4-nitrophenylazo)-benzenediazonium chloride hemi(zinc chloride), purity 30%] (**1a**) and Fast Red B salt (2-methoxy-4-nitrobenzenediazonium tetrafluoroborate, 95%) (**1b**) were purchased from Aldrich (Milwaukee, WI, USA), and Fast Red GG salt (4-nitrobenzenediazonium tetrafluoroborate, 90%) (**1c**) was from Sigma (St. Louis, MO, USA). The other diazonium salts 4-nitrobenzenediazonium chloride (**1d**), benzenediazonium chloride (**1e**), 2-methoxybenzenediazonium chloride (**1f**), 4-methoxybenzenediazonium chloride (**1g**) and 2,5-dimethoxybenzenediazonium chloride (**1h**) were prepared by diazotization of the corresponding anilines as follows: to the cold solution of 0.3 mmol of the amine in 6 cm^3 of 0.2 mol dm^{-3} HCl (1.2 mmol), 207 mm^3 of cold 10% $NaNO_2$ (0.3 mmol) solution were added, and the diazonium reagent was used immediately.

N-(1-Naphthyl)ethylenediamine dihydrochloride (98%) (**2**) was from Merck (Darmstadt, Germany).

Coupling components (Table 1) **5a–b**, **6b**, **6d**, **6h**, **6k**, **7b**, **7e–f** and **8d** were from Aldrich (Steinheim, Germany, and Milwaukee, WI, USA), **6i** was from BDH (Poole, Dorset, UK), **6f–g** and **8e** were from Fluka (Buchs, Switzerland), **3c** and **6j** were from Merck, and **3d** was from Sigma. *N*-Ethyl-*p*-toluidine (**7c**) and *N*-ethyl-2,4,6-trimethylaniline (**7d**) were synthesized from the corresponding anilines,[2] separated from impurities by preparative TLC, with use of an automatic TLC sampler and the mobile phase **I**, and extracted from the sorbent into dichloromethane–methanol (1 + 1).

The other coupling components and chemicals used have been described previously.[1] All coupling components were of 97% or higher purity, except for **7b** (96%) and **8d** (95%). The drug substances (Table 1) **3e–h**, **4c–f**, **6l–o** and **7g** were obtained from various pharmaceutical companies and they were of pharmaceutical purity.

The TLC plates were of glass coated with a 0.25 mm layer of silica gel 60 F_{254} (Merck).

Apparatus

The automatic TLC sampler was an ATS III from Camag (Muttenz, Switzerland) and the scanning densitometer was a TLC Scanner II, also from Camag. The high-performance liquid chromatography (HPLC), ultraviolet/visible spectrophotometry (UV/VIS), proton nuclear magnetic resonance spectrometry (^{1}H NMR) and mass spectrometry (MS) instrumentation have been described previously.[1]

Thin-layer Chromatography

Sample preparation

Methanolic or aqueous methanolic solutions containing 2 mg cm^{-3} each of the coupling components were prepared. For the investigation of the colour reactions on the TLC plate (Table 1), 1 mm^3 of each solution was manually applied to the plate, and the visualization procedures were carried out without prior development. For the detection limit studies, dilutions of the 2 mg cm^{-3} solutions were carried out.

Visualization methods

The plates were sprayed lightly, using a Desaga (Heidelberg, Germany) test-tube atomizer, with a filtered 0.5% m/v

Table 1 Colour reactions of coupling components with Fast Black K salt on silica gel TLC plates*

Substance	FBK	FBK + NaOH	FBK + NaOH + HCl	FBK + NaOH + NEDA†/HCl
Aliphatic primary amines—				
3a Ethylamine hydrochloride	Light red	Violet	Ochre	Ochre
3b 2-Phenylethylamine hydrochloride	Light red	Violet	Ochre	Ochre
3c Ethylenediamine hydrochloride	Light red	Red–violet	Ochre	Ochre
3d Putrescine hydrochloride	Light red	Violet	Ochre	Ochre
3e Amantadine hydrochloride	Light red	Violet	Ochre	Ochre
3f Amphetamine sulfate	Light red	Violet	Ochre	Ochre
3g Phentermine hydrochloride	Light red	Violet	Ochre	Ochre
3h Tocainide hydrochloride	Light red	Violet	Ochre	Ochre
Aliphatic secondary amines—				
4a Diethylamine hydrochloride	Orange–red	Orange–red	Violet → cream	Blue
4b *N*-Methyl-2-phenylethylamine	Orange–red	Orange–red	Violet → cream	Blue
4c Cyclopentamine hydrochloride	Orange–red	Orange–red	Violet → cream	Blue
4d Fluoxetine hydrochloride	Orange–red	Orange–red	Violet → cream	Blue
4e Methamphetamine hydrochloride	Orange–red	Orange–red	Violet → cream	Blue
4f Prilocaine hydrochloride	Orange–red	Orange–red	Violet → cream	Blue
Poly(amines)—				
5a Spermidine	Red	Red	Ochre	Blue–green
5b Spermine	Red	Orange–red	Ochre	Blue
Aromatic primary amines—				
6a Aniline	Red	Red–violet	Ochre	Brown–violet
6b *m*-Toluidine	Red	Red–violet	Brown	Brown–violet
6c *p*-Toluidine	Red	Red–violet	Ochre	Brown–violet
6d 2,4-Dimethylaniline	Red	Red–violet	Ochre	Ochre
6e 2,4,6-Trimethylaniline	Red	Red–violet	Ochre	Ochre
6f *o*-Anisidine	Red	Red–violet	Brown	Brown
6g *p*-Anisidine	Red	Red–violet	Red–brown	Brown
6h 2,5-Dimethoxyaniline	Intense violet	Intense violet	Intense blue–violet	Intense blue–violet
6i 4-Nitroaniline	Yellow	Green–yellow	Violet → ochre	Brown–violet
6j 4-Aminobenzoic acid	Red	Red	Violet → ochre	Violet
6k Ethyl 4-aminobenzoate	Red	Red	Violet → ochre	Violet
6l Carbutamide	Light red	Red	Violet → ochre	Brown–violet
6m Nomifensine maleate	Light red	Red	Violet → ochre	Brown–violet
6n Procainamide hydrochloride	Red	Red	Violet → ochre	Brown–violet
6o Procaine hydrochloride	Red	Red	Violet → ochre	Brown–violet
Aromatic secondary amines—				
7a *N*-Ethylaniline	Orange–red	Orange–red	Violet → green	Blue
7b *N*-Ethyl-*m*-toluidine	Red–violet	Brown–violet	Violet → blue–violet	Blue
7c *N*-Ethyl-*p*-toluidine	Orange–red	Orange–red	Violet → cream	Blue
7d *N*-Ethyl-2,4,6-trimethylaniline	Orange–red	Orange–red	Violet → cream	Blue
7e *N*-Ethyl-4-nitroaniline	Yellow	Yellow	Yellow	Green
7f *N*-Methyl-4-aminobenzoic acid	Orange–red	Orange–red	Violet → cream	Blue
7g Amethocaine hydrochloride	Red	Red	Violet → cream	Blue
Aromatic tertiary amines—				
8a *N*,*N*-Dimethylaniline	Brown–red	Brown–red	Violet → green	Blue
8b *N*,*N*-Dimethyl-*p*-toluidine	Orange–red	Orange–red	Violet → cream	Blue
8c *N*,*N*-Dimethyl-2,4,6-trimethylaniline	Yellow	Yellow	Cream	Yellow
8d *N*-Ethyl-*N*-methylaniline	Brown–red	Brown–red	Violet → green	Blue
8e *N*,*N*-Diethylaniline	Violet	Violet	Blue–violet	Red–violet

* Amount of substance applied = 2 μg.
† *N*-(1-Naphthyl)ethylenediamine.

aqueous solution of **1a**, then dried briefly with a hot-air blower, sprayed generously with 0.5 mol dm^{-3} NaOH and dried thoroughly, prior to one of the following procedures.

Acid treatment. The plate was sprayed with 2 mol dm^{-3} HCl and dried.

Acid coupling treatment. The plate was sprayed with a 1% m/v solution of **2** in 0.5 mol dm^{-3} HCl and dried.

Structure elucidation by TLC

For the investigation of the **1a** derivatives formed on the plate, the TLC plate was developed directly after the following application sequence. With use of an automatic TLC sampler, 3 mm^3 each of solutions of the coupling components **3a–d**, **4a–b**, **5a–b**, **6a–k**, **7a–f** and **8a–e** were applied to separate tracks of the plate, followed by over-application with 2 mm^3 of 0.1 mol dm^{-3} NaOH and 5 mm^3 of the diazonium salt solution (with **1b–h**, only **8a–e** were studied). With **1a–c**, a 1% m/v filtered aqueous solution was used; with **1d–h** a 0.05 mol dm^{-3} solution (see above) was used.

The application was performed by spraying narrow bands of 6 mm length, and the plate was dried between the application stages. The development was carried out over a distance of 7 cm in a 20 × 10 cm double-trough developing chamber from Camag, with use of mobile phase I (Fig. 1). Separate plates were then submitted to the acid treatment and the acid coupling treatment (see above).

For the investigation of the acid or acid coupling products formed on the plate, the application procedure described above was continued by over-applying 5 mm^3 of 2 mol dm^{-3} HCl or 5 mm^3 of a 1% solution of **2** in 0.5 mol dm^{-3} HCl,

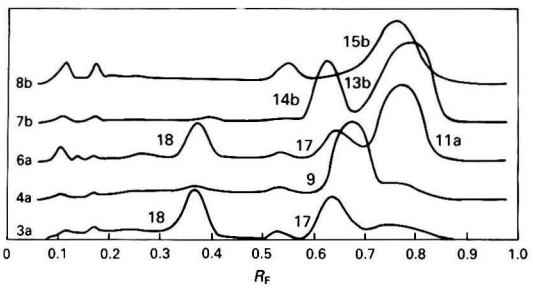

Fig. 1 Thin-layer chromatographic separation of FBK derivatives from aliphatic and aromatic amines. The pre-chromatographic reaction was carried out on a silica-gel plate by sequential application of a coupling component, NaOH and FBK, and developing with toluene–methanol (9 + 1). Absorbance detection was by reflectance at 500 nm

respectively, and the TLC plate was developed with mobile phase II. Additionally with **6a–k**, the spots obtained by spraying with the acid coupling reagent (Table 1) were scraped off, extracted with dichloromethane–methanol (1 + 1) and analysed with use of mobile phase II. After drying, the plate was sprayed with 2 mol dm^{-3} HCl to restore acidity for visual inspection.

The mobile phases were as follows:

Mobile phase I. Toluene–methanol (9 + 1).

Mobile phase II. Ethyl acetate–methanol–concentrated ammonia (80 + 15 + 5).

Structure Elucidation by Spectroscopy

Syntheses

For the preparation of **10**, 0.42 g of **1a** was dissolved in 20 cm^3 of water, and the filtered solution was added, with stirring, to a solution containing 1 mmol of **2** in 10 cm^3 of water. The precipitate formed was centrifuged, washed twice with 0.5 mol dm^{-3} HCl and suspended in 2 mol dm^{-3} NaOH. The suspension was extracted twice with dichloromethane, and the organic phase was evaporated to dryness. Yield: 134 mg.

The reaction between **1a** and the aromatic primary amines **6a–c**, the aromatic secondary amines **7a–b** and the aromatic tertiary amines **8a–b** was carried out in solution as follows: 0.42 g of **1a** was dissolved in 20 cm^3 of water, and the filtered solution was added, with stirring, to a solution containing 1 mmol of the amine in 2 cm^3 of 0.5 mol dm^{-3} HCl. Sodium hydroxide solution (2 mol dm^{-3}) was added dropwise, with stirring, until the solution was clearly alkaline (pH >9), and the reaction vessel was allowed to stand in ice for 10 min. The precipitate formed was centrifuged, washed twice with cold water and dried in air. Yields: 94 mg (from **6a**), 119 mg (**6b**), 110 mg (**6c**), 88 mg (**7a**), 124 mg (**7b**), 75 mg (**8a**) and 122 mg (**8b**).

For the preparation of **19**, 0.42 g of **1a** was dissolved in 20 cm^3 of water, and the filtered solution was made clearly alkaline (pH >9) with 2 mol dm^{-3} NaOH. The suspension formed was allowed to stand in an ultrasonic bath for 10 min, then it was centrifuged, and the supernatant phase was separated. Another basic fraction was obtained by suspending the precipitate in 2 mol dm^{-3} NaOH, sonicating and centrifuging. The combined supernatant phases were acidified with 2 mol dm^{-3} HCl, extracted twice with dichloromethane, and the organic phase was evaporated to dryness.

Purification

The products from **6–8** were separated and purified by preparative HPLC by collecting fractions from successive 0.5 cm^3 injections of 5 mg cm^{-3} solutions prepared in the mobile phase or in toluene–methanol (9 + 1). The mobile phase was toluene–methanol (99.9 + 0.1). The flow rate was 2.5 cm^3 min^{-1}, and the analytes were monitored at 480 nm.

The product **19** was separated from impurities by preparative TLC, with use of an automatic TLC sampler and mobile phase II, and extracted from the sorbent into dichloromethane–methanol (1 + 1).

The purified products were compared for identity with those formed on the TLC plate, by use of TLC with mobile phase I.

Spectroscopic analyses

Proton NMR spectra (200 MHz) were recorded in $CDCl_3$. Mass spectra were recorded with an electron energy of 70 eV, unless stated otherwise, *via* a direct inlet probe at 100–250 °C. The UV/VIS spectra were recorded in methanol.

N-{4-[2,5-*Dimethoxy*-4-(4-*nitrophenylazo*)*phenylazo*]-1-*naphthyl*}*ethylenediamine* (**10**). ^{1}H NMR: δ (ppm) 3.19 (2 H, quintet, CH_2NH_2), 3.47 (2 H, q, CH_2NH), 4.10 (3 H, s, CH_3O), 4.16 (3 H, s, CH_3O), 5.98 (1 H, t, NH), 6.69 (1 H, d, aromatic H *ortho* to $NHC_2H_4NH_2$, J = 8.9 Hz), 7.5–8.1 (4 H, m, aromatic H), 7.55 (1 H, s, aromatic H^a), 7.64 (1 H, s, aromatic H^b), 8.06 (2 H, d, aromatic H^c, J = 9.1 Hz), 8.15 (1 H, d, aromatic H *meta* to $NHC_2H_4NH_2$, J = 8.8 Hz), 8.37 (2 H, d, aromatic H^d, J = 9.1 Hz). MS (19 eV): *m/z* 499 (3%) [M^+], 456 (9) [$M - C_2H_3NH_2$], 426 (7), 322 (8), 302 (86), 272 (38), 195 (100).

4-[2,5-*Dimethoxy*-4-(4-*nitrophenylazo*)*phenylazo*]-N-*nitrosobenzenamine* (**19**). ^{1}H NMR: δ (ppm) 3.85 (3 H, s, CH_3O), 4.01 (3 H, s, CH_3O), 6.01 (1 H, s, aromatic H^a), 6.38 (1 H, s, aromatic H^b), 7.33 (2 H, d, aromatic H^c, J = 9.2 Hz), 8.26 (2 H, d, aromatic H^d, J = 9.2 Hz), 11.4 (1 H, br s, NH). MS: *m/z* 331 (4%) [M^+], 303 (100) [$M - N_2$], 181 (35), 151 (33), 138 (62), 123 (83).

The spectral data for **11a–c**, **12b**, **13a–b**, **14a–b**, **15a–b** and **16a** are presented in Tables 2 and 3.

Results and Discussion

Table 1 shows the behaviour of the coupling components (**3–8**) on the silica gel TLC plate in the FBK (**1a**) visualization and in the subsequent acid or acid coupling treatment. The colours obtained for various types of amines are summarized in Table 4. The acid coupling reaction with aliphatic secondary amines (**4**) is shown in Scheme 1. The structures of the synthesized reaction products from aromatic amines (**11–16**) are shown in Scheme 2. Fig. 1 demonstrates the TLC separation of the **1a** derivatives from selected coupling components after a reaction on the plate.

Aliphatic Primary Amines

Aliphatic primary amines (**3**) react with **1a** to produce violet spots on the TLC plate, the main coloured components being a violet 1,3-diaryltriazene (**17**) and a red primary arylamine (**18**), both derived exclusively from **1a**.[1]

Ar–N=N–NH–Ar
17

$Ar–NH_2$
18

Both the acid treatment and the acid coupling treatment produced an ochre colour. The colour change was due to **18**, which in acidic medium turned to ochre yellow, probably because of protonation of the amino and/or the azo group.[3] The compound was formed also from **17** with acid. In the acid coupling, some regeneration of **1a** from **17** and subsequent coupling with **2** with formation of a blue–green product (see below) was observed, but it did not have a contribution to the over-all ochre colour.

Table 2 ^{1}H NMR and MS data for triazenes from FBK and arylamines*

Compound No.	d	c	b	a	e	f	g	OMe	Ph–Me	NH, NH_2	Aliphatic	*m/z* (%)
11a†	8.35, 2H, d, J = 9.1	7.99, 2H, d, J = 9.1	7.49, 1H, s	7.42, 1H, s	7.62, 2H, d, J = 8.2	7.33–7.52, 3H, m		4.12, 3H, s 3.97, 3H, s		10.07 1H, brs, NH		328(27), 302(48), 288(100), 151(29), 138(81), 122(40)
11b‡	8.36, 2H, d J = 8.1	7.99, 2H, d J = 8.2	7.49. 1H, s	7.42, 1H, s		7.12–7.54, 4H, m		4.13, 3H, s 3.97, 3H, s	2.45 3H, s	10.06 1H, s, NH		420(3) [M$^+$], 392(75) [M – N_2], 362(21), 302(100), 137(43), 122(81)
11c§	8.35, 2H, d, J = 8.9	7.98, 2H, d, J = 8.9	7.49, 1H, s	7.40, 1H, s	7.54, 2H, d, J = 8.3	7.26, 2H, d, J = 8.2		4.12, 3H, s 3.96 3H, s	2.42, 3H, s	10.01, 1H, s, NH		405(18), 360(84), 302(57), 288(100), 195(82), 138(80)
13a¶	8.37, 2H, d J = 9.1	8.03, 2H, d J = 9.1			7.30–7.60, 7H, m			4.08, 3H, s and 3.99 3H, s			4.45, 2H, q, CH_2 and 1.39 3H, t, CH_3	434(100) [M$^+$], 406(12) [M – N_2], 302(25), 148(73), 135(35) 120(92)
13b‖	8.32, 2H, d, J = 9.0	7.98, 2H, d, J = 9.0	7.45, 1H, s	7.30, 1H, s		7.21–7.26, 4H, m		4.03, 3H, s 3.94, 3H, s	2.39, 3H, s		4.40, 2H, q, CH_2 and 1.33, 3H, t CH_3	448(5) [M$^+$], 420(77) [M – N_2], 405(15), 314(42), 135(41), 120(100)
15a**	8.37, 2H, d, J = 8.9	8.03, 2H, d, J = 8.9		7.42–7.55, 4H, m		7.23–7.31, 3H, m		4.08, 3H, s 4.01, 3H, s			3.81, 3H, s, CH_3	420(10) [M$^+$] 392(100) [M – N_2], 314(42), 287(52), 151(51), 122(86)
15b††	8.37, 2H, d, J = 9.0	8.02, 2H, d, J = 9.0	7.50, 1H, s	7.29, 1H, s	7.41, 2H, d, J = 8.6	7.25, 2H, d, J = 8.6		4.07, 3H, s 4.01, 3H, s	2.40, 3H, s		3.79, 3H, s, CH_3	434(3) [M$^+$], 406(100) [M – N_2], 302(27), 287(100), 151(85), 122(100)

* δ_H ppm, J = Hz.
† 1-[2,5-Dimethoxy-4-(4-nitrophenylazo)phenyl]-3-phenyltriazene.
‡ 1-[2,5-Dimethoxy-4-(4-nitrophenylazo)phenyl]-3-(*m*-tolyl)triazene.
§ 1-[2,5-Dimethoxy-4-(4-nitrophenylazo)phenyl]-3-(*p*-tolyl)triazene.
¶ 1-[2,5-Dimethoxy-4-(4-nitrophenylazo)phenyl]-3-ethyl-3-phenyltriazene.
‖ 1-[2,5-Dimethoxy-4-(4-nitrophenylazo)phenyl]-3-ethyl-3-(*m*-tolyl)triazene.
** 1-[2,5-Dimethoxy-4-(4-nitrophenylazo)phenyl]-3-methyl-3-phenyltriazene.
†† 1-[2,5-Dimethoxy-4-(4-nitrophenylazo)phenyl]-3-methyl-(*p*-tolyl)triazene.

Aliphatic Secondary Amines

Aliphatic secondary amines (**4**) react with **1a** to produce orange–red 1-aryl-3,3-dialkyltriazenes (**9**)[1] (Scheme 1). The acid treatment generated a transient violet colour that soon turned to a cream colour. The colour was tentatively assigned to a yellow compound (**19**) (λ_{max} 447 nm), which can exhibit characteristics of a diazohydroxide and an *N*-nitrosamine.

$$\text{Ar–N=N–OH} \rightleftharpoons \text{Ar–NH–N=O}$$
19

The acid coupling treatment resulted in a blue product that formed in a few minutes. The colour, which was more blue–green than blue in weaker spots was found to be due to the 4-azo coupling product (**10**) (λ_{max} 588 nm) of **1a** and **2** (Scheme 1). The coupling component (**2**) has previously been

Table 3 ^{1}H NMR and MS data for aminoazo compounds from FBK and arylamines*

Compound No.	d	c	b	a	e	f	g	OMe	Ph–Me	NH, NH_2	Aliphatic	*m/z* (%)
12b†	8.38, 2H, d, J = 9.1	8.06, 2H, d, J = 9.2	7.52, 1H, s	7.44, 1H, s	7.76, 1H, d, J = 8.5	6.60, 1H, s	6.57, 1H, d, J = 8.5	4.08, 3H, s 4.06, 3H, s	2.72, 3H, s	4.12 2H, s, NH_2		420(75) [M$^+$], 390(21), 368(8), 134(47), 121(15), 106(100)
14a‡	8.39, 2H, d, J = 8.8	8.05, 2H, d, J = 8.8	7.51, 1H, s	7.47, 1H, s	7.92, 2H, d, J = 8.6	6.67, 2H, d, J = 8.8		4.10, 3H, s 4.06, 3H, s		4.25, 1H, br t, NH	3.30, 2H, quint, CH_2 and 1.33, 3H, t, CH_3	434(63) [M$^+$], 252(5), 207(5),, 148(73), 135(38), 120(100)
14b§	8.38, 2H, d, J = 8.0	8.05, 2H, d, J = 8.0	7.51, 1H, s	7.45, 1H, s	7.81, 1H, d, J = 9.0	6.49, 1H, s	6.46, 1H, d	4.08, 3H, s 4.06, 3H, s	2.73, 3H, s	4.20, 1H, br t, NH	3.28, 2H, quint CH_2 and 1.31, 3H, t, CH_3	448(88) [M$^+$], 418(34), 368(20), 314(23), 162(39), 134(100),
16a¶	8.38, 2H, d, J = 8.9	8.05, 2H, d, J = 8.9	7.52, 1H, s	7.49, 1H, s	7.96, 2H, d, J = 9.0	6.77, 2H, d, J = 9.0		4.11, 3H, s 4.06, 3H, s			3.14, 6H, s, $(CH_3)_2$	434(100) [M$^+$] 404(5), 217(6), 148(74), 135(35), 120(93)

* δ_H ppm, J = Hz.
† 4-[2,5-Dimethoxy-4-(4-nitrophenylazo)phenylazo]-3-methylbenzenamine.
‡ 4-[2,5-Dimethoxy-4-(4-nitrophenylazo)phenylazo]-*N*-ethylbenzenamine.
§ 4-[2,5-Dimethoxy-4-(4-nitrophenylazo)phenylazo]-*N*-ethyl-3-methylbenzenamine.
¶ 4-[2,5-Dimethoxy-4-(4-nitrophenylazo)phenylazo]-*N*,*N*-dimethylbenzenamine.

Table 4 Simplified scheme of colours obtained for various types of amines with FBK and with the subsequent acid or acid coupling treatment

	FBK + NaOH	FBK + NaOH + HCl	FBK + NaOH + NEDA/HCl
Aliphatic primary amines	Violet	Ochre	Ochre
Aliphatic secondary amines	Orange–red	Cream	Blue
Aliphatic tertiary amines	No colour	—	—
Aromatic primary amines	Red–violet or red	Ochre or brown	Brown–violet
Aromatic secondary and tertiary amines	Orange–red	Cream or green	Blue

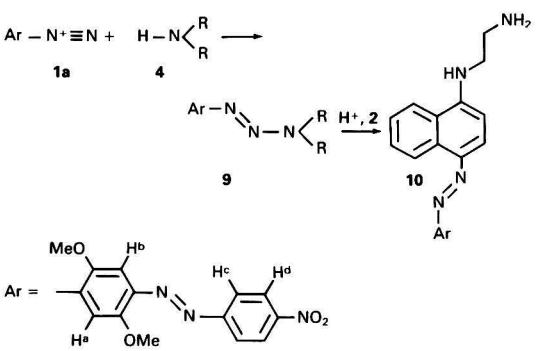

Scheme 1 Reaction of FBK with aliphatic secondary amines and subsequent coupling with *N*-(1-naphthyl)ethylenediamine (**2**)

used in the determination of sulfonamides and primary arylamines[4] and also of nitrite[5] by diazotization and coupling. On the other hand, the fact that 3,3-dialkyltriazenes in acidic medium behave like diazonium salts was already shown in the last century,[6] and this has been utilized in *Rapidogen*-type dyes.[7] However, the visualization of amines in TLC by use of the cleavage/coupling reaction is novel.

Poly(amines) showed characteristics of both primary and secondary amines as was expected. Visualization with **1a** and with the acid coupling treatment suggested a secondary amine structure, whereas the acid treatment suggested a primary amine structure.

Aromatic Primary Amines

Aromatic primary amines (**6**) were found to react with **1a** by *N*-coupling to produce red triazenes (**11**) (λ_{max} 485, 486 and 489 nm for **11a–c**, respectively) and by *C*-coupling to produce violet aminoazo compounds (**12**) (λ_{max} 535 nm for **12b**). *N*-Coupling was clearly favoured on the TLC plate, but in solution both *N*- and *C*-azo products formed. *C*-Coupling, predominantly at the *para*-position, was significant on the TLC plate only with compounds possessing ring-activating substituents in *meta*- or *ortho*-positions, especially with **6h**, but also with **6b** and to a lesser extent with **6f**. The compounds with ring-deactivating substituents (**6i–k**) reacted more weakly, and exclusively by *N*-coupling on the TLC plate. In

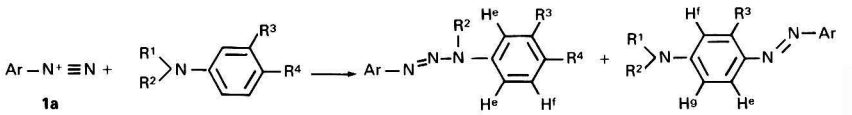

	R^1	R^2	R^3	R^4
6a	H	H	H	H
6b	H	H	Me	H
6c	H	H	H	Me
7a	H	Et	H	H
7b	H	Et	Me	H
8a	Me	Me	H	H
8b	Me	Me	H	Me

	R^2	R^3	R^4
11a	H	H^f	H^g
11b	H	Me	H^g
11c	H	H^f	Me
13a	Et	H^f	H^g
13b	Et	Me	H^g
15a	Me	H^f	H^g
15b	Me	H^f	Me

	R^1	R^2	R^3
12b	H	H	Me
14a	H	Et	H^e
14b	H	Et	Me
16a	Me	Me	H^e

Scheme 2 Reaction of FBK with arylamines

particular, the reactivity of the 4-nitro derivative (**6i**) was so weak that its native yellow colour remained dominant. Small amounts of **17** and **18** were formed from compounds with activating substituents (**6a–g**, but not **6h**).

The acid treatment produced, in most instances, an ochre colour, due to **18**, which formed in the degradation of the triazenes (**11**). The violet aminoazo derivatives (**12**) remained intact, but turned to blue–violet, which contributed to the colours from **6b**, **6f**, **6g** and **6h**. With compounds possessing ring-deactivating substituents, a violet colour developed first and turned then to ochre.

The acid coupling treatment produced variations of a brown–violet colour, consisting of an ochre yellow (**18**), a blue (**12**), and a blue–violet (from **6a–c**), a blue (from **6g**) or a violet (from **6j–k**) component. The latter components, which all had a yellow colour in basic medium, were probably from *C*-coupling between **2** and the diazonium salt from **6**. The compound **10** was not observed in the spots removed from the plate. However, if a pre-chromatographic derivatization procedure was used, **10** was observed because of an excess of intact **1a**.

Aromatic Secondary Amines

Aromatic secondary amines (**7**) were found to react with **1a** by *N*-coupling to produce red triazenes (**13**) (λ_{max} 482 and 489 nm for **13a–b**, respectively) and by *C*-coupling to produce violet aminoazo compounds (**14**) (λ_{max} 544 and 599 nm for **14a–b**, respectively). Again, *N*-coupling was favoured on the TLC plate, but in solution both *N*- and *C*-azo products formed. *C*-Coupling was significant on the TLC plate only with **7b**. The 4-nitro derivative (**7e**) was so unreactive that its native yellow colour remained dominant.

In the acid or acid coupling treatment the spots appeared similar to those obtained from aliphatic secondary amines. However, in the acid treatment, a different behaviour was observed with compounds capable of *C*-coupling. Because of small amounts of **14** present, a green shade (**7a**) or even a blue colour (**7b**) developed.

Aromatic Tertiary Amines

Aromatic tertiary amines (**8**) were found to react with **1a** by *C*-coupling to produce violet aminoazo compounds (**16**) (λ_{max} 546 nm for **16a**), as expected, but also by *N*-coupling, with a cleavage of an alkyl group, producing red triazenes (**15**) (λ_{max} 480 and 488 nm for **15a–b**, respectively). Again, *N*-coupling was favoured on the TLC plate, but in solution both *N*- and *C*-azo products formed.

This type of substitution reaction has previously been observed only under special conditions. Penton and Zollinger[8] observed the substitution of a methyl group of *N,N*-dimethylaniline by 4-methoxybenzenediazonium tetrafluoroborate in anhydrous acetonitrile. Colonna *et al.*[9] reported a similar mono-demethylation of 4-acetyl-*N,N*-dimethylaniline with 4-nitrobenzenediazonium chloride in aqueous solution, while no such reaction was observed with the other five *N,N*-dimethylanilines studied.

The acid or acid coupling treatment resulted in colours similar to those obtained with aromatic secondary amines, as was expected.

The *N*-coupling reaction of dialkylanilines on the TLC plate with different diazonium salts is of a general nature. *N,N*-Dimethyl-*p*-toluidine (**8b**) was the most reactive, followed by *N,N*-dimethylaniline (**8a**) and *N*-ethyl-*N*-methylaniline (**8d**). With **8d** it was the methyl group that was substituted. *N,N*-Diethylaniline (**8e**) reacted poorly, indicating that ethyl groups are not substituted as easily as methyl groups. *N,N*-Dimethyl-2,4,6-trimethylaniline (**8c**) was fairly unreactive, probably because of steric hindrance due to the *ortho*-methyl groups. Significant *C*-coupling was observed with **8e** and **8d**. An exact comparison of the reactivities of the diazo components (**1**) was not possible, but it appeared that the more electrophilic 4-nitro-substituted diazonium salts (**1a–d**) produced more triazenes than the others. The behaviour of **1c** and **1d** was identical. The colours of the *C*-azo dyes after the acid coupling treatment from **1a–h** were greenish blue, violet, violet, violet, blue–violet, blue, blue and blue, respectively.

Spectral Considerations

The UV/VIS maxima and the observed colours indicate a clear difference between the red triazenes and the violet aminoazo compounds. An exception is the triazene **17**, which has a violet colour[1] because of extensive conjugation. The highly conjugated aminoazo compound **10** has a distinctive greenish blue colour.

Triazenes and aminoazo compounds can be readily differentiated by their ^1H NMR spectra. The 1,3-diaryltriazenes showed an NH signal at about 10 ppm, and the 3-alkyl-1,3-diaryltriazenes showed a CH_2N or a CH_3N signal at 4.4 and 3.8 ppm, respectively. The 4-aminoazo compounds, on the other hand, showed two high-field aromatic protons.

The mass spectra of the 1,3-diaryltriazenes **11a** and **11c** revealed extensive fragmentation. These compounds were also unstable when allowed to dry on the silica gel plate. The *m*-tolyl-substituted compound (**11b**), however, was more stable and showed a molecular ion of low abundance and an abundant $[M - N_2]$ ion. The 3-alkyl-1,3-diaryltriazenes showed both an M^+ and an $[M - N_2]$ ion in various proportions. The aminoazo compounds showed an abundant M^+ without an $[M - N_2]$, in contrast to the triazenes.

Phenols and Heterocyclic Compounds

Phenols, resorcinols and heterocyclic compounds usually produce violet colours with **1a**.[1,10] These colours are apparently due to *C*-azo coupling products and turn to blue–violet,

similarly to the aminoazo compounds, in the acid or acid coupling treatment. Compounds possessing a phenolic hydroxy and an aliphatic amino group can produce mixed colours with **1a**,[10] but behave like phenols in the acid or acid coupling treatment.

Drug Analysis

With the acid coupling treatment, the identification power of TLC drug screening procedures can be significantly enhanced compared with use of **1a** alone. In particular, the differentiation of aromatic primary amines and phenols from each other and from other amines is now possible. To take some specific examples from a screening of amphetamine derivatives,[10] the differentiation of previously poorly resolved drugs such as amphetamine from nomifensine, chlorphentermine from labetalol and metoclopramide, fencamfamin from oxypertine, methoxyphenamine from carbutamide, and 3,4,5-trimethoxyamphetamine from pindolol is now possible by colour. Fortunately, there are few aromatic secondary amine drugs and the aromatic tertiary amine structures encountered in drugs (*e.g.*, imipramine) are generally unreactive with **1a**.

An improvement can also be obtained in the detection sensitivity for secondary amines by using the acid coupling treatment. Following the TLC method described previously,[1] detection limits of 0.01 and 0.04 μg were obtained for methamphetamine and methyl phenidate, respectively. These values are five times lower than those obtained with **1a** alone.[1] To obtain a high sensitivity, however, the visualization procedure described above should be strictly followed in order to decompose the excess of FBK, which causes a blue background, with NaOH and heat.

Conclusions

The sequential use of **1a** and one of the detection procedures described allows rapid, sensitive and inexpensive characterization of amines on the TLC plate. In particular, the structures often encountered in drug substances, *i.e.*, aliphatic primary, secondary and tertiary amines, aromatic primary amines, and phenols, can in most instances be readily differentiated from each other by utilizing the acid coupling treatment. The reaction of dialkylanilines with cleavage of an alkyl group was found to be of a more general nature than has been previously supposed. Pre-chromatographic derivatization on the TLC plate, with use of an automatic TLC sampler and subsequent chromatography, was found to be an ideal way of studying the present type of reaction. This method, involving the acid or acid coupling treatment, can also be used for the characterization of pure unknown amines.

The authors thank Jorma Matikainen for running the mass spectra.

References

1 Ojanperä, I., Wähälä, K., and Hase, T. A., *Analyst*, 1990, **115**, 263.
2 Dalla Croce, P., La Rose, C., and Riticni, A., *J. Chem. Res. (S)*, 1988, 346.
3 Zollinger, H., *Color Chemistry*, VCH, Weinheim, 1987, p. 106.
4 Bratton, A. C., and Marshall, E. K., Jr., *J. Biol. Chem.*, 1939, **128**, 537.
5 Jungreis, E., *Spot Test Analysis*, Wiley, New York, 1985, p. 27.
6 Wallach, O., *Liebigs Ann. Chem.*, 1886, **235**, 233.
7 Saunders, K. H., and Allen, R. L. M., *Aromatic Diazo Compounds*, Edward Arnold, London, 3rd edn., 1985, p. 409.
8 Penton, J. R., and Zollinger, H., *Helv. Chim. Acta*, 1981, **64**, 1728.
9 Colonna, M., Greci, L., and Poloni, M., *J. Chem. Soc., Perkin Trans. 2*, 1982, 455.
10 Ojanperä, I., Lillsunde, P., Vartiovaara, J., and Vuori, E., *J. Planar Chromatogr.*, 1991, **4**, 373.

Paper 2/01738E
Received April 2, 1992
Accepted June 8, 1992

Gas Chromatographic Determination of Airborne Organic Acids *via* Their Anilides

Kusum Vohra and Virindar S. Gaind
Occupational Health Laboratory, Ontario Ministry of Labour, 101 Resources Road, Weston, Ontario, Canada M9P 3T1

A gas chromatographic method was developed for the determination of airborne acetic, propionic and butyric acids collected on sampling tubes containing charcoal. On treatment with thionyl chloride followed by aniline, the acids yielded the corresponding anilides, which were quantified by gas chromatography with either flame-ionization or nitrogen–phosphorus detection. The anilides are stable and provide enhanced sensitivity of detection. The characteristic mass spectra of the anilides provide unequivocal structural confirmation of the identity and can also be used for highly sensitive quantification by selected-ion monitoring. The proposed procedure can be used to detect acetic, propionic and butyric acids at levels of 5 and 1 μg using flame-ionization and nitrogen–phosphorus detection, respectively, for a 60 dm^3 air sample.

Keywords: *Airborne carboxylic acid determination; anilide derivative; gas chromatography*

Acetic acid (AA) and propionic acid (PA) are commonly used in the food and plastics industries. Short-term exposure to air containing 125 mg m^{-3} of these acids can cause significant irritation to the eyes and the respiratory passage. The American Conference of Governmental Industrial Hygienists has adopted a threshold limit value–time weighted average (TLV–TWA) of 25 mg m^{-3} for AA and 30 mg m^{-3} for PA.[1] Air monitoring at these levels requires a sensitive and specific procedure.

There are several methods available for the analysis of airborne carboxylic acids which involve passage of air through an alkaline solution (impinger) or an air sampling tube with subsequent elution by an alkali. The solution is analysed for the acetate ion by ion chromatography.[2] However, the ion chromatographic procedure is fraught with the possibility of false positives owing to interferences, and confirmation by mass spectrometry (MS) is not available. Other procedures reported for the determination of acids include direct gas chromatography (GC)[3] and esterification followed by GC[4] or headspace GC.[5] The polar carboxylic acids are not suitable for direct GC analysis, particularly at low levels. The methyl esters of these acids, obtained by treatment with diazomethane or a methanol–sulfuric acid mixture, yield low relative molecular mass esters.[6] These esters are volatile and give mass spectra without prominent molecular ions which could be used for confirmation or quantification. Gas chromatography of carboxylic acids as *tert*-butyldimethylsilyl derivatives has also been reported.[7] The National Institute of Occupational Safety and Health (NIOSH) has published a GC procedure in which airborne acids are collected on charcoal tubes, desorbed with formic acid and analysed by GC with flame-ionization detection.[8] We found that the lower level of detection for AA was 100 μg and that formic acid was generally contaminated with AA.

This paper describes a highly sensitive and specific procedure for sampling and analysing three airborne carboxylic acids, *i.e.*, AA, PA and butyric acid (BA). The procedure is based on the derivatization reaction shown in Fig. 1 and reported previously by Umeh.[9] The efficiency of various sampling media was also evaluated.

Experimental

Reagents

Carboxylic acids (AA, PA and BA), aniline and thionyl chloride were supplied by Aldrich (Milwaukee, WI, USA); sodium sulfate (anhydrous) and sodium hydrogen carbonate were of analytical-reagent grade and were obtained from BDH (Toronto, Ontario, Canada). All solvents were of glass-distilled quality and were purchased from Caledon Laboratory (Georgetown, Ontario, Canada). Ethyl acetate was dried over anhydrous sodium sulfate prior to use. A fresh solution of aniline (10% v/v) was prepared in ethyl acetate each working day.

Sodium hydrogen carbonate solution (1 mol dm^{-3}) was prepared by dissolving 8.4 g of sodium hydrogen carbonate in 100 cm^3 of de-ionized water. A stock solution of methyl stearate (10 mg cm^{-3}) was prepared in ethyl acetate and diluted 50-fold (200 μg cm^{-3}) for use as an internal standard (IS) in the GC-FID analysis and mass spectrometric quantification.

Instrumentation and Chromatographic Analysis

A Hewlett-Packard (HP) (Avondale, PA, USA) 5880A gas chromatograph equipped with a flame-ionization detector, a GC terminal and a fused-silica capillary column (25 m × 0.2 mm i.d.) with a film thickness of 1 μm [J & W Scientific (Folsom, CA, USA) DB-5, cross-linked 5% phenyl silicone gum phase] was used. The carrier and make-up gas was He, with flow rates of 1.2 and 30 cm^3 min^{-1}, respectively. The initial temperature of the oven was held at 100 °C for 1 min, then raised at a rate of 10 °C min^{-1} to a final temperature of 280 °C. The temperature of the injector and detector was kept at 220 and 250 °C, respectively. The analyses by capillary GC with nitrogen–phosphorus detection (NPD) were carried out on an HP 5890 gas chromatograph with an HP 3396A

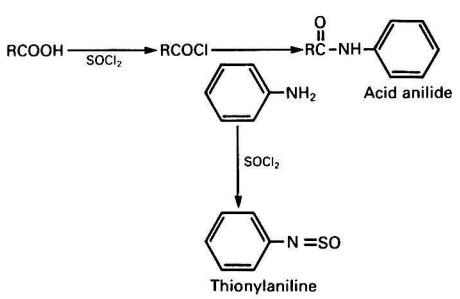

R = CH_3 (acetic acid)
R = CH_2CH_3 (propionic acid)
R = $CH_2CH_2CH_3$ (butyric acid)

Fig. 1 Derivatization reaction of acids

terminal, an HP 7673A autosampler and an HP-1 megabore column (5 m × 0.53 mm i.d., 2.65 μm methyl silicone gum). The carrier gas was helium at a flow rate of 2.0 cm^3 min^{-1}. The initial temperature of the oven was held at 100 °C for 1 min, and then raised at a rate of 10 °C min^{-1} to a final temperature of 250 °C.

The mass spectra were obtained on an HP 5985B GC–MS system equipped with an HP 7920 data system. The GC parameters were identical with those of the HP 5880A instrument. The mass spectrometer was operated in the electron impact mode at 70 eV with the ion source temperature at 200 °C.

Derivatization Procedure

The adsorbent from the front and back-up sections of the sampling tube was transferred into separate 8 cm^3 screw-capped tubes, followed by the addition of 100 mm^3 of ethyl acetate and 100 mm^3 of thionyl chloride. The tubes were agitated at room temperature for 5 min followed by the addition of 500 mm^3 of the aniline solution. The tubes were again agitated for 5 min and then heated at 65 °C for 10 min using a heating block. After cooling in an ice-bath for 2 min, 5 cm^3 of 1 mol dm^{-3} $NaHCO_3$ solution were added gradually followed by 500 mm^3 of the methyl stearate solution. The contents of the tubes were mixed with a vortex mixer and the upper organic layer was transferred into a 1.5 cm^3 screw-capped vial containing approximately 50 mg of anhydrous sodium sulfate. Calibration standards were prepared by spiking known amounts of each acid on charcoal and processing together with the samples.

Quantification was carried out by using the internal standard calibration technique for FID.

For analysis by NPD, the final ethyl acetate extract was washed with 0.5 cm^3 of 1 mol dm^{-3} HCl before injection into the gas chromatograph. Quantification in this instance was carried out by external standard calibration.

Sampling Equipment

The air sampling tubes (charcoal, Cat. No. 226-01, and silica gel, Cat. No. 226-10) were from SKC (Eighty Four, PA, USA), and the Orbo-70 tubes were kindly supplied by Supelco (Oakville, Ontario, Canada). Bendix Model 44A portable air-sampling pumps were used. The Test Atmosphere Generation System (TAGS) was manufactured by SRI (Menlo Park, CA, USA) and was used for generating a uniformly loaded test atmosphere containing the three acids.

Preliminary Evaluation of Various Sorbents for the Retention and Recovery of Spiked Acids

Three commercially available sorbents, *i.e.*, charcoal, silica gel and Orbo-70, were evaluated for the recovery of AA, PA and BA. Six tubes of each sorbent were spiked with 50 μg of AA, PA and BA. Air (10 dm^3) was pased through each of the tubes at a flow rate of 0.1 dm^3 min^{-1}. After derivatization, the spiked acids on each tube were quantified and the results expressed as mean percentage recovery (Table 2).

Evaluation of the Efficiency of Sample Collection From a Dynamically Generated Atmosphere of Acids

A test atmosphere containing AA, PA and BA was generated dynamically in the TAGS to evaluate the sampling efficiency of charcoal, which showed optimum recovery in the spiking tests. A mixture containing equal volumes of the three acids was placed in the sampling bulb of the TAGS. A carrier stream of nitrogen with a flow rate of 0.1 dm^3 min^{-1} was passed over the mixed acids kept at room temperature and further diluted with air at a flow rate of 60 dm^3 min^{-1} in the mixing chamber. Each of the 12 sampling ports of the TAGS was fitted with a precise critical orifice permitting a flow rate of 1 dm^3 min^{-1}. After equilibration for 30 min, the sampling tubes were attached to the ports and the airborne acids collected for 60 min. The front and back-up sections of each tube were analysed separately to check for any breakthrough.

Results and Discussion

GC Analysis

A typical GC-FID trace showing resolution of the anilides of AA, PA and BA is illustrated in Fig. 2 for a 1.0 mm^3 injection containing 100 ng of each acid. The retention times for the three anilides are 11.73, 12.88 and 14.02 min. Two additional peaks at 5.75 and 7.65 min were observed in all the chromatograms including those from the blanks; these were identified by electron impact MS as aniline and *N*-thionylaniline, respectively. The latter is a condensation product of thionyl chloride and aniline (Fig. 1). All the peaks were well resolved from the derivative peaks of the acids and caused no interference in the FID analysis. When using NPD, the interference from aniline and *N*-thionylaniline was minimized by agitating the reaction mixture with dilute HCl. This treatment converted the excess of aniline and *N*-thionylaniline into their water-soluble hydrochlorides.

Sensitivity and Linearity

The lowest detection levels of AA, PA and BA, detected as their anilides, were 5 μg each when using FID. Nitrogen–phosphorus detection was more sensitive and could detect 1 μg of each acid while quantification by selected-ion monitoring (SIM) using GC–MS was possible for 0.1 μg of the derivatized acids. By using a 60 dm^3 air sample, it is feasible to quantify these acids at air concentrations lower than one-tenth of the TLV–TWA levels when using FID and at still lower concentrations when using NPD.

The response of the flame-ionization detector to the anilide derived from PA was found to be linear up to 200 μg cm^{-3} with a correlation coefficient of 0.9984.

When quantifying PA by NPD, the linearity range was from 1 to 50 μg with a correlation coefficient of 0.9986.

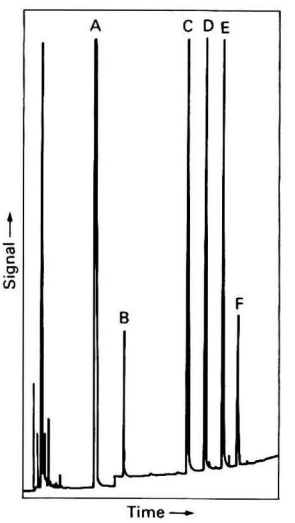

Fig. 2 Chromatographic separation of anilides derived from acids. Retention time: A, 5.75; B, 7.65; C, AA, 11.73; D, PA, 12.88; E, BA, 14.02; and F, IS, 15.03 min

Table 1 Precision data for the anilides of the acids (10 μg each)

No.	Standard : IS ratio (peak areas) AA	PA	BA
1	0.10	0.10	0.15
2	0.09	0.10	0.14
3	0.09	0.10	0.14
4	0.09	0.09	0.14
5	0.09	0.10	0.15
6	0.09	0.09	0.15
7	0.09	0.10	0.15
8	0.09	0.10	0.14
9	0.10	0.10	0.16
10	0.10	0.10	0.15
Mean:	0.09	0.10	0.15
Relative standard deviation (%):	5.4	4.3	4.7

Table 2 Mean recovery (%) of spiked acids (50 μg each)

Adsorbent	AA	PA	BA
Orbo-70	92	96	93
Charcoal	100	108	109

Table 3 Amounts of acids (μg) collected on charcoal tubes through TAGS

No.	AA	PA	BA
1*	330	180	50
2	250	140	40
3	240	150	40
4	250	150	40
5	270	160	50
6	260	150	40
Mean:	254	150	42
Relative standard deviation (%):	4.5	4.7	10

* Data not considered in calculation.

Precision

The precision of the FID analysis of replicates (n = 10) of a mixture of AA, PA and BA at a level of 10 μg of each acid is illustrated in Table 1, which shows the ratios of the peak areas of the anilide to the peak areas of the internal standard after derivatization. The relative standard deviation obtained indicates that the precision is adequate.

Evaluation of Various Sorbents for Recovery of Spiked Acids

The recovery of the acids from silica gel was very poor (<10%). The recoveries of the acids spiked on charcoal and Orbo-70 sorbents are summarized in Table 2.

Charcoal and Orbo-70 gave nearly quantitative recoveries with no breakthrough. However, the work-up of the spiked charcoal tubes was cleaner and easier compared with that of the Orbo-70 tubes. Consequently, the evaluation of sample collection from a dynamically generated atmosphere of the acids was performed on tubes containing charcoal only.

Evaluation of the Efficiency of Sample Collection From a Dynamically Generated Atmosphere of Acids

Table 3 shows the amounts of AA, PA and BA found on each tube when a dynamically generated mixture of the three acids was collected on charcoal sampling tubes.

No traces of the analytes were found in the back-up section of the tubes, showing that charcoal is an efficient adsorbent for the collection of airborne aliphatic acids for sampling rates of up to 1 dm^3 min^{-1}.

The average amounts of AA, PA and BA collected on the charcoal tubes were 254, 150 and 42 μg with relative standard deviations of 4.5, 4.7 and 10%, respectively.

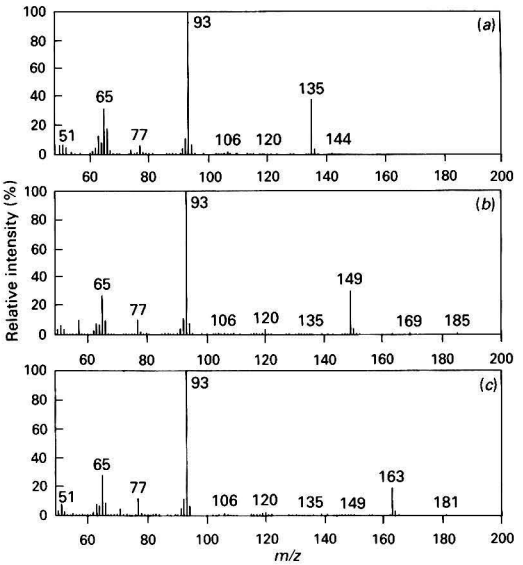

Fig. 3 Electron impact mass spectra of the anilides derived from (*a*) AA, (*b*) PA and (*c*) BA

The test atmosphere generated represents air concentrations of 4.2, 2.5 and 0.7 mg m^{-3}, respectively, for AA, PA and BA.

The difference in the amounts of the three acids collected when sampling a dynamically generated atmosphere reflects the decreasing order of the vapour pressures of AA, PA and BA.

Mass Spectra of the Anilide Derivatives

The electron impact mass spectra of the anilide derivatives of AA, PA and BA are shown in Fig. 3. Although all three anilides show m/z = 93 as the base peak, the molecular ions at m/z = 135, 149 and 163 show an abundance of 39, 36 and 21% for the anilides of AA, PA and BA, respectively, and these can be used for quantification by SIM.

Conclusions

Air sampling for AA, PA and BA can be carried out by drawing air at a flow rate of 1 dm^3 min^{-1} for 1 h through sampling tubes containing charcoal without any breakthrough. The adsorbent is used directly in the derivatization procedure, thereby eliminating the extraction step. The resulting anilide derivatives are stable and can be quantified by GC using FID or NPD.

The authors thank Dr. M. A. Nazar, Chief Scientist, Occupational Health Laboratory of the Ontario Ministry of Labour, for helpful suggestions during preparation of the manuscript.

References

1 *Threshold Limit Values and Biological Exposure Indices for 1988–1989*, American Conference of Governmental Industrial Hygienists, Cincinnati, OH, 1988.
2 Hekmat, M., and Smith, R. G., *Am. Ind. Hyg. Assoc. J.*, 1991, **52**, 332.

3 Jackson, R. B., *J. Chromatogr.*, 1966, **22**, 261.
4 Di Corcia, A., *Anal. Chem.*, 1973, **45**, 492.
5 William, K. E., and Majur, J. F., *Am. Ind. Hyg. Assoc. J.*, 1980, **41**, 1.
6 Oakley, E. T., Weissbecker, L., and Resnik, E., *Anal. Chem.*, 1965, **37**, 380.
7 Kim, K. R., Zlatkis, A., Horning, E. C., and Middleditch, B. S., *J. Chromatogr.*, 1989, **468**, 289.
8 *NIOSH Manual of Analytical Methods*, NIOSH Publication No. S169, US Government Printing Office, Washington, DC, 2nd edn., 1977, vol. 4.
9 Umeh, E. O., *J. Chromatogr.*, 1970, **51**, 147.

Paper 2/01367C
Received March 16, 1992
Accepted May 19, 1992

Determination of Ethoxyquin and Two of Its Oxidation Products in Fish Meal by Gas Chromatography

Adrianus J. de Koning and Gretel van der Merwe
Fishing Industry Research Institute, Lower Hope Street, Rosebank 7700, South Africa

A gas chromatographic procedure for the determination of the antioxidant ethoxyquin (EQ) in fish meals using methoxyquin as internal standard is described. Recoveries of EQ from spiked meals ranged from 95 to 107%. Comparison of the results obtained with the proposed method and those given by a method applied on a routine basis using chromatography on alumina shows that the results obtained with the latter method should, on average, be corrected by multiplication by a factor of 1.1 when dealing with meals having EQ contents above approximately 30 mg kg^{-1}. Meals with EQ contents of less than 30 mg kg^{-1} yield values by chromatography on alumina which are too high. In addition, gas chromatographic methods for the determination of two oxidation products of EQ, *viz.*, a dimeric oxidative coupling product and a quinolone, are described. The progressive decrease of EQ and the simultaneous formation of the two oxidation products on storage of five fish meals is demonstrated.

Keywords: *Fish meal; ethoxyquin; methoxyquin; ethoxyquin dimer; quinolone*

1,2-Dihydro-6-ethoxy-2,2,4-trimethylquinoline (**1**), commonly known as ethoxyquin (EQ), is used extensively as an antioxidant in fish meal to protect the highly unsaturated residual lipids in the meal.[1,2] In South African and Namibian fish meals EQ is normally added at a level of 400 mg kg^{-1}, whereas in South American meals it can exceed levels of 1000 mg kg^{-1}.

Ethoxyquin is determined on a routine basis in this Institute by separating it in a hexane extract of the meal from other hexane-soluble compounds by chromatography on alumina. The progress of the separation is monitored with an ultraviolet (UV) lamp as EQ is strongly fluorescent. After dilution, the amount of EQ is determined spectrophotometrically at 362 nm.[1]

The fate of EQ in fish meals was not known until Thorisson[3] showed that oxidation of EQ with *tert*-butylhydroperoxide leads to the formation of two compounds, *viz.*, a dimeric oxidative coupling product, 1,8′-di-(1,2-dihydro-6-ethoxy-2,2,4-trimethylquinoline) (**2**, EQ-dimer), and a quinolone, 2,6-dihydro-2,2,4-trimethyl-6-quinolone (**3**).

It was claimed by Thorisson[3] that the EQ-dimer (**2**) showed no antioxidant activity, whereas the quinolone (**3**) was only slightly less active than EQ. It was also found that both the EQ-dimer and the quinolone were present in a fish meal treated with EQ after storage for 1 week at ambient temperature.

In view of these results it was questionable whether the above procedure for the determination of EQ was sufficiently specific to distinguish it from the EQ-dimer and the quinolone. Hence, a gas chromatographic method using methoxyquin, 1,2-dihydro-6-methoxy-2,2,4-trimethylquinoline (**4**, MQ), as internal standard was developed and the results obtained by this method were compared with those of the routine procedure. In addition, the decrease in EQ during storage of a number of fish meals and the simultaneous formation of the EQ-dimer and the quinolone was demonstrated.

Gas chromatographic methods for the determination of EQ have been described[4–6] but these methods do not use MQ as internal standard and no analysis for the oxidation products of EQ has been carried out.

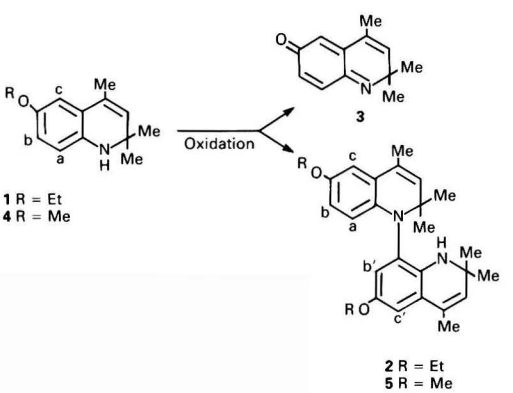

1 R = Et
4 R = Me

3

2 R = Et
5 R = Me

Experimental

Apparatus and Reagents

Ultraviolet spectra in hexane were recorded with a Varian Superscan 3 spectrophotometer and the molar absorptivity (ε) was calculated at the maximum absorption.

Elemental analyses were carried out with a Heraeus universal composition analyser.

Gas chromatography was carried out on a Hewlett-Packard 5710A gas chromatograph using a 15 m fused silica capillary column with an i.d. of 0.25 mm having a DB-1 liquid phase coating and using hydrogen as carrier gas.

Proton nuclear magnetic resonance (^{1}H NMR) spectra were recorded in $CDCl_3$ solution on a Varian VXR 200 superconducting spectrometer with tetramethylsilane (TMS) as internal standard.

All chemicals used were of analytical-reagent grade.

Fish Meals

Meals treated or not treated with EQ were obtained from a local fish meal factory. They were transported to the Institute in polypropene buckets where they were stored, after pure EQ had been added to untreated meals (see ref. 1), at 25 or 70 °C.

Preparation of Compounds

Ethoxyquin (**1**)

Pure EQ was obtained by distillation of a commercial product under high vacuum as described elsewhere.[7] It was obtained as a yellow fluorescent oil, n_D^{20} = 1.5734.

Methoxyquin (**4**)

Methoxyquin was synthesized from 4-methoxyaniline and acetone in the presence of a catalytic amount of iodine.[8] It was obtained as a yellow fluorescent oil, $n_D^{20} = 1.5843$.

1,8′-*Di*-(1,2-*dihydro*-6-*ethoxy*-2,2,4-*trimethylquinoline*) (**2**) *and* 2,6-*dihydro*-2,2,4-*trimethyl*-6-*quinolone* (**3**) *from EQ*

The EQ-dimer (**2**) and the quinolone (**3**) were prepared by oxidation of EQ with *tert*-butylhydroperoxide essentially as described by Thorisson.[3] The EQ-dimer was obtained in 36% yield as khaki fluorescent crystals, m.p. 108–109 °C (literature value[3] 107–109 °C). Ultraviolet in hexane: $\varepsilon_{375\ nm}$ = 8263 dm^3 mol^{-1} cm^{-1} [literature value[3] in light petroleum (40–60 °C boiling range): $\varepsilon_{380\ nm}$ = 5370 dm^3 mol^{-1} cm^{-1}]. The quinolone was obtained in 14% yield as a brown non-fluorescent material, m.p. 54–56 °C (literature value[3] 52–53.5 °C). Ultraviolet in hexane: $\varepsilon_{345\ nm}$ = 5386 dm^3 mol^{-1} cm^{-1} (literature value[3] in ethanol: $\varepsilon_{364\ nm}$ = 6610 dm^3 mol^{-1} cm^{-1}).

1,8′-*Di*-(1,2-*dihydro*-6-*methoxy*-2,2,4-*trimethylquinoline*) (**5**) *and* 2,6-*dihydro*-2,2,4-*trimethyl*-6-*quinolone* (**3**) *from MQ*

The MQ-dimer (**5**) was prepared by oxidation of MQ in a similar way to the preparation of the EQ-dimer. The MQ-dimer was isolated in 23% yield as yellow fluorescent crystals, m.p. 108–109 °C. Proton NMR ($CDCl_3$, 200 MHz): δ 0.96 (3 H, s), 1.16 (3 H, s), 1.21 (3 H, s), 1.29 (3 H, s), 1.99 (3 H, d, J = 1.40 Hz), 2.06 (3 H, d, J = 1.40 Hz), 3.73 (3 H, s), 3.75 (3 H, s), 4.03 (1 H, s, NH), 5.37 (1 H, d, J = 1.40 Hz), 5.45 (1 H, d, J = 1.30 Hz), 6.07 (1 H, d, J = 8.85 Hz, H^a), 6.50 (1 H, d of d, J = 8.85 and 2.93 Hz, H^b), 6.67 (1 H, d, J = 2.76 Hz, H^c), 6.71 (1H, d, J = 2.73 Hz, H$^{c'}$) 6.75 (1 H, d, J = 2.90 Hz, H$^{b'}$). Ultraviolet in hexane: $\varepsilon_{375\ nm}$ = 8349 dm^3 mol^{-1} cm^{-1}. [Found: C, 77.1; H, 7.6; N, 7.0. Calc. for $C_{26}H_{32}N_2O_2$ (404.56): C, 77.19; H, 7.97; N, 6.93%.]

The quinolone (**3**) was isolated in 17% yield.

Antioxidant Properties of the EQ-dimer (2) and the Quinolone (3)

In order to establish whether the EQ-dimer and the quinolone possess antixodant properties they were tested together with EQ in fish oil by the active oxygen method as described previously.[8]

Determination of EQ in Fish Meal

Ethoxyquin was determined in fish meals by two procedures.

Column chromatography on aluminium oxide followed by spectrophotometry

A column of alumina (Grade IV, Brockmann; 10 × 2 cm) was prepared in hexane in a glass tube (30 × 2 cm) with a sintered glass disc and a tap. Anhydrous sodium sulfate was added to a depth of 2 cm above the alumina and the glass tube was filled with hexane to about 8 cm from the top.

A 5.0 g amount of fish meal was poured onto the top of the column, the tap was opened and the hexane allowed to run until it was about 2 mm from the top of the meal. A total of 50 cm^3 of hexane was used to elute the EQ from the meal onto the alumina and the collected hexane was discarded. Ethoxyquin was then eluted with hexane–diethyl ether (9 + 1 v/v). The progress of the elution was followed with a UV lamp, and just before the fluorescent band reached the end of the column the eluate was collected in a 100 cm^3 calibrated flask. All the EQ was collected, the volume made up to 100 cm^3 with hexane and the absorbance read at 362 nm. The amount of EQ in mg cm^{-3} was found by multiplying the absorbance at 362 nm by 0.067[7] (and not 0.074[1]). With older meals it was frequently possible to distinguish a light blue fluorescent band below EQ. This band, which consists of the EQ-dimer (**2**) (see above), was always separated as effectively as possible from the EQ.

Gas chromatography using MQ as internal standard

To 5.0 g of fish meal was added a small amount (1–3 mg) of accurately weighed MQ. This was performed conveniently by using a small finely drawn glass capillary and weighing on a five decimal place balance. The meal was treated with 50 cm^3 of hexane and the mixture warmed on a water-bath until it just boiled, whereupon the hexane was filtered into a 250 cm^3 separating funnel. The extraction was repeated twice and 50 cm^3 of 1 mol dm^{-3} hydrochloric acid were added to the combined hexane extracts. After vigorous shaking, the lower layer was removed and the extraction repeated twice. The combined aqueous layers were made alkaline by the addition of about 15 g of sodium hydroxide pellets while cooling under running tap water. The alkaline solution was extracted with three 50 cm^3 portions of hexane; the combined hexane extracts were washed once with water and dried over anhydrous sodium sulfate. After filtration, the hexane was evaporated using a water jet pump on a rotary evaporator (temperature below 60 °C) and the residue taken up in a small volume (about 0.5 cm^3) of isooctane. This solution was injected into the gas chromatograph. The temperature was programmed from 100 to 150 °C rising at 4 °C min^{-1} while the injection port remained at 200 °C. Quantification was carried out with a Spectra-Physics 4270 integrator. A minimum of three injections were routinely carried out and the mean was calculated.

The procedure was checked on a matured untreated meal spiked with EQ in the range 150–850 mg kg^{-1}.

Chromatographic Properties of the EQ-dimer (2), the Quinolone (3) and EQ on Alumina

The following experiments were carried out to determine whether the EQ-dimer and the quinolone were sufficiently separated on alumina in the routine determination of EQ.

Separation of the EQ-dimer (**2**) *and EQ*

(*i*) A mixture of 1.06 mg of the dimer and 1.94 mg of EQ was placed on a column of active alumina (Grade I, 10 × 2 cm) dissolved in 2 cm^3 of hexane. Elution with hexane and hexane–diethyl ether (50 + 1 v/v) failed to elute any fluorescent material. Elution with 100 cm^3 of hexane–diethyl ether (4 + 1 v/v) eluted the dimer, as was evident from its absorption maximum at 375 nm. The absorbance at 375 nm of the 100 cm^3 solution was 0.190, corresponding to 0.99 mg (93%) of the EQ-dimer.

Elution with 100 cm^3 of diethyl ether yielded EQ. The absorbance of this solution at 362 nm was 0.252, corresponding to 1.68 mg (87%) of EQ.

(*ii*) A mixture of 0.95 mg of the dimer and 2.37 mg of EQ was separated on alumina (Grade IV, 10 × 2 cm) with hexane–diethyl ether (9 + 1 v/v) as in the normal routine determination of EQ. Separation, although more difficult to achieve than with Grade I alumina, was possible. The dimer solution (100 cm^3) had an absorbance at 375 nm of 0.158, which corresponds to 0.83 mg (87%) of the dimer. The EQ solution (100 cm^3) had an absorbance of 0.308 at 362 nm, corresponding to 2.06 mg of EQ (87%).

Separation of the quinolone (**3**) *and EQ*

A mixture of 1.09 mg of the quinolone and 1.20 mg of EQ was placed on a column of deactivated alumina (Grade IV). The fluorescent material was eluted with a mixture of hexane–diethyl ether (9 + 1 v/v) and collected in a 100 cm^3 calibrated flask. The absorbance at 362 nm was 0.159, corresponding to 1.07 mg of EQ (89%). Elution with hexane–diethyl ether (3 + 7 v/v) eluted the yellow quinolone band which was collected in

a 50 cm^3 calibrated flask. The absorbance at 345 nm was 0.550, corresponding to 0.96 mg of the quinolone (88%).

Determination of the EQ-dimer (2) by Gas Chromatography

The EQ-dimer content of a meal was determined by separating the dimer together with EQ from other hexane-soluble compounds using chromatography on alumina. The resulting solution was treated with the MQ-dimer (**5**) as internal standard and the mixture analysed by gas chromatography.

A 5.0 g amount of a fish meal was poured onto the top of a column of alumina (Grade IV, 10 × 2 cm) in hexane and all the fluorescent material eluted with hexane–diethyl ether (9 + 1 v/v). To this solution was added an accurately weighed amount of the MQ-dimer (1–2 mg weighed on a five decimal place balance). The solvent was evaporated on a rotary evaporator (temperature below 60 °C) and the residue taken up in about 0.5 cm^3 of isooctane. This solution was injected into the gas chromatograph with the temperature being programmed from 100 to 250 °C rising at 16 °C min^{-1} while the injection port remained at 200 °C. The method was verified on an untreated meal spiked with the EQ-dimer in the range 50–400 mg kg^{-1}.

Determination of the Quinolone (3) by Gas Chromatography

The quinolone was determined in the sample of meal that was analysed for EQ. This means, therefore, that MQ was used as internal standard in the determination of the quinolone. The recovery of the quinolone was determined in meals spiked in the range 10–300 mg kg^{-1}.

Results and Discussion

Synthesis of the EQ-dimer (2), the MQ-dimer (5) and the Quinolone (3)

The preparation of the EQ-dimer and the quinolone from EQ proceeded as described by Thorisson.[3]

The structure of the MQ-dimer (**5**) follows unambiguously from its preparation and its 200 MHz ^1H NMR spectrum which, like its EQ counterpart, had a broad NH signal integrating for one proton at 4.03 ppm and a coupling constant of approximately 2.8 Hz for aromatic protons $H^{b'}$ and $H^{c'}$.

Antioxidant Properties

Fish oil treated with either EQ, the EQ-dimer (**2**) or the quinolone (**3**) at the 0.01% level gave induction times at 50 °C of 23.4 h (EQ), 8.2 h (EQ-dimer), 17.4 h (quinolone) and 4.5 h (control). These results are noteworthy. The dimer, for instance, is expected to have an induction time of about half that of EQ (11.7 h), as it has only one intact EQ residue with an NH group and is twice the relative molecular mass of EQ. The value of 8.2 h is reasonably close to the calculated value of 11.7 h, from which it can be deduced that the EQ-dimer has approximately one-third of the antioxidant activity of EQ. It is, however, surprising that Thorisson[3] claims that the EQ-dimer has no antioxidant activity. The quinolone has, unexpectedly, a very marked activity which is approximately three-quarters of that of EQ.

Interference of the EQ-dimer (2) and the Quinolone (3) in the Determination of EQ

The UV/VIS spectra of EQ, the EQ-dimer and the quinolone are shown in Fig. 1. These spectra clearly show a large degree of overlap and both the dimer and the quinolone, unless they are separated from EQ, will interfere with the determination of EQ.

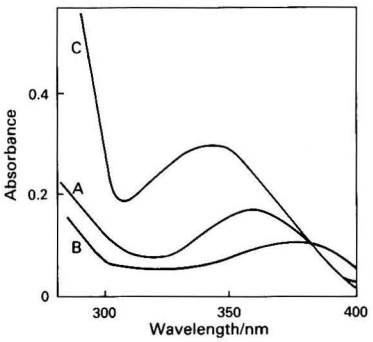

Fig. 1 Absorption spectra of A, EQ; B, the dimer (**2**); and C, the quinolone (**3**)

Table 1 Recovery of EQ added to fish meal using MQ as internal standard

EQ added/ mg kg^{-1}	EQ recovered/ mg kg^{-1}	Recovery (%)
158	148	95
212	214	101
250	262	105
400	394	99
412	440	107
633	660	104
836	870	104

Separation of EQ and the EQ-dimer (**2**)

The chromatographic behaviour of the EQ-dimer and EQ on alumina shows that the dimer is eluted first from the alumina. By using active alumina (Grade I), a mixture of hexane–diethyl ether (4 + 1 v/v) readily separated the dimer from EQ. Use of deactivated alumina (Grade IV) and hexane–diethyl ether (9 + 1 v/v), as in the routine determination of EQ, also gave sufficient separation of the dimer and EQ, although the two bands were close together and a clear-cut separation was more difficult to achieve. The results clearly indicate that the presence of the EQ-dimer can be a possible source of interference. It should be mentioned here that Spark[1] advises the inclusion of the dimer with EQ. It appears from our results that this should not be recommended if the intention is to obtain the genuine EQ content. If, however, it is the intention to obtain the antioxidant content expressed as EQ there is a case for the inclusion of the dimer as it has a reasonable antioxidant activity.

Separation of EQ and the quinolone (**3**)

This separation presented no difficulties. Calculation clearly showed that 89% of the EQ was recovered from the alumina uncontaminated by the quinolone by the normal routine procedure of eluting with hexane–diethyl ether (9 + 1 v/v). The quinolone required the much more polar solvent mixture of hexane–diethyl ether (3 + 7 v/v) to be eluted from the alumina. This result clearly demonstrates that the quinolone does not interfere with the determination of EQ in fish meal by chromatography on alumina.

Gas Chromatographic Procedure for the Determination of EQ With MQ as Internal Standard

The separation of MQ and EQ on the 15 m capillary column was excellent, MQ emerging after 3.23 min and EQ after 4.32 min. It must be mentioned here that the temperature of the injection port and the column should not exceed 200 and 150 °C, respectively, as MQ and EQ decompose at higher temperatures, which becomes evident in the appearance of

Table 2 Recovery of the EQ-dimer (**2**) added to fish meal using the MQ-dimer (**5**) as internal standard

EQ-dimer added/ mg kg^{-1}	EQ-dimer recovered/ mg kg^{-1}	Recovery (%)
53	50	94
166	153	92
200	220	110
294	272	93
376	384	102

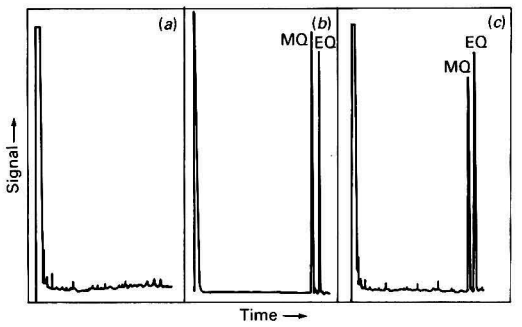

Fig. 2 Chromatograms of (*a*) meal only; (*b*) the MQ-dimer (**5**) and the EQ-dimer (**2**) only; and (*c*) meal treated with the MQ-dimer (**5**) and the EQ-dimer (**2**)

Table 3 Recovery of the quinolone (**3**) added to fish meal using MQ as internal standard

Quinolone added/ mg kg^{-1}	Quinolone recovered/ mg kg^{-1}	Recovery (%)
10	5	50
108	63	58
146	86	59
200	96	48
254	165	65
338	185	52

satellite peaks for both compounds. The decomposition of MQ and EQ probably yields a molecule of methane and 6-(m)ethoxy-2,4-dimethylquinoline.[9]

The recovery of EQ in spiked meals is presented in Table 1. Recovery ranged from 95 to 107% with a mean of 102% and a standard deviation of 3.8%, which is clearly sufficiently accurate for this work. In view of the good recovery and the specificity of the procedure the results obtained with this method were always taken as the correct results when comparing the two methods.

Determination of the EQ-dimer (2) by Gas Chromatography

By using the MQ-dimer (**5**) as internal standard, the EQ-dimer (**2**) could be readily determined. Under the conditions of the procedure, outlined under Experimental, the dimers of MQ and EQ had retention times of 7.42 and 7.80 min, respectively. The recovery of the EQ-dimer from the spiked meals is presented in Table 2. The recoveries ranged from 92 to 110% with a mean of 98% and a standard deviation of 6.9%. Examples of the separation of the two dimers in a meal together with the absence of any interfering substances in the meal are shown in Fig. 2.

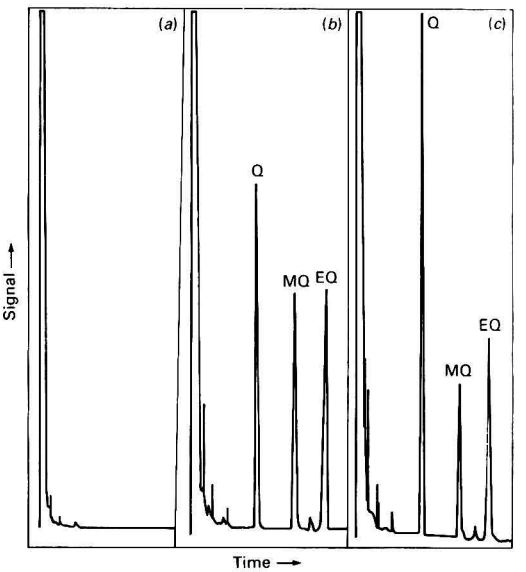

Fig. 3 Chromatograms of (*a*) meal only; (*b*) the quinolone (Q) (**3**), MQ and EQ only; and (*c*) meal plus Q, MQ and EQ

Determination of the Quinolone (3) by Gas Chromatography

In the determination of EQ in fish meals using MQ as the internal standard, the quinolone (**3**) appeared as a peak with a retention time of 1.96 min. The recovery of the quinolone from a spiked meal was, however, not quantitative; values of between 48 and 65% with a mean of 55% and a standard deviation of 5.9% were obtained (see Table 3). This is due to unequal distribution of the quinolone and MQ in hexane and the aqueous acidic or alkaline solutions. The values obtained in the determination of the quinolone were, therefore, always corrected for by multiplication by a factor of 1.8. As the amounts of the quinolone in meals were low (see below) this seems acceptable for our purposes. Examples of the chromatograms obtained when taking (*i*) a fish meal, (*ii*) the quinolone, MQ and EQ and (*iii*) a meal treated with the quinolone, MQ and EQ through the procedure are shown in Fig. 3.

Comparison of the Gas Chromatographic Procedure and Chromatography on Alumina for the Determination of EQ in Fish Meal

The results of the determination of EQ by the two methods on five fish meals of different origin and stored at 25 °C are presented in Table 4. The results showed that for EQ contents above approximately 30 mg kg^{-1}, chromatography on alumina tended to yield lower values than the gas chromatographic (GC) method, whereas for EQ contents below 30 mg kg^{-1} the reverse applied. Statistical analysis of the results from the meals with EQ contents above 30 mg kg^{-1} gives the following expression:

$$\text{EQ (by GC)} = 1.1 \times \text{EQ (by alumina)} - 2.1 \; (r = 0.99; n = 23)$$

This means that the value obtained for EQ by chromatography on alumina should be corrected for by multiplying by a factor of 1.1. The values obtained by chromatography on alumina for meals with EQ contents below approximately 30 mg kg^{-1} are much too high and the results are to be regarded as unreliable. For these meals the gas chromatographic method should be used.

Table 4 Ethoxyquin, the quinolone (**3**) and the EQ-dimer (**2**) in fish meal during storage at 25 °C

Meal history	Storage time/d	EQ/mg kg^{-1} Chromatography on alumina	EQ/mg kg^{-1} Gas chromatography	Quinolone/ mg kg^{-1}	EQ-dimer/ mg kg^{-1}	Total EQ equivalents mg kg^{-1}*
(1) Anchovy/pilchard factory meal; approximately 400 mg kg^{-1} of EQ added by factory personnel	1	198	230	2	+†	—
	212	79	83	9	86	118
	279	75	81	9	114	126
	357	80	76	9	101	116
	479	78	68	5	120	112
	573	76	61	4	120	104
(2) Maasbanker factory meal; approximately 1000 mg kg^{-1} of EQ added by factory personnel	1	938	1022	0	0	—
	184	288	297	29	92	349
	260	214	260	23	84	305
	359	208	244	7	96	281
	453	177	150	5	102	188
(3) Anchovy factory meal; 400 mg kg^{-1} of EQ added in the laboratory	20	403	394	5	0	—
	244	285	323	14	74	358
	100‡	155	238	26	98	290
	145‡	182	205	0	57	224
	216‡	146	145	7	72	174
	283‡	135	89	5	116	131
(4) Anchovy factory meal; 400 mg kg^{-1} of EQ added in the laboratory	59	164	185	21	111	238
	133	105	150	13	64	181
	186	134	134	3	98	169
	259	117	100	5	78	130
	347	79	87	22	96	136
(5) Anchovy factory meal; 400 mg kg^{-1} of EQ added in the laboratory	68	68	87	17	104	134
	181	62	30	9	124	78
	248	44	25	7	93	61
	321	62	20	4	70	46
	365	51	20	2	76	47

* See text for explanation.
† Dimer present but not determined quantitatively.
‡ Storage temperature raised to 70 °C.

Included in Table 4 are the amounts of the quinolone (**3**) and the EQ-dimer (**2**) that were generated during storage at 25 °C. There was a small and variable amount (4–30 mg kg^{-1}) of the quinolone formed in the stored meals, indicating that the quinolone is an intermediate product in the oxidation of EQ. It is not known which products are formed on further oxidation of the quinolone, but it seems unlikely that these products will interfere with the determination of EQ by chromatography on alumina, as the quinolone itself is not eluted from alumina under the conditions of the analysis.

The dimer, on the other hand, is formed in larger amounts (up to about 100 mg kg^{-1}) in the meals. All meals, except for the second meal, eventually contain amounts of the EQ-dimer which match and even exceed those of EQ. The presence of these relatively large amounts of the dimer in aged meals is probably responsible for the high values obtained by chromatography on alumina.

By using the data on the relative antioxidant efficacies of the quinolone (**3**) and the dimer (**2**) (see above), *viz.*, the quinolone has approximately three-quarters and the dimer approximately one-third of the efficacy of EQ, it is possible to calculate the antioxidant content expressed as EQ. These calculated total EQ equivalents are included in Table 4. It is evident from the results that the EQ content of a meal is normally an underestimate of its antioxidant content. It also seems unlikely that any of the three meals will be entirely deprived of antioxidant in the foreseeable future. Even if the EQ content were to drop to negligible levels there will probably still be sufficient dimer to protect the meal lipids against oxidation.

It can also be concluded that in the absence of EQ the presence of the EQ-dimer may serve as evidence to establish whether an aged meal has originally been treated with the antioxidant EQ. This question has on a few occasions been answered successfully in this Institute by analysing the meal for the EQ-dimer.

The authors thank the International Association of Fish Meal Manufacturers for financial support and Dr. J. P. H. Wessels, Director of the Fishing Industry Research Institute, for permission to publish this work.

References

1 Spark, A. A., *J. Am. Oil Chem. Soc.*, 1982, **59**, 185.

2 De Koning, A. J., and Mol, T. H., *J. Sci. Food Agric.*, 1989, **46**, 259.
3 Thorisson, S., Ph.D. Thesis, University of St. Andrews, 1987.
4 Dahle, H. K., and Skaare, U. J., *J. Agric. Food Chem.*, 1975, **23**, 1093.
5 Winell, B., *Analyst*, 1976, **101**, 883.
6 Vega, M., Saelzer, R., Mendoza, N., and Katalinic, J., *J. High Resolut. Chromatogr. Chromatogr. Commun.*, 1990, **13**, 854.
7 De Koning, A. J., *Fat Sci. Technol.*, 1987, **89**, 103.
8 De Koning, A. J., and Milkovitch, S., *Fat. Sci. Technol.*, 1991, **93**, 378.
9 Vaughan, W. R., in *Organic Syntheses, Collective Volume 3*, ed. Horning, E. C., Wiley, New York, 1955, pp. 329–332.

Paper 2/00710J
Received February 11, 1992
Accepted May 7, 1992

Determination of Trace Amounts of Water in High-purity Silane, Arsine and Phosphine by Gas Chromatography

Tianhui Ding, Baoqi Liu, Hongyi Zhang and Yanfang Liu
Department of Chemistry, Hebei University, Baoding 071002, China
Zengzhu Gao and Ziyun Li
Hongxing Monocrystalline Silicon Factory, Beijing Military Area, Baoding 071000, China

A method for the determination of trace amounts of water in high-purity silane, arsine and phosphine by gas chromatography (GC) is described. Samples are first passed through a transfer tube packed with calcium carbide to convert the water into acetylene, then through a liquid film packed column to eliminate the main hydride constituent. The analysis is performed by GC with flame-ionization detection. This method avoids contamination of the GC system.

Keywords: *Gas chromatography; high-purity silane, arsine and phosphine; water determination; trace analysis*

High-purity silane, arsine and phosphine are flammable and explosive gases, which cause serious contamination of gas chromatographic (GC) systems. Moreover, it is difficult to separate matrix hydrides from water, hence only a small number of methods have been reported. According to the SEMI Standard,[1] electrolytic analysis with a P_2O_5 cell is adopted for the determination of trace amounts of water in high-purity silane. However, this method is seriously affected by the operating conditions, environmental temperature, generation of hydrogen and oxygen, decomposition of hydride and electrode reactions. In addition, the determination of water at levels below 10 ppm was reported to be difficult[2] as it is difficult to remove traces of water in the carrier gas. In addition, adsorption of water by the GC system causes the chromatograms to tail seriously and the detection limit is increased. Hence the minimum detectable amount is 50 ppm (ref. 3) using a thermal conductivity detector. As the vapour pressure of hydrides greatly exceeds that of water, a dew-point analyser cannot be applied.

A novel column system is described in this paper. Samples are first passed through a transfer tube packed with calcium carbide to convert the water into acetylene. They are then passed through a liquid film packed column in order to eliminate matrix hydrides. Finally, the gases are determined by GC with flame-ionization detection (FID). This method eliminates hydrides which contaminate the GC system. The sensitivity is 0.04 ppm mm^{-1} and the relative standard deviation is 2.7%.

Theoretical

In order to overcome the low sensitivity of the direct determination of trace amounts of water, the method of calcium carbide conversion was used, expressed by the following equation:

$$CaC_2 + H_2O \rightarrow CaO + C_2H_2$$

The acetylene formed quantitatively was detected by FID.

A liquid film packed column was designed to eliminate the three types of hydrides. A glass column was first packed with 6201 red support (Dalian Hongguang Chemical Plant) and the required amount of an eliminating reagent to form a film. Hydrides reacted with the film and were eliminated when they were passed through the column in which 20% potassium hydroxide was used as the eliminating reagent. The reaction is as follows:

$$SiH_4 + 2KOH + H_2O \rightarrow K_2SiO_3 + 4H_2\uparrow \quad (1)$$

Perchloric acid was used for eliminating arsine and phosphine. The reactions are as follows:

$$AsH_3 + HClO_4 \rightarrow H_3AsO_4 + HCl \quad (2)$$

$$PH_3 + HClO_4 \rightarrow H_3PO_4 + HCl \quad (3)$$

Repeated experiments showed that contamination of the GC system and interferences in the analyses were avoided entirely by these methods.

Experimental

Apparatus

An SP-6000 gas chromatograph equipped with a flame-ionization detector (Beijing Analytical Instrument Factory) was connected to a six-way sampling valve (Beijing Analytical Instrument Factory). A dew-point analyser (Semiconductor Research Institute of the Chinese Academy of Sciences) was also used.

The layout of the analysis was determined by several experiments and is shown schematically in Fig. 1. Pipelines, valves and joints were made of stainless steel or brass. In order to ensure a gas-tight system and safety and reliability of analysis, washers made of red copper or poly(tetrafluoroethylene) (PTFE) gaskets were used for contact.

The set-up included three parts, as follows.

Gas chromatographic system

A six-way valve (7) that was used for quantitative injection of samples was connected to a valve (8) on the surface of the gas chromatograph. A liquid film packed column (9), that was designed to eliminate the three types of hydrides, and the valve (8) were linked.

Sample-loading system

Silane will explode if it encounters air, hence a nitrogen purging system must be used to ensure the safety of analysis. When valve 15 was switched on, a nitrogen purge eliminated any air from transfer tube 20 *via* sample valve 7 into the laboratory. The length of connection of the transfer tube and the sample bottle should be as short as possible. After loading the sample, tail gases were exhausted into the treating barrel, in which different treating liquids were present depending on the type of hydride: 20% sodium hydroxide, 5% copper(II) sulfate and 5% potassium permanganate were used for reaction with silane, arsine and phosphine, respectively.

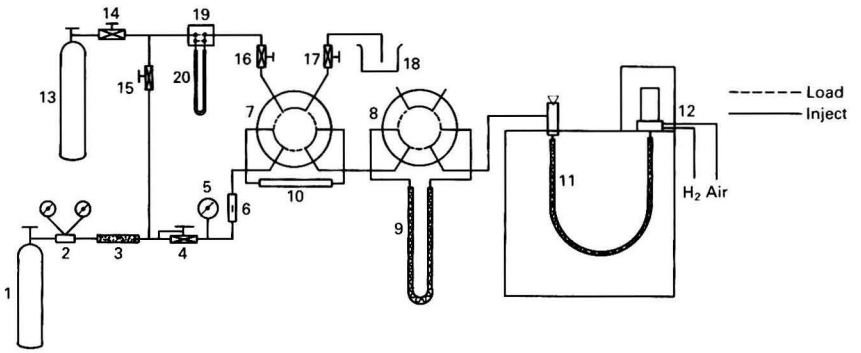

Fig. 1 Schematic diagram of the system used for the analysis. 1, Nitrogen cylinder; 2, decompressor; 3, treating tube; 4, flow controller; 5, pressure gauge; 6, rotameter; 7, six-way sample valve; 8, six-way valve; 9, sorption column; 10, quantitative tube; 11, separation column; 12, FID; 13, sample bottle; 14, decompressor; 15–17, needle valves; 18, tail gas treating barrel; 19, four-way valve; and 20, CaC_2 transfer tube

Standard sampling system

The standard sample bottle was attached to the transfer tube *via* a decompressor valve. The length of the connection should be as short as possible. This system prevented interference from adsorption of trace amounts of water.

Chromatographic Conditions

A 4 m × 3 mm i.d. stainless-steel column packed with 80–100 mesh GDX-502 organic support was used. An 80 cm × 3 mm i.d. glass tube packed with 60–80 mesh 6201 support was used as an eliminating column, in which different eliminating reagents were applied depending on the hydrides. The amount of eliminating reagent was suitable to moisten a 40 cm length of the support. The remaining 40 cm length of the support was not moistened in order to prevent the eliminating reagent from flowing into the GC system. A 30 cm × 4 mm i.d. stainless-steel column packed with 20–30 mesh calcium carbide was used for converting water into acetylene. The chart range was 5 mV, the FID range was 10 and the attenuation was 1. The injector and detector were maintained at 150 °C. The nitrogen carrier gas flow rate was 30 cm^3 min^{-1}. The oven temperature used for the GC column was 50 °C.

Procedure

After the operating conditions for the gas chromatograph had been established, six-way valve 7 was set to the Load condition. Valve 15 was then opened and high-purity nitrogen passed through the column until the air was eliminated, then valve 15 was closed.

After turning on the sample bottle, the quantitative tube was filled with sample gas and the sample valve was set to the Inject position to inject the sample into the chromatograph. These operations were repeated several times until the same peak height was obtained three times. Only by purging with the sample gas can the concentration of water in the sampling system be the same as that in the sample bottle.

The sample bottle was closed, then valve 15 was opened until the sample was entirely exhausted. After these operations, valve 15 was closed.

The above operations were repeated, replacing high-purity nitrogen with known amounts of water as the sample. The concentration of water in the high-purity nitrogen was determined with a dew-point analyser. The concentration obtained with the dew-point analyser was used as an external standard.

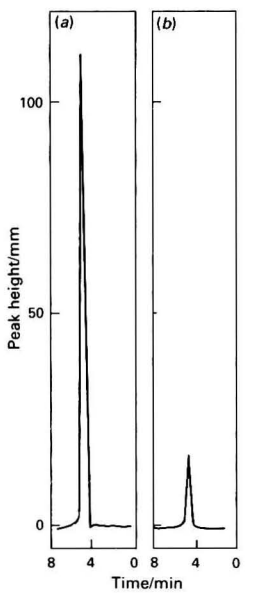

Fig. 2 Chromatogram of water in high-purity hydrides. (*a*) Standard gas containing 4.5 ppm of water; and (*b*) sample containing 0.5 ppm of water

Results and Discussion

Determination of Water

The concentration of water in high-purity nitrogen was determined as 4.5 ppm with the dew-point analyser. The water concentrations in the samples were calculated using the following equation:

$$P = Ah/B$$

where P = concentration of water in sample (ppm), A = concentration of water in high-purity nitrogen (ppm), B = peak height of water in high-purity nitrogen and h = peak height of water in sample.

The concentrations of water found were 4.0, 0.5 and 1.4 ppm in silane, arsine and phosphine, respectively. The corresponding chromatogram is shown in Fig. 2.

Precision

The concentration of water in a silane sample was determined ten times. The range was 4.43–4.79 ppm, mean 4.58 ppm, standard deviation 0.122 ppm and relative standard deviation 2.7%.

Sensitivity

The sensitivity was determined by analysing high-purity nitrogen containing 4.5 ppm of water six times. The peak heights were 110–112 mm, mean 111 mm, and the sensitivity was 0.04 ppm mm^{-1}.

Discussion

In the system shown in Fig. 1, the calcium carbide tube for converting water into acetylene is positioned very early in the rig, before the valves. Moreover, the length of the connection was as short as possible, which ensures that no moisture present owing to back-diffusion from the air was converted into acetylene. Stainless steel was used throughout for the valves and tubing. Relative to the sample types being analysed, this was satisfactory. If it is not satisfactory, a more inert material such as Hastelloy C could be considered.

The water in the sample gas stream was presumably adsorbed on the metal surfaces. However, this did not affect the results obtained because the system was purged with sample gas streams before sampling. The concentration of water in the sampling system was the same as that in the sample bottle when the moisture adsorbed on the metal was saturated. Hence, adsorption of moisture on the metal surfaces can be ignored. Also, the pipework and the valves need not be heated.

The acetylene formed by the reaction of water in the sampling gases or high-purity nitrogen with calcium carbide is proportional to the concentration of water. Hence it is not necessary to know the efficiency of conversion of water into acetylene.

Precautions

There was some water present in high-purity nitrogen. However, after the high-purity nitrogen had been purified by molecular sieves that had been frozen in liquid nitrogen, the water was eliminated. The purified high-purity nitrogen can be used to test the system for leaks to ensure that no moisture was present owing to back-diffusion from the ambient air. After injecting the high-purity nitrogen, if no peaks appeared it could be concluded that the sampling system was not leaking.

The amount of sample should not be too large, otherwise the eliminating tube would be overloaded. The volume of the quantitative tube that was used for sampling was 0.01 cm^3.

To ensure effective conversion of water into acetylene, the optimum flow rate of the sample stream was 2 cm^3 min^{-1}.

The gases in the columns must be exchanged for sample gas, otherwise the results obtained by this method would be high. Before sampling, a 20 cm^3 min^{-1} nitrogen stream was used to purge the system for 3 min to exchange the air in the system. Silane would explode if it encountered air, so purging of the system with nitrogen must be applied to ensure the safety of analysis. After this operation, the nitrogen cylinder was closed and the sample bottle was opened. The sample stream at a flow rate of 2 cm^3 min^{-1} purged the system for 12 min to eliminate entirely the remaining gas. After the above operations, the concentration of water in the sampling system was the same as that in the gas sample bottle. The calcium carbide tube needed to be repacked every week.

Conclusion

With the use of the liquid film packed column, hydrides were completely eliminated and the problems due to contamination of the GC system and interference in the analysis caused by hydrides were solved. The efficiency of the liquid film packed column was high, and much better than that achieved by liquid absorption by Ecknig and Glockl.[4] This method only required that carrier gas, hydrogen and air were purified by passage through 5A molecular sieves. The interference caused by adsorption of trace amounts of water in the GC system was avoided.

References

1 1987 SEMI Standards, Semiconductor Equipment and Materials Institute, Mountain View, CA, 1987, C_3 STD. 8–86, C_3 STD. 9–86, C_3 STD. 10–86.
2 Wang, W.-T., *Analysis of Traces of Water*, Science Press, Beijing, 1982, p. 34.
3 *Instrument Manual of Water Analyzer*, Beijing Analysis Instrument Factory, Beijing, 1990.
4 Ecknig, W., and Glockl, D., *Chem. Tech. (Leipzig)*, 1985, **37**, 214.

Paper 2/00300G
Received January 20, 1992
Accepted April 23, 1992

Determination of Forms of Sulfur in Coals and Related Materials by Eschka Digestion and Inductively Coupled Plasma Atomic Emission Spectrometry

John C. Eames
CSIRO Division of Exploration Geoscience, P.O. Box 136, North Ryde, New South Wales 2113, Australia

Robert J. Cosstick
CSIRO Division of Coal and Energy Technology, P.O. Box 136, North Ryde, New South Wales 2113, Australia

An inductively coupled plasma atomic emission spectrometric method for the determination of the forms of sulfur in coal and related materials is described. The sensitivity afforded by inductively coupled plasma atomic emission spectrometry allows sample masses in the proposed method, which involves traditional extraction techniques, to be reduced to less than one-tenth of that required by standard methods without any loss in precision. The plasma method of detection is more rapid than conventional barium sulfate precipitation techniques and still satisfies the requirements of standard procedures for the forms of sulfur in coal. Statistical analysis of results indicates no significant difference between the proposed procedure and the standard method.

Keywords: *Forms of sulfur determination; inductively coupled plasma atomic emission spectrometry; coal analysis; Eschka digestion*

Pollution of the environment has become a major concern not only to scientists, but also to the general community. One aspect is the release of SO_2 into the atmosphere as a result of burning fossil fuels. The SO_2 emitted is converted into SO_3, which may damage the environment as acid rain; SO_2 could also have an adverse effect on human health. The analysis of coal for sulfur is used to evaluate potential sulfur emissions from coal combustion or conversion processes and to check sulfur levels against contract specifications.

For decades, traditional procedures have been used to classify the forms of sulfur in coal and coke. These procedures have been embodied in standard methods,[1–4] some of which incorporate modern techniques such as atomic absorption spectrometry (AAS) as options for the detection of the relevant species. Techniques that depart even more significantly from traditional approaches have recently been developed for one or more forms of sulfur, for example, Mössbauer spectrometry.[5–7]

Although inductively coupled plasma atomic emission spectrometry (ICP-AES) has been used to determine sulfur in coal products,[8–9] this paper shows how it can be successfully adapted to the conventional techniques of extraction and isolation to provide a complete procedure for the determination of the forms of sulfur. This procedure has precision statistics equal to, or better than, those obtained by the traditional methods.

The sensitivity of the plasma emission technique enables sample masses to be reduced to one-tenth that of the traditional procedures.[1,3,4] According to studies conducted on coals and cokes by Fujimori and Ishikawa,[10] a representative analytical sample, down to 100 mg, can be taken from powders ground to <147 μm. Hence, 100 mg portions of <150 μm coal was chosen. The conventional procedure of the Standards Association of Australia (SAA)[1] for total sulfur (S_{total}) uses Eschka mixture in a mass ratio of 7:1, while in BSI[3] and ASTM[4] procedures, a mass ratio of 4:1 is used. Both these ratios are undesirably high for ICP-AES detection because of spectral and matrix effects; therefore, most of the unwanted cations were removed by ion exchange.

Pyritic sulfur (S_{pyr}) was determined indirectly *via* the pyritic iron (Fe_{pyr}) and the sulfate-sulfur (S_{SO_4}) was determined directly in the hydrochloric acid extract obtained prior to the nitric acid extraction for S_{pyr}. Vacuum filtration was used to isolate extracts from residues in the determinations of S_{pyr} and S_{SO_4}; decantation was normally sufficient for S_{total}.

Evaluation of the accuracy of the proposed method was effected by direct comparison with conventional procedures and by recovery tests. In addition, several other aspects of the technique were appraised: (*a*) the effectiveness of the ion-exchange step in the removal of potentially interfering ions without loss of analyte; (*b*) comparison of the detection of sulfate ion by plasma emission with gravimetric detection as barium sulfate; and (*c*) the validity of the use of small test portions.

Experimental

Instrumentation

All measurements were performed on a Labtest V-25 ICP-AES instrument under compromise operating conditions designed for the simultaneous multi-element analysis of geological materials. Instrumental parameters are listed in Table 1. Although the analysis of solutions with high salt contents can result in poor precision and even nebulizer blockage, this proved not to be a problem when using a modified Babington 'stop flow' nebulizer (Labtam).

The spectrometer was operated under vacuum with an argon-flushed viewing tube between the plasma and the polychromator. Spectral interferences around the 180.731 nm S and the 259.940 nm Fe lines were identified using a scanning primary slit. The only significant spectral overlap around the 180.731 nm S line came from the severe overlap of the 180.361 nm Ca line and the less severe 180.747 nm Mn line. No significant matrix interference from sodium and magnesium at

Table 1 ICP-AES operating parameters

Forward power	1450 W
Argon plasma gas flow rate	15 $dm^3 min^{-1}$
Carrier gas flow rate	1.8 $dm^3 min^{-1}$
Solution uptake rate	2.1 $cm^3 min^{-1}$
Observation height above coil	14.5 mm
Nebulizer	Labtam 'stop flow'
Torch	Demountable*

* Ref. 11.

the levels present in sample extracts was observed. The most sensitive 180.731 nm line rather than the 182.037 nm line, which does not suffer from these spectral effects, was selected in the polychromator because it afforded the best detection limit for sulfur. The well-documented aluminium recombination continuum caused no appreciable spectral interference. Spectral overlaps around the 259.940 nm Fe line were the 259.890 nm Mn line and the 259.989 nm Ti line. The relationship between interferent concentration and apparent analyte concentration was established by the method of least squares, and correction coefficients were calculated. The interference levels were consistent with those observed in other studies,[12,13] and the correction coefficients were applied to the determination of sulfur and iron.

Apparatus and Reagents

A standard commercial membrane-filtration apparatus, fitted with a 25 mm acid resistant 0.45 μm porosity membrane, was used. The resin exchange columns charged with polystyrene bead resin were of the Edgecombe configuration.[14] The Permutit Zeo-Karb 225 (14–52 mesh) resin has functional groups of sulfonic acid and was prepared by passing 30 cm^3 of 2 mol dm^{-3} hydrochloric acid through the column, followed by 60 cm^3 of water.

All the solutions used to check ICP-AES spectral interference were prepared from spectrally pure metals, or salts if metals were not available. All other chemicals were of analytical-reagent grade. Five matrix-matched (Eschka mixture) control standards containing from 1 to 100 μg cm^{-3} of S were prepared from Na_2SO_4.

Calibration standards for ICP-AES were single-element standards prepared from commercial standard solutions (Merck Titrisol) where available or from analytical-reagent grade reagents.

Procedures

Total sulfur

An accurately weighed 100 mg portion of a <150 μm sample was transferred into a porcelain crucible charged with approximately 100 mg of Eschka mixture and mixed well. A further portion of Eschka mixture was added to bring the total mass added to 800 ± 20 mg. The crucible was placed in a muffle furnace, and the temperature raised to 800 °C over about 1 h and then kept at 800 °C for 1 h. After the crucible had cooled, the contents were transferred quantitatively into a 100 cm^3 beaker containing approximately 30 cm^3 of water and dispersed with a stirring rod. Concentrated hydrochloric acid (4 cm^3) was added and the solution was boiled gently to dissolve all the sulfate. The cooled solution was transferred into a 100 cm^3 calibrated flask and diluted to the mark with water. A 30 cm^3 portion of the final solution was passed (at 4–6 cm^3 min^{-1}) through the cation-exchange column, and the 20–25 and 25–30 cm^3 fractions were collected for determination of sulfur by ICP-AES. A reagent blank and control standard (50 μg cm^{-3} of S) were carried through the same procedure.

Sulfate-sulfur

A 100 mg portion of a <150 μm sample was weighed to the nearest 0.01 mg and transferred into a 100 cm^3 conical flask. After the addition of approximately 0.2 cm^3 of methanol to wet the sample, 10 cm^3 of 5 mol dm^{-3} hydrochloric acid were added. The flask was covered with a watch-glass, and the contents were boiled gently for 15 min. The product was cooled before being filtered on a membrane filter, and the residue was washed with 5 mol dm^{-3} hydrochloric acid. The filtrate was collected in a tared vial and was adjusted to between 20 and 35 g with water. The sulfur concentration was then measured in samples and blanks by ICP-AES.

Pyritic sulfur

The residue and membrane filter from the sulfate-sulfur determination were returned to the conical flask and 10 cm^3 of 2 mol dm^{-3} nitric acid were added. The flask was covered with a watch-glass and the contents were gently boiled for 30 min. The digested sample was cooled before being filtered on a membrane filter and washed with 2 mol dm^{-3} nitric acid. The filtrate was collected in a tared vial and adjusted to between 20 and 30 g with water. The iron content was then determined in samples and blanks by ICP-AES, and the pyritic sulfur content of the samples was calculated by assuming FeS_2 stoichiometry.

Results and Discussion

Effect of Ion Exchange on Sulfate Recovery

Recovery tests were carried out using a range of control standards (1, 5, 10, 50 and 100 μg cm^{-3}) and the ICP-AES results showed that some 3–4% of the total sulfur was lost during the ion-exchange procedure. A typical ion-exchange sulfur eluent profile is shown in Fig. 1. Although significant concentrations of sodium and magnesium were eluted with the sulfur, no ICP-AES matrix interference was observed. It was concluded that the small amount of sulfur not accounted for was probably ionically retained on the ion-exchange resin by the conjugate ions, sodium and magnesium. The fact that sodium and magnesium are initially present at considerably

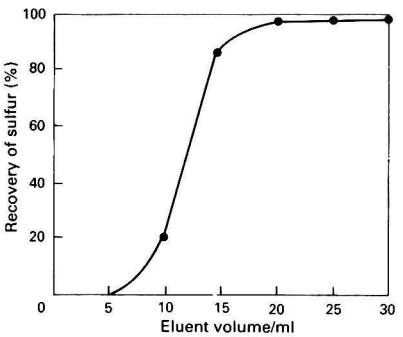

Fig. 1 Ion-exchange eluent profile showing some 3–4% sulfur loss during the ion-exchange procedure

Table 2 Comparison of ICP-AES and gravimetric determination of sulfate-sulfur in lignite combustion residues and coal samples

Sample	CSIRO sample no.	Sulfate-sulfur content (% m/v) ICP-AES	Gravimetry
Esperance lignite	88259	3.25	3.36
Esperance lignite	88260	3.27	3.26
Esperance lignite	88261	2.75	2.73
Esperance lignite	88264	3.03	3.20
Esperance lignite	88270	2.85	2.91
Esperance lignite	88271	3.41	3.49
Esperance lignite	88273	3.45	3.53
Esperance lignite	88289	2.84	2.77
Esperance lignite	88301	1.62	1.74
Esperance lignite	88302	4.02	3.87
Esperance lignite	88307	6.02	6.11
Esperance lignite	88343	2.95	3.07
Esperance lignite	88344	2.97	2.94
Esperance lignite	88346	2.11	2.13
Esperance lignite	91432	0.96	0.95
Gelliondale brown coal	91431	0.25	0.24
Loy Yang brown coal	91433	0.017	0.012
Rundle lignite	91434	0.201	0.191
Bowman's lignite	91435	0.76	0.76

Table 3 Comparison of total sulfur results in standard and other coal samples

Sample	Certified S content (%)	S found by classical method (% m/v)	S found by proposed method (% m/v)
Yallourn brown coal briquette 700 °C char	—	0.19	0.18
		0.18	0.18
Yallourn brown coal	—	0.27	0.27
		0.28	0.25
Leco calibration coal 501-001	0.52	0.50	0.50
		0.50	0.51
Newlands bituminous coal	—	0.49	0.48
		0.49	0.51
Japanese brown coal ISO/TC27WG13 (SEC-19)	—	2.70	2.73
		2.70	2.68
Leco calibration coal 767-758	2.54	2.48	2.52
		2.49	2.49
Leco calibration coal 501-022	3.48	3.38	3.39
		3.39	3.44
Gelliondale brown coal 91431	—	1.16	1.14
		1.15	1.13
Esperance lignite 91432	—	4.44	4.43
		4.48	4.46
Loy Yang brown coal 91433	—	0.27	0.26
		0.22	0.23
Rundle lignite 91434	—	1.38	1.39
		1.40	1.42
Bowmans lignite 91435	—	5.56	5.58
		5.59	5.60
ASCRM No. 9 Coal	0.35	0.34	0.35
		0.36	0.37
SARM 18 Witbank Coal	0.56	0.58	0.59
		0.57	0.57
SARM 19 Orange Free State Coal	1.49	1.46	1.48
		1.46	1.46

higher levels than that of sulfur, and even in the final 5 cm^3 analytical fraction persist at levels very much higher than the sulfur concentration, is probably sufficient to reduce the chromatographic efficiency of the resin. The sulfate recovery for coal samples should be the same as that observed for the control standards as the Eschka mixture rather than the sample accounts for the high ion concentration.

ICP-AES *versus* Gravimetric Sulfur Detection

The two methods of detection were compared by analysing for sulfate-sulfur in a number of different extracts. This approach was adopted because there are no suitable certified reference materials. The results obtained by the two methods (Table 2) were compared using the Student's two-tailed paired *t*-test.

The methods were compared by calculating the criterion:

$$t = (\bar{x}_A - \bar{x}_B)\sqrt{\frac{n(n-1)}{\Sigma(D_i - \overline{D})^2}}$$

where t is distributed as Student's t on $(n - 1)$ degrees of freedom; D_i is the positive or negative difference of the determinations carried out with the ith sample by the two methods; $\overline{D}$ is the mean difference; $\bar{x}_A$ and $\bar{x}_B$ are the arithmetic means of the results of the two methods; and n is the number of determinations carried out by the two methods.[15] The calculated absolute value for t is 1.579, and as this value is less than the two-tailed critical value at the 5% level of significance (2.093), the difference between the two methods of detection is not statistically significant.

Table 4 Comparison of results for pyritic sulfur by using 0.1 and 1.0 g sample masses

Sample	CSIRO sample no.	Pyritic sulfur content (% m/v) Proposed method*	Classical method†
Gelliondale brown coal	91431	0.11	0.10
		0.10	0.11
Great Northern seam bituminous coal	87319	0.15	0.16
		0.14	0.17
Bowman's lignite	91435	0.22	0.24
		0.24	0.23
Esperance lignite	87897	0.37	0.34
		0.36	0.35
Esperance overburden	87916	2.21	2.15
		2.24	2.17

* 0.1 g sample portion.
† 1.0 g sample portion.

Total Sulfur

As noted above, the recovery of sulfur from the Eschka sinter extract during the ion-exchange procedure was consistently low (96.5 ± 0.5%). The precision of this loss was sufficient to allow recovery correction to the sample result using a matrix-matched control standard carried through the ion-exchange procedure. Results for all samples that underwent ion exchange were corrected in this way.

The precision of both the traditional and proposed methods was consistent with the requirements of the standard procedure. The accuracy of the proposed method was confirmed by comparing the results for a range of coal samples, including some reference materials (Table 3). In all instances, individual results fell within the specified Australian Standard tolerance[16] for duplicates.

Sulfate-Sulfur

The sulfate-sulfur component of the proposed procedure was assessed by comparison of the results for lignite combustion residues and some coals with those obtained by the traditional procedure (Table 2), because no suitable certified reference materials were available.

Pyritic Sulfur

The proposed procedure was compared with the traditional method for selected samples covering a range of S_{pyr} values. Again there were no suitable certified reference materials available. The two methods differed only in the size of the sample used and in the detection of iron by ICP-AES rather than by AAS. The precision data for the traditional reference procedure and the proposed method both fell within the precision requirements specified within the Australian Standard.[16] The statistical difference between the two data sets was found to be insignificant. Results are shown in Table 4.

Conclusions

The analytical approach described, which combines the use of small sample masses with the sensitivity of the ICP-AES method of detection, satisfies the requirements of standard procedures for the determination of forms of sulfur in coal.

Statistical analysis of the results indicates that there are no significant differences between the proposed procedure and the standard method. The method described also provides a rapid alternative to standard procedures.

References

1 Australian Standard 1038.6.3.1—1986; Methods for the Analysis and Testing of Coal and Coke. Ultimate Analysis of Higher Rank Coal—Determination of Total Sulphur (Eschka Method), pp. 5–6.
2 Australian Standard 1038.11—1982: Methods for the Analysis and Testing of Coal and Coke. Forms of Sulphur in Coal, pp. 4–9.
3 British Standards Institution, BS 1016, Part 7: 1977 Methods for the Analysis and Testing of Coal and Coke.
4 *1991 Annual Book of ASTM Standards*, Section 5, Petroleum Products, Lubricants and Fossil Fuels, Volume 05.05—Gaseous Fuels; Coal and Coke, American Society for Testing and Materials, Philadelphia, pp. 289–314; 335–337.
5 Levinson, L. M., and Jacobs, I. S., *Fuel*, 1977, **56**, 453.
6 Huffman, G. P., and Huggins, F. E., *Fuel*, 1978, **57**, 592.
7 Guilianelli, J. L., and Williamson, D. L., *Fuel*, 1982, **61**, 1267.
8 Kubota, M., Reimer, R. A., Terajima, K., Yoshimura, Y., and Nishijima, A., *Anal. Chim. Acta*, 1987, **199**, 119.
9 Caroli, S., Farina Mazzeo, A., Laurenzi, A., Senofonte, O., and Violante, N., *J. Anal. At. Spectrom.*, 1988, **3**, 245.
10 Fujimori, T., and Ishikawa, K., *Fuel*, 1972, **51**, 120.
11 Eames, J. C., O'Keefe, C. J., and Dotter, L. E., *Appl. Spectrosc.*, accepted for publication.
12 Lee, J., and Pritchard, M. W., *Spectrochim. Acta, Part B*, 1981, **36**, 591.
13 Morita, M., Uchiro, T., and Fuwa, K., *Anal. Chim. Acta*, 1984, **166**, 283.
14 Edgecombe, L. J., *Fuel*, 1955, **34**, 429.
15 Eckschlager, K., *Errors, Measurement and Results in Chemical Analysis*, ed. Chalmers, R. A., Van Nostrand Reinhold, London, 1972, pp. 112–113.
16 Australian Standard 1038.16—1986: Methods for the Analysis of Testing of Coal and Coke. Acceptance and Reporting of Results, pp. 13–16.

Paper 2/02107B
Received April 24, 1992
Accepted July 1, 1992

Multi-elemental Analysis of Environmental Matrices by Laser Ablation Inductively Coupled Plasma Mass Spectrometry

Steven F. Durrant*
Department of Chemistry, University of Surrey, Guildford, Surrey, UK GU2 5XH

Laser ablation has been applied to the solid sample introduction into an inductively coupled plasma mass spectrometer for the multi-elemental analysis of several environmental matrices. Fourteen elements (Al, P, K, Ca, Cr, Mn, Fe, Ni, Cu, Zn, Rb, Sr, Ba, Pb) were determined in the Japanese National Institute of Environmental Studies certified reference materials (CRMs) No. 7 Tea Leaves and No. 1 Pepperbush; nine elements (Na, Mg, Al, P, K, Cr, Mn, Fe, Zn) were determined in International Atomic Energy Agency CRM A11 Milk Powder; and 41 elements (Li, B, Sc, Ti, V, Cr, Mn, Co, Ni, Cu, Zn, Ga, Ge, As, Rb, Sr, Y, Zr, Nb, Mo, Sn, Cs, Ba, La, Ce, Pr, Nd, Sm, Eu, Gd, Tb, Dy, Ho, Er, Yb, Ta, W, Pb, Bi, Th, U) were determined in reference sediments GSD-2–GSD-8 from the Chinese Institute of Geophysical and Geochemical Prospecting. Calibrations were based on individual elemental sensitivities derived from matrix-matched standards. Simple and full internal standardization on a minor isotope of a major matrix element are discussed. The former are helpful for analysis of the biological matrices, but the latter do not improve precisions. Comparison with certified values shows fairly good accuracy, especially considering the rapidity of the analyses. The geological analyses were particularly successful as virtually no sample preparation was necessary and the analytical results obtained were very encouraging; detection limits for each type of analysis are given.

Keywords: *Laser ablation inductively coupled plasma mass spectrometry; certified reference material; Pepperbush, Tea Leaves, Milk Powder and sediments*

Although the feasibility of the use of laser ablation (LA) for solid sample introduction to inductively coupled plasma mass spectrometry (ICP-MS) was shown seven years ago,[1] it is only in the last few years that details of real analyses have begun to be published.[2–5] This time-lag perhaps suggests the difficulties involved in fully quantitative analysis using LA-ICP-MS. However, the number of recent papers on the technique indicates that some successful treatments of the difficulties of analysis, principally the means of reliable calibration, are being found.

Direct sampling of solid material can greatly shorten sample preparation time when compared with the tedious dissolution procedures required to admit samples to the ICP *via* a nebulizer. Such dissolutions can be enormously time-consuming and occupy highly qualified people for long periods of time. Beauchemin *et al.*[6] have reported a nitric acid–hydrogen peroxide digestion procedure for the marine biological tissue reference materials for trace metals, DOLT-1 Dogfish Liver and DORM-1 Dogfish Muscle, that requires at least a full day's work. Similarly, for geological analyses, lengthy digestion procedures are typically required.[7] It can be observed also, that environmental projects involve the analysis of thousands of samples and that ease and rapidity of analysis might then be of greater importance than superb accuracy and precision.

The versatility of LA-ICP-MS for environmental applications is beginning to emerge. For example, Tye *et al.*,[2] using an Nd:YAG laser for sample ablation, determined the elements Li, B, Ti, Cr, Fe, Ni, Co, Sr, Zr, Nb, Mo, Cs, Nd, Eu, Sm, Gd and Pb in U_3O_8 with detection limits in the range 0.036–1.26 μg g^{-1}. Uranium isotope ratios were determined with precisions of about 1%. Additionally, a Japanese group determined rare earth elements plus Th and U in silicates,[8] obtaining detection limits in the range 0.02–0.86 μg g^{-1}. The same group has recently investigated LA-ICP-MS for the analysis of silicon nitride powders.[9] Imai[3] has also determined 40 elements in 12 standards from the igneous rock series of the Geological Survey of Japan using multiple free-running pulses from an Nd:YAG laser for sample mobilization; two internal standards (Ba and La) were used. Lithium tetraborate fusions of carbonate were recently analysed for Mg, Mn, Sr, Ba and Pb using Q-switched pulses, again from an Nd:YAG laser, for solid sampling.[10] However, virtually nothing has been published for biological materials beyond the work outlined recently.[11]

In this work multi-elemental analyses of two plant-based materials, a milk powder and numerous sediments, are demonstrated. Free-running pulses from a ruby laser were used to eject sample material into the central channel flow of an argon-fed ICP, with subsequent ionic detection by the Surrey prototype spectrometer. A simple approach to calibration using individual elemental sensitivities derived from matrix-matched standards was taken. Elements determined were chosen on the basis of their presence at concentrations in the standard likely to produce fair calibrations, *i.e.*, not at trace levels, and the availability of confirmatory concentrations in the analysed matrix. The efficacy of the rapid semiquantitative multi-elemental analysis of environmental matrices is demonstrated

Experimental

Apparatus

Previous work outlines the ablation system[1,4,11] and spectrometer.[12,13] Relatively slow (ms) free-running pulses from a JK 2000 ruby laser are directed onto the samples, which are held in a cylindrical glass cell. The sample sits on a turntable (32 mm diameter) that can be rotated under electronic control. A flow of argon is supplied to the cell, and it carries a fraction of the ablated matter *via* plastic tubing to the central channel of an argon-fed quartz torch that supports the ICP.

Either the laser or the electronic control unit can start data accumulation by triggering a multichannel analyser (MCA), which stores the spectra. The mass spectrometer is essentially the forerunner of the VG PlasmaQuad, lacking only the more sophisticated computer control.

* Present address: Department of Chemistry, Lederle Graduate Research Center, University of Massachusetts, Amherst, MA 01003, USA.

Sample Preparation

Plant-based material

Two plant-based certified reference materials (CRMs) from the Japanese National Institute of Environmental Studies (NIES), No. 7 Tea Leaves and No. 1 Pepperbush, were prepared by drying according to the procedures on the certificates of analysis and ball-milling in a tungsten mill with a carbonaceous binder (Elvesite 2013) for 5 min. The resulting powder was pressed in an X-ray fluorescence cup to 10 tonnes, producing a disc of 32 mm diameter and a height of about 3 mm. Each disc contained a total mass of about 2 g of which 20% m/m was binder. For use as a calibration standard, a disc of Bowen's Kale was similarly prepared.

Milk powder

The CRM A11 Milk Powder, produced by the International Atomic Energy Agency (IAEA), was prepared in the same way as the plant materials. However, as previous experience had shown that laser–sample coupling is poor with samples of a rather pale-yellow colour, 1% m/m of high-purity graphite (Spektralkohle-Pulver) was incorporated into the material to be ball-milled. A disc of National Institute of Standards and Technology (NIST) Standard Reference Material (SRM) 1549 Non-fat Milk Powder was also prepared for use as a calibration standard.

Sediment

Certified reference sediments (GSD-2–GSD-8) from the Chinese Institute of Geophysical and Geochemical Prospecting were prepared simply by drying and pressing in a 13 mm diameter steel die to form free-standing pellets. A pellet of GSD-1 was also prepared for use as a standard.

Optimization

Systematic optimization is rather tedious because there are so many parameters that influence the system response. These relate to the sample matrix, for example its surface characteristics and thermal properties in addition to the laser mode and energy, and even the polarization of the beam.[14] In this work the ion optics were opimized on the ^{12}C signal. Carbon is present, in the form of CO_2, as an impurity in the argon, and also because it desorbs from the walls of the gas lines, and is entrained from the atmosphere. The optimization procedure has been described elsewhere[15] and yields similar conditions to those obtained if a sample matrix is ablated continuously at a high repetition rate (1 Hz or more). No obvious mass discrimination effects are observed.[11]

Giant pulses (Q-switched) might be thought to be useful for analysis because of the high temperature generated, and the rapidity of the heating process, which theoretically does not permit differential evaporation effects between different elements; these considerations are particularly true for the analysis of milk powders, where laser–sample coupling is poor. However, repeated experiments on our system using giant pulses yielded only inferior sensitivities and greater memory effects than with free-running pulses.[4,11] Therefore, free-running pulses were used throughout.

Laser energy is chosen empirically to give good signal-to-background ratios but to avoid saturation effects. This is a compromise, and particularly so in multi-elemental analysis. Several saturation effects have to be considered. Firstly, for elements present at major levels in the matrix, partial saturation of the channels of the MCA covering the mass corresponding to a particular isotope will lead to counting errors and consequently poor concentration data. However, a dead time correction can be applied depending on the rate of arrival of ions at the detector. Should the counts at a particular *m/z* ratio overwhelm the memory of the MCA, this isotope is lost for the purposes of the analysis. This can be tolerated if the element is not of analytical interest or if alternative lower abundance isotopes of this element exist. A more serious problem is when too much material *per se* enters the ICP and the whole ionization process is disrupted. In such cases the laser energy must be reduced.

Multiple pulses are generally used for each spectral integration as these produce a smoother introduction of material into the plasma. Nevertheless, as the signals produced are only quasi-stable, counting errors could result with a scanning instrument. Therefore, a relatively high scan rate is employed (10 scans s^{-1}). Otherwise the system parameters are similar to those used in traditional solution nebulization ICP-MS. Table 1 summarizes the laser and spectrometer parameters used.

Table 1 System parameters for multi-elemental analysis

Spectrometer		Surrey prototype
Plasma conditions—		
Coolant flow		14 dm^3 min^{-1}
Cell flow		0.8 dm^3 min^{-1}
Forward r.f. plasma power		1500 W
Reflected power		<20 W
Interface—		
Load coil-extraction aperture separation		10.0 mm
Extraction aperture diameter		1.0 mm
Skimmer aperture diameter		0.7 mm
Ion optics		Optimized on ^{12}C
Scan details		
m/z range		4–240
Dwell time per channel		50 μs
Channels per sweep		2048
Sweeps per integration		300 or 600
Laser		
JK 2000 ruby		Free-running pulses
Ablation regime—		
Sample	Laser pulses	Standard
NIES CRMs No. 7 and No. 1	5 × 0.3 J	Bowen's Kale
IAEA CRM A11	10 × 0.8 J	NIST SRM 1549
GSD-2–GSD-8	10 × 0.1 J	GSD-1

Procedure

The ablation regimes used with the different matrices are given in Table 1. Data accumulation was triggered by the first laser pulse, as there is only about a 2 s delay before ions are registered on the MCA. A fresh sample surface was presented to each laser pulse by automatic rotation of the sample turntable.

Identical conditions were used for the analyses of the sample and standard matrices (n = 4). Calibrations were element-for-element against the sensitivities obtained from the appropriate standard.

Results and Discussion

Plant-based Material

Tables 2 and 3 show the mean elemental concentrations determined in NIES CRMs No. 7 and No. 1, respectively, together with the certified values. Two sets of LA-ICP-MS data are given for each sample. The first is with internal standardization between the mean integrals of the data sets (n = 4) based on ^{26}Mg. Magnesium is a reasonable choice as an internal standard as it is present in many materials, is easily determined by other techniques (such as neutron activation analysis) and has several isotopes, so giving a wide effective concentration range.

Without internal standardization the concentrations determined were incorrect, being about 2-fold too high. This suggests a difference, possibly in the total ablated mass,

Table 2 Analysis of NIES CRM No. 7 Tea Leaves (values given are the concentrations in μg g^{-1} dry mass)

		LA-ICP-MS					
		Simple internal standardization*		Full internal standardization†		Certified value	
Element	*m/z*	Mean	σ	Mean	σ	Mean	σ
Al	27	469	100	470	100	775	20
P	31	3320	360	3310	230	3700‡	—
K	39	14910	770	14920	1300	18600	700
Ca	44	3920	490	3920	500	3200	120
Cr	52	0.25	0.04	0.25	0.04	0.15‡	—
Mn	55	930	140	390	65	700	25
Fe	57	91	47	92	55	—	—
Ni	60	2.5	0.4	2.5	0.5	6.5	0.3
Cu	63	7	1	7	1	7	0.3
Zn	66	35	6	35	8	33	3
Rb	85	8	1	7.6	0.4	—	—
Sr	88	3.2	0.5	3.2	0.6	3.7‡	—
Ba	138	4.3	1.7	4.3	1.9	5.7‡	—
Pb	208	1	0.2	1	0.3	0.80	0.03

* Internal standardization between means only using ^{26}Mg.
† Full between-replicate internal standardization using ^{26}Mg.
‡ Non-certified value.

Table 3 Analysis of NIES CRM No. 1 Pepperbush (values given are concentrations in μg g^{-1} dry mass)

		LA-ICP-MS					
		Simple internal standardization*		Full internal standardization†		Certified value	
Element	*m/z*	Mean	σ	Mean	σ	Mean	σ
Al	27	530	120	530	110	—	—
P	31	1630	205	1620	100	1100‡	—
K	39	16560	2270	16480	1480	15100	600
Ca	44	22750	2870	22760	2180	13800	700
Cr	52	0.91	1.32	0.34	0.07	1.3‡	—
Mn	55	2160	340	940	160	2030	170
Fe	57	236	66	233	66	205	17
Ni	60	4.3	1.2	4.3	1.1	8.7	0.6
Cu	63	21	12	20	5	12	1
Zn	66	280	40	280	30	340	20
Rb	85	89	11	89	6	75	4
Sr	88	38	3	38	3	36	4
Ba	138	88	33	87	34	165	10
Pb	208	4.1	0.7	4.1	0.8	5.5	0.8

* Internal standardization between means only using ^{26}Mg.
† Full between-replicate internal standardization using ^{26}Mg.
‡ Non-certified value.

between the sample and standard. Another possibility is the production of two different particle size distributions and hence transport efficiencies to the ICP. Nevertheless, it is clear that the internal standardization used does at least give good semiquantitative data.

Full internal standardization between replicates, as well as between sample and standard, might improve precision by correcting for local changes in density or differences in laser energy. However, this approach does not appear effective, despite its success with other similar matrices.[15] It would appear that these factors, at least, are not responsible for the imprecision of the measurements. Precisions vary from less than 10 to about 50%.

A few measurements are about a factor of 2 from the true concentrations, but many are considerably better than this, which is certainly encouraging for such a rapid analysis.

Milk Powder

Table 4 shows the results of the determination of Mg, Al, P, K, Ca, Cr, Mn, Fe and Zn in IAEA CRM A11 Milk Powder. These data can be compared with those obtained by conventional solution nebulization ICP-MS[16] as well as the certified and non-certified values. In this work ^{44}Ca was used as an internal standard between the sample and standard means (n = 4). For the milk powder and the plant materials, full between-replicate internal standardization produced no significant improvements in precision. Simple internal standardization is necessary, however, as without this the concentrations determined are each about 2-fold too high.

The calibration difficulty of an individually saturated mass in the standard, for which no alternative isotope exists, occurs here with Na in Bowen's Kale. Thus Na cannot be determined in a multi-element analysis, although a separate determination using a lower laser energy could be undertaken.

On a more positive note it is interesting that for a few elements (Mg, P, K and Mn), the accuracies of the LA-ICP-MS data are superior to those obtained using sample introduction by solution nebulization. Of note, is the almost perfect agreement of the found Mn value with that derived from a multi-technique study (0.257 μg g^{-1}) by Byrne *et al.*[17] Such results are particularly important because of the tedious-

Table 4 Analysis of IAEA CRM A11 Milk Powder (values given are concentrations in μg g^{-1} dry mass)

		LA-ICP-MS		Conventional ICP-MS*		Certified value	
Element	*m/z*	Mean	σ	Mean	σ	Mean	σ
Na	23	5150	920	3880	660	4420	330
Mg	24	1150	230	1410	110	1100	80
Al	27	2.8	1.8	3	0.3	1.3†	—
P	31	10700	2460	14100	850	9100	1020
K	39	17210	2870	19100	1880	17200	1000
Ca	44	Internal standard	—	13200	540	12900	800
Cr	52	—‡	—	1.3	0.1	0.257†	—
Mn	55	0.26	0.13	0.189	0.013	0.377	0.081
Fe	57	1.3	0.5	6.54	0.03	3.65	0.76
Zn	66	77.4	18	39.4	1.3	38.9	2.3

* Conventional pneumatic nebulization ICP-MS.[16]
† Non-certified value.
‡ Element present at 2.6 ng g^{-1} in standard (too low for calibration purposes).

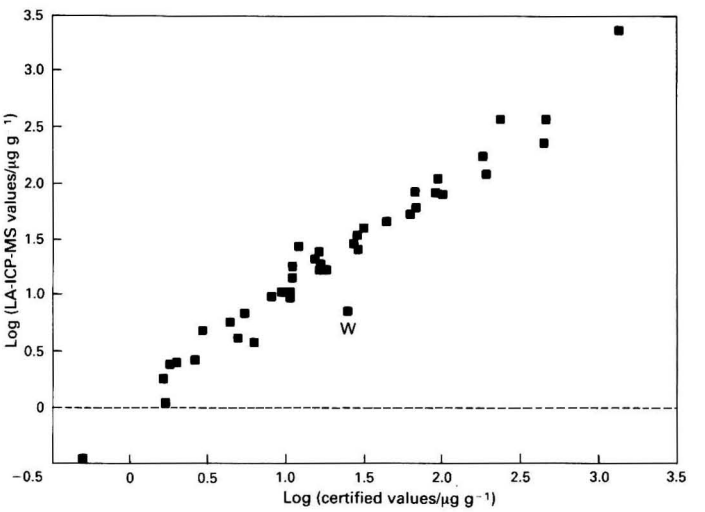

Fig. 1 Log of the LA-ICP-MS determined concentrations in GSD-2 as a function of the log of the certified concentration. Calibrated against certified values of GSD-1

ness of the conventional sample introduction approach using acid digestions for milk products. But again, the precision data are less encouraging, particularly for low level (μg g^{-1}) determinations.

Sediment

Figs. 1–7 show the logarithm of the LA-ICP-MS determined concentrations in the sediments GSD-2–GSD-8 as a function of the logarithm of the corresponding certified values. The following elements were determined: Li, B, Sc, Ti, V, Cr, Mn, Co, Ni, Cu, Zn, Ga, Ge, As, Rb, Sr, Y, Zr, Nb, Mo, Sn, Cs, Ba, La, Ce, Pr, Nd, Sm, Eu, Gd, Tb, Dy, Ho, Er, Yb, Ta, W, Pb, Bi, Th and U. No internal standardization was found to be necessary. Excellent straight lines are obtained over several decades. Only W and Zr show significant deviations from the ideal line. Both elements have rather high boiling-points, but it is doubtful if this is the cause of such large discrepancies. In fact, the poor data for tungsten are almost certainly due to contamination at the ball-milling stage. Sample and standard contamination with tungsten from the lining of the mill has been observed previously in this laboratory, although no other elements were noticeably elevated.

The boron value determined in GSD-8 also deviates substantially from the ideal line. However, sensitivity is always relatively poor for elements so low in the mass range, and possibly aggravates the usual difficulties of calibration.

Precisions (relative standard deviation) were typically in the range 15–20%, considerably better than was found with the biological matrices.

Detection Limit

Tables 5–7 show the detection limits for the analysis of the CRMs. It is not clear that the conventional 3σ of the blank definition of the detection limit is particularly applicable to LA-ICP-MS. The detection limits here are line equivalent backgrounds based on a 'gas blank'. If the ablation chamber and associated gas lines are clean, a blank spectrum obtained immediately after the firing of the laser onto an inert material, such as poly(tetrafluoroethylene), is identical with that obtained simply by integrating without the laser being fired. Hence the latter 'gas blank' was used here.

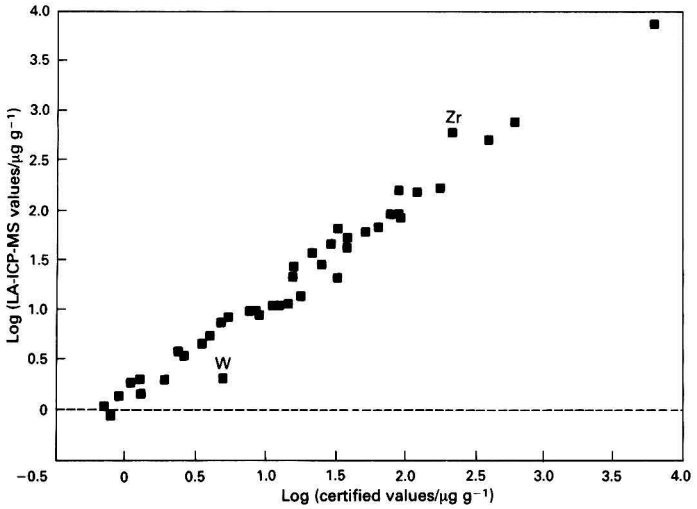

Fig. 2 Log of the LA-ICP-MS determined concentrations in GSD-3 as a function of the log of the certified concentration. Calibrated against certified values of GSD-1

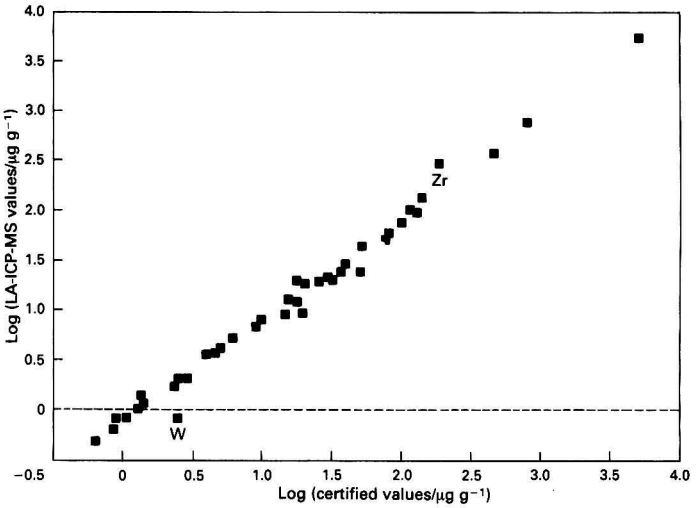

Fig. 3 Log of the LA-ICP-MS determined concentration in GSD-4 as a function of the log of the certified concentration. Calibrated against certified values of GSD-1. (Data for this sample only have also been presented in ref. 20)

Table 5 Detection limits for analysis of plant materials (values given are concentrations in μg g^{-1} dry mass). Based on line equivalent background using sensitivities from Bowen's Kale

Element	Detection limit	Element	Detection limit
Al	1.9	Ni	0.57
P	26.4	Cu	0.57
K	64.3	Zn	0.73
Ca	350	Rb	0.25
Cr	0.06	Sr	0.12
Mn	0.18	Ba	0.02
Fe	10	Pb	0.04

Table 6 Detection limits for the analysis of milk powder (values given are concentrations in μg g^{-1} dry mass). Based on line equivalent background using sensitivities from NIST SRM 1549

Element	Detection limit	Element	Detection limit
Na	10.2	Cr	0.0001
Mg	0.28	Mn	0.03
Al	0.01	Fe	0.04
P	58	Zn	1.5
K	51		

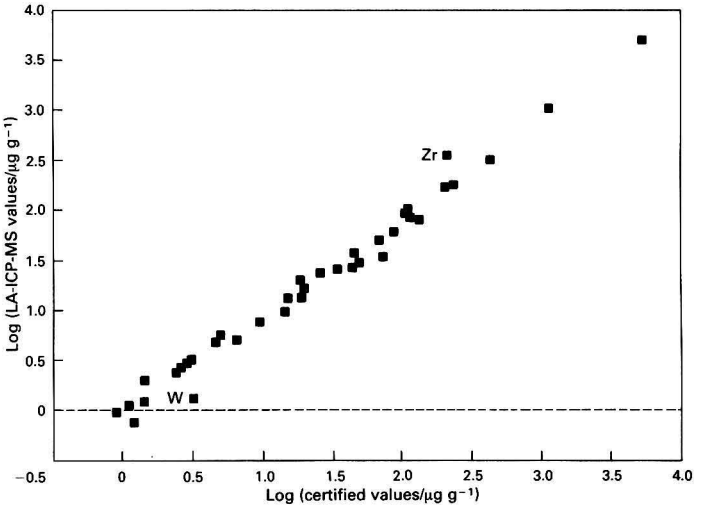

Fig. 4 Log of the LA-ICP-MS determined concentrations in GSD-5 as a function of the log of the certified concentration. Calibrated against certified values of GSD-1

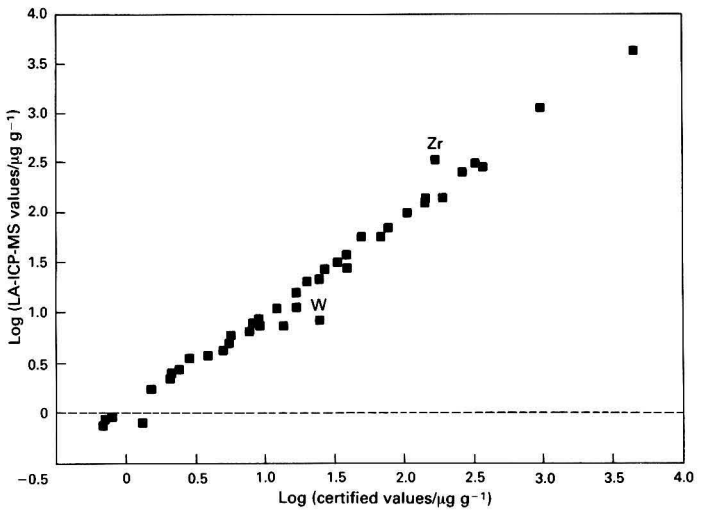

Fig. 5 Log of the LA-ICP-MS determined concentrations in GSD-6 as a function of the log of the certified concentration. Calibrated against certified values of GSD-1

Table 7 Detection limits for Chinese reference sediments (values given are concentrations in μg g^{-1} dry mass). Determined from line equivalent background using sensitivities from GSD-1

Element	Detection limit	Element	Detection limit	Element	Detection limit	Element	Detection limit
Li	0.158	Ga	0.027	Ba	0.087	Er	0.038
B	1.6	Ge	0.011	La	0.016	Yb	0.264
Sc	0.029	As	0.02	Ce	0.008	Ta	0.011
Ti	0.537	Rb	0.008	Pr	0.2	W	0.008
V	0.019	Sr	0.022	Nd	0.12	Pb	0.01
Cr	0.076	Y	0.019	Sm	0.137	Bi	0.005
Mn	0.019	Zr	0.199	Eu	0.053	Th	0.013
Co	0.027	Nb	0.013	Gd	0.077	U	0.005
Ni	0.059	Mo	0.01	Tb	0.028		
Cu	0.018	Sn	0.011	Dy	0.102		
Zn	0.164	Cs	0.014	Ho	0.015		

For the biological materials the detection limits are typical of those commonly obtained by LA-ICP-MS.[8] Those obtained for the analysis of the sediments, however, are clearly superior. Indeed they are even superior to those obtained in a very similar analysis of a series of Chinese certified reference sediments (GSS series) by LA-ICP-MS;[18] this might be due to several causes. Firstly, the sediments are supplied as fine powders and ablate in a regular way, giving better-defined pits than are obtained with the biological materials. Secondly, for a fixed ablated volume, a correspondingly greater mass of a sediment is removed compared with a biological material because of the higher density of the former. Hence, relatively high sensitivities are obtained for the sediments. As blank levels are independent of the matrix, greater sensitivity implies lower detection limits. This provides motivation to those interested in LA-ICP-MS as a technique for geological analysis. It also suggests that perhaps, even for single laser

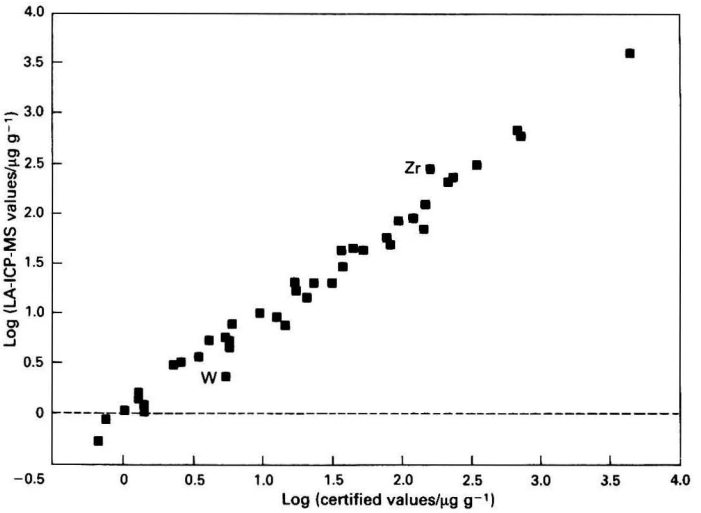

Fig. 6 Log of the LA-ICP-MS determined concentrations in GSD-7 as a function of the log of the certified concentration. Calibrated against certified values of GSD-1

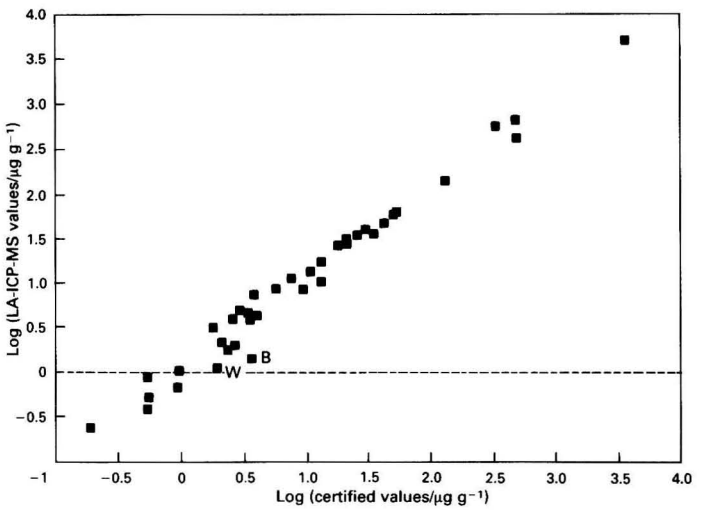

Fig. 7 Log of the LA-ICP-MS determined concentrations in GSD-8 as a function of the log of the certified concentration. Calibrated against certified values of GSD-1

shots that sample a restricted volume (2–3 μg), elemental analysis will prove possible, allowing microprobe applications.

Analytical Difficulties and Future Prospects

It can be concluded that biological matrices can be analysed by LA-ICP-MS, at least semiquantitatively. Trace analysis, however, is rather difficult for several reasons. Firstly, a well characterized matrix-matched standard needs to be available. Secondly, for the best calibrations, elements in the standard should be at similar concentrations to those in the sample, or a range of standards should be available. These criteria are rarely met in practice. Thirdly, many values in CRMs are for 'information purposes only' and so no great weight can be given to their accuracy.

Regarding calibration with CRMs in general, it is not always exactly clear what the 'precision' of the certified values signifies. Almost every reference material agency uses a different system. A related difficulty lies with the fact that concentrations are always expressed in terms of dry mass. Thus standards and samples should always be dried prior to analysis. Unfortunately, the drying procedures recommended for similar materials vary greatly. The drying process also introduces the possibility of the loss of volatile elements.

The data reported here, relating to the biological matrices, are encouraging, not only because of the complex nature of these materials, but also because of the limited mass ablated (sub-milligram per integration), which can be compared, for example, with the minimum 250 mg sample mass typically used to ensure sample homogeneity when analysing biological CRMs by more conventional techniques.

The analysis of CRM A11 Milk Powder merits additional comment. A ruby laser appears not to be very effective in ablating milk powder that is simply pressed into a disc, the

surface of the sample appearing smooth and shiny. However, the combining of the powder with a suitable graphite is at least partially successful in increasing the mass ablated by a given laser pulse energy. However, high energies (0.8 J per shot) are still necessary for reasonable sensitivity. Q-switched pulses, which might be expected to be more effective, remove very little matter. An Nd:YAG laser might be better here; firstly, as coupling to the substrate might be stronger at its wavelength (1064 nm), and secondly because it can operate at greater repetition rates (>10 Hz) than the ruby (maximum 1 Hz).

Despite the difficulties noted, some accurate determinations have been made in complex matrices. In addition, the main advantages of the analysis, *i.e.*, ease and speed, have been realized. This was particularly true for the analysis of the sediments, where the precision and especially the accuracy were extremely good. Detection limits obtained for the analysis of the sediments were also very low, especially as they represent concentrations in the solid. In the equivalent solution nebulization, a considerable dilution prior to analysis is usually required.

Simple internal standardization between sample means is sometimes required. If a suitable element is chosen a great improvement in accuracy is thereby gained. However, full internal standardization is often disappointing with regard to improvements in precision. It is also rather difficult to know *a priori* whether simple internal standardization is necessary. Hence, it ought to be habitually used for real analyses.

New developments of artificial standards, alternative calibration techniques and even laser ablation in a liquid medium[19] might further improve the performance of the technique. However, rapid semiquantitative multi-elemental analyses of difficult matrices are certainly already possible.

These analyses were undertaken at the Natural Environmental Research Council (NERC) ICP-MS Facility when it was sited at the University of Surrey, Guildford, Surrey, UK. Use of these facilities is gratefully acknowledged. I thank Dr. Alan Gray, Dr. John Williams and Dr. Neil Ward for expert advice, and Birthright for financial support.

References

1 Gray, A. L., *Analyst*, 1985, **110**, 551.
2 Tye, C., Gordon, J., and Webb, P., *Int. Lab.*, 1987, **17**, 34.
3 Imai, N., *Anal. Chim. Acta.*, 1990, **235**, 381.
4 Durrant, S. F., *Braz. J. Vacuum Appl.*, 1991, **10**, 39.
5 Marshall, J., Franks, J., Abell, I., and Tye, C., *J. Anal. At. Spectrom.*, 1991, **6**, 145.
6 Beauchemin, D., McLaren, J. W., Willie, S. N., and Berman, S. S., *Anal. Chem.*, 1988, **60**, 687.
7 Totland, M., Jarvis, I., and Jarvis, K. E., *Chem. Geol.*, 1992, **95**, 35.
8 Mochizuki, T., Sakashita, A. Iwata, H., Kagaya, T., Shimamura, T., and Blair, P., *Anal. Sci.*, 1988, **4**, 403.
9 Mochizuki, T., Sakashita, A., Iwata, H., Ishibashi, Y., and Gunji, N., *Anal. Sci.*, 1991, **7**, 151.
10 Perkins, W. T., Fuge, R., and Pearce, N. J. G., *J. Anal. At. Spectrom.*, 1991, **6**, 445.
11 Durrant, S. F., Ph.D. Thesis, University of Surrey, Guildford, Surrey, UK, 1989.
12 Date, A. R., and Gray, A. L., *Analyst*, 1983, **108**, 159.
13 Gray, A. L., and Date, A. R., *Analyst*, 1983, **108**, 1033.
14 Welch, M., *Lasers Appl.*, 1986, **5**, 67.
15 Ward, N. I., Durrant, S. F., and Gray, A. L., *J. Anal. At. Spectrom.*, in the press.
16 Emmett, S. E., *J. Anal. At. Spectrom.*, 1988, **3**, 1145.
17 Byrne, A. R., Camara-Rice, C., Cornelis, R., de Goeij, J. J. M., Iyengar, G. V., Kirkbright, G., Knapp, G., Parr, R. M., and Stoeppler, M., *Fresenius' Z. Anal. Chem.*, 1987, **326**, 723.
18 Durrant, S. F., and Ward, N. I., *Fresenius' J. Anal. Chem.*, submitted for publication.
19 Iida, Y., Tsuge, A., Uwamino, Y., Morikawa, H., and Ishizuka, T., *J. Anal. At. Spectrom.*, 1991, **6**, 541.
20 Ward, N. I., and Durrant, S. F., in *Proceedings of the International Conference on Heavy Metals in the Environment, Edinburgh, September* 1991, ed., Farmer, J. G., CEP Consultants, Edinburgh, 1991, vol. 1, pp. 588–592.

Paper 2/00890D
Received February 19, 1992
Accepted June 10, 1992

Determination of Ultrafiltrable Zinc in Human Milk by Electrothermal Atomic Absorption Spectrometry

Josiane Arnaud and Alain Favier
Laboratoire de Biochimie C, Centre Hospitalier Regional et Universitaire de Grenoble, B.P. 217, 38043 Grenoble Cedex 9, France

Percentages of non-protein-bound zinc in human milk have been reported by different workers, but ultrafiltration and zinc determination in human milk have not been comprehensively examined. However, zinc contamination and zinc membrane binding have been described for the determination of non-protein-bound zinc in serum. In this work, ultrafiltration was studied in terms of zinc contamination and zinc membrane binding. An MPS-1 micropartition system fitted with a YMT membrane was used. Zinc contamination was found to be less than 276 nmol dm^{-3} and the zinc recovery was 85 ± 4%. The conditions for electrothermal atomic absorption spectrometry were also studied. The detection limit was found to be 26.4 nmol dm^{-3} and the upper linear range was 4 μmol dm^{-3}. The precision varied from 3% (within-run) to 17% (between-run). The recovery of standard additions was 95 ± 7% (n = 30, different human milk ultrafiltrate samples). Physiological values varied from 0.46 to 84 μmol dm^{-3} (4–56% of zinc in whole human milk). Expressed in μmol dm^{-3}, zinc in human milk ultrafiltrate decreased slightly through the lactation period, whereas expressed as a percentage of the total zinc in milk, zinc in human milk ultrafiltrate remained constant from day 2 to day 69 *post partum*.

Keywords: *Zinc determination; electrothermal atomic absorption spectrometry; ultrafiltration; human milk; reference values*

Zinc is essential for normal growth and development in infants. Because the only food for neonates is human milk or formula, it is important that these foods provide adequate amounts of bioavailable zinc. Although zinc deficiency in full-term breast-fed infants has been described,[1–3] it is very rare in breast-fed compared with formula-fed infants.[4,5] Bioavailability has been documented to be higher in human milk than in formula.[6–9] This higher bioavailability could reasonably be explained by the higher non-protein-bound zinc fraction in human milk[6,10–12] but also by compounds that facilitate or reduce the zinc bioavailability.[7,8,13–15] A difference in solubility between human milk and cow's milk or formula during digestion has been reported.[6,8]

This study was carried out to develop a reliable method for the determination of non-protein-bound zinc in human milk. Non-protein-bound zinc has been previously reported by several workers,[6,9,16–19] but the ultrafiltration step has not been extensively examined, particularly in terms of contamination and membrane binding. Moreover, to the best of our knowledge, a micropartition system, more suitable for routine analysis than ultrafiltration under nitrogen in an ultrafiltration cell, has not been used previously in order to ultrafilter milk samples. The proposed method uses ultrafiltration through YMT cellulose acetate membranes. The ultrafiltration apparatus is washed with ethylenediaminetetraacetic acid (EDTA) dipotassium salt prior to use in order to remove zinc. Zinc in the milk ultrafiltrate is determined by electrothermal atomic absorption spectrometry (ETAAS). The sensitivity of this method is adequate for determining the very low (1.4 μmol dm^{-3}) zinc concentrations reported in some human milk samples.[1–3] The method is simple, rapid and reliable.

Experimental

Apparatus

Milk ultrafiltrate was prepared using an Amicon (Danvers, MA, USA) MPS-1 micropartition system fitted with a YMT cellulose acetate membrane. Silicone-rubber was used in order to reduce zinc contamination. Both YMB (Amicon) and poly(acrylonitrile)AN-69 (Rhône Poulenc, Saint Fons, France) membranes were also used for comparison. These ultrafiltration membranes had nominal molecular mass cut-offs of <30 000 Da. The zinc concentration was determined using a Perkin-Elmer Model 560 atomic absorption spectrometer fitted with an HGA-500 graphite furnace and an AS-40 autosampler. A zinc hollow cathode lamp was used as the light source (intensity 15 mA). Peaks were recorded with a Servotrace chart recorder (Sefram, Paris, France) having a full-scale pen response of 0.3 s. A chart recorder speed of 50 mm min^{-1} and a range of 10 mV were used. Peak heights were measured.

All the plasticware was made of polycarbonate, polystyrene or polyethylene. Except for the MPS-1 units, the plasticware was soaked for 16 h in 10% v/v nitric acid, then for 16 h in 10% v/v hydrochloric acid. Finally, it was rinsed with de-ionized water and dried in a stainless-steel oven at 50 °C.

Subjects

Subjects who had given verbal consent were enrolled during the first 2 months of lactation. A total of 83 lactating mothers, providing 120 individual milk samples, were selected. All the mothers were healthy and apparently well fed, as far as clinical observation was considered. There was neither albumin nor glucose in their urine and the haemoglobin concentration at delivery was 115 ± 11 g dm^{-3}, expressed as the mean ±1 standard deviation (SD). All the mothers had uncomplicated pregnancies and delivered a single full-term infant. All the infants were healthy and growing well. A description of the subjects is given in Table 1.

Samples

The breast was cleaned with de-ionized water and approximately 10 cm^3 of breast milk were hand expressed, before one of the morning feedings (9.00–11.00 a.m.), into a 30 cm^3 polystyrene bottle. Milk samples were transported on ice to the laboratory. Aliquots of the milk samples (2 cm^3) were transferred into 5 cm^3 polystyrene tubes and then frozen at −18 °C until analysis.

Reagents

The de-ionized water used for all solution preparations was processed through a system consisting of two high-capacity

Table 1 Description of mothers and their newborns

Mothers—	
Total number	83
Number of primiparae	45
Residing area:	
Urban	68
Rural	15
Race:	
Caucasian	61
Arabian	18
Asian	3
Black	1
Family income:	
Low	22
Middle	56
High	5
Age/years	26 (19–39)*
Body mass index before pregnancy/kg m^{-2}	21.5 (16.8–30.5)*
Weight gain during pregnancy/kg	12 (5–21)*
Gestional age/weeks	39.7 (36–43)*
Infants—	
Sex:	
Male	43
Female	40
Birth weight/kg	3.305 (2.370–4.300)*
Birth height/cm	49.7 (46–54)*

* Mean (range).

de-mineralizing cartridges (Crouzat, Toulouse, France) and a Milli-Q system (Millipore, Bedford, MA, USA). The resistance was at least 18 MΩ cm^{-1} and zinc was undetectable.

Ultrapure-grade hydrochloric acid (Normaton) was obtained from Prolabo (Paris, France) and nitric acid from Merck (Darmstadt, Germany).

A 3 mmol dm^{-3} solution of EDTA dipotassium salt (Fluka, Buchs, Switzerland) and a 0.1% m/v Triton X-100 (Prolabo) solution were prepared in de-ionized water.

Procedure

Sample and standard solution preparation and analysis were conducted in a class 100 000 filtered-air room.

Decontamination of the MPS-1 micropartition system

The MPS-1 units were decontaminated by soaking in 3 mmol dm^{-3} EDTA solution and sonicated for 30 min. This cleaning step was repeated twice, then the MPS-1 units were rinsed three times with de-ionized water. The MPS-1 units were placed in a beaker covered with a poly(propylene) grid and dried overnight at 50 °C in a stainless-steel oven.

Membranes were immersed in de-ionized water for 5 min. This procedure was repeated twice. The membranes were then immersed in 3 mmol dm^{-3} EDTA solution for 5 min. This procedure was repeated twice. Polystyrene tweezers (Prolabo), which had been previously decontaminated by soaking in 3 mmol dm^{-3} EDTA solution, were used to handle the membranes. The MPS-1 units were then assembled with the decontaminated polystyrene tweezers.

The assembled kit was decontaminated by adding 1 cm^3 of 3 mmol dm^{-3} EDTA solution to the sample reservoir and centrifuging at 1600*g* for 5 min. This procedure was repeated twice. Then, the empty MPS-1 micropartition system was centrifuged for 2 min, rinsed by adding 1 cm^3 of de-ionized water to the sample reservoir and centrifuging at 1600*g* for 5 min. Finally, the empty MPS-1 micropartition system was centrifuged at 1600*g* for 2 min.

Ultrafiltration of milk

A 1 cm^3 human milk sample was added to the reservoir of a decontaminated MPS-1 micropartition system, then, the latter was centrifuged in a fixed angle-head rotor (Jouan, Saint Nazaire, France) at 2500*g* for 1 h. The zinc in the ultrafiltrate was determined immediately, in duplicate, by ETAAS. The volume of the ultrafiltrate was measured and this volume was taken into account in the zinc determination.

Preparation of standard solutions

Zinc stock standard solution (75 μmol dm^{-3}) was prepared from zinc metal (Merck). Zinc (4.9 mg) was dissolved in 5 cm^3 of 11 mol dm^{-3} Ultrapur grade hydrochloric acid (Prolabo). After total dissolution, the solution was poured into a 1 dm^3 calibrated flask containing about 700 cm^3 of de-ionized water, then, the volume was made up with de-ionized water. Aliquots of the stock solution was stored at −18 °C.

Working standard solutions were prepared daily from the stock standard solution by dilution with de-ionized water. These working standard solutions contained 0.37, 0.75 and 1.50 μmol dm^{-3} of zinc.

Zinc determination

Zinc was determined in total milk using a previously described method.[20] The milk ultrafiltrate was diluted with de-ionized water (1 + 99) and zinc was determined by ETAAS using external calibration. The spectrometer was operated at 213.9 nm with a slit-width of 0.7 nm. The absorbance was measured in the peak height mode. The injection volume was 10 mm^3. A standard uncoated graphite furnace was used in all determinations. The graphite furnace heating variables and gas flow rate were determined to provide the optimum sensitivity for zinc determination. The furnace heating procedure was (*i*) drying at 110 °C for 20 s (ramp time 20 s), (*ii*) ashing at 650 °C for 30 s (ramp time 1 s) and (*iii*) atomization at 2200 °C for 5 s (ramp time 1 s). The internal gas was nitrogen and its flow rate during the atomization step was reduced to 250 cm^3 min^{-1}. Based on our previous results with serum[21] and milk[20] samples, deuterium arc background correction was not used.

Analytical Performance

The detection limit was calculated according to the criterion 3.3 SD/*S*,[22] where SD is the standard deviation of 30 replicate zinc determinations at the blank level and *S* is the slope of the calibration graph. The upper linear range was defined according to Vassault *et al.*[23] by triplicate zinc standard solution analyses (0.77, 1.5, 2.3, 3.1, 3.8 and 4.6 μmol dm^{-3} of zinc) over a 3 d period. The within-run precision was calculated from 30 replicate analyses of the same milk ultrafiltrate and from 30 replicate ultrafiltrations of the same milk, performed on the same day. After zinc determination, the milk ultrafiltrate remainders were mixed and aliquots of 200 mm^3 were frozen at −18 °C in order to evaluate the between-run precision. The latter was assessed first by 30 analyses of the same milk ultrafiltrate and second by 30 ultrafiltrations of the same milk performed over a 2 month period.

Results and Discussion

Ultrafiltration

Influence of the membrane

Zinc contamination and membrane binding were evaluated using the three membranes. Zinc contamination was assessed by filtering 1 cm^3 of de-ionized water using the decontaminated MPS-1 micropartition system. The results are presented in Table 2. Zinc contamination seemed less important with the YMT membranes. Nevertheless, although zinc was undetectable in a large number of de-ionized water ultrafiltrates [28 (AN-69), 31 (YMB) and 34 (YMT)], substantial contamination might occur; as a result, routine control was necessary.

Bloxam *et al.*[24] have also reported differences between batches.

Membrane binding was evaluated by filtering 1 cm^3 of a 38 μmol dm^{-3} aqueous zinc solution. The results are given in Table 2. The membrane zinc binding was very important on YMB and AN-69 membranes. The zinc recoveries obtained by Faure *et al.*[25] using these two membranes were better than the presented results. Nevertheless, the recovery was assessed by filtering zinc in a solution containing histidine, cysteine and sodium chloride.[25] According to our results, presented in Fig. 1, and to the results obtained by Bloxam *et al.*[24] and Brushmiller *et al.*,[6] the addition of compounds that are known to complex zinc and the addition of electrolytes affect the recovery. As shown in Fig. 1, the zinc recovery increased to values greater than 100%. This artifact is related to the use of an external zinc calibration prepared in de-ionized water. Addition of EDTA to the standards yielded a positive interference (Fig. 1). With the YMT membrane, the previously reported zinc recovery varied from 79.7 to 110%.[25,26] The acceptable zinc recovery was confirmed by duplicate filtration through the YMT membrane of 1 cm^3 of three different zinc solutions prepared in de-ionized water. The recoveries of 7.7, 15.4 and 30.8 μmol dm^{-3} of zinc were 86, 93 and 103%, respectively.

The ultrafiltrate volume was greater using YMT membranes (Table 2).

Finally, YMB or YMT membranes supplied by Amicon were found to be more suitable for routine determination than AN-69 membranes obtained from a haemodialyser. As a result, the YMT membrane was adopted in further assays.

Table 2 Zinc contamination, zinc recovery and ultrafiltrate volume using different membranes

	Membrane material		
Parameter	AN 69 Poly(acrylonitrile)	YMB Cellulose acetate	YMT Cellulose acetate
Mean zinc contamination (n = 40)*/nmol dm^{-3}	74	51	23
Undetectable results (%)	70	78	87
Maximum zinc contamination/ nmol dm^{-3}	276	276	155
Zinc recovery (n = 10)† (%)	10.5 ± 12	15 ± 3	85 ± 4
Milk ultrafiltrate volume (n = 10)‡/mm^3	252 ± 16	396 ± 9	436 ± 13

* Ultrafiltration of 1 cm^3 of de-ionized water.
† Ultrafiltration of 1 cm^3 of solution containing 38 μmol dm^{-3} of Zn.
‡ Ultrafiltration of 1 cm^3 of human milk sample. Centrifugation at 2500g for 20 min.

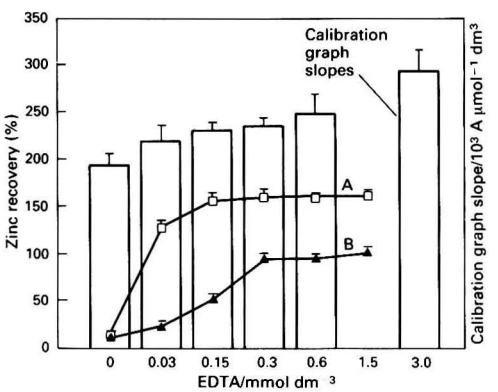

Fig. 1 Effect of EDTA on zinc recovery and on calibration graph slope. Results are expressed as mean ± 1 SD, n = 5. A, YMB membranes; and B, AN-69 membranes

Influence of the cleaning procedure

The influence of the membrane pre-treatment, prior to the MPS-1 micropartition system assembly, was evaluated. The YMT membranes were rinsed either three times with de-ionized water or three times with de-ionized water followed by three times with 3 mmol dm^{-3} EDTA solution. The MPS-1 units were then assembled. A 1 cm^3 volume of 3 mmol dm^{-3} EDTA solution was added to the sample reservoir and the MPS-1 micropartition system was centrifuged at 1600g for 10 min. The zinc concentration in the ultrafiltrate was determined using zinc standards prepared in 3 mmol dm^{-3} EDTA solution. The zinc concentration, expressed as mean (range) was found to be 821 (738–1415) nmol dm^{-3} (de-ionized water rinsing, n = 10 observations) and 158 (15–600) nmol dm^{-3} (de-ionized water and EDTA rinsing, n = 10). These results show that the pre-treatment of the MPS-1 units and membrane prior to the MPS-1 micropartition system assembly was not sufficient to eliminate zinc contamination. However, membrane pre-treatment with EDTA, prior to the assembly of the MPS-1 micropartition system, had a measurable effect on zinc decontamination.

Treatment of the assembled MPS-1 micropartition system was also studied. The YMT membranes were rinsed as described under Experimental. The assembled MPS-1 micropartition systems were washed seven times with 3 mmol dm^{-3} EDTA solution. The zinc concentrations varied from 15 to 600 nmol dm^{-3} (mean 158 nmol dm^{-3}, n = 10) in the first EDTA ultrafiltrate and from undetectable to 46 nmol dm^{-3} (mean 12 nmol dm^{-3}, n = 10) in the second EDTA ultrafiltrate, and then reached a plateau. These results indicate that two washing steps were sufficient to eliminate zinc contamination. However, because of the great variability of zinc contamination (see above), three EDTA washing steps were applied in further assays.

Centrifugation time

The centrifugation time was examined in terms of ultrafiltration rate. The ultrafiltrate volume reached a plateau within 1 h.

Table 3 Influence of the diluent and dilution rate on within-run precision and zinc recovery (n = 10 determinations, performed on the same human milk)

	Diluent					
	De-ionized water			0.1% m/v Triton X-100		
Parameter	1 + 24*	1 + 49*	1 + 99*	1 + 24*	1 + 49*	1 + 99*
Zinc concentration/μmol dm^{-3}	21 ± 0.4	23 ± 0.3	21 ± 0.6	25 ± 0.3	22 ± 0.4	25 ± 0.5
Within-run precision [RSD (%)]	2.0	1.2	3.0	1.0	2.0	2.0
Zinc recovery (%)	80 ± 6	78 ± 6	99 ± 3	64 ± 1	77 ± 2	92 ± 3

* Dilution rate.

Membrane retention of protein

Twenty-seven milk samples were ultrafiltered through the YMT membrane. The protein concentrations in these early lactation whole milks and milk ultrafiltrates, measured using a modified Lowry method[27,28] were 29 ± 9 and 2.1 ± 0.7 g dm^{-3}, respectively. These Lowry-reactive substances were not identified. Nevertheless, the Lowry method also detects cysteine, tryptophan, tyrosine and peptides, which could pass through the membrane. Using a PM-10 membrane and the Lowry method Bloxam *et al.*[24] reported a total protein concentration in the ultrafiltrate of 0.07 ± 0.013%. According to Foote and Delves,[26] the protein concentration in the ultrafiltrate is negligible. Moreover, the proteins reported to carry zinc in milk (albumin;[29-31] lactoferrin;[32] lactalbumin;[31] and caseinate micelles[30,32]) have a high molecular mass and it seems unlikely that these proteins could pass through the membrane.

Atomic Absorption Spectrometry

Influence of diluent and dilution rate

De-ionized water and 0.1% m/v Triton X-100 were selected for this test. De-ionized water is the most commonly used diluent for zinc determination by ETAAS. Triton X-100 (0.1% m/v) was the diluent used for zinc determination in whole milk[20] and, as we expressed the ultrafiltrable zinc in μmol dm^{-3} and as a percentage of the total amount in whole milk, it might be of importance to have the same diluent. Three dilutions were evaluated: 1 + 24, 1 + 49 and 1 + 99.

Zinc concentrations from these two diluents were undetectable. The detection limits were found to be 26.4 nmol dm^{-3} (de-ionized water) and 52.8 nmol dm^{-3} (0.1% m/v Triton X-100). The upper linear ranges were found to be 4 μmol dm^{-3} in de-ionized water and 3 μmol dm^{-3} in 0.1% m/v Triton X-100. The slopes of the calibration graphs, expressed as peak height absorbance/zinc concentration (μmol dm^{-3}), were found to be 0.220 ± 0.009 (0.1% m/v Triton X-100, n = 30) and 0.220 ± 0.014 (de-ionized water, n = 30).

The results of the recovery experiment and within-run precision are indicated in Table 3. The within-run precisions were similar with both diluents. The zinc recovery increased with the dilution rate and this phenomenon was still greater in 0.1% m/v Triton X-100. These results are in agreement with those obtained in whole milk.[20] Finally, the zinc concentrations were similar. As a result, de-ionized water was used in further assays.

Calibration

Zinc was determined in 74 milk ultrafiltrate samples using either an external calibration (standard solutions prepared using de-ionized water) or by the method of standard additions. The results showed acceptable agreement between the two calibration procedures. The correlation coefficient was found to be 0.90. The substantial variability in milk composition might explain the range of standard addition recoveries (80–112%) and the poor correlation coefficient (r). The Deming regression line was

$$Zn_{ext.\ calib.} = 0.99_{std.\ add.\ calib.} - 0.5\ \mu mol\ dm^{-3}$$

The zinc concentrations, expressed as means ±1 SD, were 18.9 ± 8.8 μmol dm^{-3} (by external calibration) and 19.6 ± 8.9 μmol dm^{-3} (by standard additions calibration) and were not statistically significantly different (paired Student's t-test). The external calibration procedure was adopted for practical reasons.

Validity of the Method

The proposed ultrafiltration method used an MPS-1 micropartition system fitted with a YMT membrane. Centrifugation was carried out at 2500g for 1 h. The selected ETAAS method used uncoated graphite furnace tubes and no background correction. The diluent was de-ionized water and the dilution rate was 1 + 99. The working standard solutions contained 0.37, 0.77 and 1.50 μmol dm^{-3} of zinc.

The within-run relative standard deviations (RSDs), calculated from 30 replicate analyses of the same milk ultrafiltrate and from 30 replicate ultrafiltrations of the same human milk sample, were 3 and 6%, respectively. The corresponding between-run RSDs were 12 and 17%, respectively. These values were within the degree of variation expected in view of the procedure involved. The accuracy was evaluated by measuring the recovery of standard additions. Using 74 different ultrafiltrate samples, the recoveries of 0.38, 0.77 and 1.53 μmol dm^{-3} of zinc were 94 ± 10, 92 ± 10 and 96 ± 10%, respectively. The detection limit was 26.4 nmol dm^{-3} and the upper linear range was 4 μmol dm^{-3}.

Effect of Freezing

Twenty-seven milk samples were divided into four aliquots. One was ultrafiltered and analysed immediately and the other three were kept at −18 °C for 6, 9 and 13 months prior to the ultrafiltration.

The results are given in Table 4. The zinc concentrations in the ultrafiltrates were similar before and after freezing (P >0.05, paired Student's t-test). These results are in agreement with those reported by Fransson and Lonnerdal[18] in milk ultrafiltrates and by Bloxam *et al.*[24] in amniotic fluid ultrafiltrates.

Reference Values

Zinc was measured in 120 milk samples and the corresponding ultrafiltrates. The results for non-protein-bound zinc are presented in Figs. 2 and 3. As a marked change in zinc

Table 4 Effect of freezing on the non-protein-bound zinc in human milk (n = 27 milk samples) (P >0.05)

	Month			
	0	6	9	13
Ultrafiltrable zinc (%)	18 ± 11	16 ± 11	19 ± 9	18 ± 10
Ultrafiltrable zinc/ μmol dm^{-3}	11 ± 6	11 ± 7	12 ± 7	11 ± 5

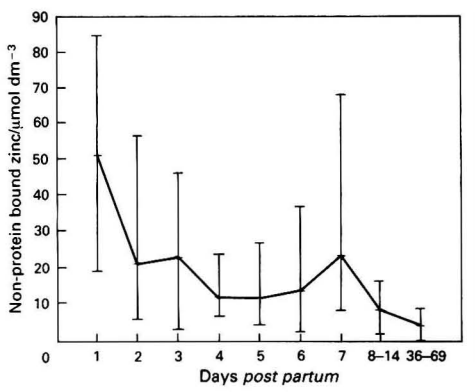

Fig. 2 Changes of non-protein-bound zinc concentration in human milk, during lactation. + = Mean zinc concentration in μmol dm^{-3}; error bars show minimum and maximum zinc concentrations, in μmol dm^{-3}. n = 5 (day 1), n = 12 (day 2), n = 22 (day 3), n = 7 (day 4), n = 18 (day 5), n = 26 (day 6), n = 20 (day 7), n = 4 (day 8 to day 14) and n = 6 (day 36 to day 69)

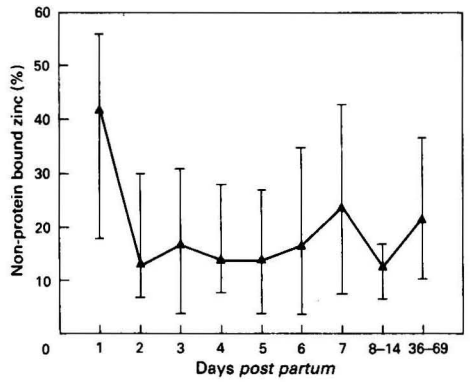

Fig. 3 Changes of the percentage of non-protein-bound zinc in human milk, during lactation. ▲ = Mean percentage; error bars indicate minimum and maximum percentages. n = 5 (day 1), n = 12 (day 2), n = 22 (day 3), n = 7 (day 4), n = 18 (day 5), n = 26 (day 6), n = 20 (day 7), n = 4 (day 8 to day 14) and n = 6 (day 36 to day 69)

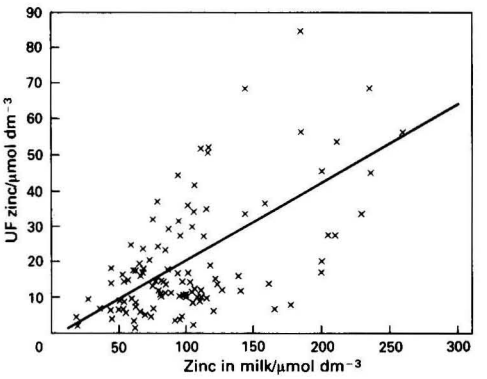

Fig. 4 Correlation between total zinc and non-protein-bound zinc concentrations (in μmol dm^{-3}) in the 120 human milk samples examined. —, Deming regression line (slope = 0.22, intercept = −2.2 μmol dm^{-3}), r = 0.59

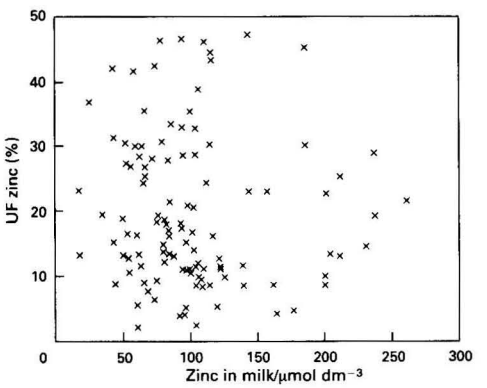

Fig. 5 Relationship between the total zinc concentration (in μmol dm^{-3}) and the percentage of non-protein-bound zinc, in the 120 human milk samples examined. r = 0.05

concentration in whole milk has been reported during early lactation,[20,31] the results are specified for the first 7 d *post partum*.

Differences among individuals were substantial. These results are in agreement with those of previous work.[16,19,33] The whole milk zinc measured in these samples was 101 ± 49 (18–261) μmol dm^{-3} [mean ± 1 SD (range)] and the concentration of non-protein-bound zinc was 20 ± 16 (1.4–85) μmol dm^{-3}. The proportion of zinc in the ultrafiltrate was 20 ± 12% (2–47) [mean ± 1 SD (range)]. These results are in agreement with those of previous work using ultrafiltration through different membranes[9,16–19] or gel-filtration chromatography,[30] but are lower than those reported by Brushmiller *et al.*[6] and Evans and Johnson.[33]

The non-protein bound zinc, expressed in μmol dm^{-3}, decreased with time in colostrum milk (days 1 and 2), and continued to decrease after day 14 *post partum* (Fig. 2). These results are in agreement with those of Lonnerdal *et al.*,[19] who noted a decrease in ultrafiltrable zinc concentration from day 0 to day 45 *post partum*. Expressed as a percentage of the total amount in whole milk, ultrafiltrable zinc decreased from day 1 to day 2 *post partum*, and then remained unchanged from day 2 to day 69 *post partum* (Fig. 3). These results are in agreement with those of Fransson and Lonnerdal,[17] who reported no significant changes in the amount of ultrafiltrable zinc from 0.5 to 12 months *post partum*. However, using high-performance liquid chromatography, Bratter *et al.*[29] reported an increase in the zinc peak co-eluted with citrate, comparing prenatal and day 4 *post partum* milk samples. Suzuki *et al.*,[31] using the same method, also noted an increase in the zinc–citrate peak from day 2 to day 5 *post partum*. However, this peak was not found in mature milk.[31]

There was a significant correlation between total zinc and non-protein-bound zinc, expressed in μmol dm^{-3}, in the 120 milk samples examined [Fig. 4, r = 0.59 (P <0.01), Deming regression line slope = 0.22 and intercept = −2.2 μmol dm^{-3}]. However, there was no correlation between zinc in whole milk and ultrafiltrable zinc, expressed as a percentage (Fig. 5, r = 0.05). These results confirm the slight decrease in non-protein-bound zinc, expressed in μmol dm^{-3}, during early lactation and the relative stability of milk ultrafiltrable zinc, expressed as a percentage.

Conclusion

A micropartition system was used in order to ultrafilter milk, the ultrafiltrable zinc then being determined by ETAAS. This method is simple, rapid, sensitive and accurate. The precision of the proposed method is adequate for bioclinical investigations. Nevertheless, extreme precautions are required against zinc contamination.

The zinc concentration in the ultrafiltrate varied widely among the samples. This great variability reflects individual differences. Factors such as age, parity, nutrition, family income and environment might affect zinc concentration. Our results are in agreement with those of previous studies.

As the low molecular mass fraction is considered to play a key role in the intestinal absorption of zinc,[6,10–12] the proposed method should be useful in order to study and compare non-protein zinc from human milk and infant formulas.

We thank Marie-Christine Bouillet, Dominique Andre and Dominique Kia for their technical assistance, Christiane Orsini for the manuscript preparation, Josette Ruinat for the collection of the mothers' milk samples and all the mothers who were involved in this study.

References

1 Bye, A. M. E., Goodfellow, A., and Atherton, D. J., *Pediatr. Dermatol.*, 1985, **2**, 308.
2 Kuramoto, Y., Igarashi, Y., Kato, S., and Tagami, H., *Acta Derm.-Venereol.*, 1986, **66**, 359.
3 Roberts, L. J., Shadwick, C. F., and Bergstresser, P. R., *J. Am. Acad. Dermatol.*, 1987, **16**, 301.
4 Hambidge, K. M., *Acta Paediatr. Scand.*, 1986, Suppl. **323**, 52.

5 Higashi, A., Matsuda, I., Masumoto, T., Saikusa, H., Yabuso, M., and Oka, Y., *Tohoku J. Exp. Med.*, 1985, **146**, 253.
6 Brushmiller, J. G., Ames, R. W., Jacobs, F. A., and Nelson, L. S., *Biol. Trace Elem. Res.*, 1989, **19**, 71.
7 Lonnerdal, B., Cederblad, A., Davidsson, L., and Sandstrom, B., *Am. J. Clin. Nutr.*, 1984, **40**, 1064.
8 Lonnerdal, B., and Glazier, C., *Biol. Trace Elem. Res.*, 1989, **19**, 57.
9 Sandstrom, B., Keen, C. L., and Lonnerdal, B., *Am. J. Clin. Nutr.*, 1983, **38**, 420.
10 Duncan, J. R., and Hurley, L. S., *Am. J. Physiol.*, 1978, **235**, E556.
11 Evans, G. W., *Nutr. Rev.*, 1980, **38**, 137.
12 Lonnerdal, B., Keen, C. L., and Hurley, L. S., *Adv. Nutr. Res.*, 1984, **6**, 139.
13 Auge, M., Nichter, K., Seibold, G., Harzer, G., and Rehner, G., in *Trace Elements in Man and Animals*, eds. Mills, C. F., Bremner, I., and Chesters, J. K., Commonwealth Agricultural Bureau, London, 1985, vol. 5, pp. 434–436.
14 Furniss, D. E., Hurrell, R. F., de Weck, D., and Finot, P. A., in *Trace Elements in Man and Animals*, eds. Mills, C. F., Bremner, I., and Chesters, J. K., Commonwealth Agricultural Bureau, London, 1985, vol. 5, pp. 544–546.
15 Kiely, J., Flynn, A., Singh, H., and Fox, P. F., in *Trace Elements in Man and Animals*, eds. Hurley, L. S., Keen, C. L., Lonnerdal, B., and Rucker, R. B., Plenum Press, New York, London, 1988, vol. 6, pp. 499–500.
16 Fransson, G. B., and Lonnerdal, B., *J. Pediatr.*, 1982, **101**, 504.
17 Fransson, G. B., and Lonnerdal, B., *Pediatr. Res.*, 1983, **17**, 912.
18 Fransson, G. B., and Lonnerdal, B., *Nutr. Res.*, 1983, **3**, 845.
19 Lonnerdal, B., Clegg, M., and Hurley, L. S., *Am. J. Clin. Nutr.*, 1981, **34**, 640.
20 Arnaud, J., Favier, A., and Alary, J., *J. Anal. At. Spectrom.*, 1991, **6**, 647.
21 Arnaud, J., Bellanger, F., Bienvenu, F., Chappuis, P., and Favier, A., *Ann. Biol. Clin.*, 1986, **44**, 77.
22 Baud, M., Cohen, R., Dumont, G., Mercier, M., Naudin, C., and Vassault, A., *Inf. Sci. Biol.*, 1989, **15**, 157.
23 Vassault, A., Grafmeyer, D., Naudin, C., Dumont, G., Bailly, M., Henny, J., Gerhardt, M. F., and Georges, P., *Ann. Biol. Clin.*, 1986, **44**, 719.
24 Bloxam, D. L., Tan, J. C. Y., and Parkinson, C. E., *Clin. Chim. Acta*, 1984, **144**, 81.
25 Faure, H., Favier, A., Tripier, M., and Arnaud, J., *Biol. Trace Elem. Res.*, 1990, **24**, 25.
26 Foote, J. W., and Delves, H. T., *Analyst*, 1988, **113**, 911.
27 Lowry, O. H., Rosebrough, N. J., Farr, A. L., and Randall, R. J., *J. Biol. Chem.*, 1951, **193**, 265.
28 Eggstein, M., and Kreutz, F. H., *Klin. Wochenschr.*, 1955, **33**, 879.
29 Bratter, P., Gercken, B., Rosick, U., and Tomiak, A., in *Trace Element Analytical Chemistry in Medicine and Biology*, eds. Bratter, P., and Schramel, P., Walter de Gruyter, Berlin and New York, 1988, pp. 145–156.
30 Lonnerdal, B., Hoffman, B., and Hurley, L. S., *Am. J. Clin. Nutr.*, 1982, **36**, 1170.
31 Suzuki, K. T., Tamagawa, H., Hirano, S., Kobayashi, E., Takahashi, K., and Shimojo, N., *Biol. Trace Elem. Res.*, 1991, **28**, 109.
32 Blakeborough, P., Salter, D. N., and Gurr, M. I., *Biochem. J.*, 1983, **209**, 505.
33 Evans, G. W., and Johnson, P. E., *Lancet*, 1976, **ii**, 1310.

Paper 2/01901I
Received April 10, 1992
Accepted May 22, 1992

Extraction Systems for the Flame Atomic Absorption Spectrometric Determination of Trace Amounts of Mercury and Palladium

Nelly Mateeva, Sonia Arpadjan,* Todor Deligeorgiev and Mariana Mitewa
Department of Chemistry, University of Sofia, 1126 Sofia, Bulgaria

Two extraction systems incorporating novel derivatives of benzothiazole are described for the determination of trace amounts of Hg^{II} and Pd^{II} by flame atomic absorption spectrometry (AAS). The extraction ability of the systems was studied both in strongly acidic (3 mol dm^{-3} HCl) and slightly acidic (pH 5) media. By using the equilibrium shift method the composition of the extracted complexes was determined. The experimental data obtained indicate that the composition of the complexes depends on the acidity of the reaction system. A procedure for the extraction, separation, preconcentration and flame AAS determination of Hg^{II} in Pb, Cu and Cd salts was developed, allowing 2×10^{-4}% Hg to be determined.

Keywords: *Extraction; N-phenyl(aza-15-crown-5) derivatives; flame atomic absorption spectrometry; mercury and palladium determination*

The synthesis and analytical application of *N*-phenyl(aza-15-crown-5)-containing chromophores is of current interest because of their complexation, extraction and photochemical properties in respect of their application as dyes and analytical reagents.[1–6]

Recently, we have synthesized a novel compound of this type, namely, 2-[4-(1-aza-4,7,10,13-tetraoxacyclopentadecyl)styryl]-3-ethylbenzothiazolium perchlorate (**L1**), by condensation of 4-formylbenaza-15-crown-5 with 3-ethyl-2-methylbenzothiazolium iodide (**L2**) in order to study its extraction properties towards a series of metal ions and its applicability as an extractant in flame atomic absorption spectrometry (AAS). For comparison, the extraction ability **L2** was also studied. The analytical data obtained are presented in this paper.

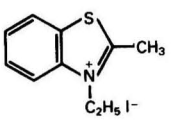

L2

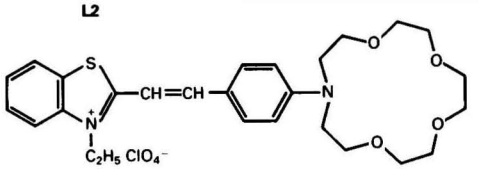

L1

Experimental

Apparatus

A Pye Unicam SP 1950 atomic absorption spectrometer with an air–acetylene flame and a Radelkis OP-208 pH meter were used. The proton nuclear magnetic resonance (^{1}H NMR) ($CDCl_3$ solutions), infrared (IR) and ultraviolet/visible (UV/VIS) spectra were recorded on Bruker 400 MHz, Specord IR 71 and Perkin-Elmer 17 spectrometers, respectively.

* To whom correspondence should be addressed.

Reagents

Stock standard solutions of metals were prepared from AAS standards (BDH). Isobutyl methyl ketone (IBMK) (Merck) was used as received.

All other reagents used were of analytical-reagent grade.

Procedures

Synthetic procedure

The starting materials, 4-formylbenzaza-15-crown-5 and 3-ethyl-2-methylbenzothiazolium iodide (**L2**), were obtained according to the Vilsmeier procedure[7] and by alkylation of 2-methylbenzothiazole with ethyl iodide, respectively. The extractant (**L1**) was synthesized by condensation of these compounds in acetic anhydride by refluxing for 30 min. The crude product was recrystallized from ethanol and converted into the perchlorate salt. For this purpose, an equimolar amount of $NaClO_4$ was added to the hot solution of the iodide. After cooling, the precipitate formed was collected and dried.

The compound was characterized by means of melting-point (m.p.), IR and ^{1}H NMR data. m.p. 224–226 °C; λ_{max} = 528.4 nm, $\log(\varepsilon/dm^3\ mol^{-1}\ cm^{-1})$ = 4.82 (ethanol); IR ($CHCl_3$): ν 1150 (C–O–C), 1600 (sh) (>C=C<), 1580 cm^{-1} (>C=C<, aromatic); ^{1}H NMR: δ 8.02 (d, J = 9 Hz, Ar), 8.00 (1 H, m, Ar), 7.88 (d, J = 15 Hz, =CH), 7.76 (d, J = 15 Hz, =CH), 7.67 (2 H, m, Ar), 7.55 (1 H, m, Ar), 6.65 (d, J = 9 Hz, Ar), 3.77 (t, J = 6 Hz, N–CH_2–CH_2–O), 3.67 (s, CH_2–O), 3.63 (s, CH_2–O), 3.63 (t, J = 6 Hz, N–CH_2–CH_2–O). [Found: C, 55.53; H, 6.22; N, 4.70. Calc. for $C_{27}H_{35}N_2O_8ClS$ (relative molecular mass = 583.11): C, 55.62; H, 6.05; N, 4.80%.]

General procedure

The pH of the aqueous solutions was adjusted by means of acetate (pH 5), borate (pH 9), HCl + KCl (pH 1) and citrate (pH 3) buffer solutions (pH meter control). The ratio of the aqueous to the organic phase was either 1 : 1 (5 cm^3 + 5 cm^3) or 25 : 2 (25 cm^3 + 2 cm^3). The initial concentration of the metal ions in the aqueous phase was in the range 0.5–15 μg cm^{-3}, depending on the sensitivity of the flame AAS measurements. The ligands **L1** and **L2** were added to the aqueous phase after dissolution in methanol (0.01 mol dm^{-3}). The extraction was carried out with IBMK for 5 min. The concentration of the elements in both phases was measured by flame based on direct calibration.

Standards for Hg^{II} in IBMK were obtained by appropriate dilution of a cyclohexanebutyric acid Hg^{II} salt oil-soluble standard for AAS (Merck) in IBMK. The standards for Pd^{II} in IBMK were prepared by dilution of an aqueous standard

Table 1 Influence of acidity on the percentage extraction of various heavy metals as complexes with **L1** or **L2** from aqueous solution into IBMK

	Extraction (%)																			
	Ag		Cd		Co		Cu		Fe		Hg		Mn		Ni		Pb		Pd	
Acidity	L1	L2	L1	L2	L1	L2	L1	L2	L1	L2	L1	L2	L1	L2	L1	L2	L1	L2	L1	L2
pH 1	<1	<1	<1	<1	<1	<1	<1	<1	<1	<1	>99	>99	<1	<1	<1	<1	<1	<1	<1	>99
pH 3	<1	>99	<1	<1	<1	<1	<1	<1	<1	<1	>99	>99	<1	<1	<1	<1	<1	<1	<4	>99
pH 5	<1	>99	<1	<1	<1	<1	<1	<1	<1	<1	>99	>99	<1	<1	<1	<1	<1	<1	25 ± 3	>99
pH 9	17 ± 5	>99	<1	<1	<1	<1	<1	<1	<1	<1	>99	>99	<1	<1	<1	<1	<1	<1	<1	>99
1 mol dm^{-3} HCl	95 ± 2	>99	<1	<1	<1	<1	<1	<1	20 ± 4	<1	>99	<99	<1	<1	<1	<1	<1	<1	28 ± 5	<1
3 mol dm^{-3} HCl	74 ± 4	>99	<1	<1	<1	<1	<1	<1	97 ± 3	>99	95 ± 3	>99	<1	<1	<1	<1	<1	<1	<1	<1
6 mol dm^{-3} HCl	24 ± 4	>99	<1	<1	<1	<1	<1	<1	>99	>99	80 ± 4	>99	<1	<1	<1	<1	<1	<1	<1	<1

Table 2 Percentage extraction of Hg^{II} and Pd^{II} from Pb, Cu, Cd and Fe salts (4 g) and sea-water using the extraction systems **L1**–IBMK and **L2**–IBMK

	Extraction (%)		
	Hg^{II}	Hg^{II}	Pd^{II}
Salt	L2–IBMK	L1–IBMK	L2–IBMK
$Pb(NO_3)_2$	>99	60 ± 4	>99
$Pb(CH_3CO_2)_2$	>99	75 ± 3	97 ± 2
$Cu(NO_3)_2$	>99	84 ± 2	98 ± 2
$Cu(CH_3CO_2)_2$	>99	70 ± 4	96 ± 3
$CdCl_2$	>99	50 ± 5	>99
$Cd(CH_3CO_2)_2$	>99	65 ± 2	98 ± 2
$Cd(NO_3)_2$	>99	75 ± 3	>99
$FeCl_3$	>99	52 ± 3	>99
$Fe(NO_3)_3$	>99	90 ± 4	92 ± 3
$FeNH_4SO_4$	>99	63 ± 5	>99
Sea-water	>99	>99	>99

Table 3 Composition [ligand (L) : metal (M)] of the complexes of metals with **L1** or **L2**, and their conditional extraction constants (K_{ex}) from aqueous solution into IBMK

		L : M		Log K_{ex}	
Metal	Aqueous phase	L1	L2	L1	L2
Ag	pH 5	1.02	—	−2.7	—
	1 mol dm^{-3} HCl	1.04	1.04	−1.2	−1.5
	3 mol dm^{-3} HCl	2.07	2.08	−3.0	−3.1
Hg	pH 5	2.02	2.05	−3.9	−4.3
	1 mol dm^{-3} HCl	1.10	1.08	−1.3	−1.5
	3 mol dm^{-3} HCl	1.03	1.02	−2.9	−2.6
Pd	pH 5	2.16	—	−4.6	—

solution of Pd^{II} with 20 cm^3 of 6 mol dm^{-3} HCl and extraction with 2% methyltrioctylammonium chloride in IBMK (saturated with 6 mol dm^{-3} HCl).

When studying the extraction of Hg and Pd from salts, for each salt investigated two parallel samples of 4 g were transferred into two extraction tubes. To one of the tubes 1.00 cm^3 of an aqueous standard solution of Pd^{II} (concentration 10 μg cm^{-3}) and 1.00 cm^3 of an aqueous standard solution of Hg^{II} (concentration 30 μg cm^{-3}) were added. The samples were dissolved in 25 cm^3 of doubly distilled water. Then, 1 cm^3 of a 0.01 mol dm^3 methanolic solution of **L1** or **L2** was added to the dissolved sample and the extraction was carried out with 2.0 cm^3 of IBMK. After the extraction, the organic phase was aspirated into the flame of the atomic absorption spectrometer without preliminary separation from the aqueous phase. The difference in the absorption values obtained for samples with and without the addition of the standard solutions was compared with the absorption of the elements in the standards for Hg^{II} and Pd^{II} in IBMK (of the same concentration as the standard addition). The recovery [R(%)] was calculated from the equation

$$R(\%) = (A_{salt\ +\ std} - A_{salt})/A_{std} \times 100$$

where $A_{salt\ +\ std}$ is the absorption value for samples with the addition of the standard solution, A_{salt} is the absorption value for samples without the addition of the standard solution and A_{std} is the absorption value for the standard solutions in IBMK.

Results and Discussion

Extraction Ability of the Ligands

Data on the effect of the acidity on the extraction of Ag^{I}, Cd^{II}, Co^{II}, Cu^{II}, Fe^{III}, Hg^{II}, Mn^{II}, Pb^{II} and Pd^{II} are shown in Table 1.

It is evident that Cd^{II}, Co^{II}, Cu^{II}, Mn^{II}, Ni^{II} and Pb^{II} are not extracted and that **L1** and **L2** are selective for Ag^{I}, Fe^{III} and Hg^{II}. The data also show that the presence of an *N*-phenylaza macrocycle group in the ligand molecule increases its selectivity.

By using the extraction system **L1**–IBMK, the quantitative, selective extraction of Hg^{II} can be achieved at high acidity or over a broad pH range, thus enabling Hg^{II} to be separated and concentrated from aqueous solutions containing other metals. However, at high salt concentrations the extraction of Hg^{II} with **L1** is suppressed (Table 2). In contrast, the ligand **L2** is capable of extracting Hg^{II} quantitatively in the presence of dissolved salts. The larger size of the **L1** molecule is probably responsible for its greater sensitivity towards the nature and concentration of the electrolyte in the aqueous phase.

Composition of the Extracted Species

By using the equilibrium shift method the composition of the extracted complexes was studied. Plots of the logarithm of the distribution coefficient (log D) *versus* the logarithm of the ligand concentration (log c_L) for Hg^{II} and Ag^{I} at three different acidities (pH 5, 3 mol dm^{-3} HCl and 1 mol dm^{-3} HCl) and for Pd^{II} at pH 5 are shown in Figs. 1 and 2. The parameters obtained from the straight-line regression equations and the conditional extraction constants are given in Table 3. The data thus obtained show metal-to-ligand ratios of 1 : 1 or 1 : 2 depending on the reaction acidity both for **L1** and **L2**. The compositions of the extracted species are: $[AgCl_2]^-[\mathbf{L1}]^+$, $[AgCl_2]^-[\mathbf{L2}]^+$, $[AgCl_3]^{2-}[\mathbf{L1}]_2^+$, $[AgCl_3]^{2-}[\mathbf{L2}]_2^+$, $[HgCl_3]^{2-}[\mathbf{L1}]$, $[HgCl_3]^-[\mathbf{L2}]^+$, $[FeCl_4]^-[\mathbf{L1}]^+$ and $[FeCl_4]^-[\mathbf{L2}]^+$ (where $\mathbf{L1}^+$ and $\mathbf{L2}^+$ are the cationic part of the complex salts). For the extraction complexes formed in slightly acidic media (pH 5) the metal-to-ligand ratio was shown to be 1 : 1 for Ag^{I} and 1 : 2 for Hg^{II} and Pd^{II}. The latter results could be explained by assuming that the ligand is monodentate, with coordination taking place *via* the S atom rather than the macrocycle.

Table 4 Determination of Hg in Pb, Cu and Cd salts by flame AAS

	Salt					
	$Pb(NO_3)_2$	$Pb(CH_3CO_2)_2$	$Cu(NO_3)_2$	$CdCl_2$	$Cd(CH_3CO_2)_2$	$Cd(NO_3)_2$
Determined/μg g^{-1}	4.2	3.8	2.6	2.5	2.3	5.4
Added/μg	5.0	5.0	3.0	3.0	3.0	5.0
Found/μg g^{-1}	9.3 ± 0.4	8.6 ± 0.3	5.5 ± 0.3	5.7 ± 0.3	5.2 ± 0.3	10.5 ± 0.3
Recovery (%)	101	98	98	103.7	98	101
RSD* (%) (n = 5)	4.3	3.5	5.4	5.3	5.8	4.8

* RSD = Relative standard deviation.

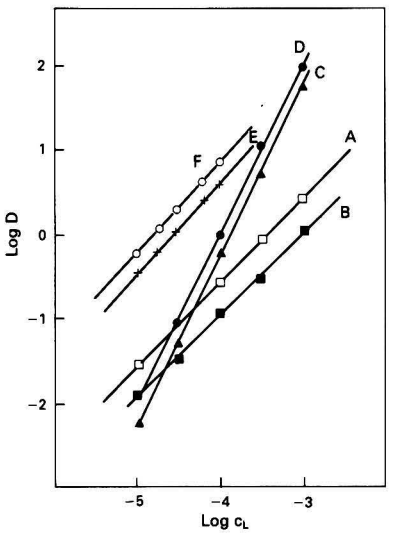

Fig. 1 Log D *versus* log c_L dependence for Hg^{II} complexes at different acidities. Extraction with: A **L1** at 3 mol dm^{-3} HCl; B, **L2** at 3 mol dm^{-3} HCl; C, **L1** at pH 5; D, **L2** at pH 5; E, **L1** at 1 mol dm^{-3} HCl; and F, **L2** at 1 mol dm^{-3} HCl

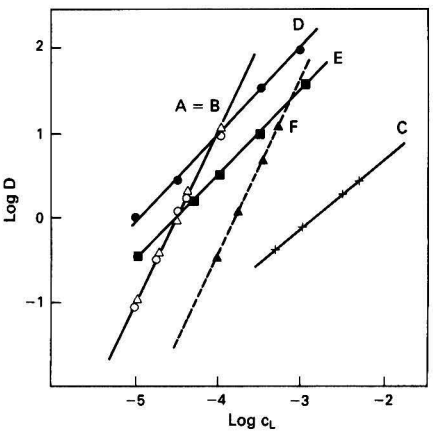

Fig. 2 Log D *versus* log c_L dependence for Ag^{I} (solid line) and Pd^{II} (broken line). Extraction with: A and B, **L1** and **L2** at 3 mol dm^{-3} HCl; C, **L2** at pH 5; D, **L1** at 1 mol dm^{-3} HCl; E, **L2** at 1 mol dm^{-3} HCl; and F, **L2** at pH 5

Determination of Hg^{II} in Pb, Cu, Cd and Fe Salts

The data presented in Table 2 indicate that it should be possible to develop an analytical procedure for the extraction, separation, preconcentration and flame AAS determination of Hg^{II} and Pd^{II} with **L2** in aqueous solutions containing high concentrations of Pb, Cu and Cd.

Analysis for the presence of Hg in salts of Pb, Cu or Cd was carried out as follows. The sample (4 g of the salt) was dissolved in 25 cm^3 of water and 1.0 cm^3 of a 0.01 mol dm^{-3} solution of **L2** in methanol was added. The mixture was shaken for 2 min and the Hg or Pd concentration in the organic phase was determined by flame AAS, with reference to blanks and standard additions samples taken through the whole preconcentration procedure. Data on the accuracy and precision of the procedure are presented in Table 4. The proposed method permits the determination of 2 × 10^{-4}% Hg and of 1 × 10^{-5}% Pd. The relative standard deviation is between 3 and 6% for concentrations of the analytes in the range from 5 × 10^{-3} to 5 × 10^{-4}%.

References

1 Lohr, H. G., and Vogtle, F., *Acc. Chem. Res.*, 1985, **18**, 65.
2 Zollinger, H., *Color Chemistry*, VCH, Weinheim, 1987, p. 316.
3 Dix, J. P., and Vogtle, F., *Chem. Ber.*, 1981, **114**, 638.
4 Takagi, M., and Ueno, K., *Top. Curr. Chem.*, 1984, **121**, 39.
5 Junek, H., Klade, M., Biza, P., Geringer, M., and Sterk, H., *Liebigs Ann. Chem.*, 1990, 741.
6 Gromov, S. P., Fomina, M. V., Ushakov, E. N., Lednev, I. K., and Alfimov, M. V., *Dokl. USSR Akad. Nauk*, 1990, **314**, 1135.
7 Dix, J. P., and Vogtle, F., *Chem. Ber.*, 1980, **113**, 457.

Paper 2/00665K
Received February 7, 1992
Accepted June 8, 1992

Combined Generator/Separator

Part 2.* Stibine Generation Combined With Flow Injection for the Determination of Antimony in Metal Samples by Atomic Emission Spectrometry

Hengwu Chen
Department of Chemistry, Hangzhou University, Hangzhou, Zhejiang 310028, People's Republic of China
Ian D. Brindle† and Shaoguang Zheng
Chemistry Department, Brock University, St. Catharines, Ontario, Canada L2S 3A1

Application of a new continuous hydride generator to the determination of antimony in metals by flow injection is described. A modified hydride generator/gas–liquid separator has been designed. The detection limit for antimony is 7.5 ng cm^{-3} for a 0.5 cm^3 sample. For solutions containing 200 ng cm^{-3} of antimony, the relative standard deviation is 0.9%. Reduction of antimony(v) to antimony(iii) is effected by off-line pre-reduction with L-cysteine. L-Cysteine also accelerates the tetrahydroborate(iii) reaction and reduces interferences from transition elements and, with the exception of selenium, other hydride-forming elements. Results are reported for the determination of antimony in iron and copper samples.

Keywords: *Flow injection; hydride generation; transition element interference reduction; antimony determination; direct current plasma atomic emission spectrometry*

Batch-wise and continuous flow hydride generation, combined with atomic spectrometry, have been applied successfully to the analysis of hydride-forming elements in various samples during the past twenty years.[1] Although slightly higher sensitivities can be obtained with the two operation modes, compared with conventional sample introduction, fairly large volumes of sample are required and considerable manipulation is involved (especially for the former). A relatively slow rate of sample throughput is another major disadvantage of the two modes.

Since Aström published the first paper on the combination of hydride generation (HG) with the flow injection (FI) technique in 1982,[2] the merits of the combination, such as small sample consumption, high precision, reduced interferences and high sample throughput rate, have attracted the interests of spectroscopists working in the field. Papers on flow injection hydride generation were reviewed in 1989 by Fang.[3] In many of these studies, attention was directed towards the development of a gas–liquid separator with a small dead-volume and a high separation efficiency. To achieve this, Wang and Fang[4] modified the volume of the Vijan-type U-tube separator, by reducing the size of the bulb and by installing a pump line to drain the effluent to waste. Thus, they reduced the risk of entrainment of liquid phase into the atomizer. Porous membrane[5] and porous tube[6–8] separators have smaller dead-volumes than the U-tube separator, therefore, the authors claim that higher sensitivities can be obtained owing to a reduction in dispersion. It has also been reported that, when using solutions with a high dissolved solids content, the lifetime of the separator made of porous material is short due to gradual blockage of the pores.[8] Recently, a flow injection hydride generator with a so called de-gassing membrane was developed by Marshall and van Staden.[9] In their arrangement, the reaction solution, rather than the gas, was passed through a cotton-gauze filter. Polymer-bound tetrahydroborate(iii) has been used to reduce arsenic in a flow injection system.[10]

Antimony determination is a routine task in environmental, geological and metallurgical analyses. Thus, over the last fifteen years, approximately 150 papers dealing with antimony determination by means of stibine generation atomic spectrometry have been published. Hydride generation and direct current plasma atomic emission spectrometry (DCP-AES) has been reported for the determination of antimony in geological samples using a batch hydride system.[11] Flow injection with HG has also been reported as a method for the determination of antimony.[12]

Similar to other hydride forming elements antimony, when determined by the generation of stibine, suffers interferences from transition metal ions in solution.[13–15] Therefore, potassium iodide,[16] ethylenediaminetetraacetic acid (EDTA),[17] 1,10-phenanthroline,[18] and thiosemicarbazide[19] have been used to reduce interference in the determination of antimony. In previous work, we reported that L-cysteine has the effect of shifting the optimum acid range to low concentration without loss of signal. L-Cysteine has also been used to pre-reduce arsenic(v) to arsenic(iii) and to reduce interferences from transition metal ions during arsine[20,21] and germane generation.[22,23] Welz and Schubert-Jacobs[24] reported that increasing the acid concentration and reducing the tetrahydroborate(iii) concentration extended the range of tolerance of transition elements in hydride generation. However, this improvement was achieved at the expense of the signal from the hydride.

A combined hydride generator/separator specifically designed for continuous hydride generation and separation from a low acid–L-cysteine medium has been developed and applied successfully to the on-line pre-reduction of arsenic(v) and to the determination of arsenic by arsine generation for a variety of samples.[25] The advantages of using low acid concentrations and L-cysteine, aside from those indicated above, include low hydrogen production, hence lower surges of gas into the plasma and extended lifetime for the equipment used owing to reduced corrosion; also, L-cysteine is a relatively innocuous reagent of low toxicity. In order to combine the merits contributed by L-cysteine to the hydride generation with the merits of FI, we have further modified the hydride generator/separator. This paper presents these modifications and their application to the determination of antimony in metal samples using FI-HG-DCP-AES.

* For part 1 of this series see ref. 25.
† To whom correspondence should be addressed.

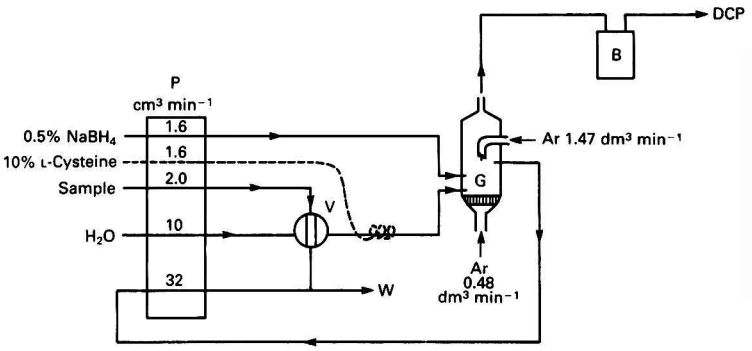

Fig. 1 Manifold for flow injection hydride generation for stibine generation. B, Buffer tank; G, hydride generator/separator; V, 4-way valve; and W, waste. The broken line indicates the experimental set-up for the investigation of on-line pre-reduction of Sb^{V}

Experimental

Instrumentation

The FI-HG manifold shown in Fig. 1 consists of a 4-channel Gilson 312 peristaltic pump, a Rheodyne 5020 4-way valve and a specially constructed hydride generator/separator. Poly(tetrafluoroethylene) (PTFE) tubing, with 0.8 mm i.d., was used to make connections. Pump tubing (from a Technicon SMA) of different diameters was used to pump the carrier, sample and reductant and to drain the spent solution to waste. To investigate the on-line pre-reduction method, an additional line was used to introduce a 10% m/v solution of L-cysteine. This line, shown as a broken line in Fig. 1 was paired with the line carrying the tetrahydroborate(III) in the peristaltic pump in the on-line pre-reduction experiments and was not used for the normal mode of determination. Fig. 2 shows the modified hydride generator/separator.

The experimental conditions for DCP-AES were described previously,[25] except that the antimony line at 231.9 nm was used.

Reagents

Antimony(III) and antimony(V) standard solutions (1000 mg dm^{-3}) were prepared from antimony trioxide and antimony pentoxide, respectively. Antimony(III) was found to be stable to oxidation for up to one week. Other reagents were prepared as described previously.[25]

Sample Preparation

Iron and steel

Add 10 cm^3 of 50% HCl and 2 cm^3 of 30% H_2O_2 to 0.5 g of sample. Digest the sample with gentle warming for about 1 h. During the digestion, add 1 cm^3 of H_2O_2 to the solution every 15 min. After the digested solution has cooled, transfer the solution together with the black residue (carbon) to a 250 cm^3 calibrated flask and dilute to the mark with distilled water. Transfer a 25 cm^3 aliquot into a 100 cm^3 beaker and dilute to about 80 cm^3 with water. Add 0.5 g of L-cysteine to the solution and adjust the pH to between 2.10 and 2.15 with 1 mol dm^{-3} HCl or 1 mol dm^{-3} NaOH. Transfer the solution into a 100 cm^3 calibrated flask and dilute to the mark with distilled water.

Copper

Add 5 cm^3 of 50% HCl and 2 cm^3 of 3% H_2O_2 to 0.1 g of sample. Digest the sample with gentle warming until the sample is completely dissolved. After the solution cools, dilute it to 80 cm^3 with distilled water. Transfer the solution to a 100 cm^3 calibrated flask. Add 2.0 g L-cysteine to the flask and adjust the pH to between 2.10 and 2.15 with 1 mol dm^{-3} HCl or 1 mol dm^{-3} NaOH before diluting to the mark with distilled water.

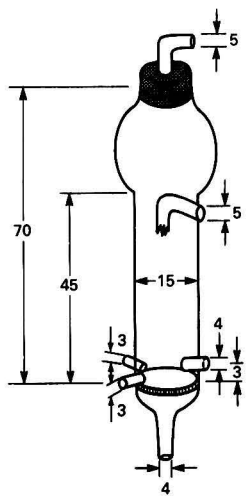

Fig. 2 Hydride generator/separator. All dimensions are in millimetres

Results and Discussion

Generator/Separator

The generator/separator, shown in Fig. 2, is significantly smaller than the device used for the continuous hydride generator,[25] and has a volume of approximately 15 cm^3. The inlet ports for the sample or carrier and reductant are at the same level, just above the frit. The two ports are also as close to each other as possible. On the opposite side from the two inlet ports is the outlet port for the waste solution, which is 3 mm above the frit. Stripping gas is introduced from below the frit and an additional flow is introduced through a side-arm, which is bent down inside the vessel and is roughly broken at the tip. With this arrangement, the direction of the carrier gas flow and the broken tip help to break any liquid film or bubbles that are able to reach this point, thus preventing any liquid from entering the gas outlet port, which is at the top of the vessel.

Reaction Coil

In the usual FI-HG manifold, the reagent ($NaBH_4$) mixes with the sample plug at a 'T' or cross connector. Then the mixture passes through a reaction coil, where the hydride is generated, before it enters a gas–liquid separator. Thus, better mixing of the reactants is achieved and higher hydride yields are obtained due to the long reaction time. With the hydride generator/separator, however, the sample plug and reductant are mixed inside the vessel and the hydride is immediately separated from the solution at the point where it is generated. Omitting the reaction coil should not reduce the sensitivity if the generation rate is fast enough to reach equilibrium in a short time. On the other hand, a decrease of interference from the matrix could be obtained due to the short residence time.[2]

Experimental results show the advantages of the generator/separator for solutions containing L-cysteine. These results are illustrated in Fig. 3. When stibine was generated at low acid concentration in the absence of L-cysteine, the peak height decreased with an increase in the length of the reaction coil [Fig. 3(*a*)]. At higher acid concentrations, peak heights increased significantly as the length of the reaction coil increased [Fig. 3(*b*)], owing to the slow rate of stibine generation in the absence of L-cysteine.[25] However, if stibine was generated in the presence of L-cysteine, elimination of the reaction coil did not reduce the sensitivity; instead an increase in peak height and a decrease in peak width at half height was observed [Fig. 3(*c*)]. This is attributed to faster generation of stibine in the presence of L-cysteine.[25] Thus a decrease in the length of the reaction coil did not reduce the yields of stibine, but resulted in a slight reduction in sample dispersion, which normally occurs in the longer reaction coil.

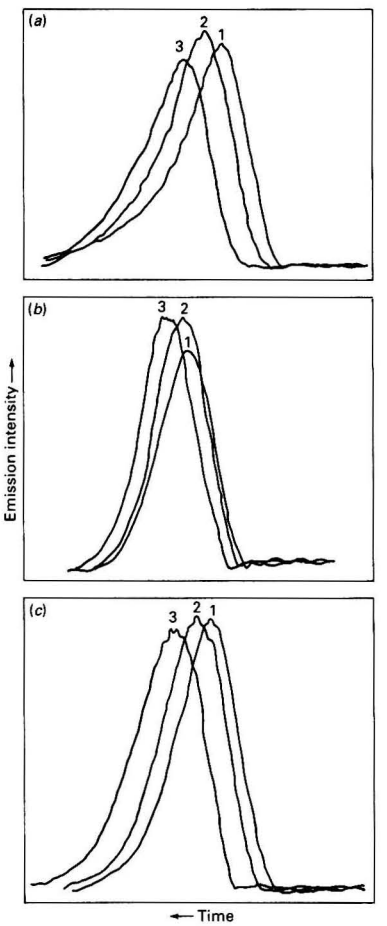

Fig. 3 Influence of L-cysteine, acid concentration and length of reaction coil on stibine generation. (*a*) 200 ng cm^{-3} of Sb^{III} in 0.02 mol dm^{-3} HCl, (*b*) 200 ng cm^{-3} of Sb^{III} in 1 mol dm^{-3} HCl and (*c*) 200 ng cm^{-3} of Sb^{III} in 0.02 mol dm^{-3} HCl with 0.5% m/v L-cysteine. 1, No reaction coil; 2, 0.5 m × 0.7 mm reaction coil; and 3, 1.5 m × 0.7 mm reaction coil

Optimization of Flow Injection Hydride Generation

Gas flow rate

Previously, we have shown that it is necessary to divide the argon flow into two different flows, *e.g.*, stripping gas flow and carrier gas flow.[25] The different roles played by the two flows are illustrated in Fig. 4. The best flow rate of stripping gas is almost the same as that reported previously,[25] but the total flow rate is smaller, which is probably due to the smaller size of the reaction vessel.

Buffer tank volume

In order to mitigate pressure fluctuation in the hydride transportation line, a buffer tank, consisting of a test tube with inlet and outlet tubes, was connected between the plasma torch and the generator/separator. Variations in peak height and relative standard deviation (RSD) with buffer tank volume are plotted in Fig. 5. A two-fold improvement in precision was obtained at a sacrifice of a 10% decrease in sensitivity and a 20% increase in the peak width at half maximum when a 20 cm^3 buffer tank was used compared with

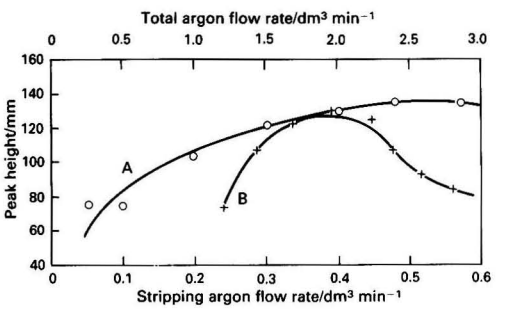

Fig. 4 Effect of total argon flow rate and stripping argon flow rate on 200 ng cm^{-3} of Sb^{III} in 0.02 mol dm^{-3} HCl with 0.5% m/v L-cysteine. A, Total argon flow rate maintained at 2.25 dm^3 min^{-1}, stripping argon flow rate varied. B, Stripping argon flow-rate maintained at 0.4 dm^3 min^{-1}, total argon flow rate varied

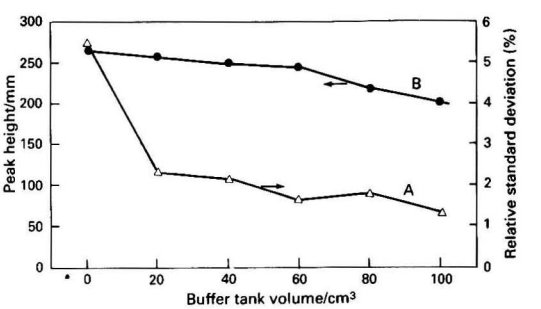

Fig. 5 Influence of buffer tank volume on A, peak height and B, relative standard deviation

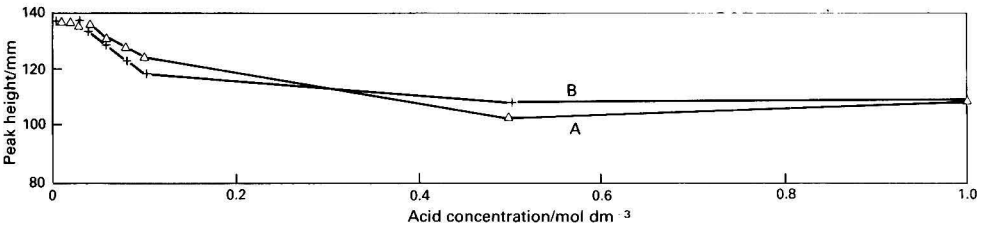

Fig. 6 Effect of acid concentration on stibine generation. A, 200 ng cm^{-3} of Sb^{III} in nitric acid with 0.5% m/v L-cysteine; and B, 200 ng cm^{-3} of Sb^{III} in hydrochloric acid with 0.5% m/V L-cysteine

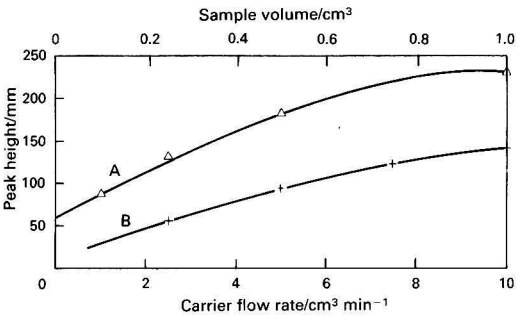

Fig. 7 Effect of carrier flow rate and sample volume. A, 200 ng cm^{-3} of Sb^{III} in hydrochloric acid with 0.5% m/v L-cysteine, different sample volumes; and B, 200 ng cm^{-3} of Sb^{III} in hydrochloric acid with 0.5% m/v L-cysteine, different carrier flow rates

the system that did not incorporate a buffer tank. Larger volumes of the buffer tank had a minimal effect on the precision, but the sensitivity decreased almost linearly with increasing volume. Therefore, a buffer tank of 20 cm^3 volume was always connected in the gas line.

Influence of acid, L-cysteine and $NaBH_4$ concentrations

The influence of acid concentration on the peak height is shown in Fig. 6. Nitric acid and hydrochloric acid have almost the same effect and the best response could be obtained in the acid range 0.01–0.04 mol dm^{-3}. A 20% increase in signal could be obtained in the presence of 0.05% L-cysteine. However, Fig. 7 shows that a further increase in the L-cysteine concentration had no effect on signal enhancement. The concentration of sodium tetrahydroborate(III) has almost no influence on the peak height, as shown in Fig. 7. As a result, 0.02 mol dm^{-3} HCl, 0.5% m/v L-cysteine and 1.5% m/v $NaBH_4$ were chosen as the best conditions for the determination of antimony.

Flow injection carrier flow and sample volume

As distilled water and dilute HCl (0.01–0.1 mol dm^{-3}) gave the same results, distilled water was chosen as the flow injection carrier. Keeping the ratio of carrier to $NaBH_4$ solution flows constant, *i.e.*, 10 : 1.6, the peak height increased with the increase of flow rate, as shown in Fig. 7. Similar observations were reported by Wang and Fang for the determination of selenium.[4] At a carrier flow rate of 10 cm^3 min^{-1}, the peak height increased with increase of sample injection volume. As can be seen in Fig. 7, a 0.5 cm^3 sample gave almost 80% of the response obtained with a 1 cm^3 sample. Therefore, a carrier flow of 10 cm^3 min^{-1} and a sample volume of 0.5 cm^3 were selected.

Pre-reduction of Antimony(v)

Owing to the difference in efficiency of stibine generation between antimony(v) and antimony(III),[26,27] antimony(v) must be reduced to antimony(III) prior to stibine generation. Potassium iodide is the most popular pre-reductant that can be used in highly acidic media, but the iodine formed in the acidic solution has been reported to cause interferences in the determination of antimony by atomic absorption spectrometry.[26,28] Yamamoto *et al.* reported that antimony(v) could be reduced on-line with 8% KI solution in high acid media when the analyte and reductant passed through a 2 m × 1.5 mm glass pre-reduction coil.[12] When L-cysteine was used on-line with the modified system shown in Fig. 1 to pre-reduce antimony(v), preliminary tests showed that the recovery of antimony(v) compared with antimony(III) approached 91% when the reaction was carried out at room temperature. If L-cysteine is added to the sample of antimony(v) solution in 0.02 mol dm^{-3} acid to give a final concentration of 0.5% m/v, before injection, full recovery could be obtained after standing for 7 min at room temperature. Thus antimony(v) is much more easily reduced to antimony(III) by L-cysteine compared with arsenic(v).[20,25] Considering the consumption of the reagent and the extra dispersion of the sample plug in on-line pre-reduction, off-line pre-reduction was chosen with the addition of L-cysteine to give a concentration of 0.5% m/v in the sample solution for iron and 2% m/v for copper.

Interference Studies

Table 1 shows the interferences from transition metal ions and the interference reducing effect of L-cysteine. From the table, it can be seen that the interference-free level is increased by more than one order of magnitude due to the presence of 0.5% m/v of L-cysteine. The most prominent feature is the elimination of interference caused by iron(III). Instead of playing a releasing effect as in the generation of arsine and hydrogen selenide,[29] iron(III) severely depressed the antimony signal, in agreement with the findings of Castillo *et al.*[30] When 0.5% m/v of L-cysteine was added to the test solution containing iron(III), the iron(III) was reduced to iron(II) and the interference was totally removed. If the iron(III) concentration was greater than 200 μg cm^{-3}, the solution became turbid due to the formation of L-cystine. A precipitate settled readily from the solution and it was unnecessary to separate the precipitate from the solution before sample loading. When L-cysteine was added to antimony solutions in the presence of copper(II) at concentrations greater than 20 μg cm^{-3}, a yellow precipitate, possibly a compound of copper(I), was observed. A similar phenomenon was reported when KSCN was used as a masking reagent for the determination of antimony in copper by means of stibine generation.[31] Although 0.5% of L-cysteine could not totally remove the interference from 1000 μg cm^{-3} of copper(II), the interference was essentially eliminated if the L-cysteine concentration was increased to between 1.0 and 2.0%. The interference reducing effect of L-cysteine is better than that of KI for nickel,[16] and EDTA for copper.[17] 1,10-Phenanthroline was only investigated for the reduction of interference from nickel for up to 50 μg cm^{-3}.[18] It should be noted that some authors have reported that the interference effect of transition metal ions depends on the

Table 1 Recovery of 200 ng cm^{-3} Sb^{III} in 0.02 mol dm^{-3} HCl in the presence of various transition elements

Element	Amount present/ μg cm^{-3}	Recovery (%) No L-cysteine	Recovery (%) With 0.5% L-cysteine
Ni^{II}	2	33	99
	20	16	86
	100	—*	68
Co^{II}	2	42	101
	20	27	99
	100	—	51
Cu^{II}	2	7	—
	20	30	98†
	200	—	97†
	1000	—	96†‡
	1000		85†
Fe^{III}	20	4	99
	200	ND§	99†
	1000	—	100†
Pd^{II}	2	ND	87
	20	—	25
Mn^{II}	20	97	102
	100	83	97
Cr^{VI}	2	3	—
	20	ND	101
	200	—	99

* Not determined.
† Precipitate formed after addition of L-cysteine.
‡ 2% m/v L-cysteine.
§ Not detected.

Table 2 Recovery of antimony(III) (200 ng cm^{-3} in 0.02 mol dm^{-3} HCl) signals in the presence of other hydride-forming elements

Element	Amount present/ μg cm^{-3}	Recovery (%) No L-cysteine	Recovery (%) With 0.5% L-cysteine
Se^{IV}	2	94	ND*†
	20	87	ND*†
Te^{IV}	2	85	82
	20	64	72
As^{III}	2	101	101
	20	101	96
	100	100	85‡
Pb^{II}	2	92	99
	20	84	100
	100	—§	100
Bi^{III}	2	5	100
	20	—	58
	100	—	30
Sn^{II}	2	91	99
	20	33	88
Ge^{IV}	2	117	99
	20	—	103
	100	139	106

* Not detected.
† Red precipitate formed after addition of L-cysteine.
‡ White precipitate formed after addition of L-cysteine.
§ Not determined.

Table 3 Determination of antimony in NIST Standard Reference Materials

Sample	Found mean ± SD (*n*)/ μg g^{-1} for copper, % m/m for iron	Certified value/ μg g^{-1} for copper, % m/m for iron
SRM 364 LA Steel, High C (modified)	0.030 ± 0.001 (3)	0.034
SRM 362 LA Steel, AISI 94B17 (modified)	0.011 ± 0.001 (4)	0.013
SRM 400 Unalloyed Copper (Cu VII)	107 ± 5 (4)	102

concentration of the interfering ion rather than the ratio of interferent to analyte as reported by the authors cited above.[32,33] For the hydride forming elements the situation was different, as shown in Table 2. Although L-cysteine reduced the depressive effects of tin(II), lead(II) and bismuth(III), and also the enhancement effect of germanium(IV), at 100 μg cm^{-3} of arsenic a small reduction in signal was observed due to the presence of L-cysteine. For selenium, signals from antimony were completely suppressed. The formation of a dark red precipitate in the test solution with 20 μg cm^{-3} of selenium suggests that selenium(IV) was reduced to selenium(0) by L-cysteine.

Limit of Detection and Calibration Parameters

The limit of detection, defined as three times the standard deviation of the blank, is 7.5 ng cm^{-3} for a 0.5 cm^3 sample. The RSD for a solution containing 200 ng cm^{-3} of antimony(III) is 0.9% (12 replicates). The linear regression equation for the calibration curve from 50–250 ng cm^{-3} was found to be $y = 1.10 + 0.7087x$. The correlation coefficient was 0.997.

Metals Analysis

For SRMs 362 and 364, low recoveries of antimony were obtained when the iron samples were decomposed with either nitric acid or *aqua regia* (3 parts HCl + 1 part HNO_3), followed by neutralization of the acid sample to pH 2. When an aliquot of the sample, which was digested with *aqua regia*, was spiked with antimony(III), the spike was fully recovered (>96%). Therefore, it is apparent that the low recovery was not caused by any interferences from nitrate and/or iron. However, hydrochloric acid plus hydrogen peroxide gave satisfactory results, as shown in Table 3. For the analysis of SRM 400, about a quarter of the calibrated flask was occupied by the yellow fluffy precipitate after it was allowed to settle (≈30 min). The precipitate did not interfere with the determination of antimony. The results shown in Table 3 are in good agreement with NIST certified values for both iron and copper SRMs. Using the experimental conditions shown in Fig. 1, the sample throughput rate was 2 min^{-1}.

Conclusions

Antimony can be conveniently determined by FI-HG with detection by DCP-AES. L-Cysteine enhances the signal compared with hydrochloric acid alone. In addition, L-cysteine reduces antimony(V) off-line and has the additional advantage that it can reduce interferences from transition elements and from several hydride-forming elements in stibine generation. The technique avoids the need for prior separation of interfering elements and is rapid (2 samples min^{-1}). The conditions required for the determination of antimony are similar to those for As, Bi, Ge and Sn, which suggests that these elements at concentrations of less than 2 μg cm^{-3} could be determined simultaneously by this technique.

The authors thank the Ontario Ministry of the Environment for funding this research (Project 434 G). Hangzhou University is thanked for providing a leave of absence for H. C.

References

1 Nakahara, T., *Prog. Anal. At. Spectrosc.*, 1983, **6**, 163.
2 Aström, O., *Anal. Chem.*, 1982, **54**, 190.
3 Fang, Z., in *Flow Injection Atomic Spectroscopy*, ed. Burguera, J. L., Marcel Dekker, New York, 1989, p. 134.
4 Wang, X., and Fang, Z., *Fenxi Huaxue*, 1986, **14**, 738 (and ref. 3 cited therein).
5 Pacey, G. E., Straka, M. R., and Gord, J. R., *Anal. Chem.*, 1986, **58**, 502.

6 Yamamoto, M., Takada, K., Kumamaru, T., Yasuda, M., and Yokoyama, S., *Anal. Chem.*, 1987, **59**, 2446.
7 Wang, X., and Barnes, R. M., *J. Anal. At. Spectrom.*, 1988, **3**, 1091.
8 Nakata, F., Sunahara, H., Fujimoto, H., Yamamoto, M., and Kumamaru, T., *J. Anal. At. Spectrom.*, 1988, **3**, 579.
9 Marshall, G. D., and van Staden, J. F., *J. Anal. At. Spectrom.*, 1990, **5**, 675.
10 Tesfalidet, B., and Irgum, K., *Anal. Chem.*, 1989, **61**, 2079.
11 Perämäki, P., and Lajunen, L. H. J., *Analyst*, 1988, **113**, 1567.
12 Yamamoto, M., Yamamoto, Y., and Yasuda, M., *Anal. Chem.*, 1985, **57**, 1382.
13 Smith, A. E., *Analyst*, 1975, **100**, 300.
14 Hershey, J. W., and Keliher, P. N., *Spectrochim. Acta, Part B*, 1986, **41**, 713.
15 Castillo, J. R., Martinez, M. C., and Mir, J. M., *At. Spectrosc.*, 1988, **9**, 179.
16 Yamamoto, M., Shohji, T., Kumamaru, T., and Yamamoto, Y., *Fresenius' Z. Anal. Chem.*, 1981, **305**, 11.
17 Henden, E., *Analyst*, 1982, **107**, 872.
18 DeDoncker, K., Dumarey, R., Dams, R., and Hoste, J., *Anal. Chim. Acta*, 1985, **169**, 339.
19 Kellerman, S. P., *Rep. MINTEK*, 1982, **M39**, 14 pp.; *Chem. Abstr.*, 1983, **98**, 26949.
20 Chen, H., Brindle, I. D., and Le, X.-c., *Anal. Chem.*, 1992, **64**, 667.
21 Brindle, I. D., and Chen, H., *Talanta*, 1991, **38**, 1137.
22 Brindle, I. D., and Le, X.-c., and Li, X.-f. *J. Anal. At. Spectrom.*, 1989, **4**, 227.
23 Brindle, I. D., and Le, X.-c., *Anal. Chim. Acta*, 1990, **229**, 239.
24 Welz, B., and Schubert-Jacobs, M., *J. Anal. At. Spectrom.*, 1986, **1**, 23.
25 Brindle, I. D., Alarabi, H., Karshman, S., Le, X.-c., Zheng, S., and Chen, H., *Analyst*, 1992, **117**, 407.
26 Sinemus, H. W., Melcher, M., and Welz, B., *At. Spectrosc.*, 1981, **2**, 81.
27 Bye, R., *Talanta*, 1990, **37**, 1029.
28 Petrick, K., and Krivan, V., *Fresenius' Z. Anal. Chem.*, 1987, **327**, 338.
29 Welz, B., and Melcher, M., *Analyst*, 1984, **109**, 577.
30 Sanz, J., Martinez, M. T., Galban, J., and Castillo, J. R., *J. Anal. At. Spectrom.*, 1990, **5**, 651.
31 Alduan, J. A., Suarez, J. R. G., Polo, A. B., and del Busto, J. L., *At. Spectrosc.*, 1981, **2**, 125.
32 Welz, B., and Melcher, M., *Spectrochim. Acta, Part B*, 1981, **36**, 439.
33 Chen, Y., and D'Ulivo, *Anal. Lett.*, 1989, **22**, 1609.

NOTE—Ref. 25 is to Part 1 of this series.

Paper 1/02921E
Received June 17, 1991
Accepted June 10, 1992

Ion-selective Electrodes for the Determination of the Antiarrhythmic Drug Bretylium

Christian Eppelsheim, Christoph Bräuchle and Norbert Hampp*
Institut für Physikalische Chemie der Universität München, Sophienstrasse 11, D-8000 München 2, Germany

Ion-selective poly(vinyl chloride) membrane electrodes and thick-film sensors for the determination of the antiarrhythmic drug bretylium in human serum are described. Ion-pair complexes of bretylium with the anionic counter ions tungstosilicate, reineckate [diamminetetracyanatochromate(III)], tetraphenylborate and dipicrylaminate were investigated as electroactive compounds for the electrode membranes. The membranes containing the bretylium–tungstosilicate complex showed the best properties with both types of transducers. The detection limits were determined to be 1×10^{-7} mol dm^{-3} for the macroscopic electrodes and 8×10^{-7} mol dm^{-3} for the thick-film sensors in 0.1 mol dm^{-3} Tris buffer at pH 7.4; slopes of 60.7 and 40.0 mV decade^{-1} respectively, were found. In pathological and non-pathological test sera, a detection limit of 5×10^{-6} mol dm^{-3} was obtained with the thick-film transducers. The potentiometric selectivity coefficients towards structurally similar compounds such as ephedrine, dopamine and epinephrine (adrenaline) ranged from $10^{-1.7}$ to $10^{-3.4}$. Response times of 5–10 s were observed in buffered aqueous solutions as well as in human serum samples.

Keywords: *Bretylium; ion-selective electrode; potentiometric detection; thick-film sensor*

In recent years the importance of electrochemical sensors has increased for a wide variety of applications. Many of them involve the principle of potentiometric ion-selective electrodes (ISEs), a principle that is based on one of the best investigated sensor principles. The ISEs can be used for the quantitative determination of inorganic[1] and organic ions.[2] A common principle for the construction of ion-selective membranes is the dissolution of a lipophilic ion-pair complex in a highly plasticized polymer matrix; ISEs sensitive to alkaloids,[3] muscle relaxants[4] and antidepressants[5] are based on this. An advantage of ion-selective sensors over many other methods of drug detection is the possibility of direct monitoring of ion activities in analyte fluids, *e.g.*, for the determination of bio-availability of a drug, without any extensive sample preparation.

Bretylium, an antiarrhythmic drug, has a quaternary ammonium group and can be precipitated by several anionic reagents.[6] The present paper reports on macroscopic ISEs containing ion-pair complexes of bretylium and on a miniaturized thick-film sensor with plasticized poly(vinyl chloride)–poly(vinyl acetate) (PVC–PVAc) copolymer membranes that contain a complex of bretylium with tungstosilic acid. This sensor incorporates the Biobrid V2.1 transducers developed by our group.[7]

Experimental

Reagents

Bretylium tosylate (BRE) was purchased from Serva. For the measurement of potentiometric selectivity coefficients the potential interfering species ephedrine hydrochloride and epinephrine hydrochloride (Sigma), and dopamine hydrochloride (Fluka) were chosen (see Fig. 1). Tungstosilicic acid (TUS), sodium tetraphenylborate (TPB), Reinecke salt (RES) and aurantia [ammonium dipicrylaminate (AUR)] (all obtained from Fluka) were used as precipitating reagents for the preparation of the ion-pair complexes. The plasticizers dibutyl phthalate (DBP) and bis-(2-ethylhexyl) phthalate (BEHP) and the membrane polymer (high molecular mass PVC) (all from Fluka), and the buffer salts Tris base and Tris hydrochloride (both from Sigma) were all of analytical-reagent grade. All solutions were prepared with doubly distilled water. As test sera, Precinorm U and Precipath U (Boehringer Mannheim) were used.

Preparation of the Electroactive Compounds

The ion-pair complexes were precipitated from 0.1 mol dm^{-3} mixtures of aqueous solutions of BRE with twice the volume of saturated solutions of TPB, RES, AUR and TUS. The precipitates were sedimented by centrifugation at 7000*g*, intensively washed with doubly distilled water and dried in an evacuated desiccator over phosphorus pentoxide for 3 d.

Preparation of the Membranes and the Electrodes

Bretylium-selective membranes

Tetrahydrofuran (THF) solutions (1.0 cm^{-3}) each containing 62 mg of PVC and 140 mg of plasticizer (DBP or BEHP) were mixed with 3.0 mg each of the different ion-pair complexes. All the complexes, except BRE–TUS, were completely dissolved in the membrane solutions. These mixtures were poured into poly(propylene) rings (diameter 23 mm) on glass plates and were covered by a sheet of filter-paper and a cover glass. The THF was evaporated within 12 h at room temperature.

Electrodes and sensors

The membrane discs were cut out, glued on to the ends of PVC modules and mounted on to electrode bodies containing an

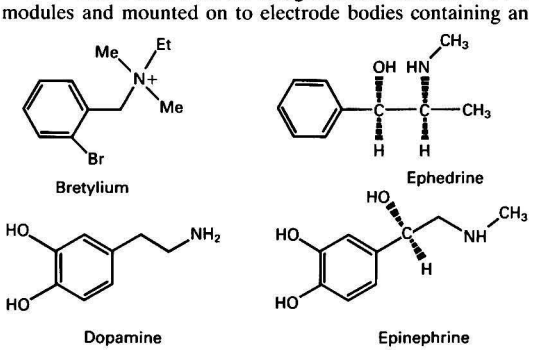

Fig. 1 Chemical structure of bretylium and the interferents tested

* To whom correspondence should be addressed.

Ag–AgCl internal lead-out (Ingold). A 3.0 mol dm^{-3} solution of sodium chloride saturated with AgCl was used as internal filling. The electrodes were stored between use in 0.1 mol dm^{-3} Tris buffer (pH 7.4) at room temperature.

Owing to the tight membrane adhesion that is required for direct mounting on the gold electrode surface, the membrane solutions for the Biobrid V2.1 thick-film sensors[8] were prepared from a PVC–PVAc copolymer instead of high molecular mass PVC. The Biobrid sensors were prepared by pipetting 2.0 mm^3 of the membrane mixture on to one of the gold electrodes of each channel of the Biobrid transducers. The difference electrodes were coated with 2.0 mm^3 of a membrane solution without an electroactive ion-pair complex. After preparation, the solvent was evaporated at room temperature in an evacuated desiccator for 12 h.

E.m.f. Measurements

Macroscopic electrodes

Potentiometric measurements with the macroscopic bretylium-selective electrodes were carried out *versus* a double-junction Ag–AgCl reference electrode (K801; Orion) at room temperature. The electrode output was recorded with a digital microprocessor pH/ion meter (pMX2000, WTW Weilheim) and plotted on a strip-chart recorder. The samples were applied from 25 cm^3 beakers, and the desired concentrations of bretylium and the other analytes were achieved by stepwise addition of small volumes of concentrated stock solutions. The sample solutions were constantly agitated by a magnetic stirrer.

Thick-film sensors

The output of each of the four potentiometric Biobrid channels was measured as the voltage difference between one ion-selective membrane and the corresponding difference membrane. The signal voltages were amplified by instrumentation amplifers (INA 110, Burr Brown) and recorded by a computer-supported data-acquisition system (AT CODAS, DATAQ Instruments). The potential of the analyte solution was earthed by an uncoated gold electrode that functioned essentially as a pseudo-reference electrode and was located between the sensing and difference electrodes of each channel. The analyte solutions were applied to the sensor, *via* a U-shaped flow cell (volume 200 mm^3), by a peristaltic pump (Microperpex; LKB Pharmacia). The measurements with the aqueous solutions were performed at a continuous flow rate of 0.4 cm^3 min^{-1}. The serum samples were analysed in a stopped-flow mode to allow the use of a small sample volume (250 mm^3). No differences between the sensor signals for the two sample application techniques were observed in tests with buffered aqueous solutions.

The potentiometric selectivity coefficients $K_{i,j}^{pot}$ were measured only for the ion-pair complex with the best properties (BRE–TUS) by the separate-solution method[9] and calculated from the equation $\log K_{i,j}^{pot} = (E_j - E_i)/S$, where E represents the e.m.f. readings measured for the primary ion (i) and the interfering ion (j), respectively, and S is the slope observed for the primary ion. The values given were evaluated from the e.m.f. readings obtained for 1×10^{-3} mol dm^{-3} solutions of the primary and the interfering ions in 0.1 mol dm^{-3} Tris buffer at pH 7.4, according to IUPAC recommendations.[10]

Results and Discussion

Calibration Data

The response curves for the macroscopic bretylium-selective electrodes are shown in Fig. 2. The characteristics of the macroscopic and the Biobrid sensors are summarized in Tables 1 and 2, respectively. The slopes of the curves for the macroscopic BRE–TUS electrodes are close to those expected for Nernstian behaviour, independent of whether BEHP or DBP is used as plasticizer. A somewhat lower slope of 40 mV $decade^{-1}$ for the BRE–TUS membranes was found on the Biobrid transducers. The reason for this could be that the plasticizer is not electrochemically inert and, owing to the differential measurements, this potential is subtracted on the Biobrid sensors. Further, there are different junction potentials between the back surface of the membrane and the Biobrid sensor (solid gold/liquid membrane) than encountered with the conventional solution/liquid membrane junction in macroscopic electrodes.[11] This behaviour corresponds to that occurring with previous measurements with the Biobrid transducer.[8] The detection limits of the macroscopic BRE–TUS electrodes was found to be 1×10^{-7} mol dm^{-3} (0.04 μg cm^3) with BEHP and 3×10^{-7} mol dm^{-3} (0.12 μg cm^{-3}) with DBP as the plasticizer in buffered solutions.

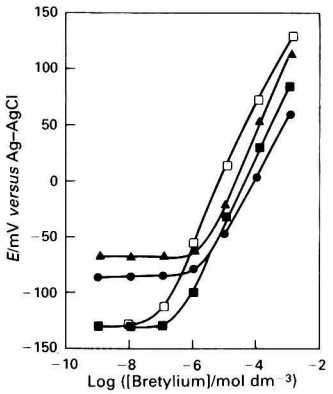

Fig. 2 Response curves of macroscopic bretylium-selective electrodes containing an electroactive ion-pair complex: □, BRE–TUS with BEHP; ■, BRE–TUS with DBP; ▲, BRE–TPB with DBP; and ●, BRE–RES with DBP as plasticizer. Measurements were made in 0.1 mol dm^{-3} Tris buffer at pH 7.4

Table 1 Calibration data for the macroscopic bretylium-selective electrodes

Ion pair/ plasticizer	Slope/mV $decade^{-1}$	Detection limit		Linear range†/ mol dm^{-3}
		mol dm^{-3}	μg cm^{-3}	
BRE–TUS/BEHP	60.7 ± 3*	1×10^{-7}	0.04	3×10^{-7}–1×10^{-3}
BRE TUS/DBP	61.3 ± 3*	3×10^{-7}	0.12	1×10^{-6}–1×10^{-3}
BRE–RES/DBP	53.0 ± 4*	2×10^{-6}	0.83	1×10^{-5}–1×10^{-3}
BRE–TPB/DBP	67.6 ± 4*	2×10^{-6}	0.83	1×10^{-5}–1×10^{-3}

* Statistical deviation for 10 electrodes.

† Not determined for concentrations higher than 1×10^{-3} mol dm^{-3}.

Table 2 Calibration data for the bretylium-selective Biobrid sensors

Ion pair/ plasticizer	Slope/mV $decade^{-1}$	Detection limit		Linear range/ mol dm^{-3}
		mol dm^{-3}	μg cm^{-3}	
BRE–TUS/DBP	40 ± 3*	8×10^{-7}	0.33	1×10^{-5}–1×10^{-1}
BRE–RES/DBP	15 ± 3*	2×10^{-6}	0.83	1×10^{-5}–1×10^{-1}

* Statistical deviation for eight independent sensor channels.

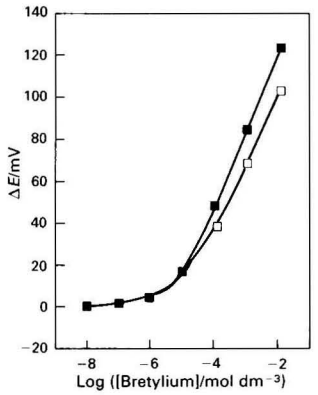

Fig. 3 Response curves of Biobrid sensors with bretylium-selective membranes containing BRE–TUS as the active ion-pair complex and DBP as plasticizer in ■, non-pathological (Precinorm U) and □, pathological (Precipath U) human sera with added bretylium tosylate

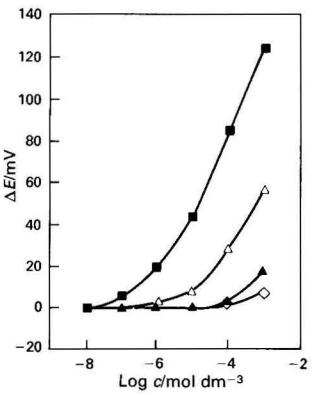

Fig. 4 Response curves of bretylium-selective Biobrid sensors (BRE–TUS/DBP) towards ■, bretylium tosylate; △, ephedrine hydrochloride; ▲, dopamine hydrochloride; and ◇, epinephrine hydrochloride in 0.1 mol dm^{-3} Tris buffer at pH 7.4

Table 3 Bretylium-selective Biobrid sensors (BRE–TUS/DBP): properties of the sensors in human sera and buffered aqueous solutions

Analyte solutions	Slope/mV decade^{-1}	Detection limit mol dm^{-3}	Detection limit μg cm^{-3}	Linear range/ mol dm^{-3}
Tris (pH 7.4)/ 0.1 mol dm^{-3}	40 ± 3*	8×10^{-7}	0.33	1×10^{-5}–1×10^{-1}
Precinorm U	37 ± 3*	5×10^{-6}	2.10	3×10^{-5}–1×10^{-2}
Precipath U	32 ± 3*	5×10^{-6}	2.10	1×10^{-4}–1×10^{-2}

* Statistical deviation for eight independent sensor channels.

Table 4 Potentiometric selectivity coefficients for the bretylium-selective electrodes and sensors

	Interfering ions		
Log $K_{i,j}^{pot}$*	Ephedrine	Dopamine	Epinephrine
Macroscopic electrode (BRE–TUS/DBP)	−2.1	−3.1	−3.4
Biobrid sensor (BRE–TUS/DBP)	−1.7	−2.7	−2.9

* For concentrations of bretylium and the interfering ions of 10^{-3} mol dm^{-3}.

Very important for any possible medical application of such a drug sensor is its performance in real biological samples with high ionic strength and protein content. Therefore, Biobrid sensors with BRE–TUS/DBP membranes were tested in non-pathological (Precinorm U) as well as pathological (Precipath U), undiluted human sera (see Fig. 3). Slopes, detection limits and linear range are reduced, compared with the same characteristics in aqueous analyte solutions, by the influence of the complex serum analytes, but remain in the analytically relevant range. The data for serum analytes are presented in Table 3.

Selectivity

The selectivity coefficients for both the macroscopic electrodes and the Biobrid sensors against ephedrine, dopamine and adrenaline (epinephrine) (see Fig. 4) are listed in Table 4. These substances were chosen for measurements because of their potential occurrence in blood serum and their relative structural similarity to bretylium. The logarithmic selectivity coefficients $K_{i,j}^{pot}$ for the Biobrid sensor are from about 0.4 to 0.5 units less than those for the macroscopic electrodes. The difference could be as a result of the different membrane matrix material used for the Biobrid sensors. Considering the physiologically and therapeutically low concentrations of the selected interfering species occurring in blood serum, the measured selectivity coefficients are not in a problematical range.

Response Times

The response times required to reach 90% of the final signal of the macroscopic electrodes were all less than 10 s over the concentration range from 1×10^{-7} to 1×10^{-3} mol dm^{-3}. The final e.m.f. readings were obtained within 30 s. The response times of the Biobrid sensors were about 5 s for 90% of the final signal and 10 s for the final reading, but depended on, and were limited by, the flow rate of the analyte solution across the electrodes in the flow cells. No significant difference of the response times between aqueous buffers and undiluted sera were observed.

Comparison of the Macroscopic Electrodes with the Biobrid Sensors

Both types of bretylium sensors (macroscopic and Biobrid) need a conditioning time of approximately 30 min in a buffer solution of the same pH as the analyte solutions. The macroscopic bretylium-selective electrodes with BRE–TUS-containing membranes showed a good performance with regard to sensitivity, linear range, slope and selectivity (see Table 1). The membranes containing the same ion-pair complexes and plasticizers were used also on the Biobrid V2.1 transducers and showed slightly poorer properties with respect to sensitivity and selectivity. Nevertheless, the calibration data obtained from measurements with Biobrid sensors (Table 2) in human sera showed that these sensors also cover the detection range needed in medical and pharmaceutical analysis. The therapeutic doses of bretylium tosylate vary between 20 and 80 μg cm^{-3} (calculated for a blood volume of 5 dm^3), depending on the manner of administration.[12] The detection limits with both types of bretylium sensor are below 0.4 μg cm^{-3}, which is at least 50 times lower than the therapeutic doses.

The main advantages of the Biobrid sensors over the macroscopic electrodes are the mechanical miniaturization,

the possibility of building a multichannel sensor,[8] which would allow the simultaneous determination of several other serum parameters, and an acceptable sample volume of 250 mm^3 that is needed for the analysis.

Conclusions

The experimental comparison of several ion-pair complexes of bretylium for their use in bretylium-selective PVC membranes showed that BRE–TUS has the best properties of the examined complexes. The membranes containing BRE–TUS provided a stable signal over a period of 7 d in continuous measurements at room temperature, whereas BRE–TPB and BRE–AUR were washed out of the membranes by the analyte solutions after 3–4 h. The BRE–RES membrane had only poor properties on the Biobrid transducer. The response times of 5 to 10 s are relatively fast and allow an acceptable sample throughput.

The BRE–TUS membranes could be successfully applied in the potentiometric determination of bretylium salts, even in complex analytes such as blood serum, without any prior sample preparation, which is necessary for most other analytical methods. Additional monitoring, however, of the serum quality is necessary, owing to the different slopes of the response curves for the sensors in non-pathological and pathological sera (see Table 3), if the deviation of 15% is not acceptable. The detection limit with the Biobrid sensors is about 100 ng in a sample volume of 250 mm^3. This value cannot compete with the detection limits obtained by high-performance liquid chromatography (10 ng)[13] and gas–liquid chromatography (5 ng cm^{-3}),[14] but these methods require expensive instrumentation and a complicated sample preparation. Electrochemical sensors such as the bretylium sensors described are suitable for on-line monitoring of analyte activities in physiological fluids and for application in the manufacture of pharmaceuticals.

We acknowledge the financial support by the 'Bundesministerium für Forschung und Technologie' (FKZ 0319474A).

References

1 Ammann, D., Morf, W. E., Anker, P., Meier, P. C., Pretsch, E., and Simon, W., *Ion Sel. Electrode Rev.*, 1983, **5**, 3.
2 Ma, T. S., and Hassan, S. S. M., in *Organic Analysis Using Ion-selective Electrodes*, eds. Belcher, R., and Anderson, D. M. W., Academic Press, London, 1982, vol. 2.
3 Eppelsheim, C., Aubeck, R., Hampp, N., and Bräuchle, C., *Analyst*, 1991, **116**, 1001.
4 Aubeck, R., Bräuchle, C., and Hampp, N., *Anal. Chim. Acta*, 1990, **238**, 405.
5 Bunaciu, A. A., Ionescu, M. S., Pălivan, C., and Coşofreţ, V. V., *Analyst*, 1991, **116**, 239.
6 Neubert, R., and Amlacher, R., *Dtsch. Apoth. Ztg.*, 1991, **131**, 2225.
7 Scholze, J., Hampp, N., and Bräuchle, C., *Sens. Actuators B*, 1991, **4**, 211.
8 Hampp, N., Eppelsheim, C., Popp, J., Bisenberger, M., and Bräuchle, C., *Sens. Actuators A*, 1992, **31**, 144.
9 Pungor, E., Tóth, K., and Hrabeczy-Pall, A., *Pure Appl. Chem.*, 1979, **51**, 1913.
10 Guilbault, G. G., *Ion Sel. Electrode Rev.*, 1979, **1**, 139.
11 Janata, J., *Principles of Chemical Sensors*, Plenum Press, New York, 1989, p. 119.
12 Garrett, E. R., Green, I. R., Jr., and Bialer, M., *Biopharm. Drug Dispos.*, 1982, **3**, 129.
13 Park, M. K., Kim, K. H., and Ha, J. Y., *Soul Taehakkyo Yakhak Nonmunjip*, 1986, **11**, 25.
14 Lai, C.-M., Kamath, B. L., Carter, J. E., Erhardt, P., Look, Z. M., and Yacobi, A., *J. Pharm. Sci.*, 1980, **69**, 681.

Paper 2/02233H
Received April 30, 1992
Accepted May 28, 1992

Comparative Study of the Voltammetric Behaviour of Guanine at Carbon Paste and Glassy Carbon Electrodes and Its Determination in Purine Mixtures by Differential-pulse Voltammetry

Markas A. T. Gilmartin and John P. Hart*
Bristol Polytechnic, Faculty of Applied Sciences, Coldharbour Lane, Frenchay, Bristol, UK BS16 1QY

Cyclic voltammetry and differential-pulse voltammetry (DPV) were used in a comparative investigation into the electrochemical oxidation of guanine at a carbon paste electrode (CPE) and a planar glassy carbon electrode (GCE). The DPV peak potential and peak current were found to be dependent on the pH of the 0.5 mol dm^{-3} phosphate buffer over the range 3.0–9.0 for both electrodes. The effect of ionic strength was investigated over the concentration range 0.05–0.5 mol dm^{-3} (pH 5.0). Slightly larger peak currents were obtained with 0.5 mol dm^{-3} supporting electrolyte at both electrodes; however, an approximate 2.5-fold increase in the anodic response was observed with the CPE. The electro-oxidation of guanine was found to occur with the production of one voltammetric peak; the product probably undergoes further oxidation to yield two peaks on the second anodic scan. Under these conditions the electrode reaction was identified as being irreversible. Systematic studies into the possible adsorption of guanine were performed on a 1×10^{-5} mol dm^{-3} guanine solution in 0.5 mol dm^{-3} phosphate buffer by DPV, utilizing CPEs and GCEs over the pH range 5.0–9.0. The peak currents did not increase with various accumulation potentials and times, indicating that the parent compound does not adsorb at either of the electrode surfaces studied. The optimum medium for quantitative determination at a CPE or a GCE by DPV was found to be 0.5 mol dm^{-3} phosphate buffer (pH 5.0). Anodic peak currents were found to be linearly related to concentration over the range 1×10^{-5}–1×10^{-7} mol dm^{-3} and 1×10^{-5}–7.5×10^{-7} mol dm^{-3} for the CPE and GCE, respectively. Guanine was successfully determined in a deoxyribonucleic acid sample, following acid hydrolysis, with use of DPV. The developed method is more sensitive than those of previous voltammetric studies.

Keywords: *Guanine; glassy carbon and carbon paste electrodes; differential-pulse voltammetry; adsorption studies; deoxyribonucleic acid analysis*

Guanine (2-amino-6-hydroxypurine) is a purine base consisting of two condensed heterocyclic pyrimidine and imadazole rings. In nature, it exists mainly as nucleoside and nucleotide constituents, in the latter form as monomeric precursors of ribonucleic acid and deoxyribonucleic acid (DNA).[1] Genetic information is stored, duplicated and transmitted by virtue of these nucleic acids. This information is contained in the sequence of purine and pyrimidine bases, with sugars and phosphate groups performing a structural role. The normal function and multiplication of cells is dependent on this complex arrangement. Guanine nucleotides also serve as energy sources (*e.g.*, guanosine triphosphate in protein synthesis on polyribosomes) and play important roles in regulatory systems (*e.g.*, cyclic guanosine monophosphate) in a wide variety of tissues and organisms, facilitating maintenance of the internal milieu.[2]

Hence, the detection and determination of purines and their corresponding nucleotides and nucleosides has become increasingly important in the field of biomedical research.[3] Indeed, the catabolism of nucleic acids, enzymic degradation of tissues, dietary habits and various salvage pathways all contribute to the presence of nucleic acid components in physiological fluids, tissues and cells; therefore, detection of elevated levels of these substances could be indicative of certain diseases.[3]

In addition, analysis for guanine is required for (*i*) the measurement of different sensitivities of adenine–thymine and guanine–cytosine (G–C) pairs in DNA to various types of denaturation; (*ii*) the measurement of G + C ratios in DNA, *i.e.*, in microbial taxonomy; (*iii*) for tracing the course of structural transitions of synthetic polynucleotides; and (*iv*) studying the interactions of nucleic acids with electrically charged surfaces,[4] effectively mimicking biological oxidation mechanisms at membrane surfaces (some of which involve enzymes).[1]

Concurrent with the biological significance of guanine, much attention has focused on its determination, and, consequently, a whole spectrum of methods have evolved to this end. The most commonly used methods involve high-performance liquid chromatography, which, when combined with electrochemical detection, addresses many of the selectivity problems encountered during the analysis of biomolecules. However, this technique generally requires a stabilization period, which may render it unsuitable for the analysis of a small number of samples. Ultraviolet spectrophotometry has been widely used for these purposes, but difficulties arise when assigning spectra unambiguously to complex mixtures containing structurally related compounds. Surface-enhanced Raman spectroscopy has excellent selectivity, but this feature is overshadowed by its limitations in sensitivity and experimental reproducibility. Additionally, these alternative methods for determining guanine require expensive and complicated equipment.

Voltammetric methods are particularly suited for the analysis of a wide variety of organic compounds[1] and it is for this reason that they have been used to investigate the electrochemistry of guanine. The inability of guanine to be reduced at a mercury electrode,[5] within an analytically useful potential range, prompted workers to investigate alternative electrode substrates. Carbon electrodes are inexpensive and provide a suitable anodic window for studying this biomolecule. In 1962, Smith and Elving[6] observed the electro-oxidation of guanine at a wax-impregnated stationary graphite electrode; these findings were reinforced by several other studies at different carbon electrodes, for example, pyrolytic graphite,[7] glassy carbon (GC)[8,9] and reticulated carbon[10] electrodes. It is, therefore, surprising that, to our knowledge, little or no attention has been paid to the application of carbon paste electrodes (CPEs) to the determination of guanine,

* To whom correspondence should be addressed.

especially when considering their inherent benefits, namely, their low cost, low residual currents and readily renewable surface.

The purpose of the present investigation was to carry out a systematic study into the voltammetric behaviour of guanine at a CPE and, for comparison, a GCE, under a wide variety of solution conditions. The results were then used in the development of a method for the determination of guanine in a purine mixture and a DNA sample by differential-pulse voltammetry (DPV).

Experimental

Chemicals and Reagents

All chemicals were of analytical-reagent grade and obtained from BDH (Poole, Dorset, UK) unless stated otherwise. Graphite (Ultra Carbon, Ultra 'F' purity, UCP-IM) was purchased from Johnson Matthey (Hertfordshire, UK). Uric acid, guanine and guanosine were obtained from Sigma (St. Louis, MO, USA). Plasmid DNA (pUC18, 512.5 μg cm^{-3}) derived from *Escherichia coli* was kindly donated by the plant molecular biology group, Bristol Polytechnic. Standard solutions were prepared daily and immediately wrapped in aluminium foil to prevent photodegradation and thermal biomolecular degradation. The supporting electrolyte used throughout this study was phosphate buffer solution, which was prepared from a 0.5 mol dm^{-3} stock solution of sodium dihydrogen orthophosphate and orthophosphoric acid. These were mixed to form a buffer solution of the required pH (a pH meter was used) and diluted with de-ionized water (if necessary) to yield the desired concentration. The dissolution of uric acid and guanine was effected in 50 cm^3 of 0.05 mol dm^{-3} sodium hydroxide following 10 min sonication using a Decon FS100 sonicator (Ultrasonics, Sussex, UK). All solutions were prepared with water that had been de-ionized by the Purite R0200-Stillplus HP system (Purite, Oxon, UK).

Apparatus

Cyclic voltommetry and DPV were performed with use of a Metrohm (Herisau, Switzerland) E612 VA-scanner in conjunction with an E611 VA-detector; these were connected to a Linseis LY18100 *x–y* plotter (Recorder Lab. Services, Surrey, UK) to record the voltammograms. A three-electrode cell was used, incorporating either a GCE or a CPE, a saturated calomel reference electrode (Russel electrodes) and a laboratory-constructed platinum-wire counter electrode. The geometrical areas of the electrode surfaces were calculated to be 0.29 and 0.21 cm^2 for the GCE and the CPE, respectively. For DPV measurements in stirred solutions, a small circular stirring disc (BDH) was placed in the bottom of the cell and rotated at a fixed rate by a Whatman Mini-MR stirrer (Maidstone, Kent, UK).

Electrode Construction and Surface Renewal

Carbon paste electrodes

The fabrication of these electrodes is based on a previously reported design,[11] consisting of a Kel-F [poly(chlorotrifluoroethylene)] barrel with a fixed depth of 3 mm. Nujol (25% by mass) was added to 0.5 g of Ultra 'F' purity graphite and vigorously mixed for 10 min, with a microspatula, in a small glass vial. The resulting paste was packed into the barrel, allowing a 3 mm depth, and the surface was smoothed with a computer punch-card in a reproducible manner. After each measurement the old paste was removed and the barrel was thoroughly rinsed with ethanol and dried with tissue; the packing procedure was then repeated for subsequent measurements.

Glassy carbon electrodes

These electrodes were cleaned in between successive runs in the following manner. The electrode was rinsed thoroughly with a jet of distilled water, the surface was polished with aluminium oxide, then the electrode was rinsed again with distilled water and finally dried with tissue paper.

Voltammetric Procedures With GCEs and CPEs

Cyclic voltammetry

Cyclic voltammograms were initially recorded with use of blank solutions of 0.5 mol dm^{-3} phosphate buffer, followed by 1×10^{-5} mol dm^{-3} guanine in the same supporting electrolyte (pH 5.0 and 7.0) with both carbon electrodes. The voltammetric conditions were as follows: initial potential, 0 V; scan rate, 20 mV s^{-1}; switching potential, +1.0 V.

The nature of the oxidation process at GCEs and CPEs was studied by investigating the effect of scan rate on the anodic peak potential (E_p) for a 1×10^{-5} mol dm^{-3} guanine solution in pH 7.0 phosphate buffer. Additionally, values for the electron transfer coefficient (αn_a) were calculated from the cyclic voltammograms for a similar guanine solution, obtained with a CPE and GCE at a scan rate of 20 mV s^{-1}.

The effect of accumulation time (t_{acc}) on the anodic signal for a similar guanine solution was investigated over the pH range 5.0–9.0 from 0 to 30 min at both electrodes. In addition, the accumulation potential (E_{acc}) was investigated on open circuit (−1.0, 0.0 and +0.5 V) with use of 1×10^{-5} mol dm^{-3} guanine (pH 7.0) in 0.5 mol dm^{-3} phosphate buffer at both electrodes. These investigations were performed in stirred solutions with allowance of a 30 s quiescence period at each of the specified accumulation times.

Further adsorption studies were performed with a 1×10^{-5} mol dm^{-3} guanine solution in 0.5 mol dm^{-3} phosphate buffer (pH 7.0) at scan rates of 20, 50, 75, 100 and 200 mV s^{-1} at both electrodes.

Differential-pulse voltammetry

The effect of ionic strength of the phosphate buffer solution (pH 5.0) on the anodic response for a 1×10^{-5} mol dm^{-3} guanine solution was studied between 0.05 and 0.5 mol dm^{-3} at both electrodes by using this technique. The instrumental parameters were as follows: initial potential, 0 V; final potential, 1.1 V; pulse repetition time, 0.4 s; pulse amplitude, 50 mV; and scan rate, 10 mV s^{-1}.

The effect of the pH of the phosphate buffer solution on the anodic response for a 1×10^{-5} mol dm^{-3} guanine solution was studied between 3.0 and 9.0 under the experimental conditions described above. The measurements were performed in triplicate. The GCEs were meticulously cleaned in the prescribed manner prior to each individual analysis; with CPEs, the paste was removed from the electrode barrel and replenished before quantitative determinations. From the relative standard deviations calculated at each pH, error bars were prepared for the three readings.

The effect of E_{acc} was studied on open circuit and between −0.1 and +0.5 V, with use of a stirred 1×10^{-5} mol dm^{-3} guanine solution in 0.5 mol dm^{-3} phosphate buffer (pH 7.0), at both electrodes, by using the same instrumental parameters as listed above.

Calibration graphs of peak current *versus* guanine concentration were prepared from the data generated through DPV studies with use of both carbon electrodes. The following operating conditions were used: initial potential, 0 V; scan rate, 5 mV s^{-1}; pulse amplitude, 50 mV; pulse repetition time, 0.4 s, and final potential, +1.1 V.

Some commonly encountered interfering species were studied by DPV with a view to testing the resolution of the voltammetric technique. A mixture of three purines (uric acid, guanine and guanosine), each at a concentration of 1×10^{-5}

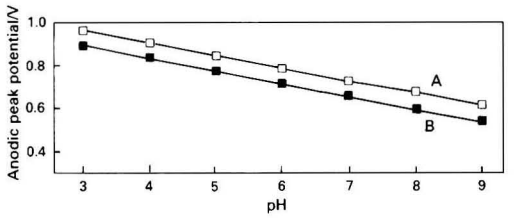

Fig. 1 Effect of pH on the anodic peak potential for a 1×10^{-5} mol dm^{-3} guanine solution in 0.5 mol dm^{-3} phosphate buffer using differential-pulse voltammetry. Scan rate, 10 mV s^{-1}; initial potential, 0 V; final potential, +1.1 V; pulse amplitude, 50 mV; and pulse repetition time, 0.4 s. A, GCE; and B, CPE

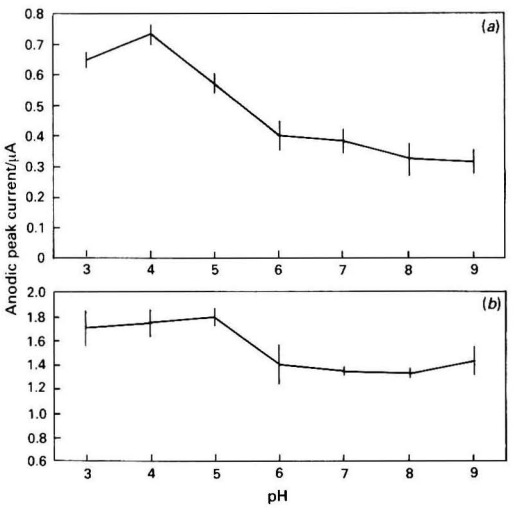

Fig. 2 (*a*) Effect of pH on the anodic peak currents obtained at a GCE for a 1×10^{-5} mol dm^{-3} guanine solution in 0.5 mol dm^{-3} phosphate buffer using differential-pulse voltammetry. Scan rate, 10 mV s^{-1}; initial potential, 0 V; final potential, +1.1 V; pulse amplitude, 50 mV; and pulse repetition time, 0.4 s. (*b*) Effect of pH on the anodic peak currents obtained at a CPE for a 1×10^{-5} mol dm^{-3} guanine solution in 0.5 mol dm^{-3} phosphate buffer using differential-pulse voltammetry. Scan rate, 10 mV s^{-1}; initial potential, 0 V; final potential, +1.1 V; pulse amplitude, 50 mV; and pulse repetition time, 0.4 s

mol dm^{-3}, in 0.5 mol dm^{-3} phosphate buffer (pH 5.0) was prepared and subjected to DPV, using the same instrumental parameters as listed above.

Determination of Guanine in a pUC18 DNA Sample by Using a CPE in Conjunction With DPV

A pUC18 DNA sample was treated by a simple modification of a well-established hydrolysis procedure;[12] briefly, this involves adding 1.17 cm^3 of a 512.5 μg cm^{-3} DNA sample to a heat-resistant, screw-topped, tapering centrifuge tube and boiling in 1.2 cm^3 of 7 mol dm^{-3} perchloric acid and 1.2 cm^3 of water for 1 h to hydrolyse the sample, liberating the purines guanine and adenine. The resulting mixture was adjusted to pH 5.0 by the addition of exactly 1.375 cm^3 of 7.0 mol dm^{-3} sodium hydroxide and 15.055 cm^3 of 0.5 mol dm^{-3} disodium hydrogen phosphate, from a microburette, and was subjected to DPV, under the following experimental conditions: initial potential, 0 V; scan rate, 5 mV s^{-1}; pulse amplitude, 50 mV; pulse repetition time, 0.4 s; and final potential, +1.1 V. The method of multiple standard additions was used to determine

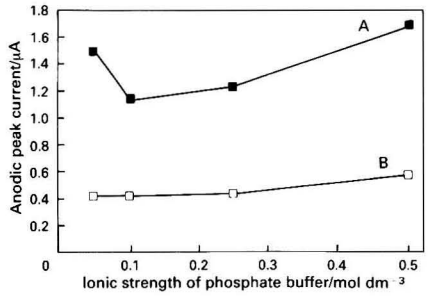

Fig. 3 Effect of ionic strength of pH 5.0 phosphate buffer on the anodic peak response for a 1×10^{-5} mol dm^{-3} guanine solution using a CPE (A) and a GCE (B) in conjunction with differential-pulse voltammetry. Scan rate, 5 mV s^{-1}; initial potential, 0 V; final potential, +1.1 V; pulse amplitude, 50 mV; and pulse repetition time, 0.4 s

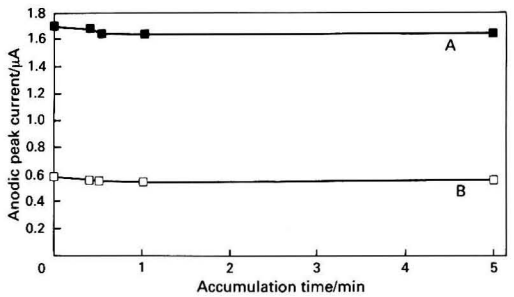

Fig. 4 Effect of accumulation time on the anodic peak currents for a stirred 1×10^{-5} mol dm^{-3} guanine solution in 0.5 mol dm^{-3} phosphate buffer (pH 7.0) at a CPE (A) and a GCE (B) using differential-pulse voltammetry. Scan rate, 10 mV s^{-1}; initial potential, 0 V; final potential, +1.1 V; pulse amplitude, 50 mV; and pulse repetition time, 0.4 s

the concentration of guanine present in the sample, wherein 0–500 mm^3 of a stock guanine solution (151.1 μg cm^{-3}) were added to 20 cm^3 of the treated sample.

Results and Discussion

Several studies have indicated that guanine is electrochemically oxidized at a variety of carbon electrodes.[1] It was also shown that guanine undergoes adsorption at a pyrolytic graphite electrode (PGE)[13,14] and a GCE[15] at pH 7.0, but the latter process becomes diffusion controlled below pH 4.0. Kenley *et al.*[8] investigated the oxidation of guanine at a GCE in pH 7.0 buffer solution, but no mention was made of adsorption at the electrode surface. Adsorption processes were reported to hamper the determination of guanine at a PGE by causing non-linear calibration graphs.[13,14] Other purines have also been found to exhibit this problem at GCEs.[16] In contrast, Wang and Freiha[17] exploited this adsorption phenomenon for the related purine, uric acid, to enhance the sensitivity of the voltammetric measurement. As adsorption seems to have occurred in at least two instances for guanine and also for structurally related purines, at various electrodes, we considered that it was important to investigate this phenomenon ourselves at a GCE and a CPE. It was hoped that we could throw some light on the nature of the electrochemical reactions of guanine at both of these carbon electrodes and then to exploit this for the quantitative determination of the substance by use of DPV.

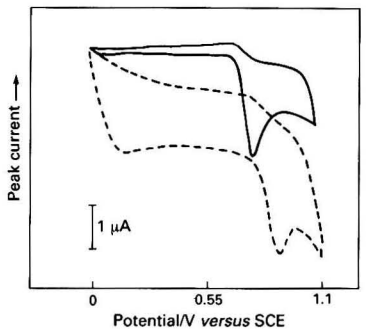

Fig. 5 Cyclic voltammetry for a 1×10^{-5} mol dm^{-3} guanine solution in 0.5 mol dm^{-3} phosphate buffer (pH 5.0) at a CPE (solid line) and a GCE (broken line). Scan rate, 50 mV s^{-1}; initial potential, 0 V; and switching potential, +1.1 V

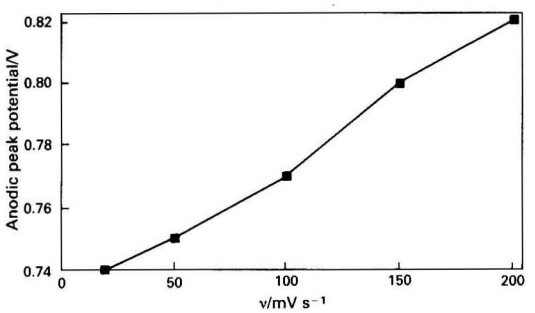

Fig. 6 Effect of scan rate on the anodic peak potential for a 1×10^{-5} mol dm^{-3} guanine solution in 0.5 mol dm^{-3} phosphate buffer (pH 5.0) at a CPE. Initial potential, 0 V and switching potential, +1.1 V

Differential-pulse and Cyclic Voltammetry of Guanine at GCEs and CPEs

The effect of pH on the electrode reaction was investigated by DPV, with use of a 1×10^{-5} mol dm^{-3} guanine solution in 0.5 mol dm^{-3} phosphate buffer, over the pH range 3.0–9.0 at both types of carbon electrodes. Fig. 1 shows that the anodic peak potential was dependent on the pH; the equation relating E_p to pH for a GCE is given by eqn. (1) and that for a CPE by eqn. (2).

$$E_p = +1.125 - 0.058 \text{ pH (V)} \quad (1)$$

$$E_p = +0.950 - 0.057 \text{ pH (V)} \quad (2)$$

The plots of peak current *versus* pH, over the same range, are shown in Fig. 2(*a*) and (*b*) for the GCE and CPE, respectively. It is apparent that the greatest peak magnitudes were obtained with phosphate buffer solution of pH 4.0 for the GCE and of pH 5.0 for the CPE. In addition, the peak currents at the CPE were more than twice the magnitude of those obtained at the GCE for each pH studied.

The effect of the ionic strength of the phosphate buffer solution on anodic peak potential was investigated by DPV over the range 0.05–0.5 mol dm^{-3}. Fig. 3 shows that slightly larger currents were obtained with the 0.5 mol dm^{-3} concentration at both electrodes; however, an approximate 2.5-fold increase in response was observed with the CPE.

It should be mentioned that it is important to fix the initial potential (accumulation potential, E_{acc}) and the time interval prior to scanning (accumulation time, t_{acc}) when adsorption studies are undertaken; both parameters could influence the degree of adsorption. Bearing this in mind, the above studies were performed after a time interval of 30 s and at 0 V. Next, the time interval was varied over the same pH range, with an

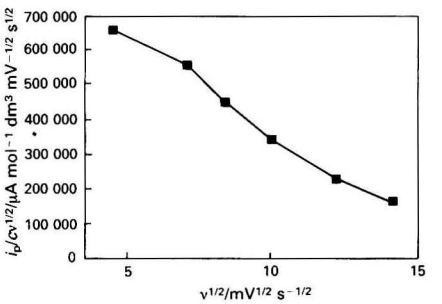

Fig. 7 Plot of $i_p/cv^{\frac{1}{2}}$ for an adsorption test for a 1×10^{-5} mol dm^{-3} guanine solution in 0.5 mol dm^{-3} phosphate buffer (pH 7.0) at a GCE

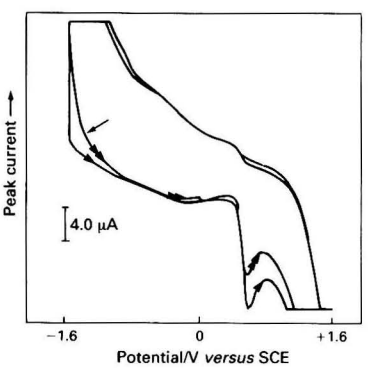

Fig. 8 Repeated cyclic voltammogram for a 1×10^{-4} mol dm^{-3} guanine solution in 0.5 mol dm^{-3} phosphate buffer (pH 7.0) at a GCE to show the subsequent oxidation reaction. Scan rate, 100 mV s^{-1}; initial potential, −1.6 V; and switching potential, +1.6 V. The arrow represents the second anodic scan

E_{acc} of 0 V. A typical plot of anodic peak current *versus* t_{acc} derived from DPV studies is shown in Fig. 4, revealing that the magnitude of the current response did not increase with accumulation time at a CPE; all of the plots at different pH values indicated that guanine itself shows no preconcentration resulting from adsorption. Similar results were obtained for a GCE. The study was repeated by using the cyclic voltammetric waveform between the potentials −0.1 and +0.3 V, and on open circuit; no increase in peak current (i_p) was observed with time at these potentials. Again, this would suggest that no significant adsorption had occurred; however, a marginally larger response was found at 0 V, which we cannot explain at present.

In order to investigate further the adsorption phenomenon and to examine the reversibility or otherwise of the oxidation process, we carried out cyclic voltammetry at different scan rates. Fig. 5 shows a typical voltammogram for guanine in 0.5 mol dm^{-3} phosphate buffer (pH 5.0). Clearly, one well-defined anodic peak was obtained at both electrodes. As no cathodic signals were observed over the potential range studied, the electrode reaction was considered to be irreversible. Further evidence for the irreversible nature of the reaction was obtained by plotting the E_p value *versus* the scan rate (v); Fig. 6 clearly shows an increase in peak potential with v, whereas reversible reactions are independent of this variable. Adsorption was investigated by plotting $i_p/cv^{\frac{1}{2}}$ *versus* $v^{\frac{1}{2}}$ (where c is the concentration of the analyte in mol dm^{-3}); an increase in the current function would indicate adsorption of this purine at the electrode surface. As no such increase occurs, the electrode reaction appears to be diffusion controlled (Fig. 7).

It has been suggested[10] that the product of oxidation at a PGE is 8-oxyguanine; this species can undergo oxidation/reduction reactions at potentials lower than that of guanine. As shown in Fig. 8 a small anodic peak appears on the second forward scan, which could be due to the more readily oxidizable 8-oxyguanine. This process at the PGE was reported to involve the loss of $2e^-$ and $2H^+$.[10] In order to ascertain the number of electrons involved in the oxidation of guanine at CPEs and GCEs we first determined the αn_a values from cyclic voltammograms by using the equation:[18]

$$\alpha n_a = \frac{0.048}{E_p - E_p/2}$$

The αn_a was 1.2 at the GCE and 1.08 at the CPE in 1×10^{-5} mol dm^{-3} guanine (pH 5.0); this suggests that the value for n_a is 2 as α values are typically 0.5. Bearing in mind that the gradients of E_p *versus* pH plots were approximately 58 and 57 mV per pH unit for the GCE and CPE, respectively, this would indicate that the number of protons involved in the reaction is two. Therefore, our results suggest that 8-oxyguanine could be the product formed at these two carbon electrodes.

Calibration, Limit of Detection and Interference Studies by DPV

As the i_p with the greatest magnitude was obtained at a CPE with 0.5 mol dm^{-3} phosphate buffer (pH 5.0), we used these solution conditions in the preparation of calibration graphs. Table 1 summarizes the DPV data for guanine at the CPE and GCE. It was found that anodic peak currents were linearly related to guanine concentrations over the ranges 1×10^{-5}–1×10^{-7} and 1×10^{-5}–7.5×10^{-7} mol dm^{-3} for the CPE and GCE, respectively. The limits of determination were 1×10^{-7} mol dm^{-3} for CPEs and 7.5×10^{-7} mol dm^{-3} for GCEs, based on a full-scale deflection of 0.5 μA.

As CPEs afforded the greatest sensitivity for the measurement of guanine [Fig. 2(*a*) and (*b*)], we used this in subsequent studies. It should be noted that the geometrical electrode area of the CPE is smaller than that of the GCE; therefore, the improvement in sensitivity of the former electrode could be due to the differences in the porosity of the electrode surfaces.

It should be stressed that we were interested in exploring the possibility of applying the CPE in biomatrices. In such samples it is likely that other electro-oxidizable biomolecules could be present; therefore, a mixture of some commonly encountered substances was subjected to DPV. Fig. 9 clearly indicates that the method, based on the use of CPEs, possesses the necesssary selectivity to permit the discrimination and determination of guanine in this mixture; it should be feasible to determine simultaneously uric acid and guanosine under the same conditions. In addition, an increase in the overpotential is observed for the oxidation of guanosine at a GCE; it is for this reason that no voltammetric signal is observed for the nucleoside at the GCE (Fig. 9).

Analytical Applications

It is envisaged that the method developed here could be applied to the classification of certain micro-organisms according to their G + C ratios and used for monitoring the effect of different modes of denaturation to DNA. The latter application is feasible as denaturation results in an unwinding of duplex DNA; this renders the guanine residues more accessible to the electrode surface owing to increased flexibility in its structure[19] and hence would provide a sensitive method for investigating any helix–coil transitions occurring in this molecule.[20] In addition, we decided to investigate the possibility of using the proposed method for the determination of guanine in a plasmid DNA sample, following acid hydrolysis. A simple hydrolysis step with perchloric acid for 1 h at 100 °C was carried out, followed by appropriate treatment to yield the desired pH for the subsequent analysis. Fig. 10 shows that two well-defined anodic peaks were obtained on the differential-pulse voltammograms, corresponding to the purines guanine and adenine; determination of guanine was performed by the method of multiple standard additions.

It is noteworthy that over a 2-fold enhancement in peak current was obtained at a CPE when compared with that of a

Table 1 Differential-pulse voltammetric data for guanine, using carbon paste and glassy carbon electrodes

Electrode type	E_p/V	Response factor/ μA μmol^{-1} dm^{-3}	Range of concentration for linear response/ μmol dm^{-3}	Precision* (%)
CPE	0.750 ± 0.01	0.12	10–0.1	3.9
GCE	0.824 ± 0.01	0.05	10–0.75	4.0

* Based on five separate measurements.

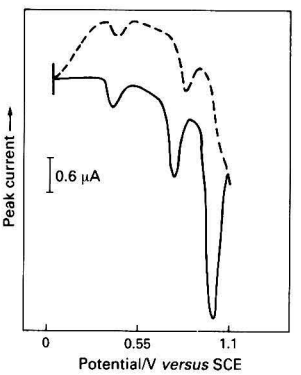

Fig. 9 Analysis of a mixture containing 1×10^{-5} mol dm^{-3} concentrations of uric acid, guanine and guanosine in 0.5 mol dm^{-3} phosphate buffer (pH 5.0) using a GCE (broken line) and CPE (solid line) in conjunction with differential-pulse voltammetry. Scan rate, 10 mV s^{-1}; initial potential, 0 V; final potential, +1.1 V; pulse amplitude, 50 mV; and pulse repetition time, 0.4 s

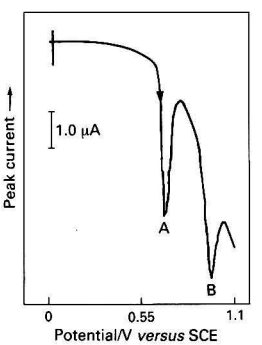

Fig. 10 Differential-pulse voltammogram of an acid-hydrolysed plasmid DNA sample (512.5 μg cm^{-3}) at a CPE, where A and B represent guanine and adenine, respectively. Scan rate, 5 mV s^{-1}; initial potential, 0 V; final potential, +1.1 V; pulse amplitude, 50 mV; and pulse repetition time, 0.4 s

similar study by Brabec with a PGE.[21] As the G + C ratios for our plasmid DNA and Brabec's calf (*Bos taurus*) thymus DNA were approximately 50 and 43%,[22] respectively, it is likely that this improved response arises as a function of the electrode surface and is not due to genetic variation between the two samples. This argument is strengthened by the fact that this enhancement of sensitivity was achieved by using an electrode with a smaller geometrical area, *i.e.*, 0.3 and 0.21 cm^2 for the PGE and CPE, respectively. Moreover, an increase in selectivity was observed at the latter electrode, as there was a 190 mV reduction in the overpotential required for the oxidation of guanine.

By using gene sequencing data obtained from Boehringer Mannheim (manufacturer's data) the theoretical number of guanine residues was calculated to be 1325. This value compares favourably with 1140 guanine bases calculated by DPV and the method of multiple standard additions. Therefore, it can be concluded that the present procedure shows promise in studies of this type.

It should be emphasized that our aim was to develop a simple, reliable and inexpensive voltammetric procedure that could be adapted to the determination of guanine in a variety of samples. Although this purine is excreted in micromolar amounts (0.4 mg per 24 h),[23] there are disorders associated with purine metabolism (*e.g.*, deficiencies in the enzyme guanase), which could conceivably elevate guanine excretion; thus, a simple analytical method would be highly desirable. The limit of detection of our method is 1×10^{-7} mol dm^{-3} (15.1 ng cm^{-3}), which is considerably lower than that previously reported for guanine[14] (*e.g.*, 5×10^{-5} mol dm^{-3}). In addition, we did not encounter any problems using a CPE, regarding non-linear calibration graphs, which had been reported previously using other electrode materials.[12–14] Therefore, we believe that the method based on DPV described in this paper could have wider applications, such as in biomedical analysis.

The authors thank Bristol Polytechnic for financial support, M. Bulman for kindly donating the plasmid DNA sample, and Boehringer Mannheim for supplying the gene sequence data. In addition, they are grateful to Dr. B. Birch for his interest in this work.

References

1 Hart, J. P., *Electroanalysis of Biologically Important Compounds*, Ellis Horwood, Chichester, 1990, p. 51.
2 Harper, H. A., in *Review of Physiological Chemistry*, eds. Harper, H. A., Rodwell, V. W., and Mayes, P. A., Lange Medical Publications, CA, 16th edn., 1977, p. 406.
3 Sheng, R., Ni, F., and Cotton, T. M., *Anal. Chem.*, 1991, **63**, 437.
4 Brabec, V., *Bioelectrochem. Bioenerg.*, 1981, **8**, 437.
5 Smith, D. L., and Elving, P. J., *Anal. Chem.*, 1962, **34**, 930.
6 Smith, D. L., and Elving, P. J., *J. Am. Chem. Soc.*, 1962, **84**, 1412.
7 Dryhurst, G., and Pace, G. F., *J. Electrochem. Soc.*, 1970, **117**, 1259.
8 Kenley, R. A., Jackson, S. E., Martin, J. C., and Visor, G. C., *J. Pharm. Sci.*, 1985, **74**, 1082.
9 Sequaris, J. M., Valenta, P., and Nurnberg, H. W., *J. Electroanal. Chem. Interfacial Electrochem.*, 1981, **122**, 263.
10 Goyal, R. N., and Dryhurst, G., *J. Electroanal. Chem. Interfacial Electrochem.*, 1982, **135**, 75.
11 Hart, J. P., Wring, S. A., and Morgan, I. C., *Analyst*, 1989, **114**, 933.
12 Brown, D. M., and Todd, A. R., in *The Nucleic Acids*, eds. Chargaff, E., and Davidson, J. N., Academic Press, New York, 1955, vol. I, p. 409.
13 Dryhurst, G., *Anal. Chim. Acta*, 1971, **57**, 137.
14 Dryhurst, G., *Talanta*, 1972, **19**, 769.
15 Yao, T., Wasa, T., and Musha, S., *Bull. Chem. Soc. Jpn.*, 1977, **50**, 2917.
16 Yao, T., Taniguchi, Y., Wasa, T., and Musha, S., *Bull. Chem. Soc. Jpn.*, 1978, **51**, 2937.
17 Wang, J., and Freiha, B., *Bioelectrochem. Bioenerg.*, 1984, **12**, 225.
18 Galus, Z., *Fundamentals of Electrochemical Analysis*, Ellis Horwood, Chichester, 1976, p. 237.
19 Brabec, V., and Dryhurst, G., *Stud. Biophys.*, 1978, **67**, 23.
20 Brabec, V., *Biophys. Chem.*, 1979, **9**, 289.
21 Brabec, V., *Biopolymers*, 1979, **18**, 2397.
22 *Molecular Biology Labfax*, ed. Brown, T. A., Bios Scientific Publishers, Oxford, 1991, p. 243.
23 Weissman, B., Bromberg, P. A., and Gutman, A. B., *J. Biol. Chem.*, 1957, **224**, 423.

Paper 2/02529I
Received May 15, 1992
Accepted June 9, 1992

Kinetic–Potentiometric Determination of Iodide With an Antimony(v) Coated-wire Ion-selective Electrode

Concepción Sánchez-Pedreño, Joaquín A. Ortuño and Ana L. Ros
Department of Analytical Chemistry, Faculty of Sciences, University of Murcia, 30071-Murcia, Spain

A coated-wire Sb^{V} ion-selective electrode has been used to study the iodide-catalysed reaction between hexachloroantimonate(v) and hydroxylamine, and a kinetic method for the determination of iodide is proposed. Under the selected experimental conditions of 1×10^{-6} mol dm^{-3} $SbCl_6^-$, 8×10^{-2} mol dm^{-3} NH_2OH, 1×10^{-1} mol dm^{-3} HCl and 25 ± 0.1 °C, iodide can be determined in the range 0.01–0.40 μg cm^{-3} with good selectivity. The method is simple and inexpensive and has been applied satisfactorily to the determination of iodide in common iodinated salts.

Keywords: *Kinetic determination; iodide; potentiometry; antimony(v) ion-selective electrode; coated-wire electrode*

Selective electrodes are of special use in potentiometric techniques applied to kinetic analysis as they are sufficiently sensitive to changes in concentration and convenient for the study of the reaction mechanism.[1,2] Glass electrodes have been used in kinetic investigations.[3,4] The iodide-selective electrode has been one of the most frequently used in the kinetic determination of metal ions based on their catalytic effect on the oxidation of iodide by different oxidants.[5–7] Other ion-selective electrodes used in kinetic analysis are the perchlorate,[8] periodate,[9] chloramine-T[10] and thallium(I)[11] electrodes. In enzymic kinetic analysis, glass (pH) and ammonia electrodes have been widely used.[12] Potentiometric enzyme electrodes have been principally used in the determination of amino acids, urea, glucose and penicillin.[12]

Coated-wire ion-selective electrodes (CWEs) consist of a film of suitable polymeric matrix, containing a dissolved electroactive species, coated on a conducting substrate. Electrodes of this type are simple, inexpensive, durable and capable of giving a reliable response.[13] A CWE for the determination of antimony(v) that responds to hexachloroantimonate(v) has recently been developed.[14] In this paper, this electrode has been applied to the kinetic–potentiometric determination of iodide based on its catalytic effect on the reaction between hexachloroantimonate(v) and hydroxylamine. No mention of a CWE or an antimony(v) ion-selective electrode in kinetic analysis has been found in the literature.

In trace amounts, iodide is important to human life. The use of iodinated salt in the diet is the most frequent way of obtaining an additional supply of iodide. Neutron activation analysis and catalytic methods are well suited for the determination of iodide in common salts at the low levels encountered.[15] The simple and inexpensive method proposed in this paper is very sensitive and selective and has been applied satisfactorily to the determination of iodide in common iodinated salts.

Experimental

Apparatus

Potentials were measured with an Orion EA940 expandable IonAnalyzer (Cambridge, MA, USA). The recorder output of the IonAnalyzer was connected to a personal computer *via* a DGH 1121 analogue-to-digital converter module. An Orion 90-02 double-junction Ag–AgCl reference electrode, containing 0.1 mol dm^{-3} KCl in the outer compartment, was used.

The construction and the characteristics of the coated-wire antimony(v) ion-selective electrode were described previously.[14] The ion exchanger of this electrode consists of the ion pair between hexachloroantimonate(v) and the 1,2,4,6-tetraphenylpyridinium cation, in a poly(vinyl chloride) matrix. The ion-selective electrode was stored dry and conditioned before being used as described.

All measurements were carried out in a cell thermostated at 25 ± 0.1 °C with continuous magnetic stirring.

Reagents

All solutions were prepared with doubly distilled water from analytical-reagent grade materials.

Standard iodide solution, 1 g dm^{-3}. Prepared by dissolving 0.1308 g of potassium iodide (Merck, Darmstadt, Germany) (dried at 105 °C for 2 h) in water and diluting to 100 cm^3 in a calibrated flask. Working solutions were prepared daily by suitable dilution with water.

Hexachloroantimonate(v) solution, 0.25 mol dm^{-3}. Prepared by dissolving antimony(v) chloride (Merck) in concentrated hydrochloric acid. Working solutions were prepared by dilution with concentrated hydrochloric acid. These solutions were stored in a refrigerator.

Hydroxylamine solution, 5 mol dm^{-3}. Prepared by dissolving hydroxylamine hydrochloride (Aldrich, Milwaukee, WI, USA) in water.

Calibration Procedure

Transfer 25.00 cm^3 of 0.1 mol dm^{-3} hydrochloric acid into the reaction cell, insert the electrodes and start the data acquisition system. Inject 400 mm^3 of 5 mol dm^{-3} hydroxylamine solution and wait until the potential has stabilized. Inject 10 mm^3 of 2.5×10^{-3} mol dm^{-3} hexachloroantimonate(v) solution and wait until the potential has stabilized again, then inject small volumes of standard solutions of iodide by micropipette to obtain final concentrations in the range 0.01–0.40 μg cm^{-3}. Calculate the slope of the potential *versus* time graph obtained and plot the slope *versus* iodide concentration.

After each experiment, introduce the electrodes into 25 cm^3 of 0.1 mol dm^{-3} hydrochloric acid and inject 10 mm^3 of 0.25 mol dm^{-3} hexachloroantimonate(v) solution and wait 5 min. This treatment leaves the electrode ready for a new measurement.

Procedure for the Determination of Iodide in Common Iodinated Salts

Weigh accurately 1 g of iodinated salt, dissolve in water and dilute to volume in a 100 cm^3 calibrated flask. Transfer an aliquot, containing up to 10 μg of iodide, into the reaction cell. Add 5 cm^3 of 0.5 mol dm^{-3} HCl, 400 mm^3 of 5 mol dm^{-3}

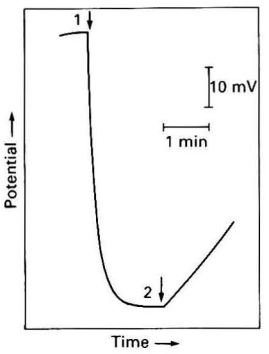

Fig. 1 Potential *versus* time graph. Conditions: $SbCl_6^-$, 1×10^{-6} mol dm^{-3}; NH_2OH, 8×10^{-2} mol dm^{-3}; HCl, 1×10^{-1} mol dm^{-3}; temperature, 25 ± 0.1 °C; and iodide concentration, 0.24 μg cm^{-3}

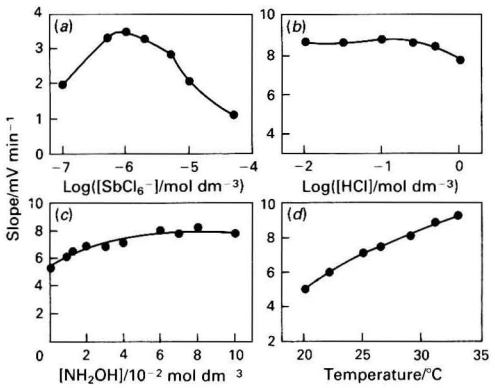

Fig. 2 Influence of reaction variables on the catalytic effect of iodide. (*a*) $SbCl_6^-$; (*b*) HCl concentration; (*c*) NH_2OH; and (*d*) temperature

hydroxylamine solution and dilute to 25 cm^3 with water. Insert the electrodes and start the data-acquisition system, then inject 10 mm^3 of 2.5×10^{-3} mol dm^{-3} hexachloroantimonate(v) solution and wait until the potential *versus* time graph becomes a straight line with a positive slope. Compare this with a calibration graph prepared for iodide in the presence of the same amount of chloride as in the sample. The chloride was added in the form of sodium chloride, prepared by the reaction of iodide-free hydrochloric acid and sodium hydroxide.[15] A similar procedure was also followed for the comparative Ce^{IV}–As^{III} method.

Results and Discussion

A typical plot of the iodide-catalysed reaction between hexachloroantimonate(v) and hydroxylamine, obtained as described under Calibration Procedure, is shown in Fig. 1. Arrow 1 corresponds to the injection of the $SbCl_6^-$ solution. A sudden decrease in potential, resulting from the response of the electrode to this anion, is observed. The potential then stabilizes, showing that the rate of the uncatalysed reaction is negligible. Arrow 2 corresponds to the injection of iodide solution, the potential showing a steady increase as a result of the iodide-catalysed reaction. The slope of the straight line obtained increases with iodide concentration. In the absence of hydroxylamine, a curved line is obtained after the injection of the iodide solution. A possible explanation for this phenomenon is discussed under Mechanism of the Catalysed Reaction.

The effect of the reaction variables was studied by altering each variable in turn while keeping the others constant. The reaction conditions chosen were those that produced the maximum slope of the straight line described above.

Effect of the Hexachloroantimonate(v) Concentration

The effect of the $SbCl_6^-$ concentration was studied by using fixed concentrations of HCl (0.1 mol dm^{-3}), hydroxylamine (0.08 mol dm^{-3}) and iodide (0.06 μg cm^{-3}) at 25 °C and by varying the hexachloroantimonate(v) concentration between 1×10^{-7} and 5×10^{-5} mol dm^{-3}. The results are shown in Fig. 2(*a*) and show a smooth maximum at about 1×10^{-6} mol dm^{-3}; hence, this concentration was selected. The blanks are negligible over the whole $SbCl_6^-$ concentration range.

Effect of Hydrochloric Acid Concentration

This was studied by fixing the concentrations of $SbCl_6^-$ (1×10^{-6} mol dm^{-3}), hydroxylamine (0.08 mol dm^{-3}) and iodide (0.17 μg cm^{-3}) and by varying the HCl concentration between 0.01 and 1 mol dm^{-3}. The temperature was kept constant at 25 °C. The results, shown in Fig. 2(*b*), show that the slope is at a maximum and constant in the range 0.01–0.5 mol dm^{-3}. A hydrochloric acid concentration of 0.1 mol dm^{-3} was selected.

Effect of Hydroxylamine Concentration

The effect of hydroxylamine concentration was studied under the following conditions: $SbCl_6^-$ (1×10^{-6} mol dm^{-3}), HCl (0.1 mol dm^{-3}) and iodide (0.15 μg cm^{-3}) at 25 °C. Fig. 2(*c*) shows the results obtained. The slope is at a maximum between 0.04 and 0.10 mol dm^{-3}. As stated above, a curved line is obtained when no hydroxylamine is added. In this instance the initial slope has been represented. A hydroxylamine concentration of 0.08 mol dm^{-3} was selected.

Effect of Temperature

The effect of temperature was studied under the conditions selected above, with 0.14 μg cm^{-3} of iodide. The increase of the slope with temperature is shown in Fig. 2(*d*). A temperature of 25 ± 0.1 °C was selected. As in all the variables studied earlier, the blanks were negligible.

Effect of Iodide Concentration

Under the selected conditions (1×10^{-6} mol dm^{-3} $SbCl_6^-$; 0.1 mol dm^{-3} HCl; 0.08 mol dm^{-3} NH_2OH; 25 °C), the slope of the straight line *E versus t* was proportional to the iodide concentration over the range 0.01–0.40 μg cm^{-3} iodide. The slope of the calibration graph was 52 mV min^{-1} μg^{-1} cm^3, with a correlation coefficient of 0.999. The relative standard deviations for 0.02 and 0.25 μg cm^{-3} (ten determinations) of iodide were 3.8 and 2.1%, respectively.

Mechanism of the Catalysed Reaction

The proposed mechanism for the catalysed reaction is:

$$2I^- + SbCl_6^- \xrightarrow{slow} I_2 + Sb^{III}\ \text{product}$$

$$I_2 + NH_2OH \xrightarrow{fast} 2I^- + \text{hydroxylamine oxidation product}$$

To derive this mechanism the following points have been taken into account.

(1) The rate of the uncatalysed reduction of $SbCl_6^-$ by NH_2OH is negligible, as shown in Fig. 1, before adding the iodide.

(2) The reported reduction of Sb^V by I^- in acidic medium;[16] this reaction only goes to completion in concentrated acid solution.

Table 1 Interferences in the determination of 0.25 μg cm^{-3} of iodide

Species tested	Limiting molar ratio, [species] : [I$^-$]
NO_3^-, SO_4^{2-}, HPO_4^{2-}, F^-, Br^-, ClO_4^-, Zn^{II}, Pb^{II}, Co^{II}, Ni^{II}, Mn^{II}, Cd^{II}, Al^{III}, Cr^{III}, Fe^{III}, As^V	1000*
(−) Pd^{II},† (−) Bi^{III}†	1
(−) Ag^I,† (+) Cu^{II}†	0.1
(+) IO_3^-,† (−) Hg^{II},† (−) Au^{III}†	0.01

* Maximum ratio tested.
† The signs before the species indicate the type of interference.

Table 2 Determination of iodide in iodinated salt

	Iodide/μg g^{-1}			
Sample*	Proposed method	Mean (± standard deviation)	Ce^{IV}–As^{III} method	Mean (± standard deviation)
1	5.79	5.60 ± 0.15	5.86	5.71 ± 0.29
	5.42		5.72	
	5.61		5.57	
	5.50		5.31	
	5.68		6.09	
2	18.59	18.01 ± 0.44	18.15	17.51 ± 0.51
	17.45		16.84	
	18.23		17.79	
	17.76		17.22	
	18.01		17.53	
3	190.0	192.7 ± 1.9	202.7	197.6 ± 4.5
	192.9		191.2	
	194.9		195.3	
	191.8		200.8	
	193.7		198.1	

* Samples from Murcia (1 and 2) and Alicante (3).

(3) The visual observation of the reduction of iodine by hydroxylamine when higher concentrations of these compounds are used.

(4) The partial reaction orders obtained under our experimental conditions; to obtain the partial order with respect to $SbCl_6^-$, the logarithmic dependence between the signal measured (potential) and the concentration of this anion must be considered.

If n represents the partial reaction order:

$$-d[SbCl_6^-]/dt = k\,[SbCl_6^-]^n \quad (1)$$

dividing by $[SbCl_6^-]$:

$$[SbCl_6^-]^{-1}\,d[SbCl_6^-]/dt = -k\,[SbCl_6^-]^{n-1} \quad (2)$$

The response of the electrode follows the Nernst equation:

$$E = E^\circ - 0.059 \log [SbCl_6^-] \quad (3)$$

$$dE/dt = -0.059 \times 0.4343\,[SbCl_6^-]^{-1}\,d[SbCl_6^-]/dt \quad (4)$$

By substituting eqn. (2) into eqn. (4):

$$dE/dt = 0.059 \times 0.4343\,k\,[SbCl_6^-]^{n-1}$$

If the reaction is first partial order with respect to $SbCl_6^-$ (n = 1):

$$dE/dt = 0.059 \times 0.4343\,k = \text{constant}$$

If this condition is fulfilled, the graph of potential *versus* time must yield a straight line. Fig. 1 shows this experimental finding. In addition, the influence of the concentration of $SbCl_6^-$ on the rate of reaction must yield a plateau in the $SbCl_6^-$ concentration range in which the first partial order is maintained. This is also obtained, as shown in Fig. 2(*a*), in the vicinity of the selected $SbCl_6^-$ concentration (1×10^{-6} mol dm^{-3}). Finally, under the selected conditions, the reaction is pseudo-zero-order with respect to hydroxylamine and H^+, as shown in Fig. 2(*b*) and (*c*), and pseudo-first-order with respect to iodide, according to the calibration graph.

Effect of Other Ions

The selectivity of the method was established by adding different amounts of potentially interfering species to samples containing 0.25 μg cm^{-3} of iodide. The limiting value of the concentration of foreign ion was taken as that value which caused an error of not more than ±5% in the determination of iodide. The results are summarized in Table 1. For foreign ions the sign of their interference is given in parentheses. It can be seen that no other anion affords the same reaction, except for iodate, because of its final reduction to iodide. Only those metal ions that form complexes with, or precipitate, iodide interfere. The interference from copper(II) occurs as a result of its catalytic effect on the indicator reaction, as we have observed.

Applications

The proposed method was applied satisfactorily to the determination of iodide in common iodinated salts. No sample pre-treatment was required. The results shown in Table 2 are compared with those of the Ce^{IV}–As^{III} method.[17] No significant difference (for a significance level of $\alpha = 0.05$) was found between the two methods by applying a two-way analysis of variance with replicates ($F_{exp} = 4.22 < F_{tab} = 4.26$).

References

1 Pérez-Bendito, D., and Silva, M., in *Kinetic Methods in Analytical Chemistry*, eds. Chalmers, R. A., and Masson, M., *Ellis Horwood Series in Analytical Chemistry*, Ellis Horwood, Chichester, 1988, pp. 229–233.
2 Mottola, H. A., in *Kinetic Aspects of Analytical Chemistry*, eds. Winefordner, J. D., and Kolthoff, I. M., *Chemical Analysis (Series)*, Wiley, New York, 1988, vol. 96, pp. 194–197.
3 Sirs, J. A., *Trans. Faraday Soc.*, 1958, **54**, 207.
4 Rechnitz, G. A., and Zui Feng, L., *Anal. Chem.*, 1967, **39**, 1406.
5 Lazarou, L. A., and Hadjiioannou, T. P., *Anal. Chem.*, 1979, **51**, 790.
6 Kataoka, M., Nishimura, K., and Kambara, T., *Talanta*, 1983, **30**, 941.
7 Kataoka, M., Yoshizawa, Y., and Kambara, T., *Bunseki Kagaku*, 1982, **31**, 171.
8 Efstathiou, C. H., and Hadjiioannou, T. P., *Anal. Chem.*, 1975, **47**, 864.
9 Hartofilax, V. H., Efstathiou, C. E., and Hadjiioannou, T. P., *Microchem. J.*, 1986, **33**, 18.
10 Koupparis, M. A., and Hadjiioannou, T. P., *Mikrochim. Acta*, 1978, **II** (3–4), 267.
11 Yang, S., and Tong, H., *Huaxue Xuebao*, 1987, **45**, 711.
12 Guilbault, G. G., in *Analytical Uses of Immobilized Enzymes*, ed. Guilbault, G. G., *Modern Monographs in Analytical Chemistry/2*, Marcel Dekker, New York, 1984, ch. 3, pp. 112–244.
13 Cunningham, L., and Freiser, H., *Anal. Chim. Acta*, 1986, **180**, 271.
14 Sánchez-Pedreño, C., Ortuño, J. A., and Alvarez, J., *Anal. Chem.*, 1991, **63**, 764.
15 Malvano, R., Buzzigoli, G., Scarlattini, M., Cenderelli, G., Gandolfi, C., and Grosso, P., *Anal. Chim. Acta*, 1972, **61**, 201.
16 Kolthoff, I. M., Belcher, R., Stenger, V. A., and Matsuyama, G., *Volumetric Analysis III*, Interscience, New York, 1957, p. 319.
17 Sandell, E. B., and Kolthoff, I. M., *Mikrochim. Acta*, 1937, 9.

Paper 1/05869J
Received November 19, 1991
Accepted February 5, 1992

Simultaneous Determination of Palladium and Nickel in Electroplating Solutions by Differential-pulse Polarography

Bharathibai J. Basu and S. R. Rajagopalan
Materials Science Division, National Aeronautical Laboratory, Bangalore-560 017, India

Differential-pulse polarography can be successfully employed for the simultaneous determination of palladium and nickel in electroplating baths. Both palladium and nickel give peaks in ammoniacal ammonium chloride and ammoniacal ammonium tartrate media that are separated by about 250 mV. When the nickel-to-palladium ratio exceeds 100, ethylenediaminetetraacetic acid (EDTA) may be added to complex nickel and thus remove the interference due to an excess of nickel. In the presence of large amounts of palladium, dimethylglyoxime is used to enhance the peak current of nickel. The palladium peak in ammoniacal ammonium chloride buffer at pH 9.0 is not affected by the presence of either EDTA or dimethylglyoxime. Hence it is possible to determine palladium and nickel simultaneously and in the presence of an excess of each other.

Keywords: *Palladium determination; nickel determination; differential-pulse polarography; dimethylglyoxime; electroplating solution*

Electroplating baths containing various amounts of palladium and nickel are used for the deposition of certain alloy compositions. Recently, palladium–nickel alloy coatings have gained acceptance as an undercoat to reduce the thickness of gold plating in the electronics and watch industries. These alloys are used as a substitute for gold as a contact material for electronics applications. There are economical and technological advantages for substituting palladium or palladium alloys for gold.[1] Economically, substantial cost reductions can be achieved owing to the lower price of palladium coupled with its lower density. Technologically, material properties of palladium such as hardness, ductility and thermal stability are superior to those of hard gold. The use of palladium–nickel alloy plating is increasing and hence it is necessary to determine the palladium and nickel contents in plating solutions, wash solutions and effluents.

Both palladium and nickel form coloured complexes with dimethylglyoxime (DMG) and this has been employed for the separation of palladium from other elements,[2] but as the sensitivity of the palladium–DMG complex is low, it is rarely used for its determination.[3] We have found that by using differential-pulse polarography (DPP), it is possible to determine palladium and nickel simultaneously and the method does not involve any tedious and time-consuming separation steps.

Wild[4] used a supporting electrolyte (SE) of 1 mol dm^{-3} pyridine and 1 mol dm^{-3} potassium chloride for the determination of Pd^{II} in nickel and palladium plating solutions. Other supporting electrolytes used are cyanide,[5] ethanolamine,[6] glycine[7] and caprolactam,[8] but it was not reported whether these media could be used for the simultaneous determination of nickel and palladium. Flora and Nieboer[9] investigated the highly sensitive peak obtained for Ni^{II} in the presence of DMG and applied this method to the determination of Ni^{II} in lake water by DPP. Later, Torrance[10] used this method for the determination of Ni^{II} and Co^{II}. This paper describes polarographic methods for the simultaneous determination of nickel and palladium in electroplating baths, effluents and wash solutions.

Experimental

Apparatus

Polarograms were recorded with a Model CL-90 pulse polarograph [Elico(p), Hyderabad, India] in conjunction with a Metrohm polarographic cell; with a dropping mercury electrode (DME) as working electrode and a mercury pool as counter electrode. A saturated calomel electrode (SCE) was used as the reference electrode and was connected to the polarographic cell *via* a potassium chloride–agar bridge. A Sargeant capillary with a natural drop time of 3 s was employed as the DME. The drop time was mechanically controlled. For DPP measurements, the pulse duration was 40 ms and the pulse amplitude was 50 mV. Purified nitrogen was used for de-aeration of the solution.

Reagents

All reagents were of analytical-reagent grade. A standard solution of palladium (1 mg cm^{-3}) was prepared by dissolving pure $Pd(NH_3)_2Cl_2$ in a sufficient volume of ammonia solution (1 + 1) and diluting to volume. A standard solution of nickel (1 mg cm^{-3}) was prepared by dissolving high-purity nickel powder in dilute nitric acid. A 1% solution of DMG in ethanol was used. Ammonium tartrate–ammonia and ammonium chloride–ammonia buffers (pH 9.0) were prepared.

Recommended Procedure for the Simultaneous Determination of Palladium(II) and Nickel(II)

Transfer a suitable aliquot of the sample solution into the polarographic cell and add 10 cm^3 of 0.2 mol dm^{-3} ammoniacal ammonium chloride buffer (pH 9.0). Pipette 0.2 cm^3 of DMG solution and dilute to 20 cm^3. De-aerate the solution and record the polarogram from −0.50 to −1.20 V *versus* SCE. Calculate the Pd^{II} and Ni^{II} concentrations in the sample by the standard additions methods.

Results and Discussion

Choice of Supporting Electrolyte

Table 1 gives the sensitivity values for Pd^{II} and Ni^{II} in the various SEs employed. The DPP conditions used were drop time = 0.5 s and pulse amplitude = 50 mV. Buffers containing 0.1 mol dm^{-3} ammonium chloride or 0.1 mol dm^{-3} ammonium tartrate at pH 9.0 ± 0.1 were used. It was found that either ammoniacal ammonium chloride or ammoniacal ammonium tartrate could be employed for the simultaneous determination of Pd^{II} and Ni^{II} as their peaks are well separated in both media. The sensitivity of Pd^{II} was almost the same in both supporting electrolytes whereas the sensitivity of Ni^{II} was higher in 0.1 mol dm^{-3} ammoniacal ammonium chloride

Table 1 Sensitivities for Pd^{II} and Ni^{II} in different SEs. DPP conditions: drop time = 0.5 s; ΔE = 50 mV; m = 1.84 mg s^{-1}

Supporting electrolyte	Sensitivity/nA (ppm)$^{-1}$ Pd^{II}	Ni^{II}
0.1 mol dm^{-3} NH_4Cl (ammoniacal) (pH 9.0)	40	110
0.1 mol dm^{-3} ammoniacal ammonium tartrate (pH 9.0)	39.2	85
0.1 mol dm^{-3} NH_4Cl (ammoniacal) (pH 9.0) + 0.01 mol dm^{-3} EDTA	42	0
0.1 mol dm^{-3} NH_4Cl (ammoniacal) (pH 9.0) + 0.01% DMG	38	1200
0.1 mol dm^{-3} ammoniacal ammonium tartrate (pH 9.0) + 0.01% DMG	36.8	1150

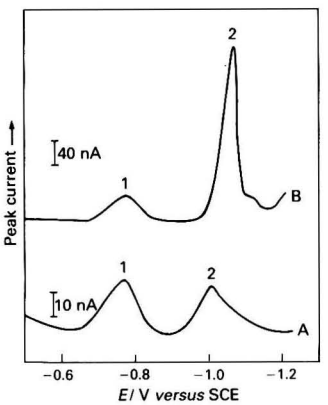

Fig. 1 Differential-pulse polarograms of Pd^{II} and Ni^{II} in ammoniacal ammonium chloride buffer with and without DMG. t = 0.5 s; ΔE = 50 mV. A, $[Ni^{II}]$ = 0.20 ppm and $[Pd^{II}]$ = 0.50 ppm. B, $[Ni^{II}]$ = 0.20 ppm, $[Pd^{II}]$ = 1.0 ppm and [DMG] = 0.01%

buffer. When the nickel concentration is very low, addition of DMG enhances the peak height of nickel. The sensitivity of Ni^{II} in the presence of DMG was comparable in both ammoniacal ammonium chloride and ammoniacal ammonium tartrate media. Addition of a small volume of 0.1 mol dm^{-3} ethylenediaminetetraacetic acid (EDTA) results in the complete removal of the nickel peak owing to complexation. The sensitivity of Pd^{II} was not affected by the presence of EDTA. Typical polarograms of Pd^{II} and Ni^{II} in 0.1 mol dm^{-3} ammonium chloride buffer (pH 9.0 ± 0.1) with and without DMG are given in Fig. 1.

The blank value for Ni^{II} in the presence of DMG in ammoniacal ammonium chloride buffer was lower than that in ammoniacal ammonium tartrate buffer. Therefore, it was preferable to use 0.1 mol dm^{-3} ammoniacal ammonium chloride buffer with DMG.

Hence it can be seen that although Pd^{II} also forms a complex with DMG, it does not interfere in the determination of Ni^{II}. Unlike nickel, there was no enhancement of the peak current for Pd^{II} in the presence of DMG. This allowed the determination of trace amounts of nickel in the presence of a large excess of palladium. Palladium(II) gave well-developed peaks in both ammoniacal ammonium chloride and ammoniacal ammonium tartrate media and these peaks were separated from the nickel peaks by about 250 mV.

Effect of Variation of DMG on the Peak Current of Nickel(II)

Fig. 2 shows the effect of varying the DMG concentration on the peak current of Ni^{II} in 0.1 mol dm^{-3} ammoniacal ammonium chloride buffer (pH 9.0 ± 0.1). A 15-fold molar

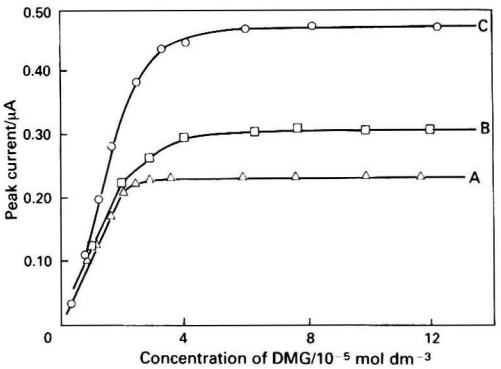

Fig. 2 Dependence of peak current on the concentration of DMG. Experimental conditions: SE = 0.1 mol dm^{-3} ammoniacal ammonium chloride buffer (pH 9.0); t = 0.5 s; and ΔE = 50 mV. Ni^{II} concentration: A, 0.16; B, 0.23; and C, 0.40 ppm

excess of DMG was sufficient to bring about the maximum peak current. This was found to be true at three different concentrations of Ni^{II}, as shown in Fig. 2. The nickel concentrations employed for this study were 0.16, 0.233 and 0.40 ppm. Flora and Nieboer[9] used a 1520-fold excess of DMG in ammoniacal citrate buffer (at a nickel level of 50 ppb) to achieve the maximum peak current. Torrance[10] also reported a 250–500-fold molar excess of DMG for the determination of 10 ppb each of Ni^{II} and Co^{II} in ammoniacal ammonium tartrate buffer (pH 8.7). We found that the amount of DMG required to give the maximum peak current for Ni^{II} was much lower in ammoniacal ammonium chloride buffer. The slightly higher DMG concentration in citrate and tartrate media must be due to the competition between the buffer components and DMG for nickel ions, as Ni^{II} forms fairly strong complexes with citrate and tartrate. As the formation constant of the $Ni(DMG)_2$ complex was high (log β = 17.24), complete complex formation could be expected to occur at a relatively low ligand-to-metal ion ratio in the absence of other complexing agents. A large excess of reagent was not favoured from a solubility point of view as the nickel–DMG complex was sparingly soluble and the solubility decreases in the presence of an excess of DMG. Hence it was possible to obtain the maximum peak current at a much lower ligand-to-metal ratio when ammoniacal ammonium chloride buffer (pH 9.0) was used.

Effect of Nickel(II) Concentration on Peak Current

In an SE of 0.1 mol dm^{-3} ammoniacal ammonium chloride at pH 9.0 and a DMG concentration of 9.38×10^{-4} mol dm^{-3}, the nickel concentration was varied and the peak currents were measured. The results are shown in Fig. 3. The peak current was found to be a linear function of nickel concentration only up to 0.5 ppm. A least-squares fit of the data was carried out by y-residual minimization and it was found that there is good linearity up to 0.50 ppm (as indicated by a correlation coefficient of 0.9995) with a slope of 1118.4 nA (ppm)$^{-1}$ and an intercept of 45.54 nA. The y-intercept corresponds to about 0.04 ppm of nickel, which results from nickel impurity in the supporting electrolyte. When the nickel concentration was increased above 0.50 ppm, the deviations from linearity became significant and at concentrations above 1 ppm the peak current decreased, as shown in Fig. 3. This could be due to precipitation of the nickel–DMG complex. The log K_s value for the equilibrium $Ni(DMG)_2(aq) \rightleftharpoons Ni(DMG)_2(s)$ was 5.68.[11] Therefore, the solubility of the complex under equilibrium conditions was $10^{-5.68}$. When the nickel concentration was increased above 1 ppm, precipitation of $Ni(DMG)_2$ began, resulting in a decrease in peak current.

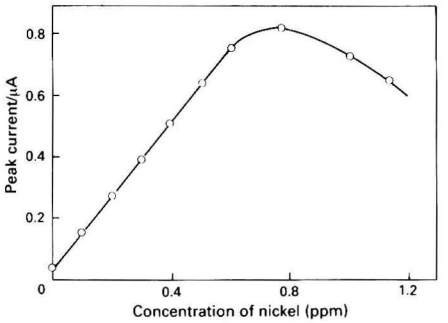

Fig. 3 Dependence of peak current on Ni^{II} concentration at a constant excess of DMG. SE and DPP conditions as in Fig. 2; [DMG] = 0.01%

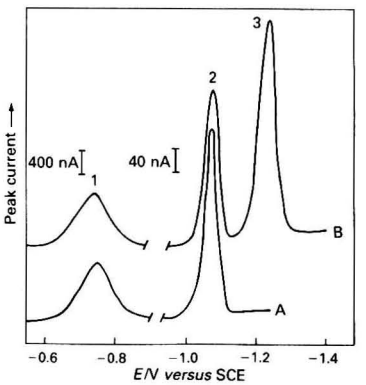

Fig. 4 Effect of Co^{II} on the adsorption peak current of Ni^{II} in the presence of DMG. A, $[Pd^{II}]$ = 25.0 ppm; $[Ni^{II}]$ = 0.25 ppm; [DMG] = 0.01% and B, $[Co^{II}]$ = 0.45 ppm; $[Pd^{II}]$, $[Ni^{II}]$ and [DMG] as in A

It was reported earlier by Flora and Nieboer[9] that the analytical application of the DMG-sensitized reaction was limited to very low nickel concentrations, as the calibration graph was linear only at Ni^{II} concentrations <100 ppb. This was true for tartrate and citrate media. However, the calibration graph was linear up to 500 ppb in ammoniacal ammonium chloride buffer (pH 9.0).

Effect of Foreign Ions

The effect of other metal ions expected to be present in electroplating baths on the simultaneous polarographic determination of Pd^{II} and Ni^{II} was investigated. It was found that comparable amounts of copper(II), iron(III), lead(II) and zinc(II) did not interfere with the simultaneous determination of Pd^{II} and Ni^{II} in an SE containing 0.1 mol dm^{-3} ammoniacal ammonium chloride buffer and 0.01% DMG. The peak current of the nickel–DMG complex was decreased by about 20% in the presence of almost double the amount of cobalt (Fig. 4).

Sensitivity and Detection Limit for Palladium(II) and Nickel(II) by DPP

It was found that the DMG enhancement factor for Ni^{II} increased as the drop time increased. Therefore, a drop time of 2 s was employed in order to obtain a higher sensitivity. The slopes of the calibration graph at a drop time of 2 s were 5350 and 80 nA μg^{-1} cm^3 for Ni^{II} and Pd^{II}, respectively.

Table 2 Determination of palladium and nickel in synthetic sample solutions

Sample no.	Amount added/μg		Amount found/μg		Error (%)	
	Pd^{II}	Ni^{II}	Pd^{II}	Ni^{II}	Pd^{II}	Ni^{II}
1	10.0	10.0	9.86	9.82	−1.4	−1.8
2	10.0	100.0	9.90	98.8	−1.0	−1.2
3	10.0	1000.0	9.85	985.0	−1.5	−1.5
4	100.0	10.0	99.5	9.85	−0.5	−1.5
5	200.0	5.0	198.5	4.95	−0.75	−1.0
6	200.0	2.0	198.5	1.98	−0.75	−1.0

The detection limit is defined as the concentration of the analyte resulting in a signal three times the standard deviation of the blank, as recommended by IUPAC.[12] The detection limits were about 10 ng cm^{-3} for Ni^{II} and 0.10 μg cm^{-3} for Pd^{II}. An even lower detection limit could be achieved for Ni^{II} provided that there was no contamination. However, often there was a blank due to the nickel impurity present in the SEs even when highly pure reagents were used. We found that the blank value for ammoniacal ammonium chloride buffer was less than that for ammoniacal ammonium tartrate buffer. The other advantages of ammoniacal ammonium chloride buffer were the relatively low DMG concentration required for maximum peak current and the wider linear calibration range for Ni^{II}.

Determination of Palladium(II) and Nickel(II) in Samples

Samples of electroplating solutions containing 10.8 g dm^{-3} of Pd^{II} and 5.0 g dm^{-3} of Ni^{II} were analysed using these DPP procedures. The DPP measurements were made in the absence of DMG as the concentrations of Pd^{II} and Ni^{II} were high in this sample. The standard deviations for six replicate measurements were found to be 0.13 for 10.77 g dm^{-3} palladium and 0.07 for 4.98 g dm^{-3} nickel.

Synthetic solutions containing ppm levels of Pd^{II} and Ni^{II} in different ratios were analysed. The DMG-sensitized procedure was used at low concentrations of nickel. The results are summarized in Table 2. It was found that this procedure permits the simultaneous determination of palladium and nickel in the presence of a 100-fold excess of the other.

References

1 Abys, J. A., Straschal, H. C., Kadija, I., Kudrak, E. J., and Blee, J., *Met. Finish.*, 1991, **89**, 43.
2 Young, R. S., *Analyst*, 1951, **76**, 49.
3 Sandell, E. B., *Colorimetric Determination of Traces of Metals*, Interscience, New York, 1965, pp. 665 and 711.
4 Wild, P. W., *Galvanotechnik*, 1970, **61**, 811.
5 Kolthoff, I. M., and Linganc, J., *Polarography*, Interscience, New York, 1965, p. 491.
6 Rao, A. L. J., and Puri, B. K., *Analyst*, 1971, **96**, 364.
7 Kopa, M., and Palogal, J., *Collect. Czech. Chem. Commun.*, 1958, **23**, 50.
8 Puri, B. K., and Kumar, A., *Analyst*, 1983, **108**, 1345.
9 Flora, C. J., and Nieboer, E., *Anal. Chem.*, 1980, **52**, 1013.
10 Torrance, K., *Analyst*, 1984, **109**, 1035.
11 Inczedy, J., *Analytical Applications of Complex Equilibria*, Ellis Horwood, Chichester, 1976.
12 Miller, J. N., *Analyst*, 1991, **116**, 3.

Paper 2/01286C
Received March 10, 1992
Accepted May 27, 1992

Determination of Chlorine, Bromine and Sodium in Fluid Inclusions by Neutron Activation Analysis

Brian A. Bennett and Susan J. Parry*
Centre for Analytical Research in the Environment, Imperial College of Science, Technology and Medicine, Silwood Park, Ascot, Berkshire, UK SL5 7TE
Maria Christoula
Department of Geology, Imperial College of Science, Technology and Medicine, London, UK SW7 2BP

A simple radiochemical procedure has been implemented for neutron activation analysis of fluid inclusions in fluorite. Samples of 100 mg or less are irradiated in a thermal neutron flux of 1×10^{16} n m^{-2} s^{-1} before crushing and leaching with NaCl carrier solution. The solution is transferred with a filtered syringe and counted immediately for Na and Cl, and after at least 5 h for Br. The recovery of the carrier is measured by re-irradiation of the sample. The detection limits are <1 μg for Cl and Na, and <10 ng for Br.

Keywords: *Fluid inclusion; neutron activation analysis; fluorite; chlorine, bromine and sodium*

The information obtained from fluid inclusions provides the main source of evidence on the chemistry of ancient fluids involved in ore genesis. The different analytical methods applied to the measurement of trace elements in fluid inclusions have been reviewed recently by Roedder.[1] Techniques include atomic absorption spectrometry, flame atomic emission spectrometry, ion chromatography, inductively coupled plasma mass spectrometry and neutron activation analysis (NAA). Neutron activation analysis was first applied in 1963 to the determination of Cu, Mn and Zn in fluid inclusions in fluorite and quartz;[2] the fluid was extracted prior to analysis. Later the benefit of radiochemical neutron activation analysis (RNAA) was applied to the determination of Na, Mn, Co, Cu and Zn.[3] This time quartz was irradiated prior to extraction of the fluid, avoiding any problems of contamination during the leaching stage. Sabouraud-Rosset[4] demonstrated the benefits of using a carrier in the analysis of gypsum to determine Cl:Br ratios in fluid inclusions. The same method was applied to quartz for Cl:Br:Na:K ratios[5] although the clean matrix of quartz provided the opportunity for Lucksheiter and Parekh[6] to determine the same ratios using instrumental NAA (INAA) with 1–2 g cylinders of quartz. Perhaps more surprisingly, INAA has also been used to measure Na, K, Cl and Br in fluorite.[7] The main interferences are from Ca when measuring Cl and Na, and from the lanthanides for the determination of Br. It was suggested that Na, K, Cl and Br were all present only in the inclusions and concluded that even iodine could be determined under favourable circumstances.

The present work aimed to measure Na:Cl:Br ratios in fluorite samples from deposits in lead, zinc and fluorite ores from the Pennines of central England and also attempted to implement INAA. However, it was not possible to obtain good data using this method because of the poor detection limits obtained. This paper describes a simple RNAA procedure adopted to provide useful Cl:Br and Cl:Na ratios.

Experimental

Materials

The mineral samples, weighing 100 mg or less, were prepared as doubly polished wafers or chips. They were weighed into polyethylene capsules (6 × 15 mm diameter) ready for irradiation. Multi-element chemical standards were prepared from stock solutions of NaCl and NaBr containing 1 mg cm^{-3}. The solutions were combined and diluted to give a standard solution containing 12.96 μg cm^{-3} of Na, 20 μg cm^{-3} of Cl and 1.00 μg cm^{-3} of Br. A single chlorine standard was prepared with 100 μg of NaCl solution dried on filter-paper in a capsule (6 × 15 mm diameter). The mixed standard was prepared as a 1 cm^3 liquid sample sealed in a polyethylene capsule (30 × 15 mm diameter). The carrier was sodium chloride solution containing Cl at 100 mg cm^{-3}.

Methods

All of the irradiations were carried out in the Consort Mark II thermal nuclear reactor at the Imperial College Reactor Centre. The reactor operates at 100 kW and has irradiation sites for long or short irradiations with thermal neutron fluxes up to 2.4×10^{16} n m^{-2} s^{-1}. The irradiations in this work were carried out either in ICIS (in core irradiation system), a pneumatic device at the centre of the core with a thermal neutron flux of 2.4×10^{16} n m^{-2} s^{-1}, or in the core tube at the side of the core with a thermal neutron flux of 1×10^{16} n m^{-2} s^{-1}.

All of the counting was performed with a pure Ge semiconductor detector (20% efficiency and 1.8 keV full width at half maximum resolution of 1.33 MeV). All measurements were made at a 2 cm distance from the detector end-cap. The gamma ray energies measured for quantitative analysis, on an ND6700 analyser were at 1368 keV of ^{24}Na, 1642 keV of ^{38}Cl, 617 keV of ^{82}Br and 554 keV of ^{80}Br for long irradiation (see Table 1).

The complete scheme of the analysis, shown in Fig. 1, consists of the following stages: (*i*) instrumental analysis for chlorine; (*ii*) radiochemical analysis for chlorine, bromine and sodium; and (*iii*) determination of the yield. The samples are first irradiated in sequence with the chlorine standards in ICIS, the pneumatic irradiation site at the centre of the core. After a 10 min irradiation and a 15 min decay, the samples are counted for 14 min.

Once the samples have been counted for chlorine instrumentally they are re-packed in clean capsules and placed, with the multi-element standards, in an outer irradiation container, and irradiated for 7.5 h at the edge of the core. The following day, after a 16 h decay overnight, the samples and standards are transferred into individual irradiation containers and irradiated sequentially for 10 min as before in order to re-activate the chlorine that has decayed overnight.

The active samples are transferred immediately into an agate mortar and crushed with 1.5 cm^3 of carrier. The carrier solution of sodium chloride is in exactly the same chemical form as the saline fluid inclusion to ensure that chemical

* To whom correspondence should be addressed.

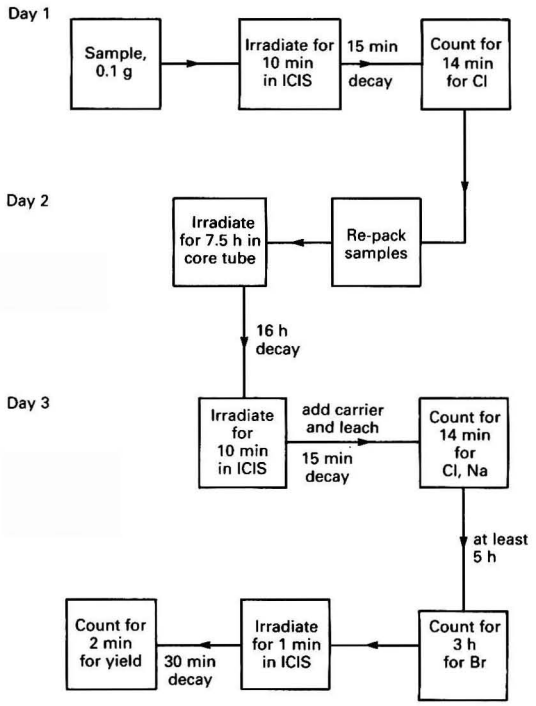

Fig. 1 Analytical procedure for the determination of Na, Cl and Br in fluid inclusions

Table 1 Nuclear properties of the elements*

Element	Nuclear reaction	Half-life	Gamma-ray energy/ keV	Gamma-ray intensity (%)
Cl	$^{37}Cl(n,\gamma)^{38}Cl$	37.24 min	1642.7	31
Br	$^{79}Br(n,\gamma)^{80}Br$	17.68 min	616.9	6.7
	$^{81}Br(n,\gamma)^{82}Br$	1.4708 d	554.4	79.9
			776.5	83.6
Na	$^{23}Na(n,\gamma)^{24}Na$	14.659 h	1368.6	100

* Source: see ref. 8.

equilibrium between the carrier and the sample is reached rapidly. Approximately 1 cm^3 of the solution is pipetted into a polyethylene capsule and then transferred with a filtered syringe into a clean polyethylene capsule for counting (after a 15 min decay) for 14 min to measure Cl and Na. Once all the samples and standards have been measured they are allowed to decay to allow the chlorine activity and short-lived interferences such as europium to reduce. After at least 5 h the samples are recounted for 3 h each for bromine.

It is important to determine the recovery of the elements during the crushing and leaching stages, as the volume of solution recovered during leaching is variable. It is measured by the re-irradiation of the carrier. As the Na and Cl in the carrier is greatly in excess of the values in the sample, re-activation will result in major activity from the carrier. Only a 1 min irradiation, 30 min decay and 1 min count is required.

Results and Discussion

The detection limits for INAA were poor: 2–4 μg for Cl and Na, and about 50 ng for Br. The separation procedure provided improvement to 1 μg for Cl and Na, and 0.5–5 ng for Br. The use of a carrier is an important aspect of the techniques as the data are corrected for any losses during the crushing and leaching stages. It is not possible to validate the method using reference materials, as there are no fluid inclusion reference standards and no other matrix would test the fluid extraction procedure. The results for fluorite in Table 2 are given to show the capabilities of the method for real unknown samples. The data serve to show the range of typical values and ratios found in real samples. The Na : Cl ratios of the fluid inclusions are in agreement with expected values for highly saline Na–Ca–Cl rich basinal brines and repeated analyses give reasonable agreement for the Cl : Br ratios. These results represent an average of the composition of all the fluid inclusions in the sample. Therefore, sometimes poor sampling reproducibility can arise from the presence of more than one generation of inclusions. This method is superior to the instrumental neutron activation methods used in this research area while providing a simple procedure that can be applied by researchers outside the field of radiochemistry. This technique can be further validated in the future using synthetic fluid inclusions of known composition, when they become available.

Table 2 Amounts of Br, Na and Cl in fluorites

Sample	Br/μg	Na/μg	Cl/μg	Cl : Br ratio	Cl : Na ratio
1	0.0612	3.77	8.22	134	2.18
	0.0584	3.64	8.62	148	2.36
2	0.0309	2.23	5.83	189	2.62
	0.0456	3.56	9.51	209	2.67
	0.0567	4.28	9.51	168	2.22
3	0.108	3.82	9.14	84.6	2.40
	0.0284	1.93	6.37	224	3.30
	0.0434	3.68	12.6	291	3.43
4	0.0087	0.657	1.45	167.2	2.21
	0.0400	3.55	7.34	183.6	2.06
5	0.0320	1.79	3.67	114	2.05
	0.0732	3.35	7.16	97.8	2.15

We are indebted to Georgina Coe for her technical assistance throughout this project. M. C. is grateful to the Greek State Scholarships Foundation and the British Council for their financial support during this project.

References

1 Roedder, E., *Geochim. Cosmochim. Acta*, 1990, **54**, 495.
2 Czamanske, C. K., Roedder, E., and Burns, F. C., *Science*, 1963, **140**, 401.
3 Puchner, H. F., and Holland, H. D., *Econ. Geol.*, 1966, **61**, 1390.
4 Sabouraud-Rosset, C., *Sedimentology*, 1974, **21**, 415.
5 Grappin, C., Saliot, P., Sabouraud, C., and Touray, J. C., *Chem. Geol.*, 1979, **25**, 41.
6 Lucksheiter, B., and Parekh, P. P., *Neues Jahrb. Mineral. Monatsh.*, 1979, **3**, 135.
7 Wickman, F. E., and Khattab, K. M., *Econ. Geol.*, 1972, **67**, 236.
8 Brown, E., and Firestone, B., *Table of Radioactive Isotopes*, Wiley, Chichester, 1986.

Paper 1/06418E
Received December 23, 1991
Accepted June 3, 1992

Automated Simultaneous Determination of Metal Ions by Use of Variable Flow Rates in Unsegmented Systems

Juliana Marcos, Angel Ríos and Miguel Valcárcel*
Department of Analytical Chemistry, Faculty of Sciences, University of Córdoba, E-14004 Córdoba, Spain

Two methods for the simultaneous determination of zinc and copper and of calcium and magnesium, based on the use of flow-rate gradients and spectrophotometric detection in unsegmented systems, are reported. The underlying chemistries of the determinations are a ligand-exchange reaction and a pH change, respectively, in completely continuous and flow-injection manifolds. By automatically changing the ligand concentration or pH, one can ascertain the contribution of each ion to the recorded signal. The performance of the two proposed methods was tested on both synthetic and real samples, involving the simultaneous determination of zinc and copper and of calcium and magnesium. Relative standard deviations between 1.5 and 5% were found for the precision of the proposed methods.

Keywords: *Variable flow rate; simultaneous determination; metal ion; flow injection; unsegmented flow system*

Simultaneous determinations are among the major issues of analytical chemistry[1] as they avoid the need to separate a mixture of components by using one of the many techniques available for this purpose. The automation capability of unsegmented flow systems is a major asset for implementation of these determinations in routine analyses.[2] In this context, the concept of simultaneous determination is related to the determination of more than one parameter per injection in the same configuration if the flow injection (FI) mode is used. Therefore, this is a wide concept involving clearly sequential determinations in some instances (*e.g.*, in using more than one detector[3,4]). Analytical methods based on the use of special FI configurations[5–8] or, more recently, on fast-scanning detectors,[9,10] are more interesting in this respect.

The recent development of flow methods based on variable flow rates[11] has broadened the scope of automated simultaneous determinations. One of the most appealing assets of variable flow rates is that they can be used to create concentration gradients or automatic abrupt changes in the concentration of one reactant. Such changes in the experimental conditions are highly useful in performing simultaneous determinations in both FI and continuous-flow systems, as shown in this work. Hence, a ligand-exchange reaction between Zincon and DCTA (*trans*-1,2-diaminocyclohexane-*N*,*N*,*N*′,*N*′-tetraacetate)[12] was used to determine zinc and copper simultaneously. Also, a pH change was used for the simultaneous determination of calcium and magnesium with Chlorphosphonazo III (CPA).[13]

Experimental

Apparatus

A Hewlett-Packard (HP) 8451A diode-array spectrophotometer (Avondale, PA, USA), equipped with an HP-9121 floppy-disk drive, an HP-9855A keyboard and an HP-7470A plotter, was used. A Gilson Minipuls-2 peristaltic pump (Worthington, OH, USA) working at a constant flow rate and a Gilson Minipuls-3 peristaltic pump that was controlled by a Commodore-64 microcomputer (Commodore Business Machines, Berkshire, UK) *via* a laboratory-built interface to set flow-rate gradients[11] were used. A Tecator TM II (Tecator, Högonäs, Sweden) chemifold and a Hellma (Jamaica, NY, USA) 178.12 QS flow cell (inner volume, 18 mm^3) were also used.

Reagents

Analytical-reagent grade chemicals were used in all instances.

Aqueous solutions of the following compounds were prepared at different concentrations: Zincon (Aldrich, Milwaukee, WI, USA), DCTA (Merck, Darmstadt, Germany), copper nitrate (Merck), zinc nitrate (Merck), calcium nitrate (Merck), magnesium nitrate (Merck), sodium chloride (Merck), CPA (Fluka, Buchs, Switzerland) and a borate buffer solution of pH 8.5.

The following British Chemical Standard (BCS) certified reference material (CRM) samples supplied by the Bureau of Analysed Samples (Middlesbrough, Cleveland, UK) were used: BCS-CRM No. 179/2 High Tensile Brass (Cast); BCS-CRM No. 385 Leaded Brass; BCS-CRM No. 390 High Tensile Brass (Wrought); BCS-CRM No. 344 70/30 Brass; BCS-CRM No. 10e High Tensile Brass; and BCS-CRM No. 5g High Tensile Brass.

Sample Pre-treatment

Approximately 0.5 g of CRM was accurately weighed and treated with nitric acid until complete dissolution, then 150 cm^3 of distilled water were added, the mixture was filtered, and the filtrate was diluted to a final volume of 250 cm^3 with water. A volume of 40 cm^3 of this stock solution was treated with concentrated ammonia in order to remove iron and aluminium by precipitation as hydroxides. The resulting mixture was filtered, the precipitate washed with ammonia solutions and these washings were added to the initial solution. The excess of ammonia in the solution was expelled by heating. The final solution was allowed to cool to room temperature and its pH was adjusted to 5.2.

Manifolds

The manifolds used are depicted in Fig. 1, namely, a completely continuous system [Fig. 1(*a*)] and an FI system [Fig. 1(*b*)]. Two pumps were needed in both instances: a conventional pump (CP) that was operated at constant flow rate, and a programmable pump (PP) that was used to set the flow gradients or change the flow rate on command by the microcomputer *via* the interface. In the completely continuous system [Fig. 1(*a*)], the sample and solution B merged at C_1, and the mixed stream was merged with solution A at C_2. In the FI system [Fig. 1(*b*)], the sample was injected into the stream of solution B, and merged subsequently with solution A at C. This last stream only started flowing after the sample was injected to allow the formation of two zones on each side

* To whom correspondence should be addressed.

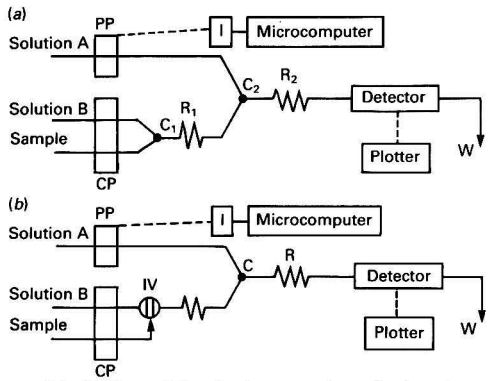

Fig. 1 Manifolds used for simultaneous determinations by completely continuous flow analysis (*a*) and flow injection (*b*). PP = Programmable pump; CP = conventional pump; I = interface; IV = injection valve; R = reaction coils; and C = merging points

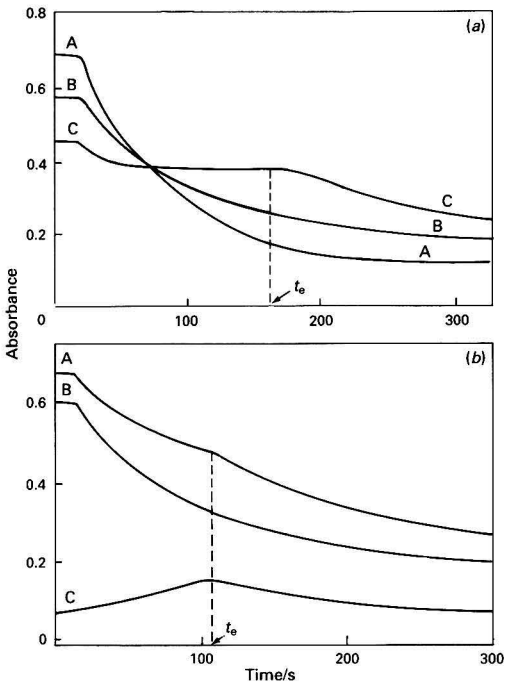

Fig. 2 Absorbance–time recordings obtained in the simultaneous determination of copper and zinc with DCTA in a completely continuous system. (*a*) Recordings obtained at three different wavelengths: A, 484; B, 534; and C, 620 nm. (*b*) Recordings obtained at A, 484 nm; B, 534 nm; and C, their difference for a sample containing zinc only. t_e = the time at which the metal–ligand stoichiometric ratio is reached

of the sample plug: one in the absence of A and the other in its presence.

Results and Discussion

Two different chemical systems were used to separate binary mixtures of zinc and copper and of calcium and magnesium at trace levels by the proposed methodology.

Use of a Ligand-exchange Reaction

Copper and zinc react with Zincon at pH 8.5 (borate buffer) to yield highly coloured 1:1 complexes with an absorption maximum at 620 nm. If DCTA is added to the medium Zincon is displaced from its complex with Zn^{II}, but not from its Cu^{II} complex, which reacts very slowly with DCTA:[14]

$$\begin{matrix} Cu^{II}\text{–Zincon} \\ + \text{DCTA} \\ Zn^{II}\text{–Zincon} \end{matrix} \longrightarrow \begin{matrix} Cu^{II}\text{–Zincon} \\ + \text{Zincon} \\ Zn^{II}\text{–DCTA} \end{matrix}$$

This differential behaviour of Zn^{II} and Cu^{II} towards Zincon and DCTA is the basis for the proposed simultaneous determination of both metal ions.

Completely continuous system

Solution A contains DCTA in a 0.02 mol dm^{-3} borate buffer (pH 8.5) and 0.02 mol dm^{-3} NaCl in order to keep the ionic strength constant. The sample (a mixture of copper and zinc solutions) is merged with a Zincon stream (solution B) at the first confluence point (C_1), so Zincon complexes are formed along reactor R_1. The flow rate of the DCTA solution is increased linearly with time (from zero to a maximum value), resulting in a gradual increase in the concentration of this reagent at C_2. The addition of DCTA resulting from increased flow rate causes both the dissociation of the Zn^{II}–Zincon complex and dilution after C_2 (both effects must be considered).

The flow rate of the Zincon and sample streams was 1.0 cm^3 min^{-1}. The Zincon concentration was kept at 2.6×10^{-4} mol dm^{-3} in order for the reagent to react with a maximum concentration of metal ions of 10 μg cm^{-3}. The flow rate of the DCTA solution was changed from 0 to 5.0 cm^3 min^{-1}, and a concentration of 2.6×10^{-5} mol dm^{-3} was used to determine zinc concentrations below 8.0 μg cm^{-3}. The flow gradient played a major role in the sensitivity to zinc; the optimum value was 0.0145 cm^3 min^{-1} and was set by using a linear flow-rate gradient.

The reaction was simultaneously monitored at three different wavelengths by using the diode-array spectrophotometer. Fig. 2(*a*) shows the typical absorbance *versus* time recordings obtained at 620 nm (the absorption maximum of the Zincon complexes), 484 nm (the absorption maximum absorbance of free Zincon) and 534 nm (the wavelength at which the molar absorptivities of free Zincon and its complexes are similar). This last curve shows the dilution undergone by these compounds within the flow system as a result of the flow-rate gradient. The initial absorbance at 620 nm was related to the copper and zinc concentrations. Such an absorbance always decreased as a result of both dissociation of the Zn^{II}–Zincon complex and dilution. The absorbance at 484 nm shows the variation of the free Zincon concentration in the system. The amount of Zincon increased on addition of DCTA until the stoichiometric ratio of Zn^{II} to Zincon was reached. Obviously, the time at which such a ratio is reached (denoted by t_e) is related to the Zn^{II} concentration. As its location on curve C [Fig. 2(*a*)] was not always clear, a new curve was defined by subtracting the absorbances at 484 and 534 nm [curve C in Fig. 2(*b*)], where the effect of dilution was cancelled.

The zinc concentration in the samples can be calculated from t_e, while that of copper can be obtained from the initial absorbance at 620 nm once the zinc concentration is known, by using the following equations (620 nm):

$$A = A_{Cu} + A_{Zn} + A_{blank}$$
$$A_{Cu} = A - A_{Zn} - A_{blank}$$

The calibration equations obtained under these conditions were

Zinc(II):

$$A_{Zn} = 0.178[Zn^{2+}] + 0.012 \qquad (r = 0.9999)$$
$$t_e = 15.05[Zn^{2+}] + 44.2 \qquad (r = 0.9998)$$

Copper(II):

$$A_{Cu} = 0.144[Cu^{2+}] + 0.005 \qquad (r = 0.9999)$$

Table 1 Results obtained in the analysis of synthetic samples of copper and zinc

(*a*) Completely continuous system				(*b*) FI system			
Concentration added/ μg cm^{-3}		Concentration found/ μg cm^{-3}		Concentration added/ μg cm^{-3}		Concentration found/ μg cm^{-3}	
Cu	Zn	Cu	Zn	Cu	Zn	Cu	Zn
2.5	2.5	2.5 ± 0.1	2.7 ± 0.1	1.4	0.3	1.3 ± 0.1	0.3 ± 0.05
5.0	5.0	5.1 ± 0.1	4.9 ± 0.2	1.0	2.1	1.0 ± 0.1	2.0 ± 0.1
1.0	6.0	1.0 ± 0.1	6.0 ± 0.1	3.1	2.1	3.2 ± 0.2	1.8 ± 0.1
1.0	0.8	0.9 ± 0.1	0.7 ± 0.1	0.1	1.1	0.1 ± 0.07	1.0 ± 0.06
0.5	4.0	0.4 ± 0.1	4.1 ± 0.1	0.2	0.1	0.2 ± 0.06	0.1 ± 0.02
3.0	7.5	2.9 ± 0.2	8.0 ± 0.2	0.5	0.5	0.6 ± 0.1	0.4 ± 0.02

Table 2 Determination of copper and zinc in certified samples

Certified brass reference material	Certified values (%)		Amounts found (%)			
			(*a*) Completely continuous system		(*b*) FI system	
	Cu	Zn	Cu	Zn	Cu	Zn
BCS-CRM No. 179/2	58.5	35.8	58.5 ± 0.3	36.8 ± 0.9	57.8 ± 0.2	43.9 ± 1.2
BCS-CRM No. 390	57.1	38.6	57.1 ± 0.2	39.6 ± 0.4	60.1 ± 0.3	37.6 ± 0.6
BCS-CRM No. 10c	61.1	31.5	57.7 ± 0.2	31.5 ± 0.3	62.8 ± 0.3	28.9 ± 0.6
BCS-CRM No. 5g	67.4	28.6	66.0 ± 0.3	31.1 ± 0.3	64.1 ± 0.3	25.3 ± 0.3
BCS-CRM No. 344	69.0	31.0	67.4 ± 0.3	31.1 ± 0.4	65.5 ± 0.3	26.7 ± 0.5

where the ion concentrations are expressed in μg cm^{-3}, and t_c in seconds. All the absorbance values correspond to the initial absorbance of the curves at 620 nm.

Synthetic samples were analysed by this method in order to test its performance. The results obtained are listed in Table 1(*a*). The method was subsequently applied to the CRM samples, as shown in Table 2(*a*). The precision of the method, expressed as the relative standard deviation (RSD) (n = 11 and P = 0.05), was between 2.0 and 2.5% for both copper and zinc.

FI system

Solution A contains 4 × 10^{-5} mol dm^{-3} DCTA in 0.02 mol dm^{-3} borate buffer and 0.02 mol dm^{-3} NaCl, while solution B contains 2 × 10^{-4} mol dm^{-3} Zincon plus the same buffer and salt. Both streams are circulated at a constant flow rate, but the DCTA stream can be halted at will. The first time the DCTA stream is stopped, the sample is injected into the other channel (flow rate, 0.8 cm^3 min^{-1}). When half the sample plug has passed by the confluence point (C), the DCTA stream is set into motion at 0.6 cm^3 min^{-1} (10 s after sample injection), thereby providing two zones of the sample plug that emerges from C (in the absence and presence of DCTA, respectively). Hence, the first portion of the peak obtained as the plug passes through the detector (measured at 620 nm) is proportional to the sum of the copper and zinc concentrations, whereas the second portion is only related to the copper concentration. Some typical recordings are shown in Fig. 3, where the two time parameters (t_1 and t_2) used for the determination have been marked. The absorbance at t_2 corresponds to the amount of copper in the sample, while that at t_1 arises from the contribution of both ions. The optimum injected sample volume was 157 mm^3.

The calibration equations obtained are

Copper(II):

$$A_{t_1} = 0.113[Cu^{2+}] - 0.001 \qquad (r = 0.9991)$$

$$A_{t_2} = 0.073[Cu^{2+}] + 0.024 \qquad (r = 0.9966)$$

Zinc(II):

$$A_{t_1} = 0.116[Zn^{2+}] + 0.002 \qquad (r = 0.9990)$$

The linear ranges of determination were 0.1–5.0 μg cm^{-3} for Cu^{II} and 0.1–3.0 μg cm^{-3} for Zn^{II}, and the RSDs were between 1.5 and 3.5% (copper), and 3.5 and 5.0% (zinc). The results found for synthetic and certified samples are shown in Tables 1(*b*) and 2(*b*), respectively.

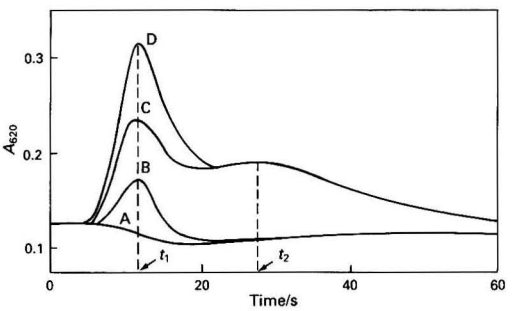

Fig. 3 Recordings obtained in the simultaneous determination of copper and zinc with DCTA by using the FI system: A, blank; B, 0.9 μg cm^{-3} Zn^{II}; C, 2.1 μg cm^{-3} Cu^{II}; and D, a mixture of the two. t_1 and t_2 are the two time parameters used for the determination (see text)

Use of pH Changes

Calcium and magnesium yield coloured complexes with CPA, which behave differently in relation to pH.[13] Hence, while both ions react with CPA at pH ≥7, only the Ca^{II} complex is formed below pH 5. These two ions were previously determined by using CPA in an FI system with two different buffers and a switching valve.[13] Our method relies on a flow-rate change resulting from a pH change, which allows the simultaneous determination of Ca^{II} and Mg^{II} in a completely continuous or FI system.

Completely continuous system

Solution A contains 60 μg cm^{-3} of CPA at pH 2.5, while solution B contains the same concentration of CPA at pH 7.2. As the PP was initially stopped, the sample stream was merged with the reagent at pH 7.2, and both complexes were formed and monitored by spectrophotometry at 668 nm. The recorded signal was constant and equal to the sum of the absorbances of

Table 3 Results obtained in the analysis of synthetic samples of calcium and magnesium

(*a*) Completely continuous system				(*b*) FI system			
Concentration added/ μg cm^{-3}		Concentration found/ μg cm^{-3}		Concentration added/ μg cm^{-3}		Concentration found/ μg cm^{-3}	
Ca	Mg	Ca	Mg	Ca	Mg	Ca	Mg
1.0	3.0	1.1 ± 0.1	2.8 ± 0.3	1.0	1.1	1.1 ± 0.1	1.1 ± 0.1
3.0	1.0	3.2 ± 0.2	1.2 ± 0.2	3.0	0.7	3.2 ± 0.1	0.6 ± 0.1
2.6	2.5	2.6 ± 0.1	2.3 ± 0.2	0.5	2.2	0.5 ± 0.1	2.3 ± 0.1
2.0	1.0	1.8 ± 0.1	0.9 ± 0.2	0.8	3.3	0.9 ± 0.1	3.3 ± 0.2
0.5	1.2	0.5 ± 0.1	1.1 ± 0.1	0.9	2.0	1.0 ± 0.1	1.9 ± 0.1
1.5	2.0	1.0 ± 0.1	2.2 ± 0.2	2.0	3.5	2.1 ± 0.1	3.5 ± 0.2

Table 4 Determination of calcium and magnesium in different types of water

	Results obtained by AAS*/μg cm^{-3}		Concentrations found/μg cm^{-3}			
			(*a*) Completely continuous system		(*b*) FI system	
Type of water	Ca	Mg	Ca	Mg	Ca	Mg
Mineral water ('Lanjaron')	34.6	11.5	35.8 ± 1.2	11.0 ± 1.0	34.6 ± 1.0	11.5 ± 0.6
Mineral water ('Centra')	71.5	10.4	71.6 ± 1.5	8.8 ± 1.0	73.1 ± 1.2	11.0 ± 0.5
Mineral water ('Sousa')	13.3	6.7	11.0 ± 1.0	7.0 ± 0.7	12.8 ± 0.6	5.4 ± 0.3
Tap water	20.0	7.5	20.8 ± 0.9	6.8 ± 0.8	20.0 ± 0.5	6.7 ± 0.2
Ground water	25.0	7.0	23.5 ± 0.7	5.8 ± 0.5	25.6 ± 0.5	3.4 ± 0.2
Rain water	10.5	0.5	11.0 ± 0.5	1.3 ± 0.1	10.8 ± 0.3	0.5 ± 0.1

* AAS = Atomic absorption spectrometry.

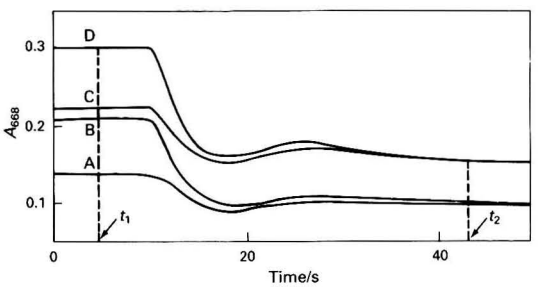

Fig. 4 Absorbance–time recordings obtained in the simultaneous determination of calcium and magnesium with CPA by using the completely continuous system: A, blank; B, 1.5 μg cm^{-3} Mg^{II}; C, 2.0 μg cm^{-3} Ca^{II}; and D, a mixture of the two. t_1 and t_2 are the two time parameters used for the determination (see text)

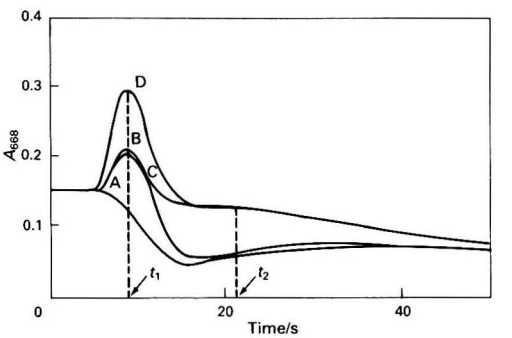

Fig. 5 Recordings obtained in the simultaneous determination of calcium and magnesium with CPA by using the FI system: A, blank; B, 1.0 μg cm^{-3} Mg^{II}; C, 2.2 μg cm^{-3} Ca^{II}; and D, a mixture of the two. t_1 and t_2 are the two time parameters used for the determination (see text)

both complexes. As the PP was started at a rate of 0.3 cm^3 min^{-1}, the pH of the system was lowered below 7, so that only the Ca^{II}–CPA complex was formed along reactor R_2. The recorded absorbance decreased as a result. This signal was proportional to the amount of Ca^{II} in the sample, while the initial signal corresponded to the sum of Ca^{II} and Mg^{II}. The Mg^{II} concentration was obtained by difference. As a result of the change in the molar absorptivity of CPA with pH, a blank recording was obtained and used in the calculations. Some typical recordings are shown in Fig. 4, where t_1 and t_2 denote, respectively, the times at which the initial and final absorbances are attained. The calibration equations obtained are

Calcium(II):

$$A_{t_1} = 0.0362[Ca^{2+}] + 0.001 \qquad (r = 0.9990)$$

$$A_{t_2} = 0.0139[Ca^{2+}] + 0.055 \qquad (r = 0.9999)$$

Magnesium(II):

$$A_{t_1} = 0.0582[Mg^{2+}] - 0.001 \qquad (r = 0.9998)$$

where concentrations are expressed in μg cm^{-3}. The linear determination ranges were 0.3–8.0 μg cm^{-3} for Ca^{II} and 0.5–5.0 μg cm^{-3} for Mg^{II}. The RSDs were 2–3% (for calcium) and 2.5–5% (for magnesium).

The results obtained by applying the proposed method to synthetic samples are listed in Table 3(*a*). Calcium and magnesium in different types of water were also determined in this fashion, the results being listed in Table 4(*a*).

FI system

The sample was injected into a stream containing 74 μg cm^{-3} of CPA [solution B in Fig. 1(*b*)] flowing at 0.8 cm^3 min^{-1}. The pH of the solution was adjusted to 7.2. A stream of CAP at the same concentration, but at pH 2.5, was used as solution A. This was propelled by the PP, which was initially stopped and was then started 5 s after injection of the sample at a rate of 0.3 cm^3 min^{-1}. This time is crucial to ensure the formation of two zones in the sample plug at different pH values along reactor R, which are detected and recorded as a 'quasi' double peak at 668 nm (see Fig. 5). The absorbance at time t_1 arises from calcium alone. A blank signal was recorded in order to subtract its contribution to the sample signals. The optimum injected sample volume was 75 mm^3.

The calibration equations obtained under these conditions were

Calcium(II):

$$A_{t_1} = 0.036[Ca^{2+}] \qquad (r = 0.9965)$$

$$A_{t_2} = 0.023[Ca^{2+}] + 0.057 \qquad (r = 0.9981)$$

Magnesium(II):

$$A_{t_1} = 0.036[Mg^{2+}] + 0.005 \qquad (r = 0.9992)$$

The determination ranges were 0.2–3.0 μg cm^{-3} for magnesium (RSD approximately 5%) and 0.5–3.0 μg cm^{-3} for calcium (RSD between 2 and 4%). The performance of this method was also tested on synthetic samples first [Table 3(*b*)] and then on different types of water [Table 4(*b*)]. The results obtained were consistent with those provided by atomic absorption spectrometry.

Conclusion

The proposed methods, which are based on the use of variable flow rates, are highly useful in implementing simultaneous determinations by using straightforward manifolds, inexpensive instrumentation (a conventional spectrophotometer can also be used) and automated methodologies. These features make them very appealing for routine analyses, as shown in this work by applying them to real samples. Higher errors were found for brass samples as a consequence of the dilution processes needed for the analysis of these types of samples (a method of trace-level analysis was applied to the major components). As a rule, the results obtained with completely continuous-flow systems were better than those provided by FI systems. However, FI systems can prove useful when small amounts or expensive samples are to be processed. Similar methods for other chemical systems could be readily developed to broaden the scope of application of this methodology.

References

1 Pérez-Bendito, D., *Analyst*, 1984, **109**, 891.
2 Luque de Castro, M. D., and Valcárcel Cases, M., *Analyst*, 1984, **109**, 413.
3 Basson, W. D., and van Staden, J. F., *Fresenius' Z. Anal. Chem.*, 1980, **302**, 370.
4 Cañete, F., Ríos, A., Luque de Castro, M. D., and Valcárcel, M., *Analyst*, 1988, **113**, 739.
5 Fernández, A., Luque de Castro, M. D., and Valcárcel, M., *Anal. Chem.*, 1984, **56**, 1146.
6 Ruz, J., Ríos, A., Luque de Castro, M. D., and Valcárcel, M., *Fresenius' Z. Anal. Chem.*, 1985, **322**, 499.
7 Ríos, A., Luque de Castro, M. D., and Valcárcel, M., *Anal. Chem.*, 1986, **58**, 663.
8 Ríos, A., Luque de Castro, M. D., and Valcárcel, M., *Anal. Chim. Acta*, 1986, **179**, 463.
9 Lázaro, F., Ríos, A., Luque de Castro, M. D., and Valcárcel, M., *Anal. Chim. Acta*, 1986, **179**, 279.
10 Cañete, F., Ríos, A., Luque de Castro, M. D., and Valcárcel, M., *Anal. Chim. Acta*, 1988, **214**, 375.
11 Agudo, M., Marcos, J., Ríos, A., and Valcárcel, M., *Anal. Chim. Acta*, 1990, **239**, 211.
12 Ferguson, J. W., Richard, J. J., O'Laughlin, J. W., and Banks, C. V., *Anal. Chem.*, 1964, **36**, 769.
13 Youxian, Y., *Anal. Chim. Acta*, 1988, **212**, 291.
14 Ridder, G. M., and Margerum, D. W., *Anal. Chem.*, 1977, **49**, 2090.

Paper 2/01250B
Received March 9, 1992
Accepted May 28, 1992

Determination of Ascorbic Acid in Pharmaceuticals and Urine by Reverse Flow Injection

Mª. Isabel Albero, Mª. Soledad García, C. Sánchez-Pedreño* and José Rodríguez
Department of Analytical Chemistry, Faculty of Chemistry, University of Murcia, Murcia, Spain

Two reverse flow injection (FI) methods, using spectrophotometric detection, are proposed for the determination of ascorbic acid. Both methods are based on its reaction with the ethylenediaminetetraacetic acid–Co^{III} complex in a medium of 5% diethylamine. In the first method, using the peak-height FI technique, ascorbic acid is determined over the range from 2×10^{-4} to 5×10^{-3} mol dm^{-3} and in the second, using the peak-width FI method, the working range is extended (2×10^{-3}–5×10^{-2} mol dm^{-3}). Both FI methods were applied to the determination of ascorbic acid in pharmaceuticals while the peak-height FI technique was also used to determine ascorbic acid in urine.

Keywords: *Ascorbic acid; ethylenediaminetetraacetic acid–cobalt(III) complex; flow injection; pharmaceuticals; urine*

Ascorbic acid participates in many different biological processes, and is important in human diet. There is a need for fast, selective and automated methods for its determination, particularly in routine analyses. Most of the methods proposed have been listed in reviews and monographs[1–4] and some have been suggested as reference methods for different types of samples.[5–7]

Flow injection (FI) has been applied to determine ascorbic acid in a variety of samples, including foods, pharmaceuticals and biological samples. Several detection techniques have been proposed, *e.g.*, potentiometric,[8] coulometric,[9,10] amperometric,[9,11–18] spectrophotometric[19–25] and spectrofluorimetric[26] techniques. Few methods are found in the literature using FI gradient techniques.[24,27]

In this work, two simple, fast and selective methods for the determination of ascorbic acid, based on the reaction between Co^{III}–ethylenediaminetetraacetic acid (EDTA) and ascorbic acid using FI techniques are described. Peak height and peak width are used as quantitative parameters. These methods have been applied, with good results, to the routine determination of ascorbic acid in pharmaceuticals and urine.

Experimental

Apparatus

The FI system consisted of a Gilson HP4 peristaltic pump, an Omnifit injection valve, a Hellma 18 mm^3 flow cell and a Pye Unicam spectrophotometer as detector. Connecting tubing of 0.5 mm bore, poly(tetrafluoroethylene) (PTFE) tubing and various end fittings and connectors (Omnifit) were used. For the peak-width measurements, a Perspex gradient tube of 2 mm inner diameter was used.

Reagents

All chemicals were of analytical-reagent grade and the solutions were prepared with doubly distilled water.

Cobalt(III)–EDTA, 4×10^{-2} mol dm^{-3}. Exactly 50 cm^3 of 0.1 mol dm^{-3} cobalt(II) nitrate (Merck) and 50 cm^3 of 0.1 mol dm^{-3} Na_2H_2EDTA (Merck) were transferred by pipette into a 250 cm^3 beaker. Dipotassium peroxodisulfate (3 g, Merck) was then added and the solution adjusted to pH 6 with ammonia solution (1 + 1; $d = 0.88$ g cm^{-3}) and boiled gently for about 20 min in order to decompose the excess of peroxodisulfate.[28] The solution was diluted to volume with doubly distilled water in a 125 cm^3 calibrated flask.

* To whom correspondence should be addressed.

Ascorbic acid stock solution, 0.1 mol dm^{-3}. Prepared by dissolving 4.4032 mg of the acid (Sigma) in 250 cm^3 of distilled water; the solution was stored at 4 °C in a dark bottle. Working solutions of ascorbic acid were prepared daily by dilution of this stock solution.

Diethylamine, 5% *v/v*. Prepared by dissolving diethylamine (Merck) in distilled water.

FI Procedures

The FI manifold shown in Fig. 1(*a*) was used. An 85 mm^3 aliquot of 5×10^{-3} mol dm^{-3} Co^{III}–EDTA solution was injected into a stream formed by the mixing of 5% diethylamine solution and the ascorbic acid sample. All streams were pumped at a rate of 0.87 cm^3 min^{-1}.

The absorbance of Co^{III}–EDTA at 540 nm was measured, and a calibration graph was obtained by plotting the peak height *versus* the concentration of ascorbic acid over the range from 2×10^{-4} to 5×10^{-3} mol dm^{-3}.

For the peak-width method the manifold shown in Fig. 1(*b*) was used. A 146 mm^3 aliquot of 5×10^{-3} mol dm^{-3} Co^{III}–EDTA solution was injected into a stream formed by the mixing of 5% diethylamine solution and the ascorbic acid sample; the absorbance was monitored at 540 nm with a plotting rate of 10 s cm^{-1}. A calibration graph was obtained by plotting the peak width expressed in seconds, measured to a preselected absorbance level of 0.1, *versus* the logarithm of the ascorbic acid concentration.

Determination of Ascorbic Acid in Authentic Samples

Pharmaceutical samples

No sample pre-treatment was needed for these analyses. An accurately weighed or measured amount of the pharmaceutical sample was dissolved in water and the solution filtered. The CO_2 was expelled from the samples by shaking, if necessary, and the sample diluted to a final volume of 250 cm^3 with doubly distilled water. The FI procedures described above were applied to the resulting solutions.

Urine samples

The proposed FI method was applied to the determination of ascorbic acid in urine. The composition of the synthetic urine was: lactic acid, 5×10^{-4} mol dm^{-3}; uric acid, 2×10^{-4} mol dm^{-3}; hippuric acid, 8×10^{-3} mol dm^{-3}; urea, 3×10^{-4} mol dm^{-3}; glucose, 3×10^{-4} mol dm^{-3}; Cl^-, 6 mg cm^{-3}; PO_4^{3-}, 0.5 mg cm^{-3}; Na^+, 4 mg cm^{-3}; K^+, 0.5 mg cm^{-3}; and Ca^{2+}, 0.5 mg cm^{-3}. Five aliquots of 100 cm^3 each, in which different amounts of ascorbic acid had been dissolved, were

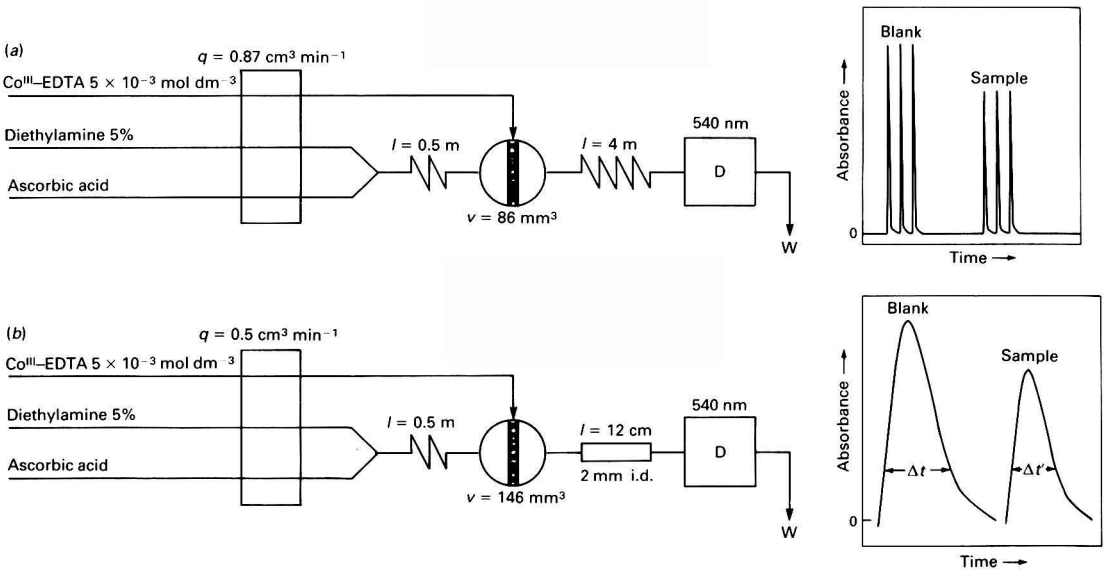

Fig. 1 FI manifolds for the determination of ascorbic acid. Recordings obtained using (*a*) peak-height method and (*b*) peak-width method

taken. The content of each aliquot was determined by following the recommended procedure.

For human urine, urine samples were obtained from an individual 2 h after he had ingested a pharmaceutical compound containing 1 g of vitamin C. Samples were collected in a polyethylene flask. Aliquots of 15 cm³ were taken, 2 cm³ of 0.1 mol dm⁻³ Na_2H_2EDTA were added and the mixture was diluted in a 25 cm³ calibrated flask with doubly distilled water. The content of each aliquot was determined by following the recommended FI procedure.

Results and Discussion

Ascorbic acid was found to reduce the Co^{III}–EDTA complex to Co^{II}–EDTA in a water–diethylamine medium (pH 12.5) and this reaction was adapted in order to develop two FI methods for determining ascorbic acid. Detection was carried out spectrophotometrically at 540 nm, the absorption maximum of Co^{III}–EDTA, by reverse FI as the analyte is pumped in both methods, the peak height being measured in the first method and the peak width in the second.

Peak-height FI Method

A schematic diagram of the reverse FI manifold is shown in Fig. 1(*a*). The solution of Co^{III}–EDTA was injected into a stream containing a mixture of the sample and diethylamine solution. Under these conditions the ascorbic acid reduced the Co^{III}–EDTA complex and the absorbance was measured spectrophotometrically at 540 nm.

In the absence of ascorbic acid (blank), a maximum peak was obtained corresponding to the initial concentration of Co^{III}–EDTA. The presence of ascorbic acid caused a decrease in the analytical signal proportional to the ascorbic acid concentration [Fig. 1(*a*)].

Flow injection and chemical variables were optimized for the proposed FI method. This study was carried out by altering each variable in turn while keeping the others constant. The optimum chemical and FI variables chosen were those that yielded maximum and constant differences between the peak height of the blank and the samples (Δh).

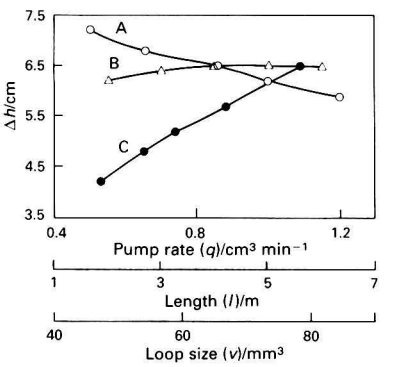

Fig. 2 Variation of Δh with: A, the pumping rate; B, reactor length; and C, loop size

It was found that a basic medium was necessary for the reaction between Co^{III}–EDTA and ascorbic acid to proceed and the best results were obtained with the use of diethylamine.

The influence of the diethylamine concentration was studied in the range between 1 and 7% v/v. The concentrations of ascorbic acid and Co^{III}–EDTA were 2×10^{-3} and 5×10^{-3} mol dm⁻³, respectively. The best results were obtained with a concentration of 5% v/v diethylamine.

Similarly, the influence of the concentration of Co^{III}–EDTA was studied in the range from 1×10^{-3} to 5×10^{-3} mol dm⁻³. A concentration of 5×10^{-3} mol dm⁻³ Co^{III}–EDTA was selected as this yielded suitable peak heights both for the blank and in the range of the calibration graph.

Fig. 2 shows the effects of the flow rate, reactor length and loop size on the differences between the signal of the blank and the sample (Δh) for an ascorbic acid concentration of 2×10^{-3} mol dm⁻³.

The effect of the flow rate on Δh was studied over the range 0.5–1.2 cm³ min⁻¹. An increase in the flow rate resulted in a decrease in Δh (Fig. 2, line A). A flow rate of 0.85 cm³ min⁻¹

was selected in order to obtain a reasonable sampling frequency.

The influence of the reactor length on Δh was studied over the range 2–6 m (inner diameter, 0.5 mm). The results (Fig. 2, line B) showed that Δh is virtually constant throughout the range studied. A 4 m reactor was selected.

The effect of the loop size on Δh is shown in Fig. 2, line C. An increase in loop size produced an increase in Δh, and a loop size of 85 mm^3 was chosen.

Determination of Ascorbic Acid

With the manifold described above and under the selected experimental conditions, *viz.*, 5×10^{-3} mol dm^{-3} Co^{III}–EDTA and 5% v/v diethylamine, a linear calibration graph between 2.0×10^{-4} and 5.0×10^{-3} mol dm^{-3} ascorbic acid was obtained. The regression equation found was $h = 11.21 \times 10^2$[ascorbic acid] + 18.4, where h is the peak height in centimetres and [ascorbic acid] is expressed in mol dm^{-3}, with a correlation coefficient (r) of 0.9985. The relative standard deviation (RSD) ($p = 0.05$) for ten determinations of 2×10^{-3} mol dm^{-3} ascorbic acid was 0.94%. The detection and quantification limits were 6×10^{-5} and 1.2×10^{-4} mol dm^{-3}, respectively, and the sampling frequency was 60 samples h^{-1}.

Peak-width FI Method

This method is based on the measurement of the peak width at a pre-determined height from the baseline. One of the problems found in routine analytical determinations is that the analyte concentrations of the sample often do not fall within the limited range of concentration covered by the calibration graphs. As the aim of this work was the routine determination of ascorbic acid, the peak-width FI method was applied to extend the useful working range for this acid. A logarithmic relationship between the peak width and the concentration of the samples was found.

The proposed FI manifold for the determination of ascorbic acid is shown in Fig. 1(*b*).

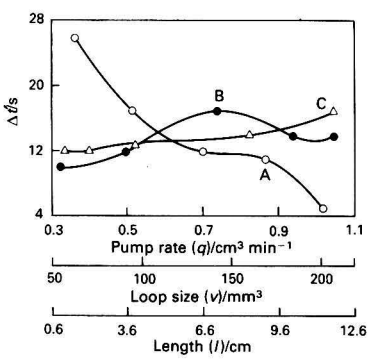

Fig. 3 Variation of $\Delta t'$ with: A, the pumping rate; B, loop size; and C, reactor length

Table 1 Calibration graphs for the determination of ascorbic acid using the peak-width method

Concentration range/mol dm^{-3}	Absorbance*	Slope	Correlation coefficient (r)
2×10^{-3}–5×10^{-2}	0.1	−26.632	0.9926
2×10^{-3}–3×10^{-2}	0.2	−20.068	0.9888
2×10^{-3}–1×10^{-2}	0.3	−18.446	0.9422

* Absorbance at which the peak width (Δt) was measured.

The effect of the FI experimental variables on Δt–$\Delta t'$ (the difference between the peak width of the blank and the samples) was studied. The results obtained are shown in Fig. 3. The selected values for the FI variables were as follows: flow rate = 0.51 cm^3 min^{-1}, with which a suitable Δt without a notable decrease in the sample frequency was obtained; and injection volume = 146 mm^3; this large volume of Co^{III}–EDTA injected ensured that wide peaks were obtained. Several tubes of 2 mm inner diameter and between 1.0 and 12 cm in length were used for the study of the influence of the gradient tube volume on Δt. The peak width increased with the volume of the tube, and hence a tube of length 12 cm (diameter = 2 mm) was selected.

The concentrations of Co^{III}–EDTA and diethylamine selected were the same as in the peak-height method.

The absorbance at which the peak width was measured influenced the sensitivity of the determination. It is advisable to measure the peak width at the absorbance level that yields the maximum difference between the blank and the sample. A plot of the peak width *versus* the logarithm of the concentration of ascorbic acid showed different linear ranges according to the value of the absorbance at which Δt was measured (as is shown in Table 1). An absorbance of 0.1 was selected because a wider range and a greater slope were obtained.

Table 2 Effect of various foreign species on the determination of 4×10^{-3} mol dm^{-3} ascorbic acid using the two FI methods

Species assayed*	Limiting molar ratio [species]: [ascorbic acid]
NO_3^-, Cl^-, CH_3COO^-, PO_4^{3-}	100
SO_4^{2-}, CO_3^{2-}, Br^-, AsO_2^-	50
SO_3^{2-}, oxalate	40
SeO_3^{2-}, citrate, tartrate, SeO_4^{2-}, lactose, starch†	20
Ca^{2+}, I^-, F^-, MoO_4^{2-}, urea, thiourea, fructose, lactic acid, gelatin†	10
Glucose, maltose, methionine, hippuric acid, glutamic acid, phenylalanine, NH_4^+, sucrose, valine, thiamine, pyridoxine, leucine	5
Nicotinamide, Zn^{2+}‡, Cu^{2+}‡, Mn^{2+}‡	1
Uric acid§, riboflavine	0.5
NO_2^-, S^{2-}	0.1

* Caffeine, aspartic acid and saccharin do not interfere.
† Mass relation.
‡ In the presence of H_2EDTA^{2-}.
§ Maximum relation assayed by the solubility of uric acid.

Table 3 Determination of ascorbic acid in pharmaceuticals

	Ascorbic acid content*			
Sample	Peak-height method	Peak-width method	Reference method	Stated
1†	162.52 (0.89)‡	162.75 (0.95)	163.34 (1.92)	166.67
2§	50.37 (0.92)	50.46 (0.87)	50.73 (1.77)	50.0
3¶	200.49 (1.17)	199.46 (1.25)	200.13 (2.53)	200.0

* Values for samples 1 and 2 in mg g^{-1}; values for sample 3 in mg cm^{-3}.

† Cebion sachets (Abbott Laboratories): vitamin C, 1 g; aromatized excipient (including 8 mg of sodium saccharin) up to 6 g.

‡ Values in parentheses are relative standard deviations in % (n = 5).

§ Frenadol sachets (Abelló Laboratories): paracetamol, 600 mg; salicylamide, 100 mg; codeine phosphate, 10 mg; caffeine citrate, 30 mg; chlorpheniramine maleate, 4 mg; ascorbic acid, 500 mg; plus excipient with attached carbohydrate groups up to 10 g.

¶ Redoxon drops (Roche Laboratories): vitamin C, 200 mg; sodium saccharin, 2 mg; plus excipient up to 1 cm^3.

Table 4 Determination of ascorbic acid in urine by the peak-height FI method

Sample	Added/ mg cm^{-3}	Found*/ mg cm^{-3}	Recovery (%)
Synthetic urine	0.296	0.298	100.8
	0.501	0.510	101.9
	0.672	0.674	100.3
Human urine	0.000	0.129	—
	0.352	0.349	99.20
	0.528	0.542	101.06
	0.704	0.699	99.25

* Average of five determinations.

Calibration Graph

The equation of the calibration graph for determining ascorbic acid is $\Delta t = -26.63 \times \log$ [ascorbic acid] -9.16 ($r = 0.9926$), where Δt is expressed in seconds and [ascorbic acid] in mol dm^{-3}. The equation is satisfied for ascorbic acid concentrations between 2.0×10^{-3} and 5.0×10^{-2} mol dm^{-3}. Hence, by using the peak width as a quantitative parameter, it was possible to determine greater concentrations of ascorbic acid than by using the peak height.

The RSD ($n = 10$) for 7.5×10^{-3} mol dm^{-3} ascorbic acid was 2.02%.

Study of Interferents in Both Methods

The effect of foreign species in both FI methods was studied. the results for the determination of 4×10^{-3} mol dm^{-3} ascorbic acid are listed in Table 2. The tolerance limit was taken as the concentration causing an error of not more than ±3% in the determination of ascorbic acid. As can be seen, the proposed methods are sufficiently selective.

Applications

The first (peak-height) method was applied to the determination of ascorbic acid in three pharmaceuticals and urine and the second (peak-width) method only to the determination of ascorbic acid in pharmaceuticals.

The results obtained for pharmaceuticals are summarized in Table 3. Reproducibility was good in all instances. The results obtained with the proposed methods were compared with those given by the standard British Pharmacopoeia.[5]

The peak-height method was also tested for its applicability to the determination of ascorbic acid in urine. A recovery experiment was performed using a mixture to simulate human urine. The data from this study are summarized in Table 4. Recovery data were obtained by adding different amounts of standard ascorbic acid to the synthetic urine samples and subtracting the results obtained from samples prepared in a similar way but with no ascorbic acid added.

The results obtained for human urine samples containing ascorbic acid, in addition to the data from the recovery study, are summarized in Table 4 and show that the components of the urine do not interfere in the determination of ascorbic acid in the samples assayed. Recovery data were obtained in a similar way to that described for synthetic urine.

We gratefully acknowledge the Dirección General Científica y Técnica for financial support (PB 90-0008).

References

1 Looke, J. R., and Moxon, R. E. D., in *Vitamin C (Ascorbic Acid)*, eds. Counsell, J. M., and Horming, D. H., Applied Science Publishers, London, 1981, p. 167.
2 Briggs, M., *Vitamins in Human Biology and Medicine*, CRC Press, Boca Ration, FL, 1981.
3 Zloch, Z., *Chem. Listy*, 1988, **82**, 825.
4 Grolubkina, N. A., and Prudnik, O. V., *Zh. Anal. Khim.*, 1989, **44**, 1349.
5 *British Pharmacopoeia 1980*, The Pharmaceutical Press, London, 1980, vol. 1, p. 39.
6 *Official Methods of Analysis of the Association of Official Analytical Chemists*, ed. Williams, S., Association of Official Analytical Chemists, Washington, DC, 1984, p. 844.
7 *The United States Pharmacopeia XXI, The National Formulary XXVI*, US Pharmacopeial Convention, Rockville, MD, 1985, p. 75.
8 Karlberg, B., and Thelander, S., *Analyst*, 1978, **103**, 1154.
9 Strohl, A., and Curran, D., *Anal. Chem.*, 1979, **51**, 1045.
10 Curran, D. J., and Tougas, T., *Anal. Chem.*, 1984, **56**, 672.
11 Fogg, A. G., Summan, A. M., and Fernández-Arciniega, M. A., *Analyst*, 1985, **110**, 341.
12 Wang, J., and Frelha, B. A., *Anal. Chem.*, 1983, **55**, 1285.
13 Uchiyama, S., Tofuku, Y., and Suzuki, S., *Anal. Chim. Acta*, 1988, **208**, 291.
14 Bradberry, C., and Adams, R., *Anal. Chem.*, 1983, **55**, 2439.
15 Ikeda, S., Satake, H., and Yohri, Y., *Chem. Lett.*, 1984, **6**, 873.
16 Lunte, C., Wong, S., Redgway, T., Heineman, W., and Chan, K., *Anal. Chim. Acta*, 1986, **188**, 263.
17 Greenway, G. M., and Ongomo, P., *Analyst*, 1990, **115**, 1297.
18 Matuszewski, W., Torjanowicz, M., and Ilcheva, L., *Electroanalysis*, 1990, **2**, 147.
19 Karayannis, M., *Talanta*, 1976, **23**, 27.
20 Karayannis, M. I., and Farasoglou, D. I., *Analyst*, 1987, **112**, 767.
21 Hiromi, K., Kuwamoto, C., and Onishi, M., *J. Biochem.*, 1980, **100**, 421.
22 Yamane, T., and Ogawa, T., *Bunseki Kagaku*, 1987, **36**, 625.
23 Hernández-Mendez, J., Alonso, A., Almendral, M. J., and García de Maria, C., *Anal. Chim. Acta*, 1986, **184**, 243.
24 Lázaro, F., Ríos, A., Luque de Castro, M. D., and Valcárcel, M., *Analyst*, 1986, **111**, 163.
25 Lázaro, F., Luque de Castro, M. D., and Valcárcel, M., *Analusis*, 1987, **15**, 183.
26 Vanderslice, J., and Higgs, D., *Micronutr. Anal.*, 1989, **6**, 109.
27 Koupparis, M., and Anagnostopoulou, P., *Talanta*, 1985, **32**, 411.
28 Chang, F., and Cheng, K., *Mikrochim. Acta, Part II*, 1979, 219.

Paper 2/01057G
Received February 28, 1992
Accepted May 14, 1992

Problem of Concurrent Measurements of Peroxonitrite and Nitrite Contents

Robert C. Plumb* and John O. Edwards
Department of Chemistry, Brown University, Providence, RI 02912, USA
Melissa A. Herman
Department of Chemistry, Worcester Polytechnic Institute, Worcester, MA 01609, USA

It has been thought that metastable peroxonitrite, $ONOO^-$, does not interfere with the determination of nitrite, NO_2^-, because of evidence that it decays by isomerization to NO_3^-. In fact, the isomerization process is quantitative only under acidic conditions; partial decomposition to NO_2^- can take place in neutral solutions and quantitative decomposition to NO_2^- can occur in basic media with a metal catalyst. A method of analysis of these systems, based on these findings, is described. The details of the solution behaviour of $ONOO^-$ have not been recognized in the 50 years of studies of the photochemistry of nitrates where both NO_2^- and $ONOO^-$ are produced. As a result analyses were in error and changes in concentration of $ONOO^-$ with experimental variables have frequently appeared as changes in NO_2^- content, which were theoretically inexplicable.

Keywords: *Peroxonitrite and nitrite determination; decomposition of peroxonitrite; nitrite colorimetric analysis*

Although peroxonitrite, $ONOO^-$ (isomeric with NO_3^-), was synthesized prior to 1904[1] its importance in natural processes has only recently been recognized. It has been shown to have a role in such diverse areas as vascular damage in humans[2] and the generation of the Mars Viking biology experiment responses[3] and has been suggested as an active ingredient in photochemical smog and polar stratospheric clouds. Thus it has become important to analyse for $ONOO^-$ in systems such as photolysed solids and solutions and to distinguish it from chemically related species.

We focus here on the problem of determination of $ONOO^-$ and NO_2^- produced in nitrates by ultraviolet (UV) photolysis because the analyses of these systems have been subject to error for many decades. The methods proposed here can be extended to other systems containing $ONOO^-$ and NO_2^-.

The following brief summary of the history of this subject shows how the analytical problem came about. Narayanswamy[4] reported in 1935 that NO_2^- was produced by UV treatment of inorganic nitrates. He measured NO_2^- in solutions prepared from irradiated crystals. Although Gleu and Hubold[5] published a review of the solution chemistry of $ONOO^-$ at about the same time, photochemical and radiation chemical researchers over the next 30 years did not recognize that $ONOO^-$ was also a product of photolysis, and as we have found, is the principal product under many circumstances. Determinations of NO_2^- employing the colorimetric procedures developed by Shinn[6] were widely used and it was assumed the NO_2^- was formed in the solid. Researchers attempted to determine the dependences of NO_2^- formation upon the nature of the cation in nitrate salts, the crystal structure and similar independent variables. As we will show, the determinations of NO_2^- contents were, in many cases, in error because they included the NO_2^- generated from $ONOO^-$ when the samples were dissolved. Even after Papée and Petriconi[7] reported in 1964 that $ONOO^-$ was produced in irradiated nitrate solutions and Yurmazova *et al.*[8] reported in 1983 that $ONOO^-$ was formed in UV irradiated solid nitrates, the analytical problems continued.

Papée and Petriconi[7] adapted a permanganate potentiometric titration, used by Gleu and Hubold,[5] to the determination of $ONOO^-$. Before titration, the peroxonitrite was stabilized, by making the solution strongly alkaline, because peroxonitrite isomerizes to NO_3^- very rapidly when protonated, according to a mechanism determined by Mahoney.[9] Because the isomerization of $ONOO^-$ to NO_3^- had been established, Papée and Petriconi[7] and Bayliss and Bucat[10] carrying out related studies assumed that peroxonitrite did not interfere with nitrite determinations and continued to employ the colorimetric procedure for nitrite. In early work, before peroxonitrite was identified as a photolysis product, Pringsheim[11] and Maddock and Mohanty[12] had encountered difficulties in explaining the changes they found in nitrite levels during photobleaching and thermal bleaching of the colour centres that are formed in irradiated solid nitrates. They questioned the validity of the nitrite determinations. The most recent investigators[8,13] of the mechanism of photolysis have also stated that problems exist with the nitrite analytical method but have not identified the source of the problem or provided an alternative.

This paper describes experiments which show that peroxonitrite interferes with nitrite determinations when performed using the previous procedures. In addition, procedures that permit concurrent determinations of the two species are presented.

Experimental

Samples for analysis were prepared by crushing and sieving analytical-reagent grade KNO_3 to $250 < d < 420$ μm and irradiating in a rotating horizontal quartz tube with 254 nm photons from Southern New England (Hamden, CT, USA) UV RPR-2537 lamps. Photobleaching was performed with the same equipment but with 300 nm photons from RPR-3000 lamps.

Nitrite determinations were all performed by standard colorimetric procedures[14] but with the controlled dissolution conditions to be described. Samples were diluted with non-irradiated KNO_3 if necessary, to limit the nitrite content of the 50–100 mg samples used for assays to less than 1 μmol.

Degeneration of Peroxonitrite in Solution

It has been found[9] that the decay of peroxonitrite in solution by the isomerization path is first-order with respect to peroxonitrite. The published pseudo-first-order rate constants[7,15–18] and the pH profile for the isomerization reaction (calculated from measured activation parameters[19] and pK_a of

* Also at Department of Chemistry, Worcester Polytechnic Institute, Worcester, MA 01609, USA.

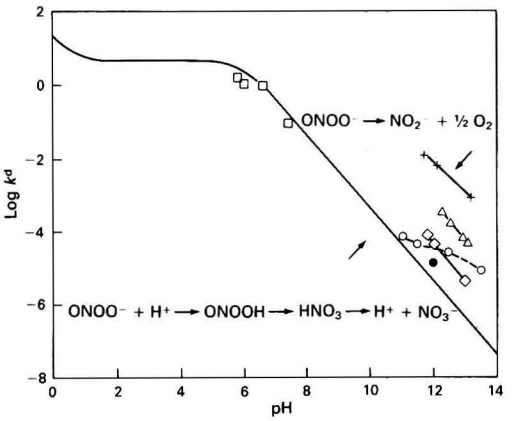

Fig. 1 Calculated pH profile (solid line) for the peroxonitrite isomerization reaction and the measured pseudo-first-order rate constants for decay of peroxonitrite in solution. □, Barat *et al.* (ref. 15); ○, Papée and Petriconi (ref. 7); ●, Petriconi and Papée (ref. 16); △, Hughes and Nicklin (ref. 17); ◇, Hughes *et al.* (ref. 18); and +, this work

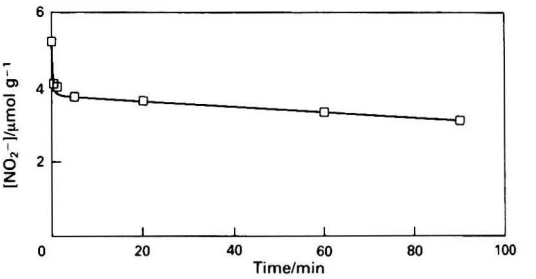

Fig. 2 Nitrite content observed on acid dissolution of samples of irradiated KNO_3, which had given a nitrite level of 28.5 μmol g^{-1} when subjected to base dissolution. HCl (0.01 mol dm^{-3}) was added to the samples while mixing with a vortex mixer and, at various time intervals after addition of acid, base was added to raise the pH to 10. The NO_2^- was then determined

peroxonitrous acid[20]) are shown in Fig. 1. The measurements of Barat *et al.*[15] in the pH range 5.8–7.4, which employed flash photolysis and transient absorption spectra, agree well with the pH profile curve for the isomerization path. Experimental results at pH ≥ 10 obtained by Papée and Petriconi,[7] Petriconi and Papée,[16] Hughes and Nicklin[17] and Hughes *et al.*[18] are substantially faster than expected for the isomerization process. Their pH dependence is indicative of an acid catalysed process. Those results were obtained by measuring the rate of loss of $ONOO^-$ without monitoring the concentrations of products. All these workers assumed that isomerization to NO_3^- was occurring. The results of similar studies by us in which the kinetics of decay were followed by measurements of products are also shown in Fig. 1. The KNO_3, which had been irradiated at 254 nm, was dissolved in solutions of varying pH with 2×10^{-4} mol dm^{-3} Cu^{II} catalyst present. After a period of elapsed time (ranging from 1 to 120 min) the solutions were acidified to isomerize the remaining $ONOO^-$, and the nitrite levels measured by colorimetry. The decrease in $ONOO^-$ as measured by NO_2^- formation obeyed first-order kinetics, as did the isomerization process.

The results demonstrate that peroxonitrite decomposes to nitrite in alkaline solution in the presence of a metal catalyst many times faster than the rate at which it is expected to isomerize. We believe that some or even a large part of the decay of $ONOO^-$ at higher pH values, which was attributed to isomerization by previous investigators, was in fact, decomposition to nitrite because the observed rate constants were substantially higher than predicted from the known activation parameters of the isomerization reaction. The variability of the results obtained by previous investigators suggests that adventitious metal catalysts may have been involved. Copper(II) was selected for the studies described here because it has been found to be effective as a catalyst in a variety of peroxide systems. As the rate constants found for decomposition to nitrite are about 1000 times greater than expected for isomerization, it is to be expected that quantitative conversion of peroxonitrite into nitrite might be achieved with a copper ion catalyst in alkaline solution.

Nitrous acid, formed by protonation of NO_2^- when nitrite containing salts are dissolved in acidic solutions, tends to disproportionate to form NO_3^- and NO. However, the rate constant for loss of NO_2^- in the acidic solutions with which we are concerned is several orders of magnitude smaller than the rate constant for isomerization of $ONOO^-$. Experimental results demonstrating these effects are shown in Fig. 2. By neutralizing the sample obtained from acidic dissolution with base before analysis for nitrite one can observe, at short times, the NO_2^- generated from $ONOO^-$, which had not yet isomerized and, at longer times, the much slower degeneration of NO_2^-. Complete isomerization of $ONOO^-$ to NO_3^- can be obtained in less than 5 min after dissolution. Neutralization of the resulting solution with base within 5 min restricts the loss of NO_2^- by decomposition to <1%.

Analytical Procedure for the Determination of Peroxonitrite and Nitrite

The kinetic studies suggest that the nitrite levels measured colorimetrically when irradiated salts are dissolved in acidic solutions measure the nitrite concentration in the salt whereas the nitrite level found when irradiated salts are dissolved in basic solutions with a metal catalyst, and given time to decompose, is the sum of the nitrite and peroxonitrite concentrations. On this basis the following procedures have been developed for analysis of irradiated Group I nitrates.

Procedure and reagents

Dissolution of samples. Weighed samples of up to 100 mg are placed in 10 cm^3 test-tubes. About 1 cm^3 of solvent is injected rapidly into the tube while swirling the powder on a vortex mixer, until dissolution is complete. For acidic dissolution 0.01 mol dm^{-3} HCl is used. To prepare the base dissolution reagent 200 mm^3 of 0.01 mol dm^{-3} $CuSO_4$ solution are added to 10 mm^3 of 0.01 mol dm^{-3} KOH just prior to use.

Treatment after dissolution. Samples from base dissolution are allowed to decompose for ≈1 h, then transferred into a calibrated flask and NO_2^- is determined colorimetrically by standard procedures.[14] Samples from acid dissolution are allowed to decompose for 5 min, then made alkaline by the addition of 2 mm^3 of 0.01 mol dm^{-3} KOH, transferred into a calibrated flask and analysed for NO_2^-.

Fig. 3 shows the nitrite levels from a series of KNO_3 samples that had been irradiated for increasing periods of time using acid dissolution, base dissolution and dissolving in unbuffered water.

The interpretation of the lower curve of Fig. 3 as the nitrite concentration and the upper curve as the sum of the nitrite and peroxonitrite levels is supported by comparison with potentiometric analysis. Triplicate potentiometric analyses[7] completed within 20 min of dissolution at pH 12.4 with no copper catalyst gave 26.0 ± 1.4 μmol g^{-1} whereas duplicate analyses of the same material by the procedures proposed here gave 26.4 ± 0.6 μmol g^{-1}. Thus, the peroxonitrite levels measured by these procedures appear to be accurate. In order to determine if isomerization in acidic solution is quantitative in

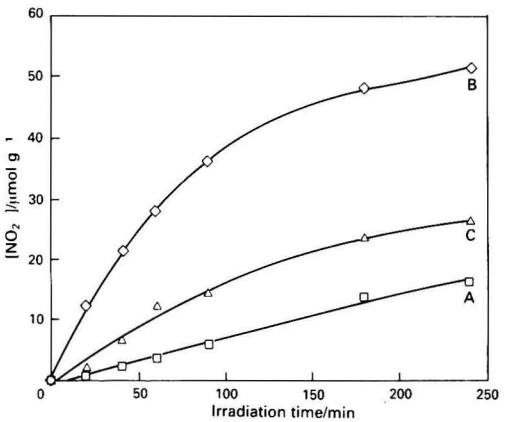

Fig. 3 Measured nitrite concentrations in samples of KNO_3 that had been irradiated at 254 nm for various time intervals, using the acid (A) and base (B) dissolution procedures described in the text and also with rapid dissolution in distilled (unbuffered) H_2O (C)

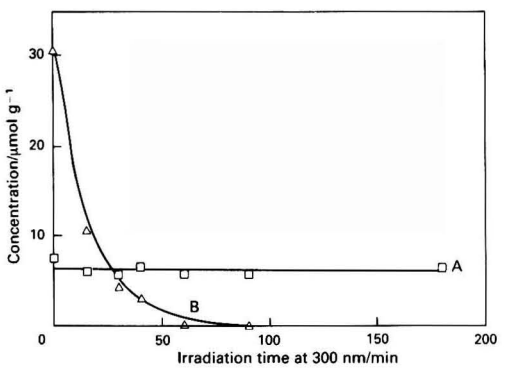

Fig. 4 Measured concentrations of nitrite (A) and peroxonitrite (B) in 254 nm irradiated KNO_3 after various periods of photobleaching with 300 nm photons

eliminating the influence of $ONOO^-$ upon the determination of NO_2^- further experiments (shown in Fig. 4) were performed. These experiments were based on the fact that the yellow colour due to $ONOO^-$ in irradiated nitrates can be photobleached with 300 nm radiation. Measurements by Fourier transform infrared spectroscopy indicate that the photobleaching process is an isomerization and does not involve NO_2^- formation.[21] When the composition changes produced by photobleaching were measured by the controlled dissolution procedures it was found that the $ONOO^-$ level decreased to zero with pseudo-first-order kinetics and the NO_2^- level was not altered. This demonstrates that $ONOO^-$, when present, does not interfere with the NO_2^- determination.

The nitrite contents measured when samples are dissolved in distilled H_2O, as in Fig. 3, show the type of error when the procedures used by the several earlier groups who have studied photolysis and radiolysis of nitrate crystals are followed. Under these conditions, both $ONOO^-$ and NO_2^- in the solid contribute to the measured NO_2^- level. Processes such as photobleaching and thermal degeneration that affect the $ONOO^-$ level will appear to change the NO_2^- level if the determinations are carried out in that way. This appears to have been the source of the spurious results that caused some previous investigators[8,11–13] to question the validity of the analytical method.

The procedures described here are considered to be directly applicable to systems where the cations in the solution do not undergo significant hydrolysis. It is anticipated that they can be extended to other systems by inclusion of suitable buffers and chelating agents in the dissolution reagents.

This work was partially supported by a research grant from the National Aeronautics and Space Administration (USA).

References

1 Raschig, F., *Z. Angew. Chem.*, 1904, **17**, 1419.
2 Beckman, J. S., Beckman, T. W., Chen, J., Marshall, P. A., and Freeman, B. A., *Proc. Natl. Acad. Sci. USA*, 1990, **87**, 1620.
3 Plumb, R. C., Tantayanon, R., Libby, M., and Xu, W. W., *Nature (London)*, 1989, **338**, 633.
4 Narayanswamy, L. K., *Trans. Faraday Soc.*, 1935, **31**, 1411.
5 Gleu, K., and Hubold, R., *Z. Anorg. Allg. Chem.*, 1935, **223**, 305.
6 Shinn, M. B., *Ind. Eng. Chem., Anal. Ed.*, 1941, **13**, 33.
7 Papée, H. M., and Petriconi, G. L., *Nature (London)*, 1964, **204**, 142.
8 Yurmazova, T. A., Koval, L. N., and Serikov, L. V., *Khim. Vys. Energ.*, 1983, **17**, 151.
9 Mahoney, L. R., *J. Am. Chem. Soc.*, 1970, **92**, 5262.
10 Bayliss, N. S., and Bucat, R. B., *Aust. J. Chem.*, 1975, **28**, 1865.
11 Pringsheim, P., *J. Chem. Phys.*, 1955, **23**, 1113.
12 Maddock, A. G., and Mohanty, S. R., *Radiochim. Acta*, 1963, **1**, 85.
13 Miklin, M. B., Kriger, L. D., Ananev, V. A., and Nevostruev, A. A., *Khim. Vys. Energ.*, 1989, **23**, 506.
14 *Standard Methods for the Examination of Water and Wastewater*, American Public Health Association, Washington, DC, 16th edn., 1985, pp. 404–406.
15 Barat, F., Gilles, L., Hickel, B., and Sutton, J., *J. Chem. Soc. A*, 1970, 1982.
16 Petriconi, G. L., and Papée, H. M., *J. Inorg. Nucl. Chem.*, 1968, **30**, 1525.
17 Hughes, M. N., and Nicklin, H. G., *J. Chem. Soc. A*, 1970, 925.
18 Hughes, M. N., Nicklin, H. G., and Sackrule, N. A. C., *J. Chem. Soc. A*, 1971, 3722.
19 Benton, D. J., and Moore, P., *J. Chem. Soc. A*, 1970, 3179.
20 Shuali, U., Ottolenghi, M., Rabani, J., and Yelin, Z., *J. Phys. Chem.*, 1969, **73**, 3445.
21 Plumb, R. C., and Edwards, J. O., *J. Phys. Chem.*, 1992, **96**, 3245.

Paper 1/05691C
Received November 8, 1991
Accepted May 12, 1992

Interaction of Hydrophobic Anions With Cationic Dyes and Its Application to the Spectrophotometric Determination of Anionic Surfactants

Mitsuko Oshima, Shoji Motomizu and Hirofumi Doi
Department of Chemistry, Faculty of Science, Okayama University, 3-1-1 Tsushimanaka, Okayama-shi, 700 Japan

The change in absorption spectra of Ethyl Violet solution on addition of anionic surfactants in an aqueous solution was used for the determination of anionic surfactants. This change is caused by the hydrophobic interaction between the bulky dye and the detergent. The contribution from the substituents of the cationic dyes and anionic surfactants to the hydrophobicity is discussed. The calibration graph is linear over the concentration range from 4×10^{-6} to 4×10^{-5} mol dm^{-3}. The molar absorption coefficient for lauryl sulfate is 1.76×10^{3} m^{2} mol^{-1} at 700 nm.

Keywords: *Hydrophobic interaction; aggregate; determination of anionic surfactants; Ethyl Violet; spectrophotometry*

Bulky cationic or anionic dyes form aggregates at high concentrations in aqueous solution.[1] These aggregates often exist in a stacked form by overlapping their hydrophobic groups, such as the benzene ring.[2] The formation of aggregates accompanies changes in the absorption spectrum. Takada *et al.*[3] reported that these changes were also caused by addition of the tetraphenylborate anion (TPB^-) to Crystal Violet or Rhodamine 6G solution at a concentration lower than that required for aggregate formation of the dyes. They supposed that TPB^- promoted the aggregation. This phenomenon seems to be a result of interaction between the anion and the cation, which has bulky and/or hydrophobic groups, when present at or near the concentration of aggregate or precipitate formation in an aqueous solution.

Generally, anionic surfactants are determined by spectrophotometric techniques, which are based on extraction of the ion associates of anionic surfactants and cationic dyes, *e.g.*, the Methylene Blue[4] and Ethyl Violet methods.[5] Although these methods are highly sensitive, the procedures are often complicated and time consuming. Sato *et al.*[6] reported that an anionic detergent when present at concentrations below the critical micellization concentration of the detergent caused changes in the absorption spectrum of a cationic dye, which were due to the formation of a dye–detergent aggregate. In this paper, anionic surfactants were determined in homogeneous aqueous solution using hydrophobic interaction with a cationic dye. The method is very simple, rapid and can be applied to the determination of lauryl sulfate over the range 1×10^{-5}–4×10^{-5} mol dm^{-3} with a 10 mm pathlength cell and 4×10^{-6}–1×10^{-5} mol dm^{-3} with a 20 mm pathlength cell.

Experimental

Apparatus

Spectrophotometric measurements were made using a Hitachi 139 spectrophotometer and a Shimadzu UV-300 scanning spectrophotometer with 0.1, 1 and 10 mm pathlength cells. A Hitachi–Horiba M-5 pH meter was used for pH measurement.

Reagents

Cationic dyes

Ethyl Violet (EV, Tokyo Kasei Kogyo), Brilliant Green (BG, Tokyo Kasei Kogyo), Crystal Violet (CV, Tokyo Kasei Kogyo), Malachite Green (MG, Wako Pure Chemicals) and Hoffmann's Violet (HV, Tokyo Kasei Kogyo) were dissolved in distilled water containing 0.04 mol dm^{-3} phosphate buffer solution (pH 6.4). When the dyes were dissolved in ethanol, buffer solution was not added. The details of the dyes used are listed in Table 1.

Table 1 Dyes tested

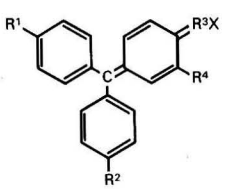

Dye	Colour Index No.	R^1	R^2	R^3	R^4	X	*C* value	Hansch and Leo value[8]
Ethyl Violet	42600	NEt_2	NEt_2	NEt_2^+	H	$Cl^- \cdot 0.5\,ZnCl_2$	14.31	3.54
Brilliant Green	42040	NEt_2	H	NEt_2^+	H	HSO_4^-	13.14	2.36
Hoffmann's Violet	42530	NHEt	NHEt	$NHEt^+$	CH_3	Cl^-	12.54	0.80
Crystal Violet	42555	NMe_2	NMe_2	NMe_2^+	H	Cl^-	11.95	0.54
Malachite Green	42000	NMe_2	H	NMe_2^+	H	Oxalate*	11.20	0.36

* $0.5\,(COO)_2^{2-} \cdot (COOH)_2$.

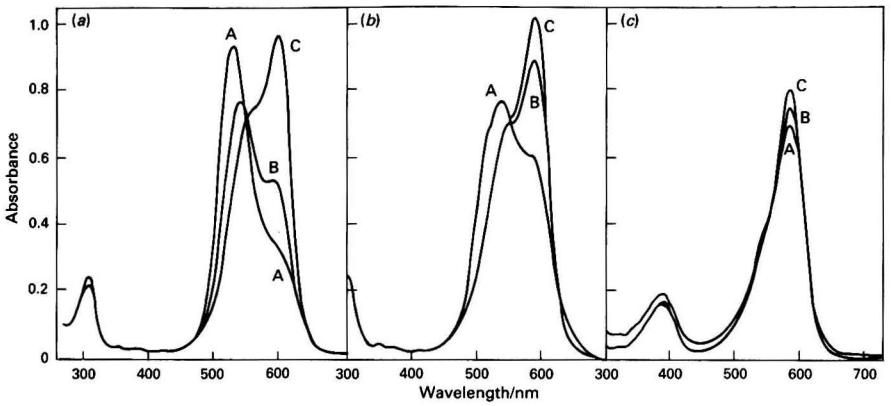

Fig. 1 Absorption spectra of cationic dyes: (*a*) EV^+; (*b*) CV^+; and (*c*) MG^+. Concentration of dyes (cell pathlength, mm): A, 1×10^{-3} (0.1); B, 1×10^{-4} (1); and C, 1×10^{-5} mol dm^{-3} (10)

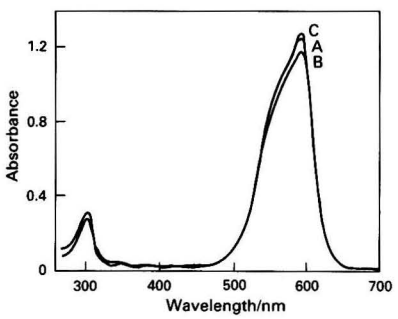

Fig. 2 Absorption spectra of Ethyl Violet in ethanol. Concentration of EV (cell pathlength, mm): A, 1×10^{-3} (0.1); B, 1×10^{-4} (1); and C, 1×10^{-5} mol dm^{-3} (10)

Anionic surfactants

These were all sodium salts. Octane-1-sulfonate, decane-1-sulfonate, dodecane-1-sulfonate (DS), tetradecane-1-sulfonate and hexadecane-1-sulfonate were all purchased from Tokyo Kasei Kogyo. Lauryl sulfate (LS, Wako Pure Chemicals; for water test, 99.9%), dodecylbenzenesulfonate (DBS, Wako Pure Chemicals; purity more than 99.2%) and di-2-ethylhexylsulfosuccinate (SSS, Kanto Chemicals; standard substance of Japan Oil Chemistry Association) were also used. The surfactants were dissolved in water after drying at 50 °C under reduced pressure (about 400 Pa) until constant mass was obtained.

Non-ionic surfactants

Poly(vinyl alcohols) (PVAs) of average molecular mass: PVA 205, 2.2×10^4; PVA 217, 7.5×10^4; and PVA 224, 10.6×10^4, obtained from Kuraray and Triton X-100 [C_8H_{17}–C_6H_4O–$(CH_2CH_2O)_{10}H$] obtained from Wako Pure Chemicals were used.

Standard Procedure

To a 25 cm^3 calibrated flask, transfer 1 cm^3 of phosphate buffer solution (pH 6.4, 1 mol dm^{-3}), 20 cm^3 of sample solution and 2 cm^3 of 1×10^{-3} mol dm^{-3} EV solution, and mix. After 5 min, add 1 cm^3 of 0.5% m/v PVA 205 solution and make up to the mark with water, then mix thoroughly. Measure the absorbance at 700 nm.

Results and Discussion

Changes in Absorption Spectra of Cationic Dyes in Aqueous or Ethanol Solution

In Fig. 1, the absorption spectra of EV, CV and MG in aqueous solution are shown at concentrations from 1×10^{-3} to 1×10^{-5} mol dm^{-3} with 0.1, 1 and 10 mm pathlength cells, respectively. The changes in the absorption spectra of BG and HV were small. In order to confirm that aggregate formation is characteristic in aqueous medium, the absorption spectra of the cationic dyes in ethanol were recorded. Fig. 2 shows the spectra of EV at various concentrations. The differences in absorbances at the wavelength of maximum absorption in Fig. 2 are due to cell errors. The cell errors were tested with *p*-nitrophenol solution at 398 nm. When the transmittance with the 10 mm pathlength cells was taken as 100%, those with the 0.1 and 1 mm pathlength cells were 98.8 and 94.5%, respectively. In ethanol, which is a more hydrophobic medium than water, the shift in absorption did not occur because the cationic dyes were dispersed homogeneously.

In aqueous solution, the higher the concentrations of the dyes, the larger the shifts of wavelengths. This tendency was strongly related to the order of the hydrophobicity of the dyes, EV>HV>CV>BG>MG, and for all except BG, agreed with the order for the *C* values,[7] which are a measure of the extractability of the cations into chloroform. The *C* values obtained experimentally were as follows: EV, 14.31; BG, 13.14; HV, 12.54; CV, 11.95; and MG, 11.20. These values are comparable to the substituent constants (π) of Hansch and Leo:[8] EV, 3.54; BG, 2.36; HV, 0.80; CV, 0.54; and MG, 0.36. These values are summarized in Table 1 with their structural relationships. Stork *et al.*[9] reported that this phenomenon seems to be caused by the formation of aggregates, which stack their hydrophobic groups as $n(C^+) \rightleftharpoons (C)_n{}^{n+}$, where C and *n* denote the cationic dye and the aggregation number, respectively. They reported a value of 2 for *n* at a concentration of about 1×10^{-3} mol dm^{-3} CV.

Selection of Cationic Dyes

Fig. 3 shows the absorption spectra of EV with LS solution added. A new absorption peak appears above 650 nm, and the absorption peaks at 540 and 600 nm decrease. These changes are different from that for the cationic dye aggregation. The shift in absorption spectra is due to the formation of the ion associate and at higher concentrations of the anionic surfactants might be due to the formation of more complex species. The changes in absorbance caused by the addition of LS

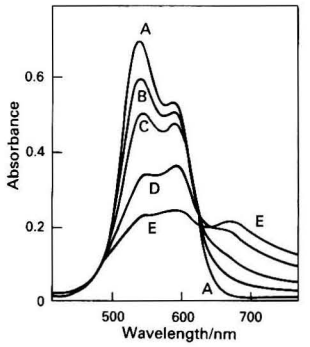

Fig. 3 Absorption spectra of Ethyl Violet with lauryl sulfate solution. EV, 8.0×10^{-5} mol dm^{-3}; PVA, 0.02%; pH, 6.6; cell pathlength, 1 mm. Concentration of LS: A, 0; B, 2.0×10^{-5}; C, 4.0×10^{-5}; D, 6.0×10^{-5}; and E, 8.0×10^{-5} mol dm^{-3}

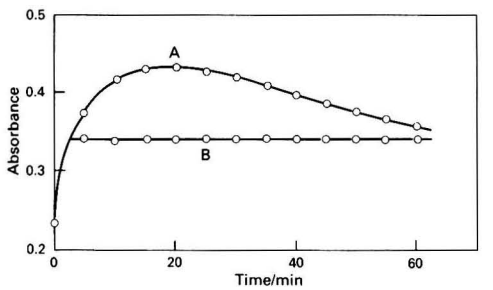

Fig. 4 Effect of standing time after mixing Ethyl Violet and lauryl sulfate. Conditions: EV, 8.0×10^{-5} mol dm^{-3}; LS, 2.0×10^{-5} mol dm^{-3}; pH, 6.6; cell pathlength, 10 mm; and λ, 700 nm. Concentration of PVA: A, 0; and B, 0.02% m/v

increased in the order of the hydrophobicity of the cationic dyes, *i.e.*, EV>CV>BG>HV>MG. Ethyl Violet was selected for the determination of the anionic surfactants. The measurements were carried out at 700 nm where the absorbance from the reagent blank was very small. The decrease in the absorbance near 540 nm on the addition of anionic surfactants appears to be larger than the increase at 700 nm, but its reproducibility is poor and the determination range limited.

Addition of Non-ionic Surfactants

The absorbances at 700 nm changed with time as shown in Fig. 4. The increase in absorbance over the first 5 min seems to be the stabilization time for the colour development and the decrease after this time seems to be the formation of the precipitate or adsorption. Therefore, the addition of non-ionic surfactants, *i.e.*, Triton X-100 and PVA, in order to maintain homogeneity was tested. Triton X-100 did not show a marked stabilizing effect. Three types of PVA were tested, PVA 205, PVA 217 and PVA 224, which had different average molecular masses; although the absorbances were almost identical for each, PVA 205 was the best in terms of reproducibility. The optimum concentration of PVA 205 was tested over the range 0.01–0.2% m/v. The lower the concentration, the higher the absorbance, but the absorbances at a level of 0.01% m/v gradually decreased with time, hence 0.02% m/v was chosen. The timing of the addition was also tested. As shown in Fig. 4, the addition of PVA 205 is recommended 5 min after the addition of the EV solution; the absorbances were then constant and stable for 1 h.

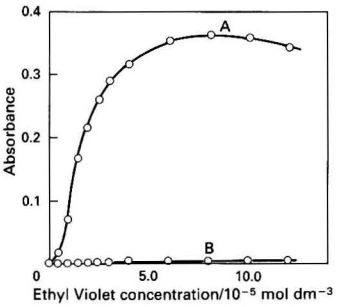

Fig. 5 Effect of Ethyl Violet concentration: A, 2.0×10^{-5} mol dm^{-3} LS; and B, reagent blank (other conditions except EV concentration are the same as in Fig. 4)

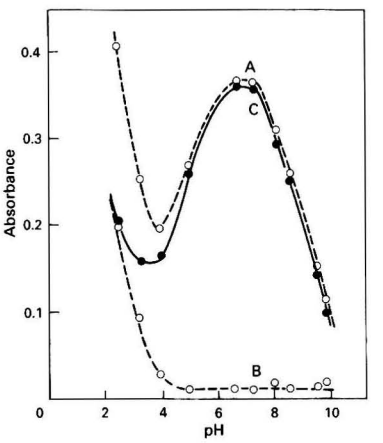

Fig. 6 Effect of pH. A, 2.0×10^{-5} mol dm^{-3} LS; B, reagent blank; and C, net absorbance (other conditions except pH are the same as in Fig. 4)

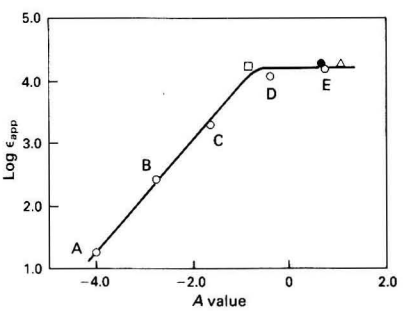

Fig. 7 Plots of log ε_{app} and A values. Alkyl sulfonate (○) with carbon numbers of the alkyl group: A, 8; B, 10; C, 12(DS); D, 14; and E, 16. □, LS; ●, DBS; and △, SSS

Effect of EV Concentration and Molar Ratio

As shown in Fig. 5, maximum and constant absorbances were obtained from 6×10^{-5} to 8×10^{-5} mol dm^{-3} of EV; a concentration of 8×10^{-5} mol dm^{-3} was chosen. From Fig. 5, it can be seen that LS reacts in a 1:1 molar ratio with EV.

Table 2 Effect of foreign ions (concentration of LS was 2×10^{-5} mol dm^{-3} and the absorbance was 0.349)

Ion	Tolerable concentration*/mol dm^{-3}
NH_4^+, Mg^{2+}, Fe^{3+}, Cl^-, SiO_3^{2-}	1×10^{-3}
Ca^{2+}, NO_3^-, SO_4^{2-}, HCO_3^-	5×10^{-4}
I^-	1×10^{-4}
ClO_4^-	1×10^{-6}

* Concentrations within 2.5% error of the absorbance of 0.349.

Effect of pH

The effect of pH is very marked, as shown in Fig. 6. This is caused by the dissociation of EV.

$$HEV^{2+} \rightleftharpoons H^+ + EV^+$$
$$K_{a_1} = [H^+][EV^+]/[HEV^{2+}] = 2.07 \times 10^{-4}$$
$$EV^+ + OH^- \rightleftharpoons EVOH$$
$$K_{a_2} = [EVOH]/[EV^+][OH^-] = 4.73 \times 10^4$$

At a pH of lower than 4, the HEV^{2+} species is dominant at the maximum absorption wavelength (440 nm) and at a pH higher than 8.5 the colour of EV^+ disappears due to a change to the colourless carbinol form (EVOH). As a result, the pH was adjusted to 6.6 with phosphate buffer solution.

Reactivity of Anionic Surfactants

The apparent molar absorption coefficients of the ion associate of EV^+ and the anionic surfactants were plotted against the *A* values (Fig. 7). The *A* value is a measure of the extractability of the anions, *i.e.*, a measure of the hydrophobicity, which is obtained experimentally by extraction into chloroform as the ion pair using a pyridylazo dye cation.[7] The values are as follows: SSS, 0.98; DBS, 0.43; LS, −1.02; and DS, −1.70. The apparent molar absorption coefficients of the ion associates are comparable to the reactivities of the anions, provided the paired cations are the same. The reaction with alkylsulfonates was accomplished when the *A* values were larger than −0.9, corresponding to more than 14 carbon atoms in the alkyl group. The reactivity of the surfactants increased in the order of their hydrophobicity, *i.e.*, SSS>DBS>LS>>DS.

Calibration Graph

Calibration graphs were linear over the range 1×10^{-5}–4×10^{-5} mol dm^{-3} of LS with a 10 mm pathlength cell, and 4×10^{-6}–1×10^{-5} mol dm^{-3} with a 20 mm pathlength cell. The apparent molar absorption coefficient was about 1.8×10^3 m^2 mol^{-1} for LS with a 10 mm pathlength cell.

Effect of Foreign Ions

Co-existing ions usually present in river waters were tested. The results are shown in Table 2. Almost all of the ions tested did not interfere with the determination; however, Ca^{2+} precipitated with the phosphate ion in buffer solutions above 1×10^{-3} mol dm^{-3}. It is noteworthy that the iodide and perchlorate ions did not interfere at the concentrations at which they usually cause large reagent blank signals in extraction spectrophotometry.

Conclusions

The proposed method is very simple and rapid, and there is no pollution from harmful solvents as the reaction is carried out in a homogeneous aqueous solution. The application to use in flow injection was examined, but there was noticeable baseline drift from adsorption of EV either onto the flow cell or the tubing walls. As the reaction is quantitative, with some improvement the determination of anionic surfactants by flow injection will be possible.

References

1 *Aggregation Processes in Solution*, eds. Wyn-Jones, E., and Gormally, J., Elsevier, Amsterdam, 1983, p. 241.
2 Craven, B. R., Griffith, J. C., and Kennedy, J. G., *Aust. J. Chem.*, 1975, **28**, 1971.
3 Takada, N., Sonoda, T., and Kobayashi, H., *Bunseki Kagaku*, 1983, **32**, E191.
4 Longman, G. F., *The Analysis of Detergents and Products*, Wiley, London, 1975, p. 499.
5 Motomizu, S., Fijiwara, S., Fijiwara, A., and Tôei, K., *Anal. Chem.*, 1982, **54**, 392.
6 Sato, H., Kawasaki, M., Kasatani, K., Nakashima, N., and Yoshihara, K., *Bull. Chem. Soc. Jpn.*, 1983, **56**, 3588.
7 Motomizu, S., *Bunseki Kagaku*, 1989, **38**, 147.
8 Hansch, C., and Leo, A., *Substituent Constants for Correlation Analysis in Chemistry and Biology*, Wiley, New York, 1979, p. 49.
9 Stork, W. H. J., Lippits, G. J. M., and Mandel, M., *J. Phys. Chem.*, 1972, **76**, 1772.

Paper 2/00683I
Received February 10, 1992
Accepted June 23, 1992

BOOK REVIEWS

Pharmaceutical Drugs

International Agency for Research on Cancer. *IARC Monographs on the Evaluation of Carcinogenic Risks to Humans. Volume 50.* Pp. 415. World Health Organization. 1990. Price Sw.Fr.65.00 ISBN 92-832-1250-9.

This volume reports the findings of a group of experts who met in 1989 to evaluate the carcinogenic risks associated with six antineoplastic and immunosuppressive agents, four antimicrobial agents and five other drugs. Included in the first category were azacitidine, chlorozotocin, ciclosporin, prednimustine, thiotepa and trichlormethine (trimustine hydrochloride). The antimicrobial agents studied were ampicillin, chloramphenicol, nitrofural (nitrofurazone) and nitrofurantoin. Cimetidine, dantron (chrysazin; 1,8-dihydroxyanthraquinone), furosemide (frusemide), hydrochlorothiazide and paracetamol (acetaminophen) were also evaluated.

Each monograph contains chemical and physical data relating to the pure substance, which will be of interest to the analytical chemist. A list of technical products and tradenames, details of production and use, as well as biological data relating to toxicity and metabolism are also given. Data on human studies are included as well as epidemiological studies. The sections on analysis are generally very short and concentrate on key references to reviews. Many of the references are fairly old. No details of the performance criteria for the analytical methods are presented.

The book concludes with a useful one-page summary of the final evaluations. This is followed by Appendix 1, which tabulates the genetic and related effects of each compound in various biological systems, both *in vivo* and *in vitro*, mammalian and non-mammalian. Appendix 2 contains activity profiles for genetic and related effects and forms a major part of the volume. This information is primarily of interest to a toxicologist and it reports the lowest effective concentration and highest ineffective concentration tested, together with a reference to the original work. There is also a cumulative cross-index covering all 50 volumes in the series. This is a useful reference since many compounds have been studied on more than one occasion by the committee of experts as new evidence is obtained. Other IARC publications are also listed.

N. T. Crosby

Iron Oxides in the Laboratory: Preparation and Characterization

By U. Schwertmann and R. M. Cornell, Pp. xiv + 137. VCH. 1991. Price DM118.00; £45.00. ISBN 3-527-26991-6; 0-89573-858-9.

This is a modest little book filled with an interesting mixture of information on the preparation and characterization of iron oxide materials. It is a book that fits snugly into a pocket of a lab coat and indeed that is where it should be kept since it contains just the sort of information that is invaluable whilst working at the bench. The preparative procedures are written in a concise straightforward manner, the resulting product is described and useful comments are added. Representative data are clearly presented and include X-ray diffraction profiles, electron micrographs (of good quality reproduction), ^{57}Fe Mössbauer and infrared spectra and colour charts. The approach is entirely systematic. The opening introductory chapter covers oxide structures and the location of these materials in the natural environment. The next two chapters are general in content describing aspects of synthetic methods and characterization, respectively. The chapter on characterization is somewhat uneven, for example, although eight pages are devoted to discussing colour measurement, there is only one paragraph dealing with Mössbauer spectroscopy, which is an important technique for these materials. The remaining chapters are short and describe preparative methods and characterization of individual oxides (goethite, lepidocrocite, feroxyhite, ferrihydrite, akaganeite, hematite, magnetite, maghemite and green rusts) and their metal ion substituted (*e.g.*, Al, Cr and Mn) counterparts.

This book succeeds in communicating the essential details of workable procedures in iron oxide chemistry. There is nothing new here, or of particular intellectual challenge, but the distillation of a vast literature into a readable, usable manual is sure to be welcomed by scientists in many fields (mineralogy, geology, soil science, corrosion and industrial pigments). In my own field of biomineralization, this book will be very useful to students involved in biogenic iron oxides. I only wish it had been published seven years ago when we started these studies; it would have then saved us a lot of time and effort in establishing reproducible routes to the controlled synthesis of iron oxides and related materials.

S. Mann

Polymers for Microelectronics. Science and Technology

Edited by Y. Tabata, I. Mita, S. Nonogaki, K. Horie, S. Tagawa. Pp. xxv + 848. VCH. 1990. Price DM280.00; £112.00. ISBN 0-89573-987-9 (VCH, New York).

The proceedings of an international symposium entitled 'Polymers for Microelectronics' (PME '89) held in Tokyo, Japan, October 29–November 2, 1989 are combined to make up this book. This was reported as being the first international meeting in this field to be held in Japan. The book comprises 67 lengthy, referee-reviewed papers presented at the meeting. The collection of articles covers many important aspects of polymers in microelectronics organized into three sections: fundamental and applied research on resists and related compounds; photosensitive polymers for optical memory and related applications; and polyimides and related functional polymers for electronics. A comprehensive index helps the reader find items of particular interest with ease.

The contents of the book clearly reflect the wide range of basic and applied research currently under investigation in this field of advanced technology. The main topics addressed in the book are photo- and radiation physics, chemistry of polymers, photoresponsive polymers, photochemical hole burning, resist materials and lithographic processes. The role of analytical chemistry in this field of research is clearly identified in the collection of articles presented. Various analytical techniques ranging from spectroscopy to gravimetry to electrochemical methods are used as tools by many of the authors. Several of the included studies monitor radiation-induced degradation of polymers. The effect of the irradiation processes are illustrated by 'before and after' spectra obtained by IR and UV spectrophotometry, electron spin resonance spectroscopy and nuclear magnetic resonance spectroscopy. The use of thermogravimetric analysis is reported in a number of papers as a means of monitoring mass changes during polymer degradation. New resist materials and new methods of developing resists are also covered in the book. Surface imaging plays an important role in these studies and the use of techniques such as X-ray fluorescence spectroscopy and scanning electron microscopy are the chosen analytical techniques for this purpose.

As polymers continue to play an important role in the microelectronics industry, this book should prove to be a

useful reference text to anyone interested in this area of research. This state-of-the-art report is particularly recommended to chemists and physicists active in this field.

Susan A. Darke

Analytical Biotechnology: Capillary Electrophoresis and Chromatography
Edited by Csaba Horváth and John G. Nikelly. ACS Symposium Series No. 434. Pp. x + 213. American Chemical Society. 1990. Price $49.95. ISBN 0-8412-1819-6.

It would perhaps have been of more immediate impact to the prospective reader if the title and subtitle of this volume had been interchanged, since this symposium volume is entirely devoted to contributions in analytical electrophoresis and chromatography. Nevertheless, such is the accelerating importance of analytical chemical techniques as applied to biotechnology, that readership among those in this area is clearly the goal of the editors. As the editors remark in their preface, no treatise yet exists in this rapidly developing area, and indeed any such would be rapidly outdated. Thus a symposium volume format can supply a valid critical overview of the state of the art in the field at the symposium time, provided that the participants are leaders in the field, and also the papers are written in a timely manner and updated as appropriate before publication.

All of these criteria apply to this volume. The first four chapters are concerned with capillary electrophoresis. The introductory chapter by Guzman, Hernandez and Terabe is written with the novice in mind; the authors cover basic ideas non-theoretically and with much practical advice on equipment and procedure. Application papers cover the use of capillary zone electrophoresis (CZE) in pharmaceutical quality control, the separation of cyclic nucleotides and on-column radioisotope detection, but unfortunately lacking is any coverage of the rapidly developing technique of CZE-mass spectrometry.

A valuable overview of liquid chromatographic strategies for biological pharmaceuticals is given by Canova-Davis and colleagues. Protein HPLC separations are a clear focus with preparative as well as analytical studies being described. In the preparative field, displacement chromatographic procedures on cyclodextrin–silica columns are described. Amino acid sequencing by means of interfaced HPLC-mass spectroscopy is introduced and is clearly seen to be of marked significance.

Necessarily, such a text as this must be selective, but the areas chosen for review represent well those where there will surely be continuing and significant developments. In this light, the book is recommended.

Peter C. Uden

Continuous-flow Fast Atom Bombardment Mass Spectrometry
Edited by R. M. Caprioli. Pp. × + 189. John Wiley and Sons. 1990. Price £27.50. ISBN 0-471-92863-1.

Without a doubt this is a book for the specialist mass spectroscopist, providing an overview of the subject from experts in the field as given at a 1989 symposium. However, it serves also to acquaint others, notably biological and separations scientists, with a field which is having increasing impact in the characterization and identification of complex samples. It is perhaps this latter group who will find it of more value since, while rapid technical advancements rapidly make the detailed descriptions of instrumentation and methodology outdated, the concepts and principles which the book's contributors describe suggest long term applications of a wide-ranging and lasting nature.

Considering these comments, there is one omission the inclusion of which would have made the text more valuable to the general reader. This is a general introductory chapter on Fast Atom Bombardment (FAB) Mass Spectroscopy itself. The underlying principles of this important technique appear only incidentally in individual chapters. This criticism aside, the concepts and applications of continuous sample introduction into FAB devices are well covered in eight chapters. The first three chapters deal with fundamentals and trace and quantitative analysis. Direct analysis of biological samples, high performance liquid chromatographic and capillary zone electrophoretic introductory modes are then discussed followed by consideration of low polarity substances and a number of specific application studies. Potential users of CF-FAB will gain a good insight into what the technique can do for them. The book is clearly designed, easily readable and of consistent format, as is not always seen in multi-author symposium volumes. The references are comprehensive and figures very clear. This is an accessible book on a complex but important subject which deserves a wide audience.

Peter Uden

Pierre Gy's Sampling and Sampling Practice Volume I. Heterogeneity and Sampling
By Francis F. Pitard. Pp. 214. CRC Press. 1990. Price £93.50. ISBN 0-8493-6658-3.
Pierre Gy's Sampling Theory and Sampling Practice Volume II. Sampling Correctness and Sampling Practice
By Francis F. Pitard. Pp. 247. CRC Press. 1990. Price £119.00. ISBN 0-8493-6659-3.

It is not immediately clear why the publishers have divided the material into two volumes as the purchase of one without the other would definitely not be recommended. Maybe the prices have something to do with it. According to Pitard, Pierre Gy has been working on the sampling theory of particulate material since 1953. This theory is characterized by an 'impeccable cartesian approach that leaves no room for the empiricist'. For those who read French impeccably, it is possible to follow the development of Gy's theory through the original literature (details of which are fully referenced) and by reading Gy's own books (published in 1979, second edition in 1982, and in 1988). For those who don't, these two volumes provide a good overview. They have arisen out of a short course of between 3 and 5 days and the aim of the texts is to provide the essential basis of a programme adapted for teaching such a short course without 'overwhelming the attendee in such a way that he (sic) will be convinced that indeed the theory of sampling is too complicated for its daily application'.

Volume I develops the thesis that heterogeneity exists independently of the sampling process and considers how it can be characterized and quantified. The concept of the continuous sampling selection error is examined in detail and is shown to consist of three components (short-range, long-range and periodic heterogeneity fluctuation errors) each of which are discussed in some detail. If these terms do not immediately sound familiar, there is no need to panic as the pace of Volume I is really quite gentle and even the reader with only the most rudimentary previous contact with chemical statistics will be able to follow the development of the argument. All the basic terms are clearly defined and the volume starts with a chapter concerned with basic statistical

concepts, in which the author states that 'probabilities and statistics are often easier to understand by drawing a simple sketch'. Pitard adheres to this guideline and both this and the later chapters are well illustrated both with simple sketches and examples to which the analytical chemist can readily relate. Volume I continues with Components of the Overall Estimation Error, and Correctness of a Sampling Strategy before the second part of the volume, concerned with heterogeneity is introduced. Pitard warns that 'the hypothesis made when we assume that a material is homogeneous is very dangerous because it allows anyone to solve all sampling problems associated with heterogeneity by oversimplifying them'. This, in effect, is the *raison d'etre* of these volumes and the remainder of Volume I is concerned firstly with developing concepts and quantitative parameters to handle heterogeneity. The following chapter deals with Constitution and Distribution Heterogeneities and Variography ('The study of a chronological set of units and the quantification of all forms of heterogeneity fluctuations carried out by this set, random or non-random, is often called variography'). The next two chapters deal with zero-dimensional and one-dimensional lots, respectively. The third part of Volume I is concerned with sampling errors and is made up of five chapters in which a number of practical worked examples are considered including, a coal shipment, a molybdenum trioxide concentrate, a molybdenum–tungsten ore deposit and a gold ore deposit. The final chapter deals with segregation and this forms the transition between the largely theoretical material of Volume I and the mainly practical content of Volume II.

However, the introduction to the second volume warns that in addition to the heterogeneity fluctuation errors considered in Volume I, there are three more independent components of the total sampling error, namely the increment delimitation error, the increment extraction error and the preparation error. Pitard pulls no punches here as he goes on to accuse the manufacturers of sampling equipment, of neglecting these errors either 'voluntarily or involuntarily'. Furthermore, he writes, 'when we consider sampling devices used for sampling the environment, waste piles, treated water, cereals, high-purity chemicals, pharmaceutical products, electronic components and so on delimitation and extraction errors become so overwhelming that we may wonder what the driving force is that leads to their concealment'. Having caught the reader's interest, Pitard proceeds to briefly consider each of the three error types mentioned above. In the second of these, a number of practical devices such as thiefs, augers and triers are exposed, along with several stream sampling techniques, as practically never correct. Following these three chapters is one concerned with preparation errors and again some strong sentiments are expressed. Consider the following 'The prevention and minimization of preparation errors can only be achieved if sampling is under the responsibility of engineers and technicians with analytical backgrounds' or 'It is not a good idea to allow production operators to control their own quality: unfortunately it is done all the time'. Pitard then considers some particular sampling problems and the five chapters deal with moisture content, particle size distribution, precious metals, high-purity materials, and liquid and solid wastes and the environment, respectively. The two final chapters in the section deal with proportional sampling and solvable and unsolvable sampling problems. In the last of these chapters Pitard discusses the cost of representativeness. In some ways it is a shame that this little 4-page chapter is hidden away towards the end of the volumes, as the material it contains provides a powerful motivation for getting to grips with the contents of these 2 volumes. The next two chapters are concerned with homogenization and the advantages of the bed blending process are stressed. The final chapter, essentially conclusions and recommendations, is another that might have been better placed earlier in the volumes as it deals with the needs for proper sampling procedures.

These are important books and anyone who considers themselves to be a card-carrying analytical chemist should be aware of the contribution of Pierre Gy to the theory and practice of the sampling of heterogeneous materials. These two volumes do the job very nicely and are highly recommended. They do, of course, raise the question of just where, in the educational processes that produce analytical chemists, are concepts such as Gy's theory to be taught?

J. F. Tyson

Sampling
By G. E. Baiulescu, Pompilia Dumitrescu and P. Gh. Zugråvescu. *Ellis Horwood Series in Analytical Chemistry.* Pp. 184. Ellis Horwood. 1991. Price £45.50. ISBN 0-13-791021-5.

With an intriguing title like 'Sampling' and an attractive cover, this is a book you want to dip into if only to see where the authors think sampling begins and ends. Curiosity is further aroused when you look at the table of contents, with just five chapters, an Introduction, History of the Sample, Homogeneity of the Sample, Chemical Analysis of the Sample, and Influence of Sampling on the Analytical Process. Clearly the approach is novel.

By page 8 it is made clear that separation is to be included, and by page 10 you can't help starting to wonder whether the authors would have been happier writing a book on separation techniques. By page 13, on which 'the analytical chemist, like an "artist", will have to learn first the "musical notes" in order to produce a "symphony" that is to characterize a sample material', my sympathy was with those who might buy this book expecting a step-by-step guide to sampling. In fairness, the authors do make it clear, on several occasions, in the text that this is not their intention.

Chapter 2, I found interesting to read, but although it is full of enthusiasm, it is rather akin to the flight of a bumble bee. The authors might have their route well planned out, but it is very difficult for anyone else to work out where they are going. Only one page (p. 39) was clear, concise, and very obviously to the point. Chapter 3 on Homogeneity also left me lost. It is full of chemistry, techniques, jargon and interest, but not very much to do with sample homogeneity. Environmental chemists looking for help will find this chapter particularly frustrating. To be honest, Chapter 4 isn't particularly useful either, the authors continuing to flutter from flower to fascinating flower. However, Chapter 5 is more valuable, and more obviously to the point as suggested by the book's title.

While I might never recommend this volume to inexperienced students, I have to admit that I enjoyed reading it. I suspect that others of the older generation might do likewise. At times I felt much as I often do in front of an abstract painting, not exactly sure what the message is, or sometimes even if there is a particular message at all. This is really a text for the philosophical analyst. However, you would need to be a dedicated enthusiast of the philosophy of analytical chemistry to invest the required £45.50!

Malcolm S. Cresser

Patterson's German–English Dictionary for Chemists. 4th Edition. By Anotin M. Patterson. Edited by George E. Condoyannis. Pp. Liii + 890. Wiley. 1992. Price £52.00. ISBN 0-471-66991-1.

The revised edition of Patterson's German–English Dictionary is a welcome update. The 3rd Edition was published in 1984 with 59 000 entries and the many advances made in all

areas of chemistry since then means that a large number of modern terms do not appear in that version. The addition of a large range of new techniques and the associated vocabulary results in the 4th Edition being substantially thicker (containing 69 000 entries) while still remaining compact.

The vocabulary is not limited to chemistry in the narrow sense but includes basic German vocabulary in related fields such as biology, biochemistry and medicine. In addition to strictly 'chemistry related' words the dictionary also includes a broad general vocabulary, a very useful feature, which obviates the need to use a second dictionary in conjunction with this one for most purposes.

Although a knowledge of German is necessary when using the dictionary, a very useful and helpful Editor's Introduction is provided, which explains the 'wise use' of the dictionary and expands on some German grammar points, an understanding of which is useful and often vital when translating from German.

Paula O'Riordan

Analytical Methods in Toxicology
By H. M. Stahr. Pp. xxxvi + 328. Wiley. 1991. Price £56.00. ISBN 0-471-85136-1.

This book presents a collection of procedures used and compiled by the Chemistry Laboratory (Veterinary Diagnostic) of the University of Iowa. The six main chapters describe procedures for measuring a range of inorganic compounds, mycotoxins, pesticides, rodenticides, drugs and vitamins and other miscellaneous compounds. There are also discussions on sample handling, safety, quality assurance and instrumentation, and also normal values in domestic animals.

The methods are easy to follow and presented with sufficient clarity to enable them to be reproduced by other laboratories. Instrumentation used includes gas chromatographs, atomic absorption spectrometers, ultraviolet/visible spectrophotometers and apparatus as simple as Conway microdiffusion units. Many of the methods presented are not new or novel but are based on well-proved techniques, and have been adopted for use in the author's laboratory. Most of the methods are therefore rigid and well proved.

The book will be particularly useful in veterinary laboratories that are required to carry out a wide range of analytical methods including toxicology and should form an important reference manual for everyday use.

John Blanchflower

Electrochemical Interfaces. Modern Techniques for *In-Situ* Interface Characterisation
Edited by Héctor D. Abruña. Pp. xviii + 589. VCH. 1991. Price DM182.00; £65.00. ISBN 3-527-27840-0 (VCH Verlagsgesellschaft); 0-89573-715-9 (VCH Publishers).

The development and application of *in situ* techniques for the study of electrochemical reactions and electrode surfaces has been one of the most exciting developments of the last decade. As a result of progress in this field it is now possible to study the electrode surface at the molecular scale and to answer questions about the nature and binding of intermediates at electrified interfaces. The implications of these advances for the rational design of electrocatalytic surfaces for fuel cells, for chemical sensors, and in many other areas are enormous. This new book provides an excellent introduction to, and survey of, techniques for the *in situ* characterization of interfaces.

The book is divided into ten chapters, each covering a different technique and each by a different author or authors. The topics covered are X-ray absorption spectroscopy (EXAFS), X-ray scattering, the use of X-ray standing waves, the measurement of surface forces, surface enhanced Raman (SERS), non-linear optical methods, infrared spectroelectrochemistry, Mössbauer spectroscopy, radioactive labelling studies, and the use of the electrochemical quartz crystal microbalance (EQCM). Of course, there are some techniques which are not covered, for example the scanning probe family (STM, AFM, SECM) and ellipsometry; nevertheless, this is a very useful text. The editor has been careful to choose his authors, all young, active American electrochemists, and to give them clear guidelines about the scope and level of their contributions. The result is a very well written and exciting book. Each chapter provides an introduction to the basic principles of the technique, a discussion of the experimental aspects and examples of the application of the technique to electrochemical problems.

This is an ideal book for surface chemists, surface physicists and materials scientists who wish to find out more about progress in this area. It will also be invaluable as a teaching resource for final year undergraduate and postgraduate courses in electrochemistry, and as a reference work for the electrochemistry community.

P. N. Bartlett

Applications of Plasma Source Mass Spectrometry
Edited by Grenville Holland and Andrew N. Eaton. The Royal Society of Chemistry. 1991. Pp. viii + 222. Price £37.50. ISBN 0-85186-566-6.

This is a book containing 21 of the papers that were presented at the Second International Conference on Plasma Source Mass Spectrometry held at the University of Durham on September 24–28, 1990. It includes applications of low and/or high resolution inductively coupled plasma mass spectrometry (ICP-MS) to various environmental (9 papers), biological (3 papers), and other (2 papers) samples, some of which describe the development of a digestion or calibration procedure. In addition, the development and application of alternative sample introduction systems (laser ablation, hydride generation with and without flow injection, and electrothermal vaporization) are discussed (4 papers). The spatial distribution of ions in the plasma (1 paper) and the design of the ion optics (1 paper) are also covered. Finally, one paper is devoted to a critical assessment of glow discharge mass spectrometry.

However, behind its attractive pink hard-cover lie numerous typographical errors, omissions, parts of sentences missing, and bad justifications. On several occasions, references are made to the wrong table or figure. In fact, some figures appear without any reference being made to them at all! The labelling of a few figures and tables is not explained, and some abbreviations are not defined. One can even find in the second of two consecutive papers by the same authors, a reference made to a procedure described in the first paper as 'will be published later'. Putting together a book is certainly a lot of work but, in this case, it certainly looks like the editors have simply combined the camera-ready manuscripts without having a look at them. Preserving the ideas and observations of the authors (as the editors rightfully did) is one thing, but preserving poor presentations is another. In a publication of this quality one should not find a faint figure with a hand-written label as on p. 90.

Furthermore, the reader should be careful not to leave his or her critical sense aside when going through this book. For instance, on p. 17 (in a paper entitled 'Direct Analysis of Semiconductor Grade Reagents by ICP-MS'), the authors say that they avoid internal standardization for fear of contami-

nating the sample, and use the method of standard additions instead, one of the reasons being that it 'does not contaminate the sample'. As both methods involve the addition of one or more (in the case of multiple additions of various elements) solutions to the sample, they both involve a high risk of contamination. The same authors also say that 'values for Ca and Fe in H_2SO_4 were measured by external calibration (instead of the method of standard additions) since both elements suffer spectral interferences on all isotopes'. How can any calibration strategy be used, unless a correction is made for these spectroscopic interferences?

Fortunately, several papers are excellent and compensate for the poorer presentation (and/or quality?) of the others. The book certainly contains valuable information for ICP-MS users and is worth the frustration of 'decoding' some of the text.

Diane Beauchemin

The Handbook of Environmental Chemistry
Edited by Otto Hutzinger. Volume 3. Part G. Anthropogenic Compounds. Pp. xi + 237. Springer Verlag. 1991. Price DM 168.00. ISBN 3-540-53198-X; 0-387-53198-X.

Four groups of anthropogenic compounds: isocyanates; nitro-derivatives of polycyclic aromatic hydrocarbons; chlorinated ethanes; and organic explosives and related compounds, are discussed in this Handbook. In my opinion, the contents of this book are far beyond the scope of traditional handbooks. It is, rather, a combination of a reference book and a textbook with the purpose of introducing the role of anthropogenic compounds in the environment by bringing together the essential knowledge in respect to the research scientists, biochemists, industrial hygienists, toxicologists, chemical analysts, etc. Although certain volumes of this Handbook are written for readers at a somewhat advanced level, the easiness of reading of this volume means it would be of interest to all levels of readers. The anthropogenic compounds discussed are presented with important as well as versatile information regarding industrial production and consumption, chemical (including photochemical) and biological reactivities in the environment, toxicological effects and toxicities, metabolic routes, regulatory exposure limits, exposure monitoring techniques, *etc.* The vast information is, of course, presented in a condensed fashion yet all the essentials are retained. Therefore, this Handbook has great value not only to professionals engaged in the various disciplines of environmental chemistry but to scientists in general who are interested in acquainting themselves with slightly advanced knowledge in related environmental issues. Discussions and reviews for individual topics are well referenced. Readers can easily expand the horizon of some specific knowledge by referring to the well documented reference lists. It is certainly convenient to have this book to hand to access useful information. Although the topics are well presented, there are only a few places in the contents that are less clear than they should be. For example, the terms for polyisocyanates, isocyanate prepolymers, isocyanate semi-prepolymers and modified isocyanates are not clearly defined. These isocyanates together with isocyanate products such as cellular, microcellular, solid polyurethanes could probably be better presented with chemical formulae and drawing-added illustrations instead of mere descriptions. Furthermore, all tables and figures should have a brief introduction in the main contents, thus making it easier for readers to scan the contents briefly (for example, Chapter 2, noticeably, has a few missing).

Weh-sai Wu

Calixarenes
By C. David Gutsche. Monographs in Supramolecular Chemistry. Pp. xii + 224. Price £39.50. The Royal Society of Chemistry. 1991. ISBN 0-85186-916-5.

This book describes the development of interest in the family of oligomers known as calixarenes. The term 'calixarene', coined by the author in 1975, associates these molecules with the shape of a chalice (Greek: calix). In functionalized calixarenes, the 'cup' portion of the molecule is described by a number of polar groups (*e.g.*, esters, ketones or amides), while the 'base' consists of non-polar aryl and *tert*-butyl groups. Calixarenes thus possess a well-defined polar cavity capable of interacting with metal ions, and alkali metal ions in particular, but are usually preferentially soluble in non-polar solvents. Although not generally as well known as their close cousins, the crown ethers, their exciting potential as hosts for a wide variety of commercially important ions and molecules, coupled with their ease of synthesis and functionalization, makes the calixarenes a potential source of many useful materials.

For the analyst, the main areas of exploitation will be those which can take advantage of the selectivity of complexation which they offer, such as the development of novel sensor or chromatographic stationary phases. From the teaching point of view, several well characterized compounds can be easily synthesized from readily available precursors (Aldrich) using simple equipment, and the products identified using IR, UV/VIS and NMR spectroscopic techniques.

The book itself is superbly written and produced, with an excellent review of the historical background of research into calixarenes, and a series of chapters in which the author describes how to make, prove, shape, embroider, fill and use these molecular baskets. It is completed by a comprehensive subject index and two compound indexes. My only reservation is that the applications section of the book is not as well covered as it could be, but this is perhaps more a reflection of the speed of developments in calixarene applications, most of which have been published in the literature after this monograph.

To conclude, I recommend this book as a useful source of information and ideas for anyone interested in applications involving host–guest chemistry. In addition, the book itself is an example of how a specialized scientific text can be turned into a very readable story. When is the paperback coming out?

Dermot Diamond

Spectroscopic Properties of Inorganic and Organometallic Compounds: Volume 24
Senior Reporter, E. G. Davidson. *Specialist Periodical Report.* Pp. xiv + 492. Price £149.50. The Royal Society of Chemistry. 1991. ISBN 0-85186-223-3.

This topical series of reviews maintains the very high standard one expects from the Specialist Periodical Reports, and in particular this series. The volume is produced directly from the authors manuscripts, which speeds publication and cuts costs, although the quality varies from publication quality laser printed copy to traditional, harder to read, monospaced fonts reminiscent of electric typewriter copy. It is unfortunate, that despite these measures the price in most cases will limit this work to library shelves rather than the offices and laboratories where it really belongs.

The first of eight chapters, NMR, by B. E. Mann is the longest and most thorough (191 pp. 3357 references). It also includes an appendix with a cross-listing of references by nucleus with the exception of the three common spin 1/2

nuclei. Arranged by element, topics include: stereochemistry and complexes; dynamic systems (fluxional molecules, equilibria and the course of reactions); and a section on solids (46 pp.), a growing area of study. All have extensive coverage of the non-NMR literature where much of this information is buried.

Two speciality chapters, NQR by Dillon and Rotational Spectroscopy by Carpenter, show that there is significant activity in these areas of spectroscopy, not routinely considered by the inorganic chemist contemplating spectroscopic methods.

Vibrational Spectroscopy by Davidson is split into three chapters (121 pp.), the first two based on the Main Group and Transition Elements with the third focused on the Coordinated Ligand. This breaks an immense topic into more manageable units.

A very thorough chapter on Mössbauer Spectroscopy (825 refs.) by Clark *et al.* indicates continuing vibrant activity in a field confined by the number of sources readily available. Rankin and Robertson conclude with a short chapter on structure determination by electron diffraction.

The only important topic missing from this series is the application of mass spectroscopy to inorganic and organometallic compounds, an area of growing importance over the past decade as new sources have been developed that can handle non-volatile ionic systems as well as covalent molecules were handled in the past.

No inorganic chemist should be without ready access to this valuable series.

Jack M. Miller

Applied Inorganic Chemistry
By T. W. Swaddle. Pp. xii + 331. University of Calgary Press. 1991. Price £24.50. ISBN 0-9191813-58-5.

This book by Professor Swaddle is intended as a text for third and fourth year chemical engineers and deals with an area of chemistry neglected in both engineering and pure chemistry programmes. So much time is spent in our curricula on structure, bonding, spectroscopy and exciting new inorganic molecules and reactions, that students often do not realize the vast industrial and agricultural importance of inorganic chemicals, in particular the main group elements. This book does a superb job of meeting those needs and is an ideal length for a single term course. It deals almost entirely with the chemistry, both thermodynamics and kinetics, being treated as an integral part of the chemical discussions. As the course was given to engineers, no time is spent on unit operations that often form the heart of texts on industrial chemistry. While it is noted that the specific technologies are often ephemeral, the addition of a basic chapter on unit operations would make it more useful for the pure chemistry student without having to use supplementary materials. That being said, it is still the best book on the market to fill this necessary niche in our curricula, and the next time I have occasion to teach our industrial chemistry course I will use it.

Chapter topics include chemical energetics, the atmosphere and atmospheric pollution and agricultural chemicals. These are followed by a series of chapters dealing with various main group elements, ionic solids, defects, inorganic solids as heterogeneous catalysts and interstitial compounds of metals. Solution chemistry topics include ions, water conditioning, redox and corrosion. There then follows a good chapter on extractive metallurgy, and a brief introduction to organometallics and homogeneous catalysis. Chapters have suggested readings, although not always from the most up-to-date materials, and a series of useful exercises.

The material is presented not as a series of dry facts but rather as a series of chemical examples showing the problems and pitfalls and reasoning behind particular processes. It is readable. Although the specific engineering aspects are not covered, and the references are not all to the 1980s and 1990s, the author is clearly aware of modern chemical process technology used in the wide variety of industries covered.

I recommend this book to anyone looking for a text in this area.

Jack M. Miller

CUMULATIVE AUTHOR INDEX

JANUARY–OCTOBER 1992

EUROANALYSIS VIII

The Eighth European Conference on Analytical Chemistry

will be held at the

University of Edinburgh
September 5–11, 1993

Organized by the Analytical Division of The Royal Society of Chemistry on behalf of WPAC/FECS

Scientific Programme

Euroanalysis VIII will cover developments in instrumentation and methodology in all areas of analytical chemistry, with emphasis on industrial, biomedical and environmental analysis. The programme will be designed to appeal to both practising analytical chemists in industry and those in academia who are teaching and carrying out research.
The programme will consist of invited keynote lectures and contributed oral and poster papers. In order to ensure high quality, all contributed papers will be refereed.

Social Programme

A comprehensive programme is being planned for participants and accompanying persons. It will include half- and full-day excursions, and various evening events including a whisky tasting and a Buffet Reception at the Royal Museum of Scotland.

Publication

All of the invited lectures will be published in a collected volume as the proceedings of the conference. Authors of contributed papers will be encouraged to submit manuscripts for publication in either *The Analyst* or the *Journal of Analytical Atomic Spectrometry* (*JAAS*).

Topics

Some of the topics covered are:

Industrial Analysis	Validation of Analytical Measurements, Process Control Analysis, Materials Analysis (including Surface Analysis), Energy Related Analysis
Pharmaceutical and Biomedical Analysis	Pharmaceutical Methods and Drug Metabolism, Forensic Science, Bioselective Methods, Trace Elements in Medicine
Environmental Analysis	Atmosphere, Soils/Sediments, Food/Drink,Water
Instrumental Techniques	Separation Science, Molecular Spectroscopy, Atomic Spectrometry, Electroanalytical Techniques, Expert Systems and Chemometrics,Coupled Techniques, Sensors, Laser-based Techniques, Flow Analysis

Conference Secretariat: Honorary Chairman, E.J. Newman

Conference Presidium: D.T. Burns, Belfast (Chairman); J.F.K. Huber, Vienna; L. Niinisto, Espoo; P.G. Zambonin, Bari

Secretary and Conference Organizer: Miss P.E. Hutchinson,
Analytical Division, The Royal Society of Chemistry, Burlington House,
Piccadilly, London W1V 0BN, UK
Tel. 071 437 8656; Fax 071 734 1227; Telex 268001

All correspondence and requests for further information should be addressed to the Conference Organizer.

FIRST FOLD HERE

THE ANALYST READER ENQUIRY SERVICE
For further information about any of the products featured in the advertisements in this issue, write the appropriate number on the postcard, detach and post.

FOLD HERE

THE ANALYST READER ENQUIRY SERVICE

OCT'92

For further information about any of the products featured in the advertisements in this issue, please write the appropriate number in one of the boxes below.
Postage paid if posted in the British Isles but overseas readers must affix a stamp.

PLEASE USE BLOCK CAPITALS LEAVING A SPACE BETWEEN WORDS *Valid 12 months*

1 NAME

2 COMPANY

PLEASE GIVE YOUR BUSINESS ADDRESS IF POSSIBLE. IF NOT, PLEASE TICK HERE ☐

3 STREET

4 TOWN

5 COUNTY
POST CODE

6 COUNTRY

7 DEPARTMENT
DIVISION

8 YOUR JOB TITLE
POSITION

9 TELEPHONE NO

OFFICE USE ONLY RECD PROCD

FOLD HERE

Postage will be paid by Licensee

Do not affix Postage Stamps if posted in Gt. Britain, Channel Islands, N. Ireland or the Isle of Man

BUSINESS REPLY SERVICE
Licence No. WD 106

Reader Enquiry Service
The Analyst
The Royal Society of Chemistry
Burlington House, Piccadilly
LONDON
W1E 6WF
England

NEW EDITION

OVER 81,000 SPECTRA

EIGHT PEAK INDEX OF MASS SPECTRA

4th Edition

The essential tool for mass spectrometrists

NOW AVAILABLE – the **new 4th Edition** of the highly regarded ***Eight Peak Index of Mass Spectra.***

This quality compilation is recognised by many mass spectrometrists as the most useful index of mass spectra in print today.

THE *EIGHT PEAK INDEX* EMPOWERS YOU TO:

- ★ identify unknowns rapidly and easily
- ★ locate spectra of compounds quickly by formula or molecular weight
- ★ match spectra simply through direct peak intensity comparison
- ★ find spectra relevant to your area of interest – a wide variety of compound types are included
- ★ access the data at any time with no machine-time restrictions
- ★ use the data with confidence – extensive checks on all records have been performed

Probably the best printed index of mass spectra in the world!

For more information about the ***NEW*** edition, simply contact us at the address below for a copy of our detailed leaflet:

ROYAL SOCIETY OF CHEMISTRY

Information Services

Sales and Promotion Department
Royal Society of Chemistry
Thomas Graham House
Science Park, Milton Road
Cambridge CB4 4WF, United Kingdom
Tel: +44 (0) 223 420066.
Fax: +44 (0) 223 423623.
Telex: 818293 ROYAL

Circle 004 for further information

ANALAO 117(10) 1537–1656 (1992) October 1992

The Analyst

The Analytical Journal of The Royal Society of Chemistry

CONTENTS

0003-2654(1992)10-X

Typeset and printed by Black Bear Press Limited, Cambridge, England